In vitro analysis of lytic peptide to target breast and prostate cancer.

Jannoo, Riaz

In Vitro analysis of lytic peptide to target breast and prostate cancer

By

Riaz Jannoo

This thesis is submitted to Swansea University in fulfilment of the requirements for the degree of Doctor of Philosophy (PhD)

Swansea University
Prifysgol Abertawe

College of Medicine

March 2015

ProQuest LLC.
789 East Eisenhower Parkway
P.O. Box 1346
Ann Arbor, MI 48106 – 1346

Abstract

In the United Kingdom 1 in 3 will develop some form of cancer during their lifetime. Despite the development of new drugs and use of combinational therapies, mortality rates have not improved. Between 1979 and 2008, incidence rates for cancer in the United Kingdom increased by 26% The second most common cause of cancer deaths is prostate cancer in men and breast cancer in women, the first being lung cancer. Current methods for treating cancer involve radiation therapy and chemotherapy. However, resistance to these therapies is common.

Targeting of cell surface receptors specifically or over expressed in cancer cells has painted a new insight in anti-cancer therapy. The Gonadotropin-releasing hormone receptor (GnRHR), luteinizing hormone/choriogonadotropin receptor (LHCGR) and Interleukin-13 receptor alpha 2 (IL-13Rα2) are overexpressed in some human tumours, including prostate and breast cancer. IL-13, GnRH and βCG ligands bind to the cell surface receptors IL-13Rα2, GnRHR and LHCGR respectively.

The gene expression of GnRHR, LHCGR and IL-13Rα2 in a wide range of human cancer tissues as well as in 2D cultured (monolayers) prostate and breast cancer cell lines was analysed. Their levels were shown to be overexpressed, indicating their potential use for diagnosis and targeting treatment.

Unlike 2D monolayer cultures, 3D spheroid cultures achieve *in vivo*-like conditions in cancer. We therefore developed quick, easy and reproducible 3D tumour models of prostate and breast cancer cell lines and used them to validate the cancers target ability for the lytic peptides.

Both 2D monolayer and 3D spheroid cultures of breast and prostate cancer cells over-expressing IL-13Rα2, GnRHR and LHCGR were targeted using Pep-1, [D-Trp^6]GnRH and βCG(ala) peptides conjugated covalently to a membrane disrupting lytic peptide (Phor21). The lytic peptide drugs [D-Trp^6]GnRH-Phor21, Pep-1-Phor21 and Phor21-βCG(ala) conjugates were shown to selectively kill prostate and breast cancer cells with their toxicity dependent on the expression levels of the respective receptors at the cell surface.

Declaration

This work has not previously been accepted in substance for any degree and is not being concurrently submitted in candidature for any degree.

Signed ..... (Candidate)

Date.....4/12/15.....

STATEMENT 1

This thesis is the result of my own investigations, except where otherwise stated. Where correction services has been used, the extent and nature of the correction is clearly marked in a footnote(s).

Other sources are acknowledged by footnotes giving explicit references. A bibliography is appended.

Signed..... (Candidate)

Date.....4/12/15.....

STATEMENT 2

I hereby give consent for my thesis, if accepted, to be available for photocopying and for inter-library loans ~~after expiry of a bar on access approved by Swansea University.~~

Signed ..... (Candidate)

Date....4/12/15.....

Contents

Acknowledgment

This PhD has not been easy. The last four years, I have realised how much I hate western blotting, and I still can't bloody get it right. But I'm done now WOOP WOOP!! First I would like to thank my supervisor Professor Venkateswarlu Kanamarlapudi for giving me the opportunity to work with him and learn from him throughout my graduate career. I would also like to say a BIG thank you Dr Paula Row for her help and expertise, and Dr Zhidao Xia for teaching me how to make cool cancer spheroids. I would also like to thank Dr Sian Owens and Jonathon Davies for teaching me, helping me and for putting up with me; I know I can be a headache sometimes.

I would also like to thank the people who made me smile; the new people in the office; whole lot of you are like breath of fresh air, including Salman. Rachel Smith, Lleucu Davies, and Aled Bryant you guys made the office really fun, which kept me going. I also like the fact that every Christmas and Birthday present I got was alcohol related. I don't know why. I will also like to thank Aiysha Thompson. From undergrad to the end of the PhD, you have helped me a lot and to this day I still don't understand how you were able to fit into a very small tent, a very small bin and a locker. I'm really going to miss those days. Thank for keeping me sane and happy all these years

Finally, I would like to give my thanks to my family and step family, who have supported me all throughout my life, who never ask what I have achieved but only cares whether I am happy or not.

This work is part-funded by the European Social Fund (ESF) through the European Union's Convergence programme administered by the Welsh Government.

So thank you all so very much for everything I really don't think I would have finished without help. I'm looking forward for the future.

List of Figures

List of Tables

Abbreviations

5-aza 5-aza-2′deoxycytidine

AP-1 Activator protein 1

cAMP cyclic adenosine monophosphate

CG chorionic gonadotropin

CHO: Chinese hamster ovary cells

CT Computed tomography

DAG 1, 2 diacylglycerol

DU145 human prostatic carcinoma cell line

E2 estradiol

EC_{50} half maximal effective concentration

EGF Epidermal growth factor

EGF-R Epidermal growth factor receptor

EPR Enhanced permeability and retention

FSH Follicle stimulating hormone

FTIR Fourier transformation infrared

GnRH Gonadotropin-releasing hormone

GPCR G protein-coupled receptor

hCG human chorionic gonadotropin

HEK293 Human Embryonic Kidney

HPG hypothalamic pituitary gonadal

HPLC High-performance liquid chromatography

HT-29 Human colon adenocarcinoma grade II cell line

IL-13Rα2 Interleukin-13 receptor subunit alpha-2

Jak-Stat Janus kinase signal transducers and activators of transcription

JNK cJun N-terminal kinase

LH Luteinizing hormone

LHCGR luteinizing hormone/human chorionic gonadotropin hormone receptor

LHRH Luteinizing hormone releasing hormone

LNCaP androgen-sensitive human prostate adenocarcinoma cell line

MAPK Mitogen-activated protein kinase

MCF-10A mammary epithelial breast cell line

MCF7 Human breast adenocarcinoma cell line

MDA-MB-231 Human breast carcinoma cell line.

MDA-MB-435S. Human breast carcinoma cell line.

MDR Multidrug resistance

MMP Matrix metallo proteinases

MRI Magnetic resonance imaging

NF-kB Nuclear factor kB

Nrf2 Nuclear factor erythroid 2-related factor 2

PC-3 human prostatic carcinoma cell line

PEG polyethylene glycol

PET Positron emission tomography

PNT-2 Human prostate normal

RT-PCR Reverse transcriptase polymerase chain reaction

SPECT Single-photon emission tomography

SPIONs Superparamagnetic iron oxide nanoparticles

TRH Thyrotropin releasing hormone

TSA Trichostatin A

TSH Thyroid stimulating hormone

$ZnCl_2$ Zinc chloride

Amino Acid Abbreviations

Amino Acid	3 Letter Abbreviation	1 Letter Abbreviation
Alanine	Ala	A
Arginine	Arg	R
Asparagine	Asn	N
Aspartate	Asp	D
Aspartate or Asparagine	Asx	B
Cysteine	Cys	C
Glutamate	Glu	E
Glutamine	Gln	Q
Glutamate or Glutamine	Glx	Z
Glycine	Gly	G
Histidine	His	H
Isoleucine	Ile	I
Leucine	Leu	L
Lysine	Lys	K
Methionine	Met	M
Phenylalanine	Phe	F
Proline	Pro	P
Serine	Ser	S
Threonine	Thr	T
Tryptophan	Trp	W
Tyrosine	Tyr	Y
Valine	Val	V

1. General Introduction

1.1. Introduction

Cancer has become the leading cause of death worldwide and the second leading cause of death in developed countries (Jemal et al, 2011). In 2008, globally it is estimated that 12.7 million people were diagnosed with cancer and approximately 7.6 million patients died of cancer (Figure 1.1). The most common forms of cancer diagnosed worldwide are lung cancer in males and breast cancer in females, which account for the greatest number of cancer related deaths (figure 1).

In developed countries the incidence rate of cancer has increased, which is likely to continue due to an increased aging population and changes to lifestyles. Breast cancer incidence rates in Western countries have shown to be increased between the 1980s and 1990s due to increase in use of post-menopausal hormone therapies. Increase in cancer rates due to changes to lifestyles (change in diet, increased obesity and smoking) could explain why incidence rates for colorectal cancer are high (Jemal et al, 2011). However it is important to note that the increase in number of cancer cases is partly attributable to the development of effective and highly sensitive screening techniques.

In the United Kingdom (UK), 1 in 3 will develop some form of cancer during their lifetime . Despite the development of new drugs and use of combinational therapies, mortality rates are still not improving. In 2009, 408,381 people were diagnosed with cancer and 156,090 died of cancer in the UK ; the highest mortality occurred due to lung cancer (UK, 2009). Between 1979 and 2008, incidence rates of cancer in the UK increased by 26% with a 13% increase in men and a 34% increase in women (UK, 2009).

In the UK, the most common cause of cancer death in men is prostate cancer and breast cancer in women (figure 2) (UK, 2009). These cancer types develop a heterogeneous population of cells that are both dependent and independent of hormones (estrogen/androgen) and undergo irregular differentiation and proliferation (Catz & Johnson, 2003). Patients with prostate or breast cancer are usually treated with a combination of radiotherapy or chemotherapy therapy and hormonal therapy. Doxorubicin and 5-fluorouracil are examples of drugs that are used in chemotherapy (Delena et al, 1975). Drugs used in hormonal therapy

include leuprolide for treating prostate cancer and tamoxifen for treating breast cancer (O'Regan & Jordan, 2001; Tammela, 2004). Patients with an aggressive form of prostate or breast cancer are initially treated by surgery (prostatectomy for prostate cancer and mastectomy for breast cancer) (Meijers-Heijboer et al, 2001; Tan et al, 2011).

Current treatments cannot cure but only prolong patient's lives. Chemotherapeutic drugs are usually given when the cancer disease starts to spread to other parts of the body. Although chemotherapeutic drugs are effective, they destroy rapidly dividing both cancer and non-cancer cells, and hence their usage can cause serious side effects by destroying healthy tissue and organs (Jang et al, 2003). Moreover, these drugs are unable to target dormant cancer cells and slow growing tumours (Pantel & Otte, 2001). Although the hormonal therapy has been shown to reduce tumour size, its usage can cause the disease to remerge and differentiate into a more aggressive form, making the treatment therapy ineffective (Pantel & Otte, 2001; Tammela, 2004).

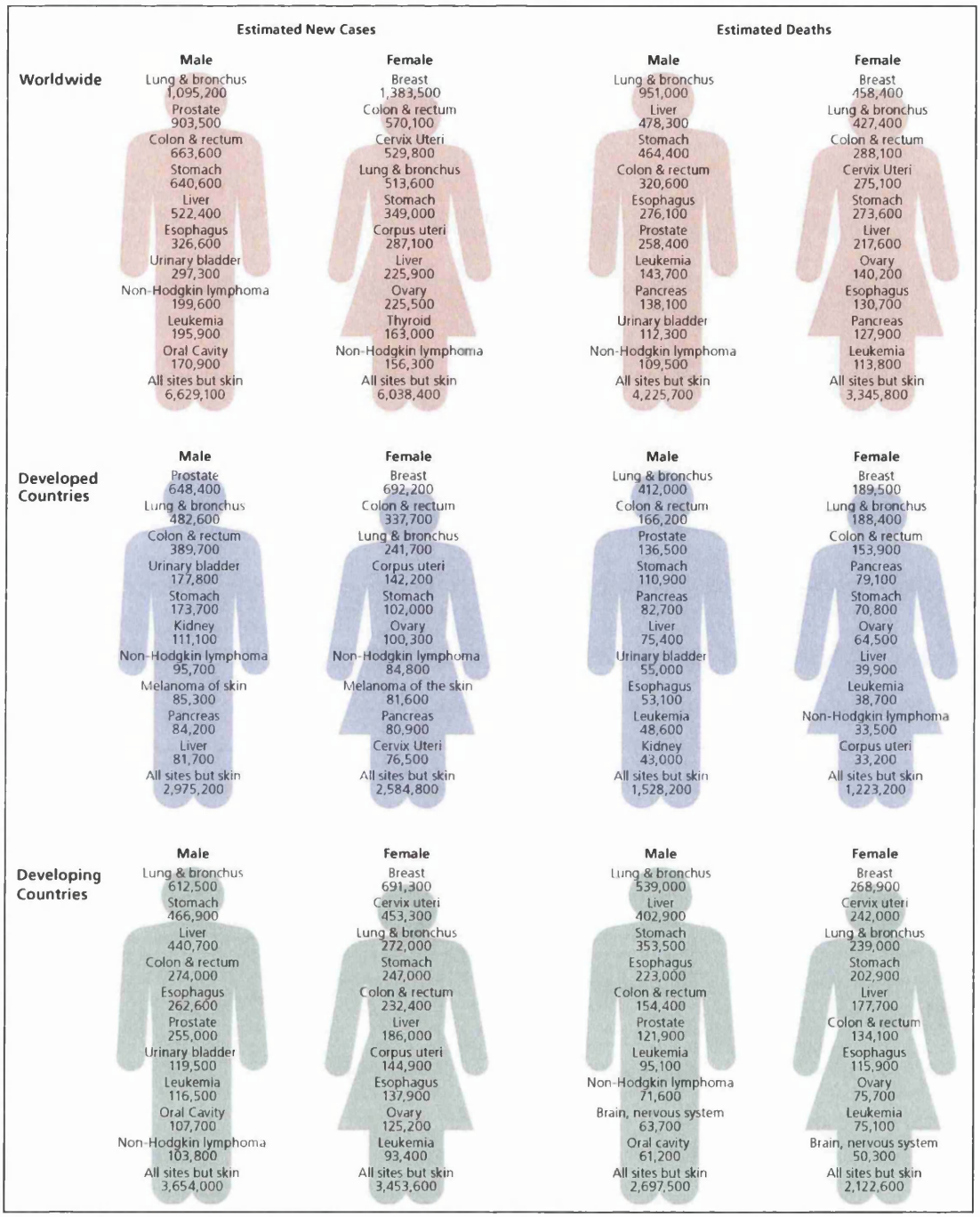

Figure 1.1. Worldwide cancer incidence and death rates in 2008. This figure [taken from (Jemal et al, 2011)] shows the estimated numbers of diagnoses and deaths related to different cancer types in 2008.

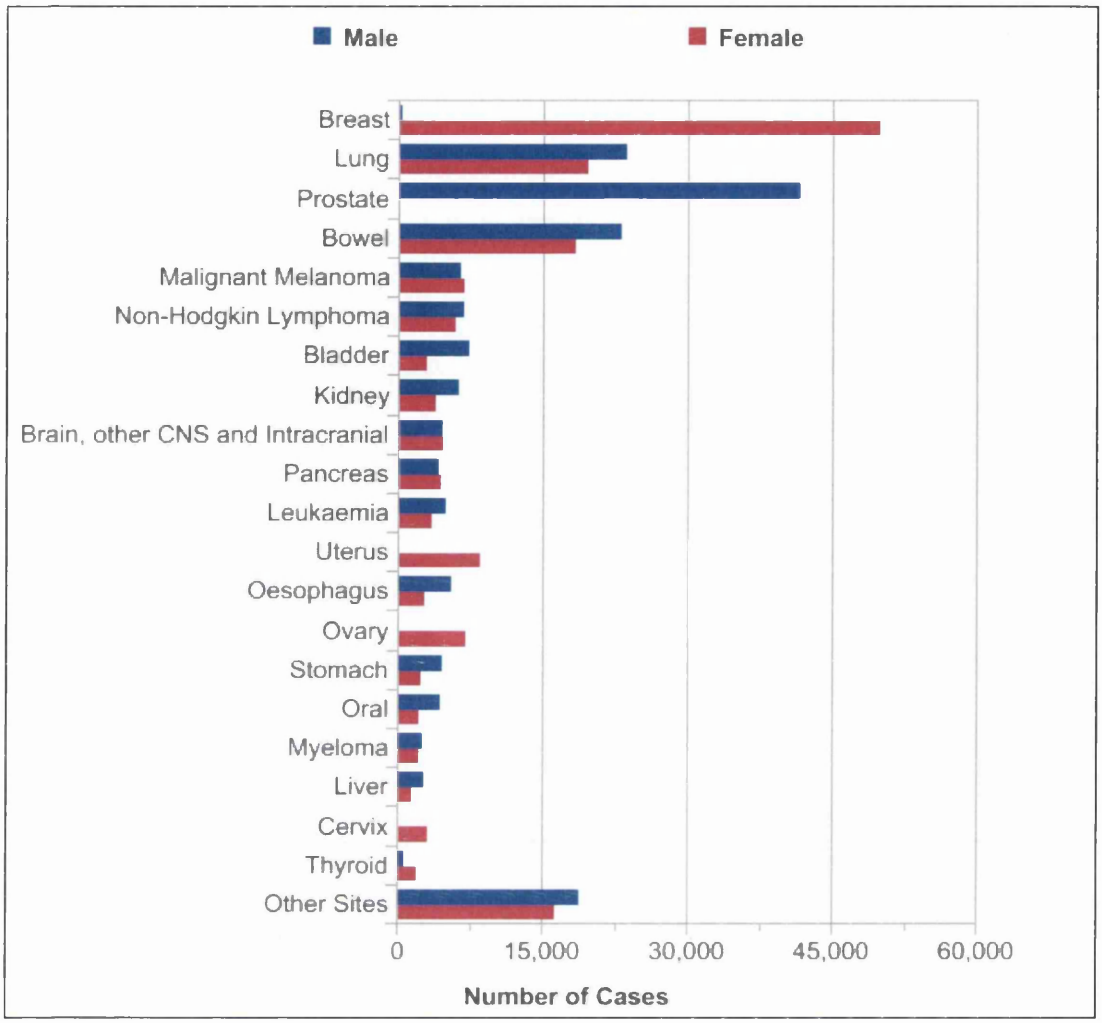

Figure 1.2. The top ten most commonly diagnosed cancers in the UK in 2011. The top ten most commonly diagnosed cancers in the UK in 2011 are shown for males and females. This graph is taken from the Cancer Research UK (CRUK) website (www.cancerresearchuk.org).

1.2. Cancer Classification

There are an overwhelming number of cancers types that have been identified, and each type consists of multiple subtypes that are able to grow in a single organ or tissue type. These are generally classified based on their tissue location. The most common form of cancer is carcinoma (cancer develops from epithelial cells), accounting for over 80% of all cancers located within epithelial cells (Weinberg, 1983; Weinberg, 2002). This type of cancer is further divided based on histological features into two types: squamous cell carcinoma and adenocarcinoma. Carcinoma with features such as intercellular bridges, keratinization, and squamous pearls is called Squamous cell carcinoma whereas carcinoma with glandular appearance is known as adenocarcinoma.

Carcinomas of the skin and cervix fall under the subtype squamous cell carcinomas whereas breast and prostate carcinomas come under adenocarcinoma subtype. In some cases, carcinomas are able to invade other parts of the body forming a malignant tumour (Hanahan & Weinberg, 2000; Hanahan & Weinberg, 2011). Malignant tumour cells acquire a number of traits for survival. These include:

1) The Ability to proliferate without any growth signals or factors

2) The Ability to inhibit or not respond to any signals or factors that prevents proliferation

3) The Ability to resist apoptosis

4) The Ability to replicate with no off switch

5) The Ability to sustain angiogenesis

6) The ability to invade surrounding tissues and metastasize

Carcinomas can also be graded (I-IV) based on the degree of cellular and tissue maturity seen in the transformed tissue compared to the appearance of epithelial tissue from which the carcinoma originates (Edge & Compton, 2010).

Grade 1- the tumour cells proliferated slowly and are well differentiated.

Grade 2- the tumour cells are moderately differentiated.

Grade 3- the tumour cells proliferated faster and spread faster than tumours in the lower grades.

Grade 4- is considered high grade, undifferentiated cells that proliferate faster and spread faster. In this case the cells have spread away from the site of origin.

Although the strength of correlation can be highly variable, there is a good correlation between carcinoma grading and cancer prognosis. The higher the grade of the carcinoma, the worse is its prognosis.

Since my research work is concerned with targeting of prostate and breast cancer, I discuss these two cancer types in further below.

1.2.1. Prostate cancer

Prostate cancer is the second most leading diagnosed cancer type and the sixth leading causes of cancer death in males worldwide. 14% (903,500) of the total new cancer cases and 6% (258,400) of the total cancer deaths in males in 2008 were caused by prostate cancer (Jemal et al, 2011). The development of PSA testing, that detects tumours as well as other cancers, has identified the rates of cancer worldwide. The death rate for prostate cancer has been decreasing in many of the developed countries such as United States, Australia, Canada and the United Kingdom; due to the improvement of treatment. In contrast, in developing countries, incidences of metastatic PSA and mortality rates have increased (Jemal et al, 2011).

90% of men diagnosed with prostate cancer, are at the early stages. These types or primary tumours are within the prostate and is often curable with treatments such as surgery or radiation therapy. However, diagnosing at the early stages of prostate cancer is difficult; symptoms do arise until there are at the advance stages of the cancer. Like most solid tumours, if prostate cancer is not detected early, the tumour can metastasise to distant organs, such as liver, lungs, brain and the bone. Patients diagnosed with prostate cancer at early stages, have a 5 year survival of 100%; however this drop significantly to 31% with patents diagnosed with advance stages of the disease (Datta et al, 2010).

Bone metastases can occur in up to 90% of patients with advance prostate cancer (Roodman, 2004). At this stage, it is usually considered incurable, and can have a severe detrimental effect on the patient's quality of life, causing severe pain, hypercalcemia and spinal cord compression (Mackiewicz-Wysocka et al, 2012; Roodman, 2004).

Current screening method for prostate cancer is the measurement of Prostate-Specific Antigen (PSA) levels in the patient's blood and a digital rectal examination (DRE). This

would then be followed by a transrectal ultrasound guide (TRUS) biopsy. Histological examination of TRUS biopsy tissue is currently used for cancer diagnosis and will then characterised the prostate tumour based on the Gleason scoring system, which will dictate subsequent clinical management of the patient's cancer (Raja et al, 2006)

PSA is a serine protease, which in the presence of prostate cancer, increases in the blood. This biomarker is currently being used to detect prostate cancer and is responsible for improving detection of the disease at an early stage. The current cut-off point for biopsy recommendation is 4.0ng/ml (Obort et al, 2013). However the test cannot distinguish between indolent prostate cancer, and aggressive prostate cancer. Also 15.2% of all prostate cancer cases, PSA levels have been below 4.0ng/ml, and 26.9% of patients had a PSA level of between 3.1 and 4.0 ng/ml (Benedettini et al, 2008).

DRE is a technique that requires inserting a lubricated gloved finger through the rectum; to estimate the condition of the prostate gland. It is a fairly accurate technique identifying the pathologic condition of the gland (Basler & Thompson, 1998). However the sensitivity of DRE is limited because the cancer might not have a different pathology from the surrounding tissue, or even manifest beyond the reach of the examining finger (Sutton et al, 1991).

Patients with elevated levels of PSA would then undergo a TRUS biopsy to give a definitive diagnosis of prostate cancer. It assesses the presence and grade of the tumour by taking samples of the prostate for pathological assessment.

The treatment of the diagnosed prostate cancer is crucially dependent on the presentation of the disease (stage and grade of the cancer). Patients with tumours that are poorly differentiated are treated by Radical prostatectomy and radiotherapy. However it is estimated that about 30% experience a form of relapse of the disease to a more aggressive metastatic state (Zietman et al, 2004). Patients that are diagnosed with the more aggressive form of the cancer, is mainly treated with drugs that targets androgen receptors. Current treatment to regulate the hormonal signals are orchiectomy, anti-androgens, and LHRH agonists (Isbarn et al, 2009).

The major problem associated with the removal of the prostate is incontinence which is experienced in many cases (Grossmann *et al.,* 2001). Impotence is another side effect of surgery caused in a large part due to the nerves controlling an erection being located on either side of the prostate becoming damaged or removed during surgery (Mason and Moffat, 2010). Many patients with prostate cancer will therefore rather live with the cancer and take

the risk of the cancer not progressing rather than the possibility of being incontinent or impotent for the rest of their lives (especially if they are relatively young). However, there are a number of alternative treatment options available to the patient depending on the grade and stage of the prostate cancer. The first treatment that should be provided is a hormonal treatment administered over 2-3 years in combination with radiotherapy in patients with poorly differentiated tumours (Heidenreich et al, 2008; Isbarn et al, 2009). Hormone therapy is usually given in a course for 6-9 months then the PSA levels are monitored. If there is an increase of PSA levels occur, a second treatment of hormonal treatment is administrated.

If the cancer has progressed and no longer responds to hormone treatments anti-androgens or Stilboestrol may be given. Docetaxel is administered as a chemotherapeutic option for patients who have bone metastasis. This is given via injections into a drip once every three weeks; this improves the average survival rate to 3 months. In this case there can be severe side effects including hair loss, diarrhoea, tiredness, anaemia, sickness and vomiting (Demir et al, 2014).

Prostate cancer has a high incidence rate in the UK. This increase over the years could be due to better awareness and improved detection methods. The ability to target and detect prostate cancer makers offers promising new waves of diagnostic and treatments by allowing early identification of patients that are at risk of aggressive metastatic disease. There is also the need to develop specific and personalized treatments for patients that would otherwise face poor clinical outcome

1.2.2. Breast cancer

Breast cancer is the most common malignancy among females and the fifth common causes of cancer death worldwide, account for 10.4% of all cancers (Organization, 2015). Localised breast cancer at an early stage accounts for 60% of breast cancers that are diagnosed. At the early stages that survival rate is 98% (Etzioni et al, 2003; Pantel et al, 2003). Diagnosing the tumour after the breast cancer have metastasised, reduces that survival rate to 27% (Wong & Pavlakis, 2011).

Breast cancer is a disease that can be classified as one of three distinct forms: ductal carcinoma, were a tumour is formed at the ducts. Lobular carcinoma us were a tumour is formed in the lobes; and inflammatory breast cancer, which presents as warm, red, and swollen breasts.

Currently Nottingham Prognostic Index (NPI) is the most common prognostic method for cases diagnosed with breast cancer. This test incorporates additional factors such as hormonal receptor status and age to predict the best possible treatments for patients with breast cancer in the UK

Besides the life style, the cause of breast cancer is mostly related to the differences in hormonal exposure during life time. These include early menarche, late menopause, nulliparity, late pregnancy and hormone replacement therapy. Other risk factors are associated whether a member of a family has been diagnosed in the past. BRCA1 and BRCA2 are two genes that code for tumour suppressor proteins. BRCA1 and BRCA2 mutations account for about 20 to 25 percent of hereditary breast cancers, and it is estimated that 5-10% of all breast cancers cases are caused by inherited genetic alterations (Easton, 1999; Fackenthal & Olopade, 2007).

Breast cancer is a heterogeneous disease, and over the years, gene expression profiling has improved our understanding of the molecular mechanism associated with this particular disease (Curtis et al, 2012; Miller, 2007; Weigelt & Reis-Filho, 2009). Sotiriou & Pusztai measured mRNA using DNA microarray, to find molecular signals that could influence the progression of the breast cancer and their potential in clinical care (Sotiriou & Pusztai, 2009). They concluded that the profiling results showed that estrogen-receptor (ER)–negative and ER-positive breast cancers can originate from distinct cell types and can play a role in metastatic progression (Sotiriou & Pusztai, 2009). Perhaps these tests improve on clinical and diagnostic results that would benefit the patient outcome.

Diagnosis first occurs by the patient self-examination or if there are abnormal areas that have been detected during a medical check-up. After screening using a mammogram the next step is to take a biopsy of the tissue. From there on the histopathological analysis of the tissues sample will then indicate whether the tumour is benign or malignant. If the tumour is malignant further analysis is needed to confirm whether it is a non-invasive or invasive form of breast cancer. In invasive breast cancers, the tumour cells have spread to the surrounding stroma area by passing through the basement membrane (Vajpeyi, 2005). In the case of non-invasive tumour type the most common cancer type is ductal carcinoma in situ (Burstein et al, 2004). The most common type of tumour in invasive breast cancer is invasive ductal carcinoma counting for 50-80% of cases (Weigelt et al, 2005; Weigelt & Reis-Filho, 2009). The Nottingham Grading System assesses the histological grade of the tumour, which then can give the best possible treatment for that patient. It is based on the evaluation of the

tumour characteristics (tubule or gland formation, nuclear pleomorphism, and mitotic count). With this grading system the tumour samples are place into three categories; either Grade 1 (differentiated), Grade 2 (moderately differentiated), or Grade 3 (poorly differentiated) (Elston & Ellis, 2002). As well as the histological type and grade, the sample is also analysed for at least three different biomarkers through immunohistochemistry; estrogen receptor alpha (ERα), progesterone receptor (PR), and human epidermal growth factor receptor 2 (HER2). ≥ 1% tumour nuclei stained is the cut-off point to determine whether the patient is ERα and PR positive or not (Hammond et al, 2010). HER2 status is given when positive staining result in > 30% of the tumour cells. HER2-negative status is given when the staining is less than 10% of the tumour cells. If the staining is between 10% and 30%, fluorescence in situ hybridization (FISH) is used, were the average HER2 gene copy number that is above 4, will be grouped into the HER2-prositive group (Wolff et al, 2014). After surgical removal of the tumour mass, the histologic grade and ERα, PR, and HER2 status is assessed again to confirm complete removal. The TNM classification system, determines the pathological stage of the tumour. It combines information about the tumours size (T), lymph node status (N), and distant metastasis (M). Stage I and II are considered as early stage breast cancer, stage III as locally advanced breast cancer, and Stage IV as metastatic breast cancer (Uehiro et al, 2014).

The appropriate treatment for the patient with invasive breast cancer depends on the stage and grade of the tumour. At the early stages of the disease, surgery followed by radiotherapy is the likely course that patient will take. If the disease is in the advance stages, then the tumour will be characterised based on its clinicopathological features. In one subgroup the tumour will be tested whether the cells have lack of ERα, PR, and HER2 receptors. This is known as triple-negative breast cancer, accounting for 15% of all breast cancer cases (Bauer et al, 2007; Dent et al, 2007; Rakha & Ellis, 2009). Patients that are diagnosed with triple-negative breast cancer are treated with adjuvant chemotherapy to reduce any relapse and mortality (Joensuu & Gligorov, 2012; Metzger-Filho et al, 2012). In this case the patients will be given a range of drugs, in combination or in sequences. These include epirubicin (anthracyclines), paclitaxel (taxanes), cyclophosphamide (alkylating agents), and or 5-fluorouracil (antimetabolite). These anticancer agents target high proliferating cells by inhibiting cell proliferation and DNA replication, resulting in the cells to become apoptotic and die. However these agents target cancer cells, but also normal cells, which can cause severe side effects. Cells from bone marrow can be effected and cause immunosuppression. Severe side

effects can also affect the hair follicles which can result in hair loss and cells that are affected in the digestive tracts can result in mucositis. Other side effects include fatigue, nausea, and vomiting (Bilici et al, 2012; Joensuu & Gligorov, 2012; Metzger-Filho et al, 2012).

The overexpression of anti-metabolites HER2 receptor can also be characterised into a subgroup. The overexpression of the HER2 receptor accounts for 20 - 30% of all breast cancer tumours and has the second poorest prognosis in breast cancer (Heil et al, 2012; Press et al, 1997; Vu & Claret, 2012). However patients with HER2 receptor positive can be treated with trastuzumab, a monoclonal antibody that directly targets HER2, with a combination of adjuvant chemotherapy agents (Arrondeau et al, 2012; Slamon et al, 2001). In year 2000 it was approved in the European Union, and since 2006, trastuzumab has been used and approved to treat HER2-positive non-metastatic breast cancer and other types of cancers (Arrondeau et al, 2012; Slamon et al, 2001). There have been several actions that have been reported regarding trastuzumab. Trastuzumab have been reported to trigger the internalisation and degradation of HER2 through activating tyrosine kinase – ubiquitin ligase c-Cbl, thus activating the proteolytic pathway (Klapper et al, 2000). The antibody can also attract immune cells. Once bound to cancer cells expressing HER2 triggering and antibody-dependent cellular cytotoxicity (Clynes et al, 2000). In 2007, in combination with capecitabine (anti-metabolites), Lapatinib was approved by the FDA as a HER2-positive breast cancer target. Lapatinib is a dual specific tyrosine kinase inhibitor directed against HER2 and the epidermal growth factor receptor (EGFR) (Cetin et al, 2014; Geyer et al, 2006; Xia et al, 2002). In 2012, Pertuzumab a monoclonal antibody directed against HER was approved by the FDA. This antibody binds to a different binding site to that of trastuzumab. Pertuzumab inhibits dimerization of HER1, HER2 and HER3; which is essential for the activation, leading to cancer cells to proliferation and resistance to therapy (Adams et al, 2006). Currently Pertuzumab is used in combination with trastuzumab and docetaxel (Baselga et al, 2012).

The last subgroup is characterised by the expression of ERα and PR. This group accounts for 70 - 80% of all breast cancer cases. In this case it has a more favourable prognosis and is characterised by proportion of postmenopausal women (Anders et al, 2008; Heil et al, 2012). Further classification of the subgroup is required for the best possible treatment. Histologic grading or abundance of a cell proliferation marker (Ki-67), together with assessment tumour size, and lymph node status is required to test whether the patient has low or high risk form of the disease (Coates et al, 2012; Goldhirsch et al, 2013). Patients that are undergoing

chemotherapy can also benefit from adjuvant endocrine therapy (Early Breast Cancer Trialists' Collaborative et al, 2011). Tamoxifen is a endocrine therapy drug given to premenopausal women (Hubalek et al, 2010; Jankowitz et al, 2013). Tamoxifen is a luteinizing hormone-releasing hormone (LHRH) agonist blocking estrogen receptor (Hubalek et al, 2010; Jankowitz et al, 2013). Anastrozole is another endocrine therapy drug that blocks the production of estrogens by inhibiting the activity of the enzyme aromatase, which has the function to convert androgens to estrogens (Baum et al, 2003; Dowsett et al, 1995; Kaufman et al, 2009). Patients with locally advanced or primary inoperable breast cancer can also be treated neoadjuvant therapy. This is to shrink the size of the tumour to enable it to be surgically removed. Women whose tumour can be removed by mastectomy, may instead undergo neoadjuvant therapy enhance the chance for breast conserving surgery (Fisher et al, 1998; Mauri et al, 2005). This treatment is given before primary therapy (Kaufmann et al, 2006; van der Hage et al, 2001).

There have been good progress over the years, for the treatment of breast cancer, however there still numbers of cases were the patient relapses or the diseases have become far more aggressive. Therefore, new therapy options with special focus on targeted therapeutics need to be continuously evaluated in clinical trials. However, together with development of new drugs and combinatorial strategies, the development of new biomarkers is needed to provide the best possible treatment for the patients.

1.3. Cancer Diagnosis

Detecting and treating cancer by targeted means at the earliest possible stage of cancer will improve the quality of life and the life expectancy of patients. Currently invasive detection methods are used for diagnosis of cancer at the early stages. The histological examination can quantify metastases by counting tumour cell colonies but lack the sensitivity to differentiate between normal cells and cancer cells (Morikawa et al, 1988). Genetic screening techniques are more sensitive than the histological sectioning for cancer diagnosis but they are costly and time consuming(Tschentscher et al, 1997).

Non-invasive detection of cancer generally involves the use of X-ray, Ultrasound, Magnetic resonance imaging (MRI), Positron emission tomography (PET) and Computed tomography (CT) (Warner et al, 2004). MRI and CT scans are more sensitive as they are independent of tissue depth and do not require a radio isotope (Warner et al, 2004). Additionally, MRI can distinguish between pathologic tissue and normal tissue. But one limiting factor of this scan

is the cost of the machine and its running (Fletcher et al, 1999; Robson & Offit, 2004). MRI is widely used in the medical field; from imaging the brain to detecting where tumours are growing in the body (Harisinghani et al, 2003).

Contrast agents such as gadolinium chelates can also be introduced into patients to enhance the detection of tumours (Hagspiel et al, 1995; Limanond et al, 2004). This technique is highly sensitive and delivers good contrast images that can easily identify different soft tissues of the body. To achieve the best image, the signal to noise ratio must be optimised. There are a number of ways to increase the resolution (Harisinghani et al, 2003):

1. Extend the scanning time

2. Increase field strength

3. Increase the concentration of contrast agents

4. Increase the retention of particles

Recently iron oxide based nanoparticles such as Superparamagnetic iron oxide (SPION) have been developed for tumour detection, which have several advantages over gadolinium chelates. SPION has low toxicity compared to gadolinium chelates and detection limit is far greater (Savranoglu et al, 2006). However, both contrast agents are non-specific and have limited use as diagnostic tools for targeting tumour cells. Several types of iron oxide nanoparticles have been investigated as contrast agents, which include Fe_3O_4 magnetite, $Fe^{2+}/Fe^{3+}{}_2O_4$ ferrimagnetic, α-Fe_2O_3 hematite, γ-Fe_2O_3 maghemite, ε-Fe_2O_3 and β-Fe_2O_3. Both magnetite and maghemite, with their superior magnetic properties, are useful not only as contrast agents but also nontoxic to cells (Stephen et al, 2011; Sun et al, 2007; Wu et al, 2008). But once they are administered, the nanoparticles have been shown to be confined only to liver, spleen and bone marrow instead of targeting tumours (Parhi et al, 2012; Ruggiero et al, 2010). Sensitivity can be dramatically increased by using contrast agents that target cells and remain in the tissue during the imaging procedure (Savranoglu et al, 2006).

The cellular uptake of a nanoparticle based contrast agents can have advantages for MRI screening if the contrast agent is specifically up-taken by cancer cells only. This would increase retention, improve resolution and specificity of the image (Kobayashi & Brechbiel, 2003). Specific cellular uptake nanoparticle based contrasts agent could be increased by coupling them with the ligand of a cell surface receptor that is highly or only expressed in

cancer cells. This will facilitate endocytosis of the nanoparticles bound to the receptor on the cell surface.

1.4. Cancer Treatments

1.4.1. Radiotherapy

Patients whose cancer can be cured are given radical radiotherapy as a potential treatment. For treating prostate cancer high energy x-rays are used to kill the cancer cells. Currently there are two methods: external beam radiotherapy, which is preformed once a day for five days for 4-8 weeks. This treatment is the most common form of radiotherapy. It uses a high dose of radiation on the prostate gland only, without affecting the surrounding tissue. Or internal radiotherapy (brachytherapy); this treatment radiates the prostate gland, were a fine needle is inserted into the rectum. In this case the patient will only get one or two treatments. The side effects associated with this treatment include inflammation of the urethra and bladder, and damage to the bowels which could lead to diarrhoea. Long term side effects are erection problems, problems passing urine and frequent or loose bowel movements (Bolla et al, 1997; Kirkpatrick, 1998; Pilepich et al, 2005; Wachter et al, 2002).

For breast cancer, radiotherapy is given after surgery to reduce the risk of the cancer returning (Clarke et al, 2005; Overgaard et al, 1999). The main aim for external beam radiotherapy (EBRT) is to remove any cells that remain in the breast and surrounding area after surgery. In this case treatments are once a day for 3 weeks. The side effects are reddening and soreness of the skin, swelling and small red marks on the skin (Clarke et al, 2005)

1.4.2. Chemotherapy

Chemotherapeutic drugs are currently used to treat cancer. These have limitations such as side effects and do not target specific areas (Pantel and Otte 2001). Additionally since they interfere with cell division and proliferation of fast growing cells; they have little to no effect on slow growing tumours or dormant cancer cells (Pantel and Otte 2001). The majority of chemotherapeutic drugs can be divided in to alkylating agents, antimetabolites, anthracyclines, and other anti-tumour agents; all of which prevent cells from proliferating (cancer.org, 2011). In order to have an effect on tumours, dosage has to be within a manageable limit (cancer.org 2011). If the dosage is too low, it would be ineffective against the tumour. If the dosage is too high it can cause severe side effects and damage peripheral

tissue. One of the side effects is the destruction of bone marrow cells, which leads to a reduction in erythrocytes, leukocytes, and platelets causing hematotoxicity, hepatotoxicity and cardiotoxicity (UK, 2009). Since the production of erythrocytes and leukocytes is impaired, patients become anaemic and more prone to infections. Other side effects of chemotherapy include nausea, alopecia and fatigue (UK, 2009). While some of these drugs are clinically useful, the duration of clinical response for many of these drugs is rather short lasting and resistant tumour cells often emerge (UK, 2009).

1.4.3. Targeted Cancer Therapy

Targeted cancer therapies have made huge progress over the years, especially with the discovery of cell surface receptors that are overexpressed or only expressed in cancer cells. Furthermore, the development of monoclonal antibodies (mAbs) against these receptors has increased the importance of targeted therapy for cancer. In fact several mAbs are now approved for clinical use and are very effective against number of cancers. These include Erbitux® (cetuximab); a drug that inhibits metastatic colorectal cancer by binding to epidermal growth factor receptor (EGFR) (Mendelsohn & Baselga, 2003). Herceptin® (trastuzumab), a mAb used against metastatic breast cancers overexpressing HER2 (Slamon et al, 2001).

However, the targeting cell surface receptors with mAbs can be problematic in some cancers due to the size the antibodies, a 150kDa mAb penetration of the entire tumour mass can be difficult. Additionally the Fc region of the antibody binds to the reticuloendothelial system, resulting in high non-specific uptake of cytotoxic drugs or toxins into bone marrow, liver, and spleen, leading to severe toxicities (Hudson & Souriau, 2003; Todorovska et al, 2001). Due to their selective uptake by some tissues such as bone marrow and liver, mAbs are better in treating cancer that originates from these tissues.

Peptide based therapies are an alternative, if not more effective, to mAbs in treating cancer. These molecules are able to penetrate the entire tumour due to their size (3-5kDa), they are chemically stable, easy to synthesize, and can be conjugated to a cytotoxic drug or a toxin. In some cases, replacing natural L-form amino acids with D-form amino acids can increase not only the peptide stability but also its binding affinity (Schally & Nagy, 1999; Sethi et al, 2014; Yang et al, 2012; Zelezetsky et al, 2005). Papo et al showed that alteration of the composition of a peptide drug increases the stability by preventing enzymatic degradation (Papo et al, 2003).

Tumour tissue morphology is different to that of normal tissues. The requirement for nutrients and oxygen is greater in malignant tissues, which therefore require the development of new blood vessels (neovascularisation) or rerouting of existing blood vessels near the tumour mass for constant supply of nutrients and oxygen (Maeda et al, 2000). This causes an imbalance, resulting in tumour blood vessels being highly disorganised and dilated with numerous pores showing enlarged gap junctions between endothelial cells and compromised lymphatic drainage (Bignold et al, 2006). These features allow drugs to diffuse and concentrate in the tumour interstitium. Fast proliferating tumour cells causes capillary vasculature to become blocked, leading to hypoxia and eventually necrosis of the tumour tissue. The basement membrane of the tumour vasculature is often aberrant. This leads to leakiness and increased permeability to counterbalance the high oxygen and nutrient requirements for the fast proliferating tumors (Olesen, 1986; Padera et al, 2004; Weindel et al, 1994). However the interstitium of tumours are denser than that of normal tissues, thus reducing the diffusion of compounds into the interstitium. This phenomenon is called the enhanced permeability and retention effect (EPR) (Maeda et al, 2000). With the absence of a lymphatic network and high interstitial pressure, the transport of any cancer drug will be governed by the physiological and physicochemical properties of the interstitium and by the physicochemical properties of the molecule itself (Brigger et al, 2002; Kuszyk et al, 2001).

The goal of cancer therapy is to remove malignant cells, whether they are singly spread in the periphery or have developed as a tumour. The idea of conjugating drug molecules with ligands (of cell surface receptors that are highly or only expressed in tumour cells) allows targeting specifically to the tumour cells. This approach can avoid any side effects to vital organs; only destroying areas where tumour cells accumulate (Minko et al, 2004). The increase in specific binding of the drug to the tumour cells can not only reduce the dose but also increases the efficacy. With high efficiency and recycling of receptors to the surface of the tumour cells, cellular uptake through the receptor can be highly specific in destroying cancer cells (Dharap et al, 2003). Targeted chemotherapy, which can traffic to tumour cells, is a new and modern strategy, designed to improve the effectiveness of cytotoxic drugs whilst decreasing toxicity. The effectiveness of any anticancer drug can be limited by multidrug resistance (MDR) of tumour cells. For example, ovarian cancer may become resistant to treatments due to MDR (Friedlander et al, 2013). However, a number of studies have indicated that targeted chemotherapy with cytotoxic peptide analogs can overcome any chemo resistance caused by MDR (Keller et al, 2006; Keller et al, 2005).

One of the methods for identifying cancer targets and thereby anticancer agents that have gathered a lot of interest is the combinatorial library method. This allows the identification of ligands that are associated with cancer associated cell receptors. Currently there are six combinatorial library methods that have been used so far (Aina et al, 2007). Of the six, there are two methods that have been widely used in identifying targets for cancer associated receptors and they are phage-display library and the One-Bead-One-Compound (OBOC) library methods. These methods use live cells or proteins that are related to cancer as screen probes. OBOC library method is a screening method that is chemistry based to identify peptide ligand discovery, to identify novel ligands for molecular imaging, protein inhibition and direct therapy for cancer (Cha et al, 2012; Cho et al, 2013). This method uses 90μm-sized beads, each containing a novel ligand and is screened in parallel against cell surface targets. This can be used to identify peptide ligands that are resistant to proteolytic degradation. This can identify any peptides that can be used for in vivo applications (Cha et al, 2012; Cho et al, 2013).

One other example is screening using Phage Display Peptide Library (Ph.D.). This method was used to identify a peptide target for human bladder cancer cells (HT-1376) (Lee et al, 2007). This screen identified a peptide (CSNRDARRC) that showed the ability to bind to human bladder cancer cells but not to normal mouse bladder cells. The specific peptide was then validated by testing its binding to urothelial tumours. Peptide based targeting of receptors is certainly an approach that can increase the specificity of targeting tumours. Recently, a number of synthetic peptides conjugated with cytotoxic agents to target cancer cells have shown potential as specific chemotherapeutic drugs (Gaspar et al, 2013)

1.5. Passive targeting

Nanoparticles that are within 10-100nm and uncharged can have the ability to passively target tumours tissues. They would have the ability to avoid the reticuloendothelial system (RES) and kidney clearance; remain in the bloodstream, and thus have a greater chance of reaching tumours tissues. Hydrophobic coating allows the nanoparticles to be delivered to the liver through the RES. Any hydrophobic particles, as compared to hydrophilic, have an enhanced absorbability of blood serum (Brannon-Peppas & Blanchette, 2004b; Wang et al, 2001). Blood flow in a tumour can also be a challenge as the tumour is heterogeneous (Brannon-Peppas & Blanchette, 2004a). However the leakiness of the tumour vasculature system, and its lack of lymphatic drainage, allows for enhanced permeation and retention

effect (EPR) (Brannon-Peppas & Blanchette, 2004a; Robinson, 2000). The main advantage of the EPR effect is that it provides accumulation of the drug inside the tumour and protects the healthy tissues from the toxic effects of the drugs (Moghimi et al, 2001). The major disadvantage associated with the EPR effect is that it can work only on solid tumours and not on spreading tumours or metastatic tumours (Robinson 2000).

With passive targeting, the drug delivery system must be transported through the blood system and through the vascular wall into the surrounding tissues and finally through the tumour interstitial space. This multiplex process can only occur by the function and morphological characteristics of both the drug and the tumour (Shenoy et al, 2005). One example of nanoparticle delivery through the RES is Endorem. It is a contrast agent consisting of dextran-coated iron oxide particles with a size of 62-150 nm in diameter. Following intravenous injection, it is trafficked to the liver and spleen *via* the RES and therefore can be used as a diagnostic tool for liver cirrhosis (Hundt et al, 2000; Robinson, 2000).

1.6. Active Targeting

Recently more attention has been focused on the identification of specific antigens and receptors that are only expressed in cancer cells. Therefore the targeting molecule must be expressed homogeneously in all tumour cells, including metastatic cells, but not expressed in healthy normal cells.

For active targeting, the cancer drug must have several characteristics to be effective. They are:

(1) The drug must only target cancer cells

(2) It must be efficient in both uptake through the receptor-mediated endocytosis and delivery to tumour cells

(3) The drug must be stable throughout the whole process and not be degraded

(4) The drug should not be recognised by macrophages.

Interestingly, several cell surface receptors (such as EGF, transferrin, IL-13, GnRH and LH/CG receptors) are over-expressed in tumour cells compared to normal cells (Leuschner et al, 2003a; Yoon et al, 2011) In addition, some intracellular proteins (heat shock protein 70 [HSP70], HSP90, glucose related protein 78 [GRP78], actin, cytokeratin, vimentin etc.)

display on surface of cancer cells can also be used as molecular targets (Weidle et al, 2011). Studies have shown that these receptors can be exploited to target tumour by drug-ligand complexes or ligand-nanoparticles complexes. One such example is interleukin-13 fused to *Pseudomonas aeruginosa* exotoxin (IL-13-PE38), which has high affinity for IL-13 receptor α2 (IL-13Rα2), show specific binding to the cancer cells that express high levels of IL-13Rα2 at the cell surface (Kioi et al, 2004). However in phase III trials, IL-13-PE38 was found to target IL-13Rα1 and IL-4R prompting to develop a new generation of peptides that specifically target IL-13Rα2 (Joshi et al, 2002; Kunwar et al, 2007).

Over the years, βCG and GnRH/LHRH conjugated drugs have gathered a lot of interest in targeted chemotherapy. This is because elevated levels of these ligand receptors (LHCGR and GnRHR/LHRHR) have been found on the surface of prostate, breast and ovarian cancer cells (Ji et al, 2002; Lojun et al, 1997; Tao et al, 1997b). Failure to treat cancer patients often arises from intrinsic or acquired drug resistance of the tumours to the anticancer drugs. The resistance occurs over a range of drugs with different structures and also different targets. This phenomenon limits the effectiveness of chemotherapy in a variety of common malignancies and is called MDR (Ozben, 2006). With the need of more specific drugs to treat cancer, βCG and GnRH/LHRH can prove to be very effective carrier molecules to not only reduce side effects but also overcome drug resistance of tumours. A recent study showed that βCG-doxorubicin conjugate can specifically target ovarian cancer cell lines with increasing cytotoxicity compared to doxorubicin alone (Gebauer et al, 2004b).

AEZS-108 (AN-152) is a drug that consists of a conjugation of [D-Lys^6]LHRH and doxorubicin. Recently AEZS-108 has been approved for Special Protocol Assessment (SPA) for an upcoming Phase III registration trial in endometrial cancer by the U.S. Food and Drug Administration (FDA) (Medical, 2012). In 2010, a phase I trial was designed to determine the maximum tolerated dose of AEZS-108. The selected dose was 267 mg/m^2 at 3 week intervals, which was then carried to phase II drug trials (Emons et al, 2010). In Phase II trials overall repose rate was 30.8 % and a clinical benefit rate was estimated at 74.4 % (Engel et al, 2012b). Compared to doxorubicin alone, overall response rate is higher with a 9 % difference and the overall survival after administration of single agent AEZS-108 is similar to that reported for modern triple combination chemotherapy (Temkin & Fleming, 2009). Phase II trials indicated that AEZS-108 exhibits antitumor properties with low or without any toxic side effects (Engel et al, 2012b) (figure 1.6). This study highlights the potential of targeting

receptors that are overexpressed in tumour cells and how targeting specific receptors can lower toxicity.

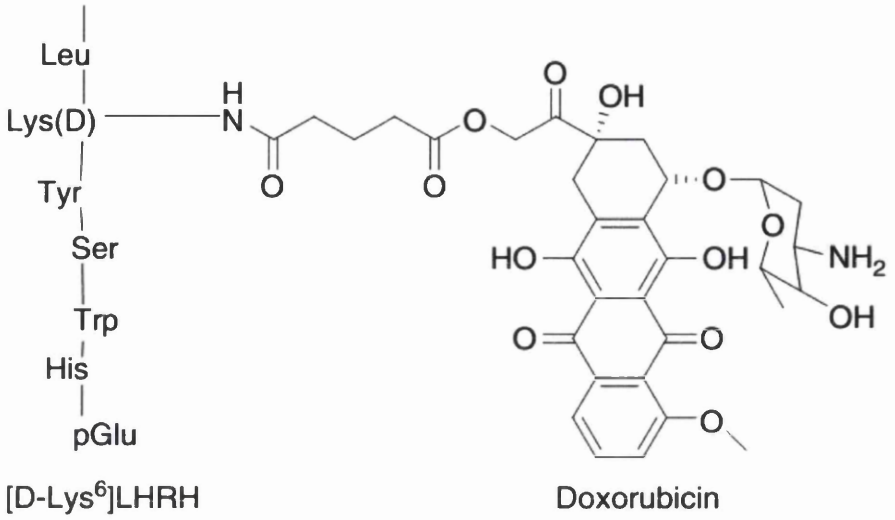

Figure 1.6. Structure of LHRH analog AEZS-108. Doxorubicin conjugated to [D-Lys^6]LHRH.

Since I have concentrated my efforts in studying the targeting of LHCGR, GnRHR and IL-13Rα2 in breast and prostate cancers, I have reviewed these receptors below.

1.7. Receptors

1.7.1. LHCGR

Luteinizing hormone (LH), follicle-stimulating hormone (FSH) and human chorionic gonadotropin (hCG) are glycoprotein hormones, known as gonadotropins. LH and FSH are secreted from the pituitary gland, regulating reproductive processes and function in vertebrates (Bowen, 2004). This is controlled by the secretion of GnRH from the hypothalamus. The hormone CG is produced during pregnancy, where it is secreted from the placenta. Both LH and CG share the similar homology sequence, enabling the two peptides to bind LHCGR with high affinity.

Gonadotropin plays a crucial role in the regulation and the development of reproductive organs. They are regulated by a system called the hypothalamic pituitary gonadal (HPG) axis (figure 1.7.1). This maintains a homeostasis of hormones by positive and negative feedback from the receptors such as GnRHR, LHCGR and FSHR (Emanuele et al, 2002).

Once GnRH is released from the hypothalamus, it binds to GnRHR on the pituitary gland and causes LH and FH release into the peripheral circulation. These gonadotropins target their receptors, which are expressed on the gonads, and regulate the functions of the ovary and testes as well as the release of sex steroid hormones e.g. testosterone, estrogen and progesterone (Gilbert, 2010).

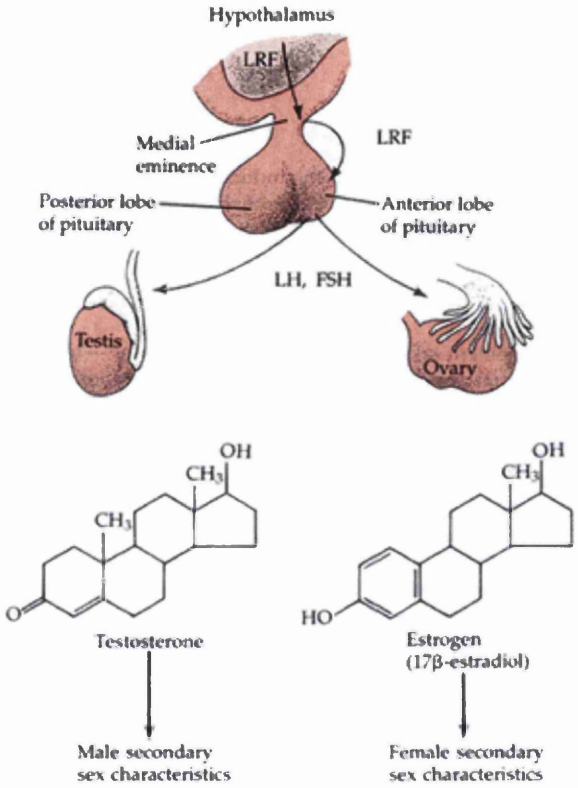

Figure 1.7.1. Hypothalamus-pituitary-gonadal axis in mammalian sexual development. The binding of GnRH to GnRHR, cause the release of LH and FH from the pituitary gland. LH and FH binds to their receptors on the testis and ovary and cause the release of sex steroid hormones testosterone, estrogen and progesterone (Gilbert, 2010).

Both LH and CG are heterodimeric proteins. Both have the common α-subunit and the hormone specific ß-subunit. The α-subunit has 92-96 amino acids whereas the ß-subunit has 117 amino acids in LH and 145 amino acids in CG (Morgan et al, 1975; Ujihara et al, 1992). It has been shown that LH stimulation on a mutant LHCGR causes its normal cellular trafficking and normal desensitization but impaired cyclic adenosine monophosphate (cAMP) production. However hCG-stimulation of the mutant receptor caused a normal cAMP response, suggesting functional difference between the two hormones in binding to the receptor. LHCGR lacking exon 10 was found to induce less cAMP production when stimulated with LH (Muller et al, 2003). It has also been suggested that CG is more potent and have a higher binding affinity to the receptor compared to LH (Rahman & Rao, 2009).

CG hormone is secreted from the placenta during pregnancy. In early pregnancy, cytotrophoblastic cells proliferate and invade the maternal endometrium to form the anchoring villi; at this point they secrete CG α subunit. These cells differentiate into syncytiotrophoblasts, which secrete both CG α and β subunits (Cole, 2009).

Human LH and CG half-life are different. LH has a half-life ranging from 1-2 hours, were as hCG has a half-life ranging from 28-31 hours. The reason for the difference in half-life is that CG is heavily glycosylated and has a long C-terminal (Casarini et al, 2012; Choi & Smitz, 2014; Cole, 2010; Trinchard-Lugan et al, 2002).

The mutations in LHCGR can cause human diseases such as pseudohermaphroditism in males and primary amenorrhea in females (Shenker, 2002). Some mutations in LHCGR can make the receptor become constitutively active and thereby cause accumulation of cAMP in unstimulated cells. Accumulation of intracellular cAMP via a mutant LHCGR has been shown to result in tumour formation as well as Leydig cell hyperfunction and hyperplasia (Shenker 2002).

Expression of LHCGR has been reported mainly in gonadal cells such as the testicular Leydig cells and the ovarian theca, granulose and luteal cells (Ascoli et al, 2002; Pakarainen et al, 2007). However there is evidence to suggest its expression in non-gonadal tissues such as human blood vessel, uterus and placenta (Singh et al, 1995; Zhang et al, 2001). Interestingly LHCGR is over expressed in tumours of breast, endometrial, ovary and prostate (Gebauer et al, 2003; Lenhard et al, 2012b; Noci et al, 2008; Tao et al, 1997b).

LHCGR belongs to the glycoprotein hormone receptor subfamily of G protein-coupled receptors (GPCRs) superfamily (Ziecik et al, 2007). GPCRs contain seven transmembrane domains and hence they are also known as 7-TM or heptahelical receptors (Kroeze et al, 2003). The seven TM domains have three extracellular regions and three intracellular loops (Arora et al, 1995). This particular receptor is encoded by a single gene located on chromosome 2 (2P21) (Simoni et al, 1997). Like other GPCRs, LHCGR interacts with heterotrimeric G proteins, which consist of three subunits (α, β and γ). The G proteins activation through ligand binding to the receptor leads to production of both cAMP and Inositol 1,4,5-trisphosphate(IP3) secondary messengers (Ascoli et al, 2002). Therefore LHCGR is able to independently activate two G protein dependent signalling pathways, the cAMP/protein kinase A (PKA) pathway and the diacylglycerol (DAG)/protein kinase C (PKC) pathway (Ascoli et al, 2002). The activated LHCGR, by binding of its ligand to the receptor, couples with the heterotrimeric G protein containing G_Q type of $G\alpha$ subunit (Dufau, 1998). This results in dissociation of the heterotrimer G-protein to α and $\beta\Upsilon$ subunits, activation of phospholipase C (PLC), and hydrolysis of phosphatidylinositol bisphosphate (PIP2) to IP3 and DAG (Ascoli et al, 2002; Dufau, 1998). IP3 is then released into the cytoplasm causing the release of sequestered calcium from the endoplasmic reticulum. DAG remains at the membrane and activates PKC (Ascoli et al, 2002; Dufau, 1998). The activated LHCGR also couples with the $G\alpha_s$ subunit containing heterotrimeric G protein, which results in activation of adenyl cyclase (AC) and thereby cAMP production and PKA activation.

In ovarian cancer cells, LHCGR activates PI 3-kinse (PI3K) and PKA, which up regulate the expression of matrix metalloproteinase (MMP)-2 and -9. Once LHCGR is stimulated, expression of both CD44, IL-6, EGFR and erythroblastic leukaemia viral oncogene homologue 2, neuro/glioblastoma derived oncogene homologue (avian) (ERBB2) are increased. The increased expression of c-MYC, and prohibitin is also observed in LHCGR stimulated cells (Figure 1.7.2) (Mertens-Walker et al, 2012).

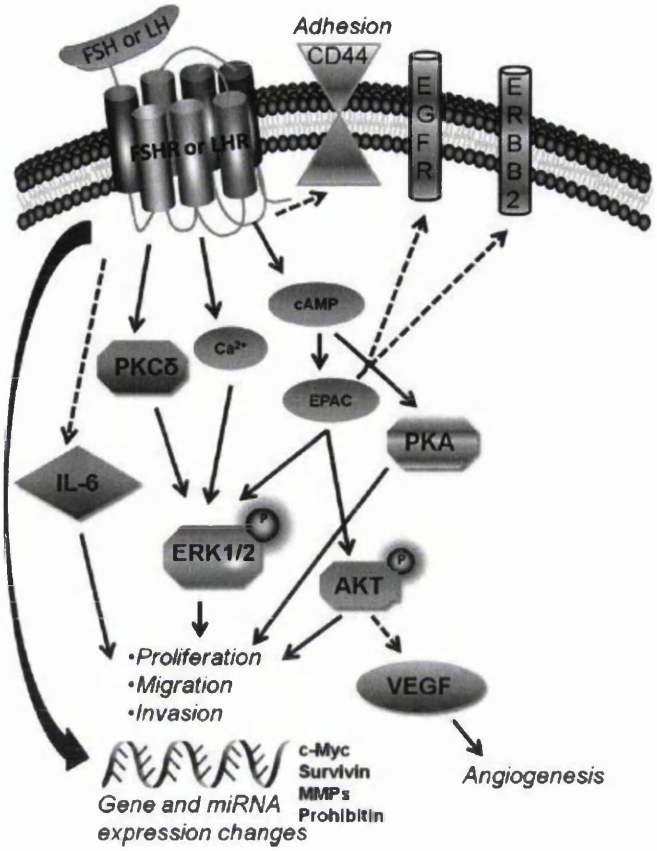

Figure 1.7.2. Gonadotropin-induced pathways in immortalised ovarian normal and cancer epithelial cells. Broken line arrows indicate up-regulation by FSH and/or LH; solid arrows indicate activation of signalling pathways with subsequent biological consequences (Mertens-Walker et al, 2012).

Once GPCR's are activated by an agonist, it usually results in a decrease in the receptors' response. This desensitization allows the termination of the signal pathway. However, over desensitization would cause the receptor to lose its responsiveness to its stimuli (Ferguson, 2001). Upon desensitization, LHCGR forms self-associated aggregates on the surface of the cells, with the long term effect being down-regulation of the LHCGR mRNA. However, evidence has shown that LH ligand causes the down-regulation of the receptor in gonads (Pakarinen et al, 1990) and the up-regulation in adrenal glands (Beuschlein et al, 2003; Kero et al, 2000; Piltonen et al, 2002). One possibility for this variation is the increase in the expression of mevalonate kinase (Mvk). Wang and Menon have shown that the expression of Mvk and cholesterol biosynthesis enzymes is up-regulated when gonads stimulated with hCG. Their study also suggested that the up-regulation of Mvk led to the down-regulation of LHCGR by MvK binding to LHCGR mRNA (Wang & Menon, 2005).

1.7.2. GnRHR

GnRH also known as LHRH was first discovered by Schally and Guellerin, for which they received noble prize in medicine in 1977. GnRH regulates the release of FSH and LH from the pituitary gland, which in turn regulates gonadal functions (Bowen, 2004). The function of GnRH and its analogues are mediated by high affinity GPCR GnRHR/LHRHR, which expressed on the cell surface of the gonadotrophic cells (Ando et al, 2001). These cells are located in the pituitary gland and once stimulated they synthesise and release gonadotropins; LH and FSH into blood circulation, which regulate the reproductive processes in vertebrates (Schally et al, 2001).

Manipulation of the neuroendocrine cascade by GnRH inhibition leads to down regulation of the sex steroids levels and has been widely used in pharmacological castration, where androgen and estrogens ablation is required (Schally et al, 2001). The activation of GnRHR by agonists causes pituitary desensitisation due to sustained stimulation whereas the competitive GnRH antagonists (compete with native GnRH for the same receptor) cause an immediate cessation of the release of the sex steroids (Schally et al, 2001). GnRH analogues are routinely used in the clinic for the treatment of cancers of the reproductive organs namely breast and prostate carcinoma, central precocious puberty, *in vitro* fertilisation procedures and many benign gynaecological disorders (Schally et al, 2001).

Different isoforms of GnRH have been isolated, sharing at least 50% sequence identity, and they are widely expressed among vertebrates (Millar et al, 2004). GnRHR expression has

been shown in various cancers of reproductive tissues and their corresponding cell lines (Millar et al, 2004).

Like LHCGR, GnRHR belongs to the glycoprotein hormone receptor subfamily of GPCRs (Grundker & Emons, 2003). Studies have shown that most tumours over express GnRH receptors (Tammela, 2004). The typical characteristic of this type of receptors is their tendency to work via secondary messenger signalling pathways, including molecules such as DAG and calcium to exert activation or deactivation of signalling proteins downstream (Grundker & Emons, 2003). The general mechanism for these GPCRs involves the binding of the ligand to the extracellular domains, followed by a conformational change in the intracellular portions of the helices. This receptor activation then causes a propagation of the signal (Grundker & Emons, 2003) (figure 1.7.3.).

GnRHR detected in breast and ovarian cancers has shown to be identical to that located in the pituitary gland, showing the same nucleotide sequence (Millar et al, 2001). Interestingly, studies have shown that the receptor located in the pituitary gland functionally differ from that expressed in breast and ovarian cancers (Millar et al, 2001). Pituitary GnRHR has been shown to have high affinity binding sites for agonists whereas the receptor expressed in cancer cells were shown to have low affinity binding sites, with high receptor expression (Moretti et al, 2002; Szende et al, 1991).

Approximately 80 % of ovarian cancer tissues tested has been shown to express high levels of GnRHR (Nagy & Schally, 2005). The over-expression of GnRHR has also been observed in breast and prostate cancer cells (Nagy & Schally, 2005). In most cancer cells, cell proliferation and the metastatic properties of tumours are thought to be regulated by GnRHR (Aguilar-Rojas & Huerta-Reyes, 2009). Once stimulated, the receptor activate phosphotyrosine phosphatase (PTP), causing the down regulation of cell proliferation by inhibiting mitogenic signal transduction of growth factor receptors. However, the receptor over-expression in tumours is also associated with the phosphorylation of EGFR and thereby the down regulation of EGFR mRNA expression (Grundker et al, 2000). In human ovarian and endometrial cancer cells; GnRH stimulates the activation of the *c-jun* N-terminal kinase/activator protein-1 (AP-1) pathway. It was found that JNK is involved in inhibition of cell proliferation induced by α1B-adrenergic receptor in human embryonic kidney (HEK) 293 cells (Yamauchi et al, 2001). In a study in rats, *c-jun* mRNA levels decrease and endometrial epithelial cell proliferation were suggested to be linked cancers (Bigsby & Li, 1994). Due to

anti-proliferative activity of GnRH, super active agonists might become efficacious drugs for the treatment of GnRHR expressing cancers (Bigsby & Li, 1994).

In prostate and ovarian cancer cells, GnRH binding to GnRHR causes the dissociating of $G_{\alpha i}$ protein (Kraus et al, 2001). $G_{\alpha i}$ coupling is poorly understood and it is suggested that activation is involved in the anti-proliferative effects. The signalling cascade results in the activation of caspase and the trans-membrane transfer of phosphatidylserine (PS) to the outer membrane, as well as JNK and p38 (Kraus et al, 2001).

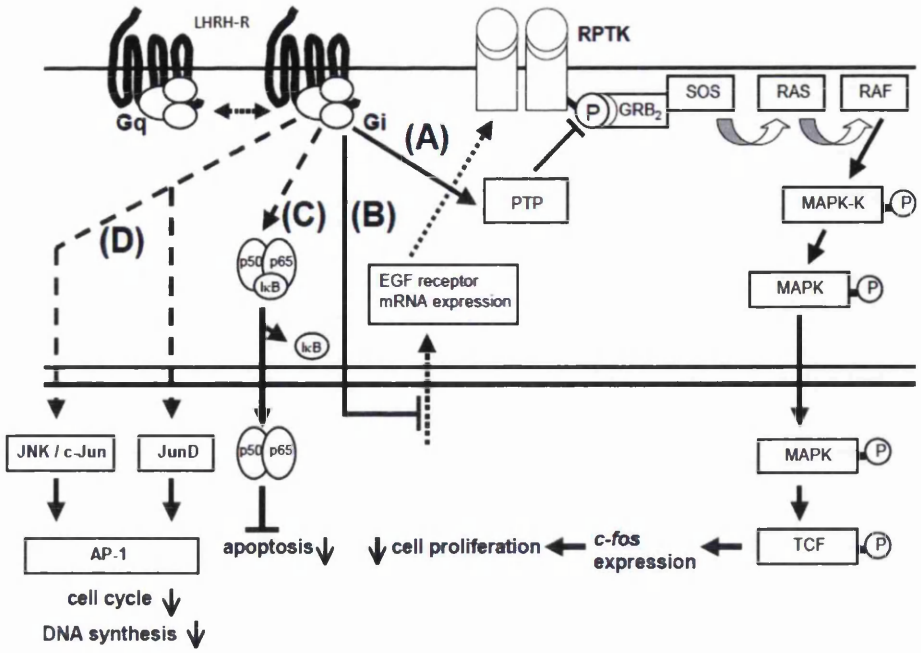

Figure 1.7.3. LHRHR/GnRHR signalling in human gynaecological cancer cells: A) GnRHR activates a phosphotyrosine phosphatase (PTP), which inhibits the mitogenic signal transduction of growth factor receptors resulting in down-regulation of cell proliferation B) GnRHR down-regulates EGFR mRNA expression. C) Activated GnRHR induces nucleus factor κB (NFκB) activation. The activated NFκB translocates to nucleus and induces expression of anti-apoptotic proteins at mRNA level. D) GnRHR activates c-Jun N-terminal kinase (JNK), induces JunD-DNA binding and stimulates activator protein (AP-1) activity, resulting in reduced proliferation as indicated by increased G0/1 phase of cell cycle and decreased DNA synthesis (Grundker & Emons, 2003)

1.7.3. IL-13Rα2

IL-13 is referred to as a pleiotropic cytokine that regulates immune response against infection as well as a mediator for inflammatory respiratory diseases (Minty et al, 1993). IL13 is a 14 kDa glycosylated protein, which consists of a four α-helical hydrophobic core, produced by Th2 helper cells. It is characterised as a type 2 cytokine, as it binds to two different types of receptors; Interleukin 4 receptor alpha (IL-4Rα)/Interleukin 13 receptor alpha 1 (IL-13Rα1) and Interleukin 13 receptor alpha 2 (IL-13Rα2) (Zurawski et al, 1993). IL-13 binds to IL-13Rα2 at a higher affinity than that of IL-4Rα /IL-13Rα1. IL-13Rα2 is classified as a monomeric receptor with a 17 amino acid cytoplasmic tail (Andrews et al, 2006; Hershey, 2003; Kawakami et al, 2001). IL-13 receptors have been found in many cell types ranging from basophils, eosinophils, mast cells and endothelial cells to fibroblasts, smooth muscle cells and respiratory epithelium (Hershey, 2003) (figure 1.7.4).

IL-13Rα2 has shown to be overexpressed in variety of malignancies; including brain tumours, renal cell carcinoma, squamous cell carcinoma of head and neck, ovarian cell carcinoma, pancreatic cancer, breast and prostate cancer (Fujisawa et al, 2009; Gonzalez-Moreno et al, 2005; Jarboe et al, 2007; Kawakami et al, 2003; Kioi et al, 2006a; Kioi et al, 2006b; Puri et al, 1996; Zhao et al, 2014). Therefore, IL-13Rα2 has gathered a lot of interest as a possible drug target for treating cancer.

Several previous studies found that IL-13Rα2 is overexpressed in ~75% of WHO grade IV glioblastoma multiforme (GBM) patients (Wykosky et al, 2008). IL-13Rα2 is a very interesting target for GBM; in fact a cytotoxic drug composed of IL-13 and a modified bacterial toxin (Pseudomonas exotoxin 38) (IL-13-PE38) has been developed, for GBM therapy (Kioi et al, 2004). However phase III clinical trials on IL-13-PE38 have shown that this drug can be non-specific since it can also target both IL-13Rα1 and IL-4R (Debinski et al, 1995; Kunwar et al, 2007). So new and more specific IL-13Rα2 cytotoxic drugs with mutated forms of IL-13 have been designed and are soon to enter in to clinical trials (Madhankumar et al, 2004; Pandya et al, 2012)

IL-13Rα2 is reported to be a decoy receptor since it is neither mediates IL-13 induced cellular responses nor activates any downstream signalling on its own (Rahaman et al, 2002). However, it has been demonstrated that IL-13 signals through IL-13Rα2 to induce tumour growth factor (TGF)-β1 production, leading to inflammation and fibrosis *in vivo* (Fichtner-Feigl et al, 2006). Further analysis in the same study revealed that IL-13 signals through IL-

13Rα2 to activate an AP-1 variant transcription factor, which then binds on TGF-β1 promoter to induce TGF-β1 production (Fichtner-Feigl et al, 2006).

Bernardi et al. have been able to use successfully IL-13 Rα2 antibody attached gold-coated silica nanoshells to target and kill high-grade glioma cells that over-express IL13Rα2. Their study also demonstrated the ability of targeted gold coated nanoshells killing of cancer cells through photothermal ablation. Since the gold nanoparticles were able to convert near-infrared laser light into heat, they concluded that an efficient way of treating brain cancer is with a localised near-infrared laser light (Bernardi et al, 2008). This idea opened an area of research that can improve the specificity of targeting and the effectiveness at a lower concentration, and allow retention of the nanoparticles in the cells.

One area of research interest is the conjugation of IL-13 with bacterial cytotoxin called *Pseudomonas* exotoxin. However there are several problems in using protein based toxins, one of which is activation of the immune response leading to the generation of antibodies, especially when the toxin is of non-human origin (Baker et al, 2010). Also due to their relatively large molecular size, the ligand or antibody-conjugated toxins are unable to penetrate the whole tumour. To over-come these difficulties, bacterial lytic peptides instead of cytotoxin agents have been used in cancer targeted therapy (Bogacki et al, 2008; McGregor, 2008). The lytic peptides immune response is generally low or no repose at all also due to their relatively small size (14-40 amino acids). Since the lytic peptides are relatively small, they are also able to penetrate further into tissues (Bogacki et al, 2008; McGregor, 2008). Therefore peptide based drugs would be able to overcome many of the limitations exhibited by protein based drugs (discussed lytic peptides further in section 1.9).

After different forms of mutated IL-13 created a peptide from a phage display library termed Pep-1 was found to have high affinity and specificity in binding to IL-13Rα2 (Pandya et al, 2012). Pep-1 has a peptide sequence of CGEMGWVRC and has been shown to bind at a site different to that of IL-13 on IL-13Rα2. As a result, Pep-1 binding to IL-13Rα2 is not inhibited by the cytokine. Similarly, Pep-1 neither binds to IL-13Rα1/IL4R complex nor it inhibits IL-13 binding to IL-13Rα1/IL4R. Therefore, unlike IL-13-PE38, Pep-1 conjugated drug is more specific in targeting IL-13Rα2 over-expressing tumors. Using infrared fluorescence imaging in nude mice, it has been found that Pep-1 is able to traffic and bind to subcutaneous and orthotopic human GBM xenografts expressing IL-13Rα2 once injected intravenously (Pandya et al, 2012). Pep-1 can be conjugated with the lytic peptide Phor21 (Pandya et al, 2012).

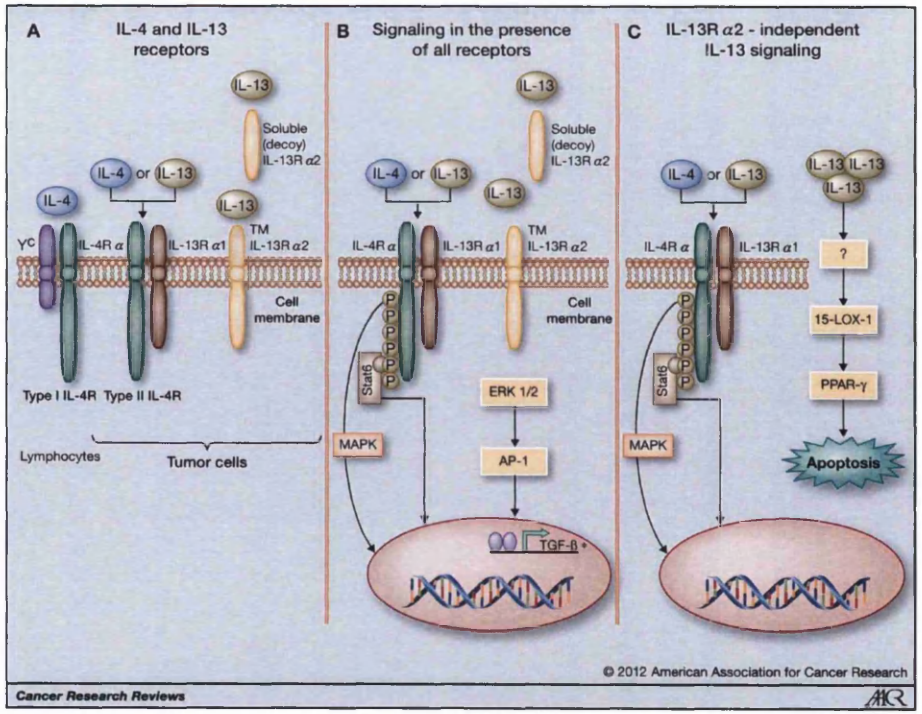

Figure 1.7.4. Schematic view of IL-13 signalling mediated by IL-13Rα1/IL-4R and IL-13Rα2. A) receptors for IL-4 and IL-13 are composed of 4 different subunits, IL-4Rα (green), γ-chain (γc; purple), IL-13Rα1 (red), and IL-13Rα2 (yellow). IL-4 and IL-13 both bind and signal through type II IL-4R. Type II IL-4R and IL-13Rα2 are present on tumour cells. B) in the presence of al signalling receptors, IL-4 and IL-13 can both bind type II IL-4R and phosphorylate Stat6, leading to increased proliferation and apoptotic resistance. JNK/MAPK and p38 pathways are also activated downstream of IL-4, and possibly IL-13 signalling, through type II IL-4R. IL-13 can also bind soluble or transmembrane IL-13Rα2, potentially leading to induction of TGF-β expression, downstream of ERK 1/2 and AP-1. *, note this pathway has thus far only been delineated in other cell types, but is speculated to occur in epithelial cancer cells. C) in the absence of IL-13Rα2, IL-13 may have enhanced signalling through type II IL-4R and/or signalling directly resulting in expression of 15-LOX-1 (Hallett et al, 2012).

1.8. Ligand-drug uptake by cells

The ligand-drug molecules are up-taken by cells through cell surface receptor mediated endocytosis. Receptor mediated endocytosis involves 4 stages (Koenig & Edwardson, 1997):

1. Formation of endosome through receptor endocytosis on the cell surface

2. The recycling of the endosome to the plasma membrane

3. Degradation of the receptor in lysosome,

4. Delivery of de novo synthesized receptors to the plasma membrane.

The classical pathway of receptor mediated endocytosis involves GPCR kinases (GRKs), β-arrestins, clathrin-coated pits and dynamin GTPase. However, GnRHR internalised through β-arrestin independent manner and recycles through the endosomal compartment (Koenig & Edwardson, 1997).

1.9. Lytic Peptides

Membrane disrupting peptides also known as lytic peptides play a key role as a defence mechanism against pathogens in organisms without immune systems, such as bacteria and invertebrates. Understanding the characteristics and biomedical importance of lytic peptides might prove to be advancement in developing new and resistance free therapies for diseases such as cancer.

Lytic peptides are generally short with 14-40 amino acids, containing cationic and hydrophobic residues, increasing their interaction with microbial membranes. In the membrane environment, they are able to form amphipathic secondary structures that can disrupt negatively charged membranes, promoting rapid cell death and reduce the risk of any resistance (Figure 1.9.1) (Zhong & Chau, 2008).

As lytic peptides do not rely on cellular uptake, they are able to overcome problems of multidrug resistance. However lytic peptides on their own have limited specificity in targeting cancer cells. There are studies being undertaken to synthesise lytic peptides fused with ligands that bind specifically to cancer cells (Johnstone et al, 2000). Combining peptides with chemotherapy will enhance treatment for various cancers by not only targeting rapidly dividing cells but also slow proliferating cancer cells and dormant tumour cells. Most lytic peptides are short, linear and cationic with multiple Arg and Lys residues. In non-polar

environment they form secondary structures such as α-helix and β-sheet and disrupt any cellular membrane that is negativity charged. They bind to the surface of the membrane through electrostatic interaction. Above a threshold concentration, the lytic peptides insert into and disturb the cell membrane and ultimately cause cell death due to membrane disintegration. As the potency does not rely on cellular internalisation, lytic peptides have a chance to circumvent the multidrug resistance (MDR), a predominant hindrance to current chemotherapy (Johnstone et al, 2000). More recently, compelling evidence has shown these peptides to be candidate as novel anticancer agents (Curtis et al, 2014).

Recent studies have shown that the lytic peptides have the ability of killing drug resistant tumour cells as quickly and efficiently as drug sensitive parental cells. When combined with other chemotherapeutics, efficiency increases against tumour cells that have developed drug resistance (Johnstone et al, 2000). With a growing demand for alternative antibiotic and anticancer therapeutics, lytic peptides have gathered a lot of interest in both academia and pharmaceutical companies.

There are many different factors that render cells resistant to chemotherapy drugs. One important factor in the resistance of tumour cells to treatment is the inability of the drug to reach or distribute into the tumour. Another problem associated with anticancer chemotherapy drugs is the ability to induce high toxicity to the surrounding tissue. One other factor that needs to be considered is that most drugs are active in cells that are dividing or proliferating, and at a given time, a large proportion of tumour cells are not dividing or proliferating and therefore irresponsive to the drug. Most drugs such as doxorubicin have become inactive and ineffective to tumour cells through a mechanism similar to ATP-driven efflux pumps, pumping drugs out of the cell (Gillet & Gottesman, 2010; Hansel, 2005; Harris & Hochhauser, 1992; Labialle et al, 2005).

However lytic peptides also have some disadvantages, which have to be addressed before any clinical testing. The toxicity of lytic peptides on normal tissues is a major concern in a systemic use. This issue can be addressed by modifying the peptide sequence to target a specific cell type. Another disadvantage is the degradation by proteases and the inhibition by anionic components in the blood serum. This gives lytic peptides poor pharmacokinetic properties. The substitution of natural L-amino acid with D-amino acid in the ligand can increase the peptide stability preventing any degradation (Sahl, 2006).

There are a number of cellular alterations that occur when a normal cell advances into a malignant cell, which could progress further into a tumour (Hanahan & Weinberg, 2000). One alteration that has undergone intensive study is the ability to avoid apoptotic cell death. Cells with the ability to evade apoptosis are recognised as anticancer resistance cells (Johnstone et al, 2002). In order for tumour cells to survive and proliferate under stressful conditions, they need to develop a resistance to apoptosis and there are several methods to do so (Hanahan & Weinberg, 2000). p53 is a tumour suppressor protein that induces apoptosis by activating transcription of pro-apoptotic BCL-2 proteins in the context of DNA damage (Vousden & Lane, 2007). Any mutation or loss of function to p53 will result in a failure to induce apoptosis under stressful conditions (Donehower et al, 1992). Another modification that can occur involves BCL-2 family of proteins such as Bax and Bak (Kondo et al, 2000; Rampino et al, 1997). Exploring non-apoptotic types of cell death might therefore provide new opportunities for a more effective anticancer approach. One example for non-apoptotic cell death is necrosis.

Necrosis is described as an uncontrolled form of cell death. This method causes the loss of membrane integrity resulting in the release of intracellular components into the microenvironment, which can cause an inflammatory response. Growing evidence has shown necrosis to be controlled and regulated. One example of this is the activation of PARP-1, a protein involved in DNA damage repair. DNA-alkylating agents cause necrotic cell death via activation of PARP-1. This necrosis occurs with equal effectiveness in cells with or without functional apoptosis (Zong et al, 2004).

Most lytic peptides disrupt and diffuse the target cell membrane causing necrosis, making it difficult for any cell to become resistant (Hancock & Diamond, 2000; Shai, 2002). Compared to normal mammalian cells, which are predominantly composed of zwitterionic phosphatydilcholine (PC) and sphingomyelin phospholipids, cancer cells are mostly composed of phosphatidylserine (PS) (3-7 times of that in normal cells) on the inner leaflet of the membrane. It gives the structure an overall negative charge on the outer membrane (Utsugi et al, 1991). Since lytic peptides are positivity charged, they are more likely to bind to the negatively charged cancer cells.

Lytic peptides must undergo conformational changes in order to interact with the membrane. The peptide needs to be hydrophilic to undergo conformational changes in an aqueous environment. This enables the lytic peptide to interact with the membrane and exposing the hydrophobic region of the lipidic constituent of the membrane. There are two mechanisms

that have been proposed for lytic peptide interaction with the membranes and both differ from each other (Shai, 1999) (figure 1.9.3).

1) Barrel-stave model describes the amphipathic α-helices structure of the lytic peptide forming a transmembrane pore by inserting into the hydrophobic core of the membrane (Ehrenstein & Lecar, 1977). Once the pore has formed, intracellular components are released into the surrounding environment, leading to cell death (Ehrenstein & Lecar, 1977).

   This is a multistep process that involves the binding between the hydrophilic part of the lytic peptide and hydrophilic lipid head group. The lytic peptide then inserts into the hydrophobic core of the membrane. However this then becomes energetically unstable, and involves a bundle formation to enable the lytic peptides to insert into the membrane core. Once inserted into the membrane the helix structure becomes stabilised. This decreases main-chain polarity by promoting more extensive Hydrogen-bonding. This allows deeper penetration of the lytic peptide into the hydrophobic region of membrane core bilayer (Shai, 1999; Zelezetsky et al, 2005). The hydrophobic part of the lytic peptide interacts with the hydrophobic alkyl chains of the lipid, leaving the hydrophilic side of the lytic peptide to face inwards forming a transmembrane pore (Ben-Efraim et al, 1993). These peptides must be neutral or less positive in charge. Otherwise once a pore is formed a heavily charged peptide will cause electrostatic repulsion (Ben-Efraim et al, 1993). This mechanism is then at a disadvantage, because it will bind to normal and cancer cells. However there are a very small number of lytic peptides that adopt this mechanism. One example is Alamethicin; a lytic peptide that causes cell lysis of bacteria and erythrocytes (Sansom, 1993).

2) Carpet model describes the lytic peptide, not penetrating the hydrophobic core of the membrane, but in direct contact with the lipid head of the cell membrane causing a bilayer curvature (Pouny et al, 1992).

   This mechanism is also a multistep process, which causes the membrane to permeabilize. This involves a high concentration of the lytic peptides to cover the surface of the membrane, forming a carpet. The peptides are then absorbed by

electrostatic interactions. Lytic peptides are positively charged and interaction with the negatively charged cancer cells becomes greater. This is an advantage as the lytic peptides will selectively lyse cancer cells but not normal cells (Shai & Oren, 2001). Once in contact with the peptide, the membrane structure is disrupted and bends, forming a pore (Oren & Shai, 1998). This mechanism is preferred over the barrel-stave mechanism.

Phor21-βCG (ala), [D-Trp^6]GnRH-Phor21 and Pep-1-Phor21 are conjugated lytic peptides that target LHCGR, GnRHR and IL-13Rα2 respectively. As previously indicated, these receptors are highly expressed in cancer cells such as breast and prostate cancer cells but not when compared to that in corresponding normal cells. βCG (ala), [D-Trp^6]GnRH and Pep-1 bind to their receptors with high affinity (Emons et al, 1993; Halmos et al, 2000; Pandya et al, 2012; Rahman & Rao, 2009). Phor21 is a lytic peptide with 21 amino acids. This lytic peptide has shown to reduce or destroy tumours once conjugated with a 15 amino acid CG β subunit or a 10 amino acid GnRH, killing cells that over-express their receptors (Bodek et al, 2003; Leuschner et al, 2003b; Leuschner & Hansel, 2005; Nagy & Schally, 2005). Using cell viability assays, Phor21-βCG (ala) and [D-Trp^6]GnRH-Phor21 have been shown to specifically target cancer cells but not normal cells (Bodek et al, 2003; Leuschner et al, 2003b; Leuschner & Hansel, 2005; Nagy & Schally, 2005) (figure 1.9.2).

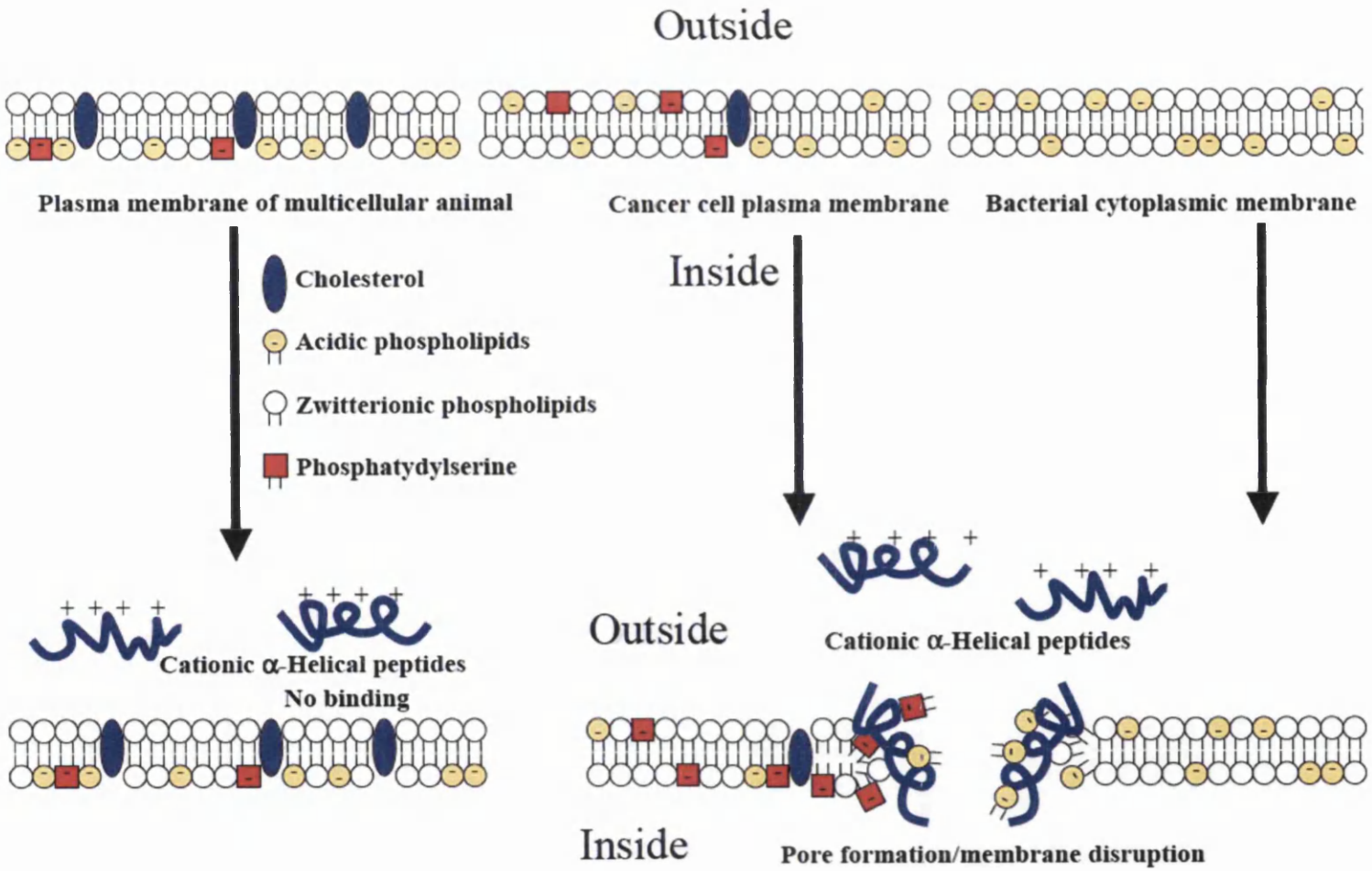

Figure 1.9.1. Characteristics of lytic peptides. Lytic peptides are positively charged, linear, amphipathic and α-helical in a hydrophobic environment, and are able to destroy rapidly negatively charged membranes (bacteria or cancer cells) with much less effect on positively charged membranes (normal somatic/eukaryotic cells) (Rivero-Muller et al, 2007).

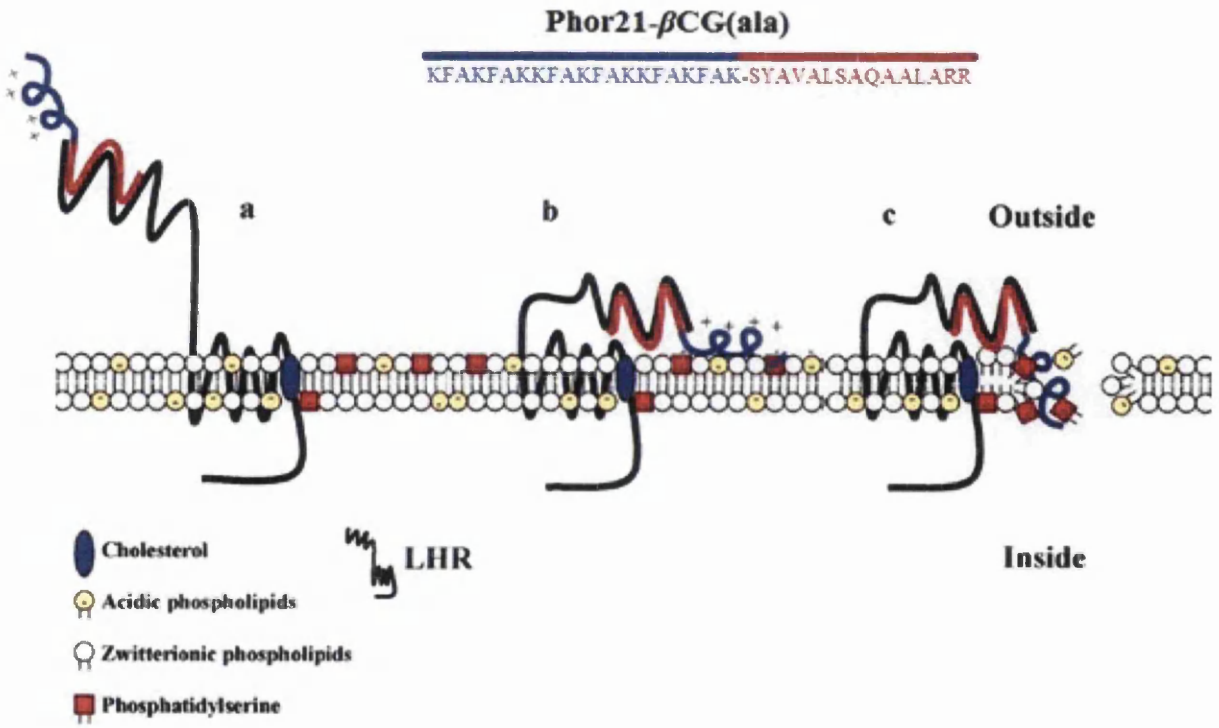

Figure 1.9.2 Phor21-βCG(ala) conjugate structure and mode of action. Phor21-βCG(ala) conjugate is a fusion polypeptide conformed of 21 amino acids of Phor21 and the 15 amino acids of the chorionic gonadotropin β (CGβ) subunit responsible for LHCGR high affinity binding. Thus it binds to the LHCGR (a) and becomes more stable, exposing the Phor21-helix molecule in a close proximity of the cell membrane (b). Cancer cell membranes possess high membrane potential which helps the Phor21-helix to bind and disrupt the adjacent membrane (c). Taken and adapted from (Rivero-Muller et al, 2007).

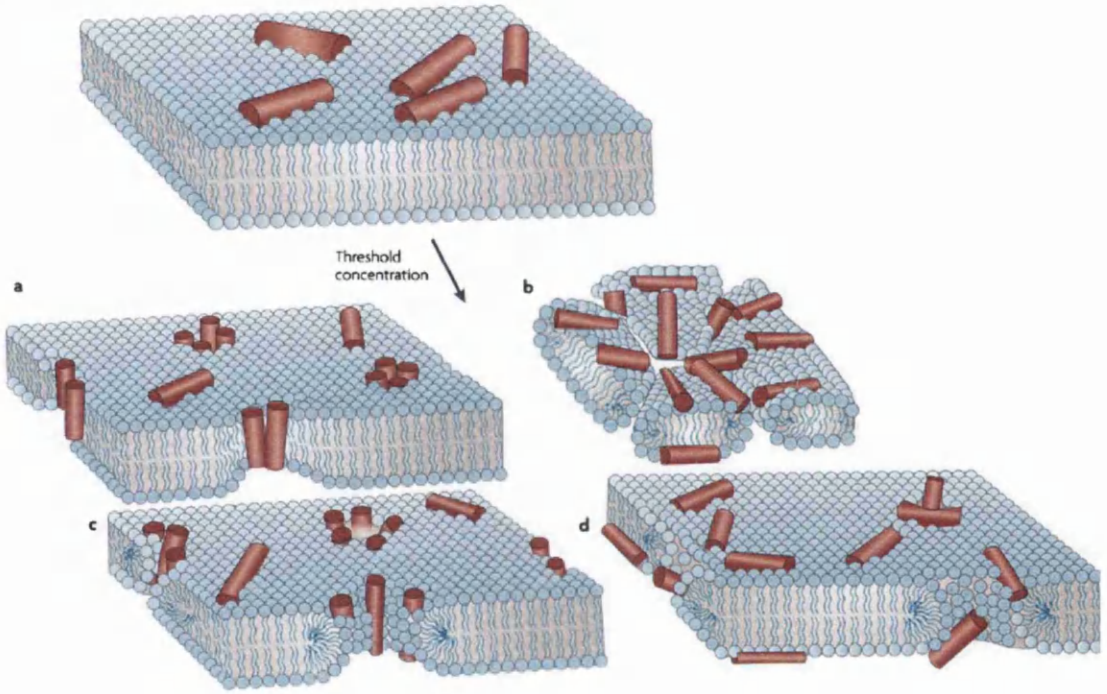

Figure 1.9.3. Schematic drawing of the mechanisms of antimicrobial peptide interacting with Membranes (Melo et al, 2009; Oren & Shai, 1998). Models describing the interactions of linear cationic amphipathic peptides with membranes. A) Barrel-stave pores. The peptide insets in the bilayer associate and form a pore. The peptides line the pore lumen in a parallel direction relative to the phospholipid chains, which remain perpendicular to the bilayer plane. B) Carpet mechanism. Peptides align parallel to the bilayer and, after reaching a threshold, it ruptures the membrane that disintegrates the membrane. C) Toroidal pores. Similar to the barrel-stave pores, the peptides insert perpendicular in the bilayer and induce a local membrane curvature in such a way that the pore lumen is lined partly by peptides and partly by phospholipid head groups. D) Disordered toroidal pores. A recent modification to the toroidal pore proposes that less-rigid peptide conformations and orientations are formed; the pore lumen is lined by the phospholipid head groups (Melo et al, 2009; Oren & Shai, 1998).

Hecate-βCG is a lytic peptide that was first developed by William Hansel and his research group. It is a conjugation of a synthetic analog of melittin (from bee venom) to βCG component. Hecate-βCG is a 38 amino acid peptide were, Hecate is 23 amino acid and βCG 15 amino acid long (Hansel et al, 2007a). However the dosage used *in vivo* was relatively high at 8-10mg/kg in prostate and breast xenografts. So a more potent compound was synthesised contain three identical 7-amino acid sequences (KFAKFAK) called Phor21 (Hansel, 2005; Leuschner & Hansel, 2005). Conjugated with βCG(ala), Phor21-βCG(ala) was found to be effective in destroying human breast cancer xenografts in nude mice, at a much lower does than Hecate-βCG (Hansel, 2005; Leuschner & Hansel, 2005).

No work to date has been performed on conjugating Phor21-βCG(ala) with SPION (superparamagnetic iron oxide nanoparicle). However one group showed SPION-Hecate–LHRH is detectable in mice for one week after injections, suggesting a more practical source for treating cancer, and most importantly serving as a monitoring tool for treatment response (Leuschner et al, 2005).

Although rapid killing by membranolytic's have been associated with lytic peptides, there are also non-membranolytic activities, which can be deployed. There is also ability to block receptors, expressed on angiogenic endothelial cells, preventing formation of the vasculature structure required for tumour cells survival (Lee et al, 2011; Rosca et al, 2011; Shang et al, 2012).

In some cases these peptides can penetrate intra-cellular and activate apoptotic pathways (Ausbacher et al, 2012). For example RGD-tachyplesin binds and kills cancer cells at low concentrations. Chen et al studied the effect of this peptide on human prostate cancer and melanoma cells (Chen et al, 2001). Their findings indicated that tachyplesin facilitates lytic peptides internalisation by the binding to integrin's on tumour and endothelial cells, this then affects the membrane function to trigger apoptosis (Chen et al, 2001).

These peptides can also trigger both necrotic and apoptotic signals. In one case A_9K;a short designed amphiphilic peptide developed by Xu et al shown to not only disrupt cell membranes but also induce cell apoptosis (Xu et al, 2013). Table 1.9 shows the primary sequence of some of the peptides with anticancer activity.

Peptide	Cancer cell	Selectivity	Activity	Amino acid sequence	References
D-peptide A	Human cervix, glioma, lung, mouse myeloma, african green monkey kidney	Yes	Cell membrane disruption	RLYLRIGRR	(Iwasaki et al, 2009)
D-peptide B	Human cervix, glioma, lung, mouse myeloma, african green monkey kidney	Yes	Cell membrane disruption	RLRLRIGRR	
D-peptide C	Human cervix, glioma, lung, mouse myeloma, african green monkey kidney	Yes	Cell membrane disruption	ALYLÀIRRR	
D-peptide D	Human cervix, glioma, lung, mouse myeloma, african green monkey kidney	Yes	Cell membrane disruption	RLLLRIGRR	
D-K6L9	Human prostate	Yes	Necrosis via membrane depolarization	LKLLKKLLKKLLKLL	(Papo et al, 2006)
NRC-03	Human breast	No	Cell membrane lysis with possible pore formation in mitochondria and ROS production	GRRKRKWLRRIGKGVKIIGGAALDHL	(Hilchie et al, 2011)
NRC-07	Human breast	No	Cell membrane lysis with possible pore formation in mitochondria and ROS production	RWGKWFKKATHVGKHVGKAALTAYL	
Gomesin	Murine melanoma, human breast, colon and cervix adenocarcinoma	-	Cell membrane disruption	ZCRRLCYKQRCVTYCRGR	(Rodrigues et al, 2008)
Hepcidin TH2-3	Human cervix, hepatocellular carcinoma, fibrosarcoma	Yes	Cell membrane disruption	QSHLSLCRWCCNCCRSNKGC	(Chen et al, 2009a)
Dermaseptin	Human prostate and breast	Yes	Cell membrane disruption	GLWSKIKEVGKEAAKAAAKAAGKAALGAVSEAV	(van Zoggel

B2					et al, 2012)
PTP7	Human lung, prostate, breast and hepatocellular carcinoma	Yes	Apoptosis induction	FLGALFKALSKLL	(Kim et al, 2003)
MG2A	Human cervix and lung, melanoma, rat glioma	Yes	Necrosis and apoptosis	GIGKFLHSAKKFGKAFVGEIMNSGGKKWKMRRNQF–WVKVQRG	(Liu et al, 2013)
HNP-1	Mouse colon and breast	-	Mediation of antitumor immunity	ACYCRIPACIAGERRYGTCIYQGRLWAFCC	(Wang et al, 2009)
Tachyplesin	Human prostate	-	Activation of the classic complement pathway	KWCFRVCYRGICYRRCR	(Chen et al, 2005)
Temporin-1CEa	Human breast	Yes	Membrane disruption, calcium release, ROS production	FVDLKKIANIINSIF	(Wang et al, 2012)

Table 1.9. Peptides and their respective oncolytic properties against solid tumour

EP-100 is a cancer drug, which is currently undergoing phase II trials (Pharmaceuticals, 2009). It is a conjugation between LHRH and the lytic peptide CLIP 71. With the phase I study, they determined the safety and the maximum dose of EP-100 against ovarian cancer. The drug was well tolerated with a maximum tolerated dose of 40 mg/m^2 (Pharmaceuticals, 2012). 1 patient out of 97 experienced elevated liver enzyme levels. However this patient was reported to have liver metastasis and elevated transaminases at baseline and that no other patients in the same cohort or subsequent cohorts experienced increases in liver enzymes. One other important factor was that there was no antibody production against EP-100 in any of the observed patients (Pharmaceuticals, 2012). With promising results from phase I, phase II is currently underway with a selected dose of 30-40 mg/m^2, twice a week for 3 weeks. The randomised phase II study will compare EP-100 combined with paclitaxel versus paclitaxel alone with patients with histologically confirmed epithelial ovarian carcinomas (Pharmaceuticals, 2012).

Using peptides as potential anticancer drug has its advantages as well as flaws. One of the main disadvantages of lytic peptides usage as anticancer is its inability to traffic to tumours whilst sustaining a low toxic effect on the surround normal tissue. Their low resistance to proteolytic cleavage in the blood can cause a major problem with their stability. The success of any lytic peptide drug depends on the sequence, overall charge, its secondary structure, oligomerisation ability, amphipathicity and hydrophobicity whilst maintaining high serum stability (Gaspar et al, 2013). Identifying the amino acids that give the lytic peptide its properties will reduce the cost by producing shorter fragments that retain biological function. In some cases the shorter the peptide the more efficient it is in disrupting the cell membrane, thus increasing its cytotoxicity (Fadnes et al, 2011).

Most lytic peptides contain arginine (R) residues to increase their interaction with the zwitterionic phospholipids in cell membrane, resulting in cell membrane disruption. Lysine (K) is also a cationic residue; together they (R and K) can form a peptide that binds negatively charged cells whilst simultaneously avoiding hemolytic events. D-amino acids can also be used to increase the stability of the peptide. In a hydrophobic environment, the hydrophobicity of the peptide, should also be considered, which can modulate the anticancer activity (Huang et al, 2011). When the hydrophobicity of an amphipathic peptide, V13K, was manipulated by changing an alanine to a leucine, it increased the peptide activity against human cervical cancer cells (Huang et al, 2011). All in all, these peptides, once optimised can point us into a new direction of chemotherapeutic drugs. They can also work in a synergistic

fashion with other existing agents, preventing any MDR mechanism and also reducing any side effects on healthy tissues and organs.

Lytic peptides action is not only limited to the disruption of the plasma membranes. Other mechanisms do exits which can cause the swelling of the mitochondria, which indices the release of cytochrome c and apoptosis events (Mai et al, 2001). In some cases the lytic peptide can cause the production of reactive oxygen species (ROS). Hilchie et al developed two lytic peptides named NRC-03 and NRC-07 to target breast cancer cells. Their results demonstrated that these peptides were able to induce apoptosis by activation of reactive oxygen species (ROS) production and mitochondrial membrane destabilization. Despite that fact there was no targeting moiety, they found that there was significate cell death in cancer cells compared to the normal cells (Hilchie et al, 2011). Kawamoto et al developed a lytic peptide that targets cell membrane-associated glycoprotein called Transferrin receptor (TfR). The research group developed a 32 amino acid lytic peptide and tested on 12 cancer and 2 normal cell lines. They found that the lytic peptide drug effectively killed cancer cells by inducing apoptotic cell death, without effecting normal cell lines. Testing further demonstrated that the lytic peptide induced annexin V-PI- and caspase 3 & 7-PI-positive cells, resulting in the collapse of mitochondrial membrane potential in cancer cells (Kawamoto et al, 2011). In some cases the lytic peptide can induce two action modes. Xu et al developed an antibacterial peptide drug called A_9K. This lytic peptide caused membrane disruption and cell apoptosis. They demonstrated that interaction with A_9K caused mitochondrial dysfunction by causing F-actin rearrangement and decrease in the transcription of BCL-2 and c-myc genes, in cancer cells (Xu et al, 2013).

1.10. 3D Cell Culture

In 2008, an estimated 12.7 million new cases of cancer occurred worldwide (UK, 2012). With such high cases it is understandable that the majority of drugs in the market today are being used to treat cancer patients. According to national cancer research institute (NCRI) more than £500 million was spent on cancer research with a significant amount being spent on developing and screening new anticancer drugs (Institute, 2013). However most clinical trials show very little success, with only 4% of anticancer drugs being recommended by NICE (national institute for health and care excellence (Excellence, 2013). Overall the current anticancer drug development process is draining away money and also it is inefficient.

Failing early in the developmental stages enables the cost of failed molecules to remain relatively low.

One major obstacle associated with drug development is the inability to identify effective and ineffective therapies early on in the drug development process (Balis, 2002). Before any drug therapy can undergo clinical trials, it must first undergo pre-clinical screening and target validation to provide information about the mechanism of the drug action, how efficient the drug is and how toxic it is to cancer cells and neighbouring normal cells (Alanine et al, 2003; Arlt, 2005; Balis, 2002; Bleicher et al, 2003). These pre-clinical screening processes *in vitro* and *in vivo* have to be further developed to identify poor candidates early on in the drug development process. However other factors also complicate the pre-clinical screening process including the biology of cancer cells themselves. Firstly, this disease has a high heterogeneity, where the tumour mass can contain a variety of subpopulations of cells with differing metastatic potential causing resistance and impeding the action of the drug (Kamb et al, 2007). Secondly, the tumour microenvironment can also cause resistance impeding any drug action, which is not shown in *in vitro* testing (Teicher, 2009).

Research and the pharmaceutical industries commonly use *in vitro* models to evaluate and aid drug development and discovery (Shoemaker, 2006). For high-throughput screening procedures, *in vitro* assays are typically used, involving the growth of cancer cells in a two-dimensional (2D) cell culture monolayer (Johnson et al, 2001; Voskoglou-Nomikos et al, 2003). This relative simple way of performing drug analysis has enabled the measurement of drug uptake and effectiveness in a simple, quick and a controlled manor.

Despite the advances towards the understanding of cancer biology by *in vitro* 2D cultures, it is still disputed that 2D cultures do not fully represent native tissue where cells are in a three-dimensional (3D) microenvironment (Teicher, 2006). It is apparent that 2D based assays are a poor indicator for anticancer drugs *in vivo*. As a result a very low number of drugs are being developed and very low number of drugs have passed approval processes using 2D based assays (Kola & Landis, 2004). *In vivo* animal models have the advantage in mimicking physiological conditions compared to 2D models. However this type of model is more complex, more expensive and introduces variables that could cause discrepancies in the overall experiments (Teicher, 2006).

In vivo models are more complex and require human tumour xenografts implanted into a murine animal. One important factor when using these models is the difference between

human beings and animal test subjects (Seok et al, 2013; Shanks et al, 2009; Whiteside et al, 2008). There have been a number of studies highlighting the differences between human tumour xenografts results and the results from phase II clinical trials (Johnson et al, 2001; Liotta & Kohn, 2001; Voskoglou-Nomikos et al, 2003). A drug compound can be highly effective in murine models but can be ineffective or even toxic to humans once undergoing phase II clinical trials (Johnson et al, 2001; Voskoglou-Nomikos et al, 2003).

With such high limitations in both 2D cell cultures and in animal models, it is apparent that an alternative system needs to be developed. An alternative is a 3D *in vitro* model (Griffith & Swartz, 2006; Rangarajan et al, 2004).

3D cell culture models are considered to be placed between 2D cell culture and whole animal models (Griffith & Swartz, 2006; Rangarajan et al, 2004). These models have shown similar characteristics to that of animal models (Lin & Chang, 2008). Reflecting on the morphology and signalling that would have been missed or absent in 2D models (Lin & Chang, 2008).

One common method of 3D cell culture is the formation of a spheroid. This method resembles avascular tumours with oxygen and nutrient gradients. The spheroids are generated by simply placing the cells in an environment that prevents cell attachment on the surfaces or placing the cells in a matrix gel (Kunz-Schughart et al, 2004; Shaw et al, 2004). This type of model allows heterologous co-culture of tumour cells with other cell types, either being fibroblast, immune or endothelial cells (Kunz-Schughart et al, 2001). Studies have shown a resemblance between tumour spheroids and their tumour counterparts. These properties include structural, morphological and functional differentiation, similar manor of growth kinetics and similar properties when resisting drugs (Mueller-Klieser, 2000). One characteristic of tumour spheroid is that it has a well-structured cellular composition, where the outer rims consist of proliferating cells and the inner centre layer has necrotic cells (Sutherland et al, 1971). This resembles the physiological morphology of tumours; as with increasing distance from blood vessels, there is a decrease in proliferating cells (Gabbert et al, 1983).

Tumour cells grown as spheroids have shown to synthesize and deposit matrix proteins, similar to those observed *in vivo*. One research group cultured HT29 colon cancer spheroids and showed that the cells deposited a thick filamentous network on the cell surface, similar to that shown *in vivo*. They also showed that this filament structure was not detected in similar quantities in monolayer cultures (Santini & Rainaldi, 1999).

One major advantage of using spheroid models especially in screening for anticancer drug candidates is the ability to identify resistance once applying a drug of interest (Friedrich et al, 2009; Lin & Chang, 2008). Identifying drug resistance before *in vivo* testing or clinical trials will not only save money it will also provide a better understanding of the drug that might have not been identified in monolayer cultures (Miller et al, 1985). There can be many characteristics that could explain the resistance of drugs to spheroids compared to monolayer cultures. Monolayers do not fully represent the true growth kinetics in cancer cells (Torisawa et al, 2005). Monolayer cell culture exhibit exponential cell proliferation until limited by the surface available whereas tumour spheroids show a phase exponential growth as the number of non-proliferating and necrotic cells increase and growth rate declines (Gimbrone et al, 1972). Also these culture methods are developed to mimic the 3-D microenvironment of a cell in a living organism, so perhaps the increase in cell to cell contact, the enhanced deposition of tumour-derived extracellular matrix (ECM) within the spheroid and the low proliferation rate could all contribute to resistance to a drug (Bates et al, 2000; Hamilton, 1998).

However, using spheroid also has its own limitations, one of which is the difference in diffusion rates in spheroids for oxygen and essential nutrients (Friedrich et al, 2007; Lin & Chang, 2008). This characteristic with spheroid models can reduce the activity of a drug compound (Graff & Wittrup, 2003). The lower diffusion rate can have a negative impact on results; making it difficult to distinguish between whether the drug is inefficient or whether the drug has a poor penetration (Thurber & Wittrup, 2008).

The use of fibrous meshwork called extracellular matrix (ECM) is highly important when generating a spheroid model. 2D cultures lack the ability to form a tumour like structure. They lack the ability to generate a 3D microenvironment of different cell types or even form various architectures that is sometime seen in tumours (Rejniak et al, 2013; Russnes et al, 2010). ECM is a vital component in studying cancer treatments, enabling complex biochemical and physical signals by allowing cell-cell or cell-matrix interactions. These signals are essential for realizing important cellular functions, such as cell adhesion and motility (Abbott, 2003; Cukierman et al, 2001).

Artificial ECM such as Matrigel (which is composed of soluble proteins derived from the Engelbreth-Holm-Swarm [EHS] mouse tumour basement membrane) can be used to culture cells for 3D tumour models. This forms a gel at room temperature and therefore allowing microscopic examination of the cultures (Hayashi et al, 2004).

Matrigel can be used in tumour biology to study drug effectiveness. When 3D cultured in Matrigel, normal prostate cells are able to form acini-like structures in contrast to malignant prostate cells (Webber et al, 1997). Furthermore, normal cells often do not proliferate on basement membrane matrix whereas malignant cells can proliferate on Matrigel (Webber et al, 1997)

Overall 3D cell culture can provide a way to visualize how cancer cell would grow and organize in vitro and how drugs will react to the environment.

1.11. Project Aims

Endocrine tumours such as ovarian granulosa, testicular Leydig cell and many adrenocortical tumors have one thing in common: they all express LHCGR, GnRHR and IL-13Rα2. The objective of this study was to investigate the expression of LHCGR, GnRHR and IL-13Rα2 in a cancer tissues sample array and investigate further by targeting the receptor using a lytic peptide in both 2D and 3D models.

The specific aims of the study were:

1. To investigate the expression of LHCGR, GnRHR and IL-13Rα2 at mRNA level using cancer tissue array cDNA
2. Given the result from the tissue array, prostate and breast cells lines grown in 2D culture were used to investigate further as a model for the efficacy of three different lytic peptide conjugated ligands, Phor21-βCG (ala), [D-Trp^6] LHRH-Phor21 and Pep-1-Phor21.
3. To investigate the molecular mechanism underlying the mode of cell death caused by Phor21-βCG (ala), [D-Trp^6] LHRH-Phor21 and Pep-1-Phor21.
4. To increase the efficacy of Phor21-βCG (ala), [D-Trp^6] LHRH-Phor21 and Pep-1-Phor21 by up regulating the expression of their receptors.
5. To develop a 3D model that mimics *in vivo* studies
6. To study the effect of Phor21-βCG (ala), [D-Trp^6] LHRH-Phor21 and Pep-1-Phor21 on 3D culture spheroids.

2. Materials and Methods

2.1. Materials

Applichem, Lutterworth, Leicestershire, UK

Sodium Dodecyl Sulphate (SDS)

BD, Oxford, Oxfordshire, UK

25 G Needles

Bioline Reagents Ltd, London, UK

SensiMix Plus SYBR & Fluorescent Kit

Biorad, Hemel Hempstead, UK

Precision Plus TM All Blue Protein Ladder, N,N,N',N'-Tetramethylethylenediamine (TEMED)

Fisher Scientific UK Ltd, Loughborough, Leicestershire, UK

Butanol, Ethanol, Isopropanol, Glycerol, Methanol, Sulphuric Acid

Ge Healthcare Life Science, Little Chalfont, Buckinghamshire, UK

Amersham ECL Select Western Blotting Detection Reagent.

Life Technologies Ltd, Paisley, UK

Applied Biosystemss High-Capacity cDNA Reverse Transcription Kit

Melford Laboratories Ltd, Ipswich, Suffolk, UK

Glycine, Tris-Base, Tris-HCL

Merck Chemicals Ltd, Beeston, Nottingham, UK

Millipore Polyvinylidene Fluoride (PVDF)

National Diagnostics, Hessle, East Riding Of Yorkshire, UK

30% Acrylamide Solution

New England Biolabs Ltd, Hitchin, Hertfordshire, UK

Non-Fat Dry Milk Powder

Qiagen, Crawley, West Susses, UK

RNeasy Mini Kit

Sigma-Aldrich Company Ltd, Poole, Dorset, UK

5-Aza 2'deoxycytidine (AZA), Ammonium persulphate (APS), Bicinchoninic acid solution A (BCA), Bovine serum albumin (BSA), Bromophenol blue, $CaCl_2$, Copper(II) sulfate solution, Trichostatin A (TSA), Dimethyl sulfoxide (DMSO), Nonidet-P40, $MgCl_2$, 2-Mercaptoethanol, Paraformaldehyde (PFA), Phosphate buffered solution (PBS), Ponceau S, Potassium acetate, Protease cocktail inhibitor, NaCl, NaH_2PO_4, NaOH, Triton X-100, Tween-20

Thermo Fisher Scientific, Cramlington, Northumberland, UK

1-Step Ultra TMB (3,3',5,5'-Tetramethylbenzidine), Pierce SuperSignal West Pico Chemiluminescent Substrate, Restore PLUS Western Blot Stripping Buffer

2.2. Antibodies

Ge healthcare life science, little Chalfont, Buckinghamshire, UK

Goat anti-rabbit IgG-Horseradish peroxidase (HRP) conjugate, sheep anti-mouse IgG-Horseradish peroxidase (HRP) conjugate

Santa Cruz biotechnology, Inc., Dallas, TX, USA

Mouse anti-Interleukin-13 Receptor alpha-2 (IL-13Rα2) monoclonal antibody, Rabbit anti-Gonadotropin-releasing hormone receptor (GnRHR) polyclonal antibody (Price et al, 2013). Rabbit anti- N-terminus luteinizing hormone/choriogonadotropin receptor (LHCGR) Monoclonal antibody

2.3. Pharmacological compounds

Peprotech, Rocky Hill, HJ, USA

Recombinant Human Epidermal Growth Factor (EGF)

Thermo Fisher Scientific, Cramlington, Northumberland, UK

Pep-1 (CGEMGWVRC), Phor21 (KFAKFAKKFAKFAKKFAKFAK), Pep-1-Phor21 (CGEMGWVRCKFAKFAKKFAKFAKKFAKFAK), βCG(ala) (SYAVALSAQAALARR), Phor21-βCG(ala) (KFAKFAKKFAKFAKKFAKFAKSYAVALSAQAALARR), [D-Trp^6]GnRH ([Pyr]-HWSY-*W-LRPG, *W = D-Trp) and [D-Trp^6]GnRH-Phor21 ([Pyr]-HWSY-*W-LRPGKFAKFAKKFAKFAKKFAKFAK)

2.4. Tissue Culture disposables

American Type Culture Collection, Rockville, USA

HEK 293, MCF-10A, MCF-7, MDA-MB 231, PNT-2, LNCaP, DU145, PC3 cells

BD, Oxford, Oxfordshire, UK

1ml and 50ml Sterile Syringes

Biosera, Uckfield, East Sussex, UK

Dulbecco's Modified Eagle's Medium (DMEM) With Sodium Pyruvate, L-Glutamine, 4.5 G/L Glucose, Foetal Bovine Serum (FBS), Roswell Park Memorial Institute (RPMI) 1640 Medium

Greiner Bio One, Stonehouse, Gloucestershire, UK

0.2-10ul, 20-200ul, 100-1000ul Pipette Tips, 6cm^2 and 10cm^2 Tissue Culture Plates, 6 Well. 12 Well, 24 Well Plates and 48 Well plates, 0.5ml, 1.5ml and 2ml Microfudge Tubes, 3ml Pasteur Pipettes.

Merck Chemicals Ltd, Beeston, Nottingham, UK

GeneJuice Transfection Reagent, Millipore Millex-GP 0.22um Sterile Filters

Sigma-Aldrich Company Ltd, Poole, Dorset, UK

Penicillin-Streptomycin-Glutamine (PSG), Phosphate-Buffered Saline (PBS), Sterile-Filtered Trypsin-EDTA 10X

VWR International Ltd Lutterworth, UK

15ml and 50ml Sterile Centrifuge Tubes

2.5. Buffer and Solutions

10X Phosphate Buffered Saline (PBS Buffer)

137 mM NaCl, 2.7 mM KCl, 10 mM Na2HPO4, 1.5 mM KH2PO4; pH 7.4. 1X PBS was made by diluting 10X by 1:10 in double distilled water (ddH2O).

SDS-PAGE and western blotting buffers and solution

Running Buffer (4x)

1.5 mM Tris-HCL, 0.4% SDS, at pH 8.8

Sample Buffer (5x)

5% SDS, 125mM Tris-HCL, set at pH 6.6, 50% glycerol, 0.025% bromophenol blue, 5% 2-Mercaptoethanol.

Stacking gel (4x)

0.5 mM Tris-HCL, 0.4% SDS, at pH 6.8

Transfer buffer (1x)

70% ddH_2O, 10% Tris-glycine (10x), 20% methanol.

Tris buffered saline (TBS) (10x)

250 mM Tris-HCL/ 1.5mM NaCl, set at 7.5

Tris buffered saline (TBS)/tween-20

TBS (10x), 0.1% tween-20

Tris-glycine (10x)

0.25mM Tris-base, 1.92M glycine.

2.6. Tissue Culture

Only adherent cells were used in this study. Tissue culture was carried out in a class II hood Mars Air Flow (ScanLaf, Lynge, Denmark) using a sterile technique at all times. All equipment was wiped with 70% (v/v) ethanol before use in the hood. All cells were maintained at 37°C in a 5% CO_2 humidified environment in a Galaxy S incubator (Galaxy S incubator Wolf Laboratories, York, UK).

2.6.1. Preparation of growth media

HEK293, MCF7 and MDA-MB 231 cell lines were maintained in Dulbecco's Modified Eagles Media (DMEM) (Biosera, Uckfield, East Sussex, UK) supplemented with 10 %(v/v) fetal bovine serum (FBS) (Biosera, Uckfield, East Sussex, UK), 2mM L-glutamine, 100U/ml penicillin and 0.1mg/ml streptomycin (Sigma-Aldrich Company Ltd, Poole, Dorset, UK).

PNT-2, LNCaP, DU145 and PC3 cell lines were maintained in RPMI-1640 (RPMI) (Biosera, Uckfield, East Sussex, UK) supplemented with 10 %(v/v) fetal bovine serum (FBS) (Biosera, Uckfield, East Sussex, UK)), 2mM L-glutamine, 100U/ml penicillin and 0.1mg/ml streptomycin. MCF-10A cell line was maintained in Ham's F12:DMEM (50:50) culture medium (F-12) containing 5% horse serum (HS), (Biosera, Uckfield, East Sussex, UK), 2mM L-glutamine, 100U/ml penicillin and 0.1mg/ml streptomycin, 20 ng/ml epidermal growth factor (EGF)(Peprotech, Rocky Hill, NJ, USA), 0.1mg/ml cholera toxin (CT) (Sigma-Aldrich Company Ltd, Poole, Dorset, UK), 10mg/ml insulin (Sigma-Aldrich Company Ltd, Poole, Dorset, UK), and 500 ng/ml hydrocortisone (Sigma-Aldrich Company Ltd, Poole, Dorset, UK) (FSM).

2.6.2. MCF-10A

MCF-10A is non-transformed epithelial cell line derived from human fibrocystic mammary tissue. These cell lines are defined as normal breast epithelial cells. MCF-10A cell lines were kindly donated by Dr Richard Clarkson and his group from the School of Biosciences at University of Cardiff UK.

2.6.3. MCF-7

MCF-7 is a tumourigenic breast epithelial cell line that is originated from pleural effusion of a 69 year old female patient with breast adenocarcinoma. The phenotypic characteristic of this cell line is an ER and PR positive breast cell line that is non-invasive.

2.6.4. MDA-MB 231

MDA-MB 231 is a tumourigenic breast epithelial cell line that is originated from pleural effusion of a 51 year old female patient with breast adenocarcinoma. The phenotypic characteristic of this cell line is an ER and PR negative breast cell line that is highly invasive.

2.6.5. PNT-2

PNT-2 is a non-tumourigenic normal prostate epithelium cell line. Its origins are from a prostate of a 33 year old male at post mortem.

2.6.6. LNCaP

LNCaP is a human prostate adenocarcinoma cell line, derived from a needle aspiration biopsy of the left supraclavicular lymph node of a 50-year-old Caucasian male, diagnosed

with metastatic prostate carcinoma. The phenotypic characteristic of this cell line is an ER and AR positive prostate cell line.

2.6.7. DU145

DU145 is a human prostate adenocarcinoma cell line, derived from vertebral column and right femoral neck of a 69-year-old Caucasian male. The phenotypic characteristic of this cell line is an ER and AR negative prostate cell line.

2.6.8. PC3

PC3 is a human prostate adenocarcinoma cell line, derived from a bone metastasis of a grade IV prostatic adenocarcinoma from a 62-year-old male Caucasian male. The phenotypic characteristic of this cell line is an ER and AR negative prostate cell line.

2.6.9. HEK 293

HEK 293 is an embryonic kidney cell line, derived from embryonic kidney explants, derived from human embryonic kidney cells. HEK 293 are a hypotriploid human cell line that contains cells of endothelial, epithelial and fibroblastic nature.

2.6.10. Maintenance and passaging of cell lines

Cell lines media was replaced ever two days by aspirating the media and replace with pre-warmed media. Once the cells reached 70-90% confluency they were passage into a dilution depending on the growth rate of the type of cell line.

After the aspirating off the media, the cells were washed with 1ml of pre-warmed 1x Trypsin-EDTA (0.05% trypsin, 0.04% EDTA in PBS (without CaCl2 or MgCl2)). This was aspirated and another 1ml of pre-warmed 1x Trypsin-EDTA was added and then placed into an incubator at 37°C until the cells have detached from the surface of the plate. Once the cells were detached, they were collected and resuspended in 10ml of pre-warmed FSM. The cell suspension was then vortexed and then split accordingly, with the desired volume of cells place into a dish and the unwanted cells discarded. Media was added to the dish of cells to make up 10mls and the cells returned to the incubator.

2.6.11. Resuscitation of cell lines

Frozen cell lines were removed from the liquid nitrogen and place into a sterile water bath at 37°C. Cells were removed from the water bath as soon as they were defrosted and place in 15ml of pre-warmed media. The cells were then carefully resuspended and placed in 10cm^2 dish. The revived cells were maintained at 37°C, 5% carbon dioxide in a 10cm^2 dish.

2.6.12. Producing frozen aliquots

Cells were grown to 90% confluency. After which they were trypsinised and resuspended in 10ml of FSM as described in section 2.210. The cells were than centrifuge (DJB Labcare Ltd, Buckinghamshire, UK) at 500 x g at 24°C for 5 minutes, after the supernatant was then removed. The pellet was resuspended in 1ml of cryopreservation medium (SFM, 25% FBS, 10% (v/v) dimethyl sulfoxide (DMSO)).This acts as a cryopreservant during storage. The resuspended cells were then transferred to a sterile 2ml cryovial. The cryovial was the placed in a cryopreservation pot Nalgene® Mr. Frosty container (Thermo Fisher Scientific, Cramlington, and Northumberland, UK). These pots were filled with isopropanol and placed in the -80 °C freezer and stored overnight. The container will ensure freezing occurs at -1°C per minute. After which the vials was transferred to liquid nitrogen for long term storage.

2.6.13. Counting of cells using a haemocytometer

Cells were trypsinised as describe in section 2.1.3. Once being resuspended in 10ml in pre-warmed media, cells were counted using a haemocytometer. The haemocytometer chamber and cover slip were first cleaned and wiped down with 70% (v/v) ethanol. The cover slip was placed onto the haemocytometer chamber. 10µl of the cell suspension was pipetted into the chamber underneath the coverslip. The cells were counted by using an inverted microscope. This was performed twice and the average cell count was calculated. The cell suspension was diluted appropriately for each experiment to unsure the correct seeding density.

2.6.14. Treating cell lines

Cell lines were grown to 30-50% confluency for the start of any treatments. Note this depends on the growth rate of each cell line. Media supplemented with any pre-treatment was added to cell line. The cells were than pelleted or scraped as described in section 2.1.6 and section 2.2.1 respectfully. A non-treated control cell line was grown as described in section 2.1.3.

2.6.15. Producing cell pellets

Cell line pellets were produced for extraction of mRNA. Once the cells reached 90% confluency or reached the end of the treatment period. The cells were washed with PBS and detached from the dish with 1 x Trypsin-EDTA as described in section 2.1.3. Cells were resuspended in culture media and transferred to a test tube, than centrifuged at 500 x g at 24°C for 5 minutes. The supernatant was removed and the cell pellet was washed with 1 ml of PBS followed by a second centrifuged step and washed again. Before snap freezing the suspension was again centrifuged and the supernatant was removed. The pellets were then transferred to -80 °C for storage until needed.

2.7. Protein expression preparation and quantification

2.7.1. Protein Extraction

Cells were cultured to 80% confluency. The medium was aspirated and the cells were washed thrice with cold PBS and then lysed Radioimmunoprecipitation assay (RIPA) lysis buffer (10mM Tris-HCL, pH 7.5, 10mM EDTA, 1% NP-40, 0.1% SDS, 150mM NaCl and 0.5% sodium deoxycholate) and 1% proteinase inhibitor cocktail. They were scraped off the dish and collected in to a centrifuged tube. The lysate was subsequently passed through a 25 gauge needle $\geq$ 10 times. Than incubated at 4°C for 15 minutes, after which the tubes were centrifuged at 14,000xg for 10 minutes. The supernatant was collected and placed into a fresh 1.5ml collection tube, and the pellet was discarded. 10µl aliquot of each sample was taken to determine the protein concentration (section 2.7.2). 5x sample buffer was added to the remaining samples, and diluted down to 1x and boiled for 5 minutes at 100°C using a Grant heating block. Protein samples were stored at -20°C until ready for use.

2.7.2. Protein quantification

Protein concentrations of whole cell lysate in RIPA buffer were determined by a Bicinchoninic Acid Protein assay. Protein standards were made from 2mg/ml of BSA in ddH2O to the concentration of 0.2, 0.4, 0.6, 0.8 and 1mg/ml. 10µl of the protein standards were added into well of 9-well pate, in duplicate. Protein samples were diluted in ddH2O (1:5 and 1:10) and plated to the same plate, in duplicate. A reaction mixture of copper II sulphate

and BCA solution (1:50 v/v) was made. 80µl of the reaction mixture was added to each well either containing protein standards or protein samples. The plate was incubated for 30 min at 37°C in an Incucell incubator. The absorbance was measured at 490nm using a Biotek microplate reader (Northstar Scientific Ltd, Leeds, UK). The standard curves were fitted using Microsoft Office Excel 2010 (Microsoft Corporation, WA, USA) and the unknown protein concentration was determined by using the standard curve.

2.8. Protein Analysis

2.8.1. SDS-Polyacrylamide Gel Electrophoresis

SDS-Polyacrylamide Gel Electrophoresis (SDS-PAGE) was used to separate proteins for western immunoblotting analysis. Polyacrylamide Resolving Gels were cast using a Mini-Protein III system (Bio-Rad, Herts, UK). Spacer plates and short plates were cleaned using 70% (v/v) ethanol. They were then clamped together using a casting frame. A 10% Polyacrylamide Resolving Gels were prepared using the components as listed in table 2.1 below. The solution was than mixed and poured in between the spacer plates and short plates. Water saturated butanol was added to remove bubbles and to level the edge. 10% resolving gel was allowed to set for 30min; the Water saturated butanol was washed off with ddH_2O. The stacking gel was mixed and poured onto the Resolving Gels and a 15 well insert comb was added. The gel was left to polymerise for 15min. After the gel is set the comb was removed and the wells were rinsed with ddH_2O.

Plates were placed into the electrode assembly, and transferred into a mini tank (Bio-Rad, Herts, UK) containing 1x running buffer. Protein samples containing sample buffer were loaded into the wells alongside with 5ul Precision plus protein Kaleidoscope ladder. Electrophoresis was ran at a 200 volts for 40 minutes or until the loading dye reacted the bottom of the gel using PowerPac basic 300 (Bio-Rad, Herts, UK).

	Resolving gel	Stacking gel
	10%	5%
Reagent (ml)	~20-150kDa	
ddH_2O	4.2	1.75
4x Running Gel Buffer	2.5	0.75
30% Acrylamide	3.3	0.5
Ammonium Persulfate (APS)	1 small spatula	½ spatula
Tetramethylethylenediamine (TEMED)	0.01	0.005

Table 2.4.1. Components in Resolving gel and Stacking gel. A table showing all the components used for resolving and stacking gel.

2.8.2. Semi-Dry Membrane transfer

The semi-dry method was used to transfer proteins from the gels to PVDF membrane (IPSN07852). PVDF membrane and filter papers were cut to the size of the gel. The PVDF membrane was activated in methanol for 30 seconds and washed with ddH_2O. The PVDF membrane and filters were placed in transfer buffer and placed in the fridge until needed. Once the electrode pack had finished the gels were removed from the plates and placed in transfer buffer. At the same time Trans-Blot® Turbo Semi Dry (Bio-Rad, Herts, UK) was set up as shown in figure 2.2 and set to run at 25 volts for 30 minutes.

2.8.3. Immunoblotting

After the run as finished, the cassette was disassembled and the PVDF membrane was placed in ponceau red stain to visualise the proteins. Once proteins had ben stain to ensure transfer had occurred, the membrane was then placed in TBS-Tween 20, to remove the stain. TBS-Tween 20 was then removed and placed in blocking buffer (5% (w/v) powdered non-fat skimmed milk (Marvel, Lincolnshire, UK) prepared in TBS-Tween 20). After incubating for 60min on the SSL4 see-saw rocker (Stuart, Standfordshire, UK) or overnight at 4°C, the membrane was placed in a sealed bag with 2ml of the primary antibody diluted in 5% (w/v)

milk-TBS-Tween 20. The working dilutions and sources of the antibodies can be found in Table 2.3. After 60min or overnight at 4°C incubation rocking, the membrane was washed 5 times for 5 min with TBS-Tween 20. After which the membrane was sealed again and incubated with secondary antibody conjugated to horse-radish peroxidase (HRP) for 60 minutes. The membrane was then washed 5 times for 5 min with TBS-Tween 20.

The membranes were viewed with chemiluminescence reagents ECL Western blotting detection reagent (GE Healthcare) or Amersham ECL Advance™ Select Western Blotting Detection Reagent. The reagent was made up by adding equal volumes of reagent A and B together. The membrane was place onto the reagent mixture for 5min for chemiluminescence reagents ECL Western blotting detection reagent or 1min for Amersham ECL Advance™ Select Western Blotting Detection Reagent. After the incubation the membrane was placed on a ChemiDoc™ XRS system (Bio-Rad, Herts, UK). The membrane was exposed for 1, 10, 30, 60, 120, 240 seconds using Quantity One Software (Bio-Rad, Herts, UK). The membranes are stored at 4°C. The images were densitometry analysed using ImageJ software (Miller, 2007).

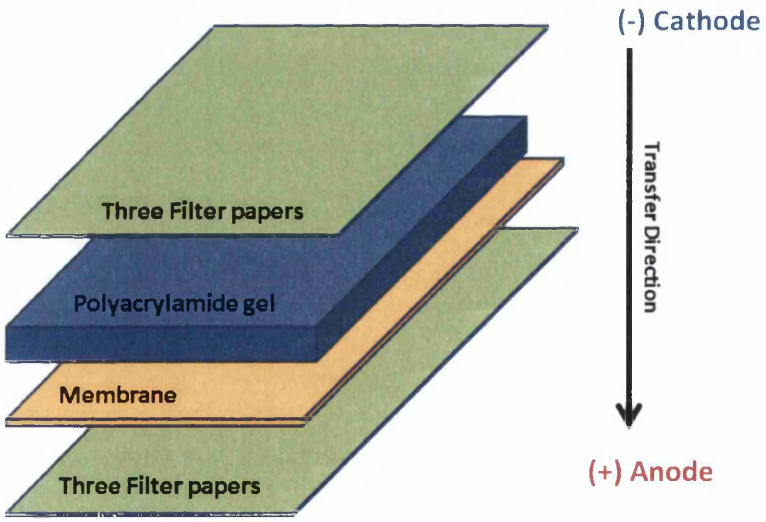

Figure 2.4.3 Transfer cassette set-ups for western blot. The polyacrylamide gel and PVDF membrane are sandwiched between filter paper and sponges and encased within the clamping system where it undergoes voltage for the transfer of proteins from the gel to the membrane.

2.8.4. Stripping and Reprobing

Membranes that have been visualised are sealing in a bog with 2ml of immunoblot stripping buffer (Thermo Fisher Scientific, Cramlington, Northumberland, UK) and allowed to incubate for 15min at room temperature rocking. After the membrane has been stripped, the membranes were washed twice with ddH2O for 1min, followed by once with TBS-Tween 20 for 5min. The membrane was then blocked for 1 hour and then reprobed with primary than with secondary and finally visualised with developing solution as described in section 2.8.3.

2.9. RNA Extraction

2.9.1. RNeasy Mini kit

RNA was extracted from cell pellets collected from section 2.1.6 using RNeasy Mini Kit (Qiagen). Cells were first homogenised by resuspension of the cell pellet in 350µl of RLT Buffer, containing 10% β- mercaptoethanol. The lysate was homogenised by passed through a 20 gauge needle ≥ 5 times. After, equal volume of 70% ethanol was added to each sample, than shaken vigorously for 15-30 seconds. The whole homogenate was added to an RNeasy spin column and centrifuge for 15 seconds at 8000 x g. After discarding the flow-through 700 µl Buffer RW1 was then added to the RNeasy spin column and centrifuge for 15 seconds at 8000 x g. The flow-through was then discarded and 500 µl Buffer RPE was then added to the RNeasy spin column and centrifuge for 15 seconds at 8000 x g. flow-through was removed and 500 µl Buffer RPE was then added to the RNeasy spin column and centrifuge for 2 minutes at 8000 x g. This step dries the spin column membrane, ensuring that no ethanol is carried over during RNA elution. Residual ethanol may interfere with downstream reactions. The RNeasy spin column was then placed onto a new 1.5 ml collection tube, were 40 µl of µl RNase-free water was added. This was followed by centrifugation at 8000 x g for 1 minute. RNA was stored at -20°C.

2.9.2. Quantification of RNA samples

A NanoDrop1000 spectrophotometer (NanoDrop Technologies, Wilmington, USA) was used to quantify RNA samples. Initially, 1µl of the solution used to elute RNA during preparation (RNase free water) was used as a reference for zero absorbance. 1µl of RNA sample was then added to the spectrophotometer. The NanoDrop was configured to read absorbance at 260nm and 280nm. NanoDrop output readings consisted of a 260/280 ratio and a ng/µl concentration. Purity of the DNA and RNA preparations was assessed using the 260/280 ratio; DNA was considered pure if the ratio was ~1.8 and RNA considered pure if the ratio was ~2.0. The spectrophotometer calculated the ng/µl concentrations using a modification of the Beer-Lambert equation that correlates absorbance with concentration: RNA concentration (ng/µl) = (A260 x e)/b, where:

A260=Absorbance at 260nm, e=extinction coefficient (ng-cm/ml), b=path length (cm).

RNA with an absorbance ratio at 260 and 280 nm (A260/A280) between 1.8 and 2.2 was deemed indicative of pure RNA. The presence of protein or phenol results in high absorption at 280nm, producing a lower A260/A280 ratio. A ratio at 260 and 230 nm (A260/A230) between 1.8 and 2.2 was also considered acceptable. Lower ratios indicated the carry-over of guanidinium salts.

2.10. Gene Expression Analysis

2.10.1.cDNA synthesis

cDNA was synthesise from 1µg per 20µlof total RNA using MultiScribe Reverse Transcriptase (Applied Biosystems, Cheshire, UK). All reactions were under sterile conditions. cDNA synthesis was performed according to the manufacturer's protocol.

Component	Volume (µL)
Nuclease free H_2O	3.2
10x RT buffer	2
25x dNTP mix (100nM)	0.8
10x RT random primers	2
RNase inhibitor	1
MultiScribe Reverse Transcriptase	1
Total	10

Samples were incubated at:

Temperature (°C)	Time (min)	
25	10	Preheating activation
37	120	Synthesis
85	5	Denaturation
4	∞	Hold

2.10.2.Real-time polymerase chain reaction (RT-PCR)

Real-time polymerase chain reaction (RT-PCR) was carried out on four selected genes to assess gene expression in cancer cell lines. Real-Time PCR used a SYBR green method from Bioline SensiFAST SYBR® & Fluorescein Kit (Bioline Reagents Ltd, London, UK). Briefly cDNA was synthesised from normal and cancer cell lines RNA and used in the real time assay.

Each sample were thoroughly mixed by vortex and pipetted in duplicated into a 96-well Multiplate™ Unskirted PCR Low-Profile plate (Bio-Rad, Herts, UK). Plates were sealed with optical Microseal® 'B' Adhesive Seals (Bio-Rad, Herts, UK). After the plates were centrifuged briefly and placed into a Bio-Rad CFX 96 Real Time Detection System (Bio-Rad, Herts, UK). PCR cycles used were as follows.

		Cycles	Temp	Time
1.	Polymerase activation	1	95°C	2 min
2.	Denaturation		95°C	5 sec
3.	Annealing	40	60°C	10 sec
4.	Extension (acquire at end of step)		72°C	15 sec

Melt curve:

55°C -95°C 10 seconds at each temperature point.

After each PCR run, an additional melt analysis was performed to assess the [Tm] of the PCR amplicon; this verified the specificity of the amplification reaction.

Primers	**Sequence (5'-3')**
Human luteinizing hormone/choriogonadotropin receptor	
LHCGR 3'	CAAGTGATAGTCGAGTGAGACCGGC
LHCGR 5'	AGCCGCAGAAGCCCAGTTCG
Human luteinizing hormone-releasing hormone receptor	
GnRHR 3'	CTGTCCGACTTTGCTGTTGC
GnRHR 5'	ATGCCACTGGATGGGATGTC
Interleukin-13 receptor subunit alpha-2	
IL-13Rα2	GGAGGGTTAACTTTTATACTCGGTGT

3'	
IL-13Rα2 5'	TAACCTGGTCAGAAGTGTGCC
β-Actin	
β-Actin 3'	AGGTCCAGACGCAGGATGGCATG
β-Actin 5'	CAGCCATGTACGTTGCTATCCAGG

Table 2.6.2 List of Primers used for this study.

Results were normalised on the basis of an endogenous RNA control, in this case the β-Actin. The data in this study was analysed using the ΔCt method of relative expression: the mean of threshold cycles (Ct) for normal tissue was subtracted from the Ct's of the experimental samples (including individual data for normal tissue) (ΔCt). The fold change of this difference was calculated by $2^{\Delta\Delta Ct}$.

2.10.3.Multiplex Real-time polymerase chain reaction (RT-PCR)

In this section, the primers and probes were selected using the mRNA sequences of IL-13α2, LHCGR, GnRHR and β-Actin from NCBI database. The sequences of primers and probes are summarized in Table 2.5, which were synthesized by Eurofins Genomics (Eurofins MWG Operon, Germany). The multiplex qPCR was carried out using Quanti-Tect Multiplex PCR No ROX Kit (Qiagen. 204743). The multiplex qPCR was optimised using a total reaction volume of 10μl. Master Mix was prepared according to the manufacturer's protocol. Primer and probe concentration for one reaction was set at 400nM and 200nM respectfully and the qPCR was carried out using a Bio-Rad CFX 96 Real Time Detection System (Bio-Rad, Herts, UK). Measurements for the target gene were normalised to produce a result of ΔCT (difference between target gene and β-Actin). Fold changes between the average of normal tissues (control) and the samples were quantified as $2^{-(\Delta CT\ sample-\Delta CT\ control)}$.

Primer	Sequence	Label	Concentration (μM)	Temp (°C)
IL-13Rα2-For	GGCATTGAAGCGAAGATACAC		100	57.9
IL-13Rα2-Rev	ATACGCAATCCATATCCTGAAC		100	56.5
IL-13Rα2-Probe	GGCAATGCACAAATGGATCAGAAGTTCAA	5'-FAM, 3 BHQ-1	100	
LHR-For	TCTACACCCTCACCGTCATC		100	59.4
LHR-Rev	AGCCATCCTCCAAGCATAATC		100	57.9
LHR-Probe	TCACCTGGACCAAAAGCTGCGATTAAGAC	5'-HEX, 3 BHQ-1	100	
GnRHR-For	GCCATCAACAACAGCATCC		100	56.7
GnRHR-Rev	GTCGCAGAGAGCAGAAAAAG		100	57.3
GnRHR-Probe	AACCTCCCCACTCTGACCTTGTCTGGAAA	5'-Cy5, 3 BHQ	100	
β-Actin-For	CACGAAACTACCTTCAACTCC		100	57.9
β-Actin-Rev	AGTGATCTCCTTCTGCATCC		100	57.3
β-Actin-Probe	TGGACATCCGCAAAGACCTGTACGCCAA	5'-RED, 3 BHQ	100	

Table 2.6.3 List of Primers used for multiplex RT-PCR.

The following thermal profile was used:

Step	Time	Temperature
PCR initial heat activation:	15 min	95°C
Denaturation	60 s	94°C
Annealing/extension	90 s	60°C
Number of cycles	**50-60**	

2.11. Enzyme linked immunosorbent assay (ELISA)

Cell surface expression was assessed by ELISA using unpermeablised cells (Kanamarlapudi et al, 2012b). 60-80 % confluency of cells were plated into poly-L-lysine (0.1 mg/ml in PBS) coated wells of a 48-well plate and allowed them to adhere to the surface of wells by incubating at 37°C/5% CO_2 in a humidified incubator. After 24h of incubation, cells were serum starved for 2 hours. The medium was aspirated, washed 3 times with SFM and then incubated with 100µl of SFM per well at 37°C/5% CO_2 in a humidified incubator. Cells were then fixed with 4% (w/v) paraformaldehyde for 5 min on a SSL4 see-saw rocker (Stuart, Standfordshire, UK). The PFA was then aspirated off and washed 3 times with TBS, followed by a 45 minute incubation with blocking buffer (1% bovine serum albumin [BSA] made in TBS [1% BSA/TBS]). Cells were then incubated with 100µl of anti-IL-13Rα2 mouse monoclonal (diluted 1:800 in 1% BSA/TBS) for 2 hours, rocking at room temperature. Cells were washed 3 times with TBS and then incubated with 100µl of HRP-conjugate anti-mouse IgG (diluted 1:5000 in 1% BSA/TBS) for 1 hour, rocking at room temperature. Cells were washed 3 times and developed by incubating with 100µl 1-step Ultra TMB-ELISA substrate (Bio-Rad) for 15 min. 30µl of the developed solution was transferred in triplicate to a 96-well plate and the reaction was stopped by adding equal volume of 2M H_2SO_4 (sulphuric acid). Absorbance of the reaction mixture was read at 450nm using a Biotek microplate reader (Northstar Scientific Ltd, Leeds, UK). The data was analysed to show the receptor expression compared to the control as a percentage (Thompson & Kanamarlapudi, 2014).

2.12. Cell Viability Assay

Cell viability was assessed using alamar blue assay. Cells were plated into 96-well μclear half area black plate and incubated at 37°C/5% CO_2 in a humidified incubator. After 24 hours, the medium was replaced with complete medium containing 10% (v/v) alamar blue The fluorescence of the medium was read after 30 min incubation (considered as zero) and every 3 hours afterwards. The fluorescence was assessed at 570nm (excitation) and 630nm (emission) using a POLAR star Omega microplate reader (BMG Labtech, Buckinghamshire, UK). Each concentration was performed in duplicates with 3 independent cell preparations

2.13. Cytotoxicity Assay

Cell cytotoxicity was assessed using CellTox™ Green Cytotoxicity Assay (Promega). Cells were plated into 96-well μclear half area black plate and incubated at 37°C/5% CO_2 in a humidified incubator. After 24 hours, the medium was replaced with FSM containing 0.1% (v/v) CellTox Green Dye and a set concentration of test compound incubated with cells at 37°C/5% CO_2. The fluorescence of the medium was read after 30 min incubation (considered as zero). The fluorescence was assessed at 490nm (excitation) and 525nm (emission) using a POLAR star Omega microplate reader (BMG Labtech, Buckinghamshire, UK). Each concentration was performed in duplicates with 3 independent cell preparations.

2.14. Cell viability, cytotoxicity and apoptosis assays

Cell viability, cytotoxicity and apoptosis of cells were determined by ApoTox-Glo ™ Triplex Assay (Promega), according to the manufacturer's protocol. Cells were plated into 96-well μclear half area black plate and incubated at 37°C/5% CO_2 in a humidified incubator. After 24 hours, the medium was replaced with complete medium containing test compound. After 6 hours of incubation at 37°C/5% CO_2. Cell viability and cytotoxicity was determined by adding 10μl of glycylphenylalanyl-aminofluorocoumarin (GF-AFC) substrate and 10μl of bis-alanylalanyl-phenylalanyl-rhodamine 110 (bis-AAF-R110) substrate to 2 ml of assay buffer. 10μl of the cell viability and cytotoxicity reagent was added to each test well and controls. The plate was then placed in the incubator for 1 hour at 37°C/5% CO_2. Cell viability was measured at 400 nm (excitation) and 505 nm (emission). Cytotoxicity was measured at 485 nm (excitation) and 520 nm (emission). Apoptosis was determined by adding 10ml

Caspase-Glo 3/7 buffer to Caspase-Glo 3/7 substrate to form Caspase-Glo 3/7 reagent. 50 µl of the reagent was added to all test wells and allowed to incubate for 30 min at room temperature, after luminescence was measured. All readings were taken using a POLAR star Omega microplate reader (BMG Labtech, Buckinghamshire, UK). Each concentration was performed in duplicates with 3 independent cell preparations.

2.15. Cell Transfection

Cells were transfected with expression plasmid FLAG-IL13Rα2 (Daines et al, 2006) or Myc-LHCGR (Kanamarlapudi et al, 2012b) or an empty control plasmid (pcDNA3) using JetPRIME transfection reagent (Polyplus) according to the manufacturers' instructions. HEK293 cells were grown plated on the appropriate tissue culture dish and placed in a 37°C/5% CO_2 humidified incubator. After 24 hours, the appropriate volume of JetPRIME buffer. 2-4 µg of plasmid DNA was diluted in JetPRIME buffer and the appropriate volume of JetPRIME transfection reagent (2 µl/µg DNA) was added to it, which then incubated at room temperature (RT) for 15 min. The DNA-JetPRIME mixture was added drop wise to the cells grown to 60-80 confluent plate, gently rocked the cell culture plate to mix and incubated the culture plate at 37°C/5% CO_2 in a humidified incubator. 1 day after transfection, the medium was replaced. The cells were used for experimentation 2 days after transfection.

2.16. Generating Spheroids

2.16.1. Functional Assays

Monolayer cells were detached with 1x Trypsin / EDTA to generate a single cell suspension. The cell suspension was diluted to 1x105/ml. 20µl of the diluted cells was pipetted onto Terasaki plate (Greiner bio-one), rotated 180° and allowed to incubate for one day at a setting of 5% CO2 humidified atmosphere at 37°C to generate a spheroid. Day one the spheroids were extracted from the Terasaki plate and pipetted into single wells of U-bottom surface repellent, 96 well plates (CELLSTAR Greiner bio-one), and grown in incubator at a setting of 5% CO2 humidified atmosphere at 37°C for a further 24hours. The media was replaced supplemented with 0.1% (v/v) CellTox™ Dye with test compound and allowed to incubate for 15min at a setting of 5% CO2 humidified atmosphere at 37°C. The resulting fluorescence

was read on a plate reader at every 3 hours were the fluorescence was detected at 490 nm (excitation wavelength) and 525 nm (emission wavelength) using a microplate reader for fluorescence (POLARstar).

2.16.2. Generation of spheroids using Matrigel

Monolayer cells were detached with 1x Trypsin / EDTA to generate a single cell suspension. The cell suspension was diluted to 1x105/ml. The cells were than stained green using the fluorescent vital membrane dye Vybrant DiO (Molecular Probes) at a dilution of 1 in 200 for 10 minutes. The labelled cells were then centrifuged at 350xg for 5 minutes. The supernatant was then removed and resuspended in warm media. 20µl of the labelled cells was pipetted onto Terasaki plate (Greiner bio-one), rotated 180° and allowed to incubate for 24 hours at a setting of 5% CO2 humidified atmosphere at 37°C to generate a spheroid.

On day zero, reconstituted basement membrane (rBM; Matrigel™ BD Biosciences) was thawed on ice overnight and added at a final concentration of 50% (v/v) with ice cold media and pipetted into a 96 well fluorescence plate (Greiner bio-one). After 24 hours the spheroids were extracted from the Terasaki plate and pipetted into the Matrigel and allowed to incubate for 3 hours with or without test compound. Cell viability was assessed using LIVE/DEAD staining (Invitrogen). Samples were incubated in serum-free, phenol red-free medium containing 2 µM ethidium homodimer I at room temperature for 40 minutes. Spheroids were then washed three times with serum-free, phenol red-free medium and immediately imaged using confocal microscopy LSM 510 microscope (Carl Zeiss, Inc).

2.17. Statistical Methods

2.17.1. Student's t-test

Student t-test was used to test the significance of two means. Student's t-test were carried out in GraphPad and in all cases were two-tailed, two sample unequal variance. $P<0.05$ was considered significant.

2.17.2. ANOVA

One –way ANOVA was used to measure variance between more than two means, using GraphPad. Significance was taken as $p<0.05$.

3. Differential expression of IL-13Rα2, LHCGR, and GnRHR and in normal and malignant human tissues

3.1. Introduction

Cancer is one of the most leading causes of human death in both developed and developing countries. Every year, approximately 15 million people are diagnosed with cancer world-wide and half of them die with cancer (Jemal et al, 2011). In the UK, about 300,000 are diagnosed with cancer every year and the most prevalent cancers are lung, bowel and gender specific breast and prostate, which accounts for 50% of the cases (Jemal et al, 2011). Cancer is a disease, which defined as an uncontrolled growth, resistance to antigrowth signals, apoptotic evasion, unlimited replicative potential, angiogenesis and invasion/metastasis (Jemal et al, 2011). The spread of caner from the primary tissue to invade neighbouring and distant organs (secondary tissues) is often termed as cancer metastasis. Metastasis is the process by which the cancer cells with an invasive phenotype invade to and through the lymphatic or circulatory system (Jemal et al, 2011). Patients who have been diagnosed with cancer are treated with anticancer drugs to prevent both relapse (the return of the tumour cells at the site of origin) and metastasis (Ruggiero et al, 2010). Conventional treatments have prolonged the lives of patients with cancer; however they are not a cure. Given that the majority of cancer related deaths are due to metastatic disease, it is essential for the identification of prognostic and predicative markers that may modulate metastasis and for therapeutic evaluation of anti-cancer compound targets (Parhi et al, 2012; Ruggiero et al, 2010).

The tumours are normally graded from scale I-IV base on the guidelines from the American Joint Committee on Cancer (AJCC) staging system. The tumours are graded based on the tumour size, lymph node involvement and level of metastasis. By staging the cancer, it is possible to identify the severity of the patient's cancer. This will influence the appropriate treatment for the patient. Low stage cancers (stages I and II) are considered benign. These types of cancers are located on the primary organ and never spread to other parts of the body. High stage cancers (stages III and IV) are considered as regional and distant. These types of cancers spread beyond the primary organ and invade to nearby lymph nodes or tissues and

organs. Cancers can also be classified based on their histopathological assessments which correlate with the disease aggressiveness and patient outcome (Jemal et al, 2011). For example, the Gleason grading is the most common grading system for prostate cancer. This scoring is based on their gland architecture indicating the aggressiveness of the cancer. By using the scale of 6-9, the tumour grade can be scored based on the level of differentiation of the cells, with well differentiated cells having a low grade and poorly differentiated tumours having a high grade and being aggressive (Jemal et al, 2011). The Nottingham grade is a well-established method in providing prognostic information of breast cancers, by grading its severity and the prognosis of cancers (UK, 2009). The scale ranges from 1-3, combining nodal status, tumour size and histological grade.

The targeting of cell surface receptors that are specifically or over expressed in cancer cells has painted a new insight in anti-cancer therapy. The importance of three such receptors (gonadotropin-releasing hormone receptor [GnRHR], luteinizing hormone/chorionic gonadotropin hormone receptor [LHCGR] and interleukin 13 receptor α2 [IL-13Rα2]) as targets for cancer treatment and diagnosis has gathered a lot of interest (Dharap et al, 2005). During the past 20 years, several studies have shown elevation of LHCGR as well as GnRHR expression in prostate, breast and uterine cancers (Ji et al, 2002; Lojun et al, 1997; Tao et al, 1997b). However, the expression of LHCGR and GnRHR in peripheral organs is relatively low, making them potential drug targets (Ziecik et al, 2007). Similarly IL-13Rα2 has been shown to be overexpressed in several cancers such as brain tumours, breast and prostate cancer (Fujisawa et al, 2009; Gonzalez-Moreno et al, 2005; Jarboe et al, 2007; Kawakami et al, 2003; Kioi et al, 2006a; Kioi et al, 2006b; Puri et al, 1996; Zhao et al, 2014). In this chapter, we concentrated our efforts in analysing the expression of the three receptors LHCG, GnRH and IL-13Rα2. Therefore these receptors discussed further below.

3.1.1. GnRHR

GnRHR belongs to the glycoprotein hormone receptor subfamily of G protein-coupled seven-transmembrane domain receptor (GPCR) superfamily (Grundker & Emons, 2003). Studies have shown that most tumours overexpress GnRHR (Tammela, 2004). The typical characteristic of GPCRS such as GnRHR is their tendency to work via secondary messenger signalling pathways, including those mediated by cyclic AMP (cAMP), diacylglycerol (DAG) and calcium (Ca^{2+}), to exert activation or inactivation of downstream signalling proteins (Grundker & Emons, 2003). GPCRS are also known as seven-transmembrane domain (7-TM) or heptahelical receptors. The receptor contains a seven α helical membrane

spanning domains, which are connected through three extracellular and three intracellular loops (Arora et al, 1995). In addition, many GPCRs contain an amino-terminal extracellular ligand binding domain and a carboxyl-terminal intracellular domain required for binding to the signalling proteins. The general mechanism for GPCRS activation involves the binding of the ligand to the extracellular domains, followed by a conformational change in the intracellular portions of the helices. The activated GPCR then causes a propagation of the signal by binding to hetero-trimeric G-proteins and thereby elevating the levels of second messengers such as cAMP, Ca^{2+} etc. (Grundker & Emons, 2003).

GnRHR detected in breast and ovarian cancers has shown to be structurally identical to the receptor (showing the same nucleotide sequence) located in the pituitary gland (Millar et al, 2001). However, GnRHR located in the pituitary gland is functionally different from that expressed in breast and ovarian cancers (Millar et al, 2001). This is because GnRHR expressed in pituitary gland has high affinity for GnRH agonist whereas the receptor over expressed in most cancers has low affinity for the agonist (Moretti et al, 2002; Szende et al, 1991).

Miller et al. first reported in 1985 that 85% of human prostate cancer specimens had a high affinity for the GnRH analogue Decapeptyl (Miller et al, 1985). The incidence rate for GnRHR overexpression was found to be near 80% in epithelial ovarian cancers and over 50% in breast cancers including triple-negative breast cancer (Engel et al, 2012a; Leung & Choi, 2007). Endometrial carcinoma specimens show similar rate of expression (Engel et al, 2012a). GnRHR mRNA overexpression was also found in endometrial, ovarian and prostate cancer. This evidence was backed up by analysing GnRHR protein levels, by using immunohistochemistry, in these tissue types (Curtis et al, 2014). Breast, endometrial, ovarian and prostate cancers are associated with the reproductive organs that in turn are affected by the pituitary/gonadal axis. Interestingly GnRHR has also shown to be expressed in non-reproductive organs associated cancers (Limonta et al, 2003; Nagy & Schally, 2005). These cancers include oral and laryngeal cancers (Krebs et al, 2002), renal cell carcinomas (Sionvardi et al, 1992), brain tumors (van Groeninghen et al, 1998), melanomas (Moretti et al, 2002), liver cancers (Pati & Habibi, 1995), ductal pancreatic carcinomas (Friess et al, 1991) and adenocarcinomas of the colon (Ben-Yehudah & Lorberboum-Galski, 2004). However, the expression of GnRHR is relatively low in normal prostate, testes, breast, and ovary or absent in normal non-reproductive tissues. These findings indicate alterations in GnRHR expression in many cancers and therefore can be used as a target for cancer diagnosis and therapy (Nagy & Schally, 2005).

Recently an isoform of GnRH ligand (GnRH-II) with a higher anti-proliferative property has been identified in ovarian and endometrial cancers (Bedecarrats & Kaiser, 2003; Kang et al, 2000). The native receptor for GnRH-II is still unknown. However, Wu et al reported the ability of GnRH-II in promoting cell migration and invasion of endometrial cancer -by activating ERK1/2 and JNK pathways through GnRHR (Wu et al, 2013). The identification of GnRH-II in human tissues has led to a search for its receptor in human tissues. In one study, GnRH antagonists have been shown to behave differently in tumour tissue, where GnRH antagonists have agnostic effects. Furthermore, another receptor, instead of GnRHR, mediating anti-proliferative effects of cetrorelix, a GnRH antagonist, on endometrial and ovarian cancer cells has been identified (Grundker et al, 2004). However, it is not yet known whether the cetrorelix effects mediating receptor act as the receptor for GnRH-II or not.

3.1.2. LHCGR

LHCGR is also a GPCR that is characterised by a large N-terminal extracellular domain with high-affinity for its native ligands LH and CG (Ziecik et al, 2007). LHCGR plays an important role in reproductive biology in male and females. The receptor is mainly expressed in gonadal somatic cells, where its physiological role is only confined to its actions in the testes and ovaries (Rivero-Muller et al, 2007). Gonadal somatic tumour cells are rare but very difficult to diagnose, and therefore come under fatal groups of malignancies. Testicular tumours are the most common malignancy in men between 15-34 years of age (Schwartz, 2002). Ovarian carcinomas are often called the "silent killer". This is because they are difficult to detect and often diagnosed in the late stages (stage III or IV) (Schwartz, 2002). Majority of human ovarian cancers are epithelial tumours, and approximately 70% of them show high expression of LHCGR. In breast cancer, there is overwhelming evidence to suggest that 72% of human breast cancers overexpress LHCGR (Lojun et al, 1997). LHCGR has also been found to show increase in expression levels in prostate cancer (Tao et al, 1997b). The development of LHCGR targeted anti-cancer drugs could lead to a more efficacious therapy for many human cancers.

3.1.3. IL-13Rα2

IL-13Rα2 is a monomeric receptor of IL-13 cytokine, which plays an important role in allergic inflammation in many tissues. This receptor affinity to IL-13 is higher than that of the other IL-13 receptor IL-13Rα1. It shares 37% homology at protein level with IL-13Rα1 but does not bind to IL-4 receptor (Andrews et al, 2002). It is considered as a negative regulator or decoy receptor of IL-13 because it lacks any motifs required to mediate signal transduction

(Pandya et al, 2012).IL-13Rα2 has been shown to be overexpressed in cancers such as human paediatric brain tumors, brainstem glioma, renal cell carcinoma, squamous cell carcinoma of head and neck, ovarian cell carcinoma, prostate carcinoma, breast cancer and also in pancreatic cancer (Joshi et al, 2008). In ovarian cancer, 83% of specimens found to show overexpression of IL-13Rα2 (Kioi et al, 2006a). In grade IV glioblastoma multiforme (GBM), 75% patients have been found to show overexpression of IL-13Rα2 (Kioi et al, 2006a). This is a relatively new target that has been associated with cancer invasion and metastasis. A cytotoxic drug composed of IL-13 conjugated with a modified bacterial toxin (*Pseudomonas* exotoxin) has undergone phase III clinical trials for targeting GBM, which overexpress IL-13Rα2.

There is an over whelming evidence to suggest that different cancer types show increase in the expression of GnRHR, LHCGR and IL-13Rα2. Whether the alterations in the expression of these receptors wide spread or not are still unknown. So there is a need for analysis of these receptors expression in cancers over a wide range of tissues. In this chapter, an Origene's TissueScan Cancer Survey cDNA array (381 samples covering 18 different cancers) was used to investigate the expression of GnRHR, LHCGR and IL-13Rα2 genes by qPCR. GnRHR mRNA expression found to be significantly increased in breast, pancreatic and prostate cancer. Similarly, LHCGR gene expression was increased in breast, endometrial and prostate cancer and decreased in kidney cancer. IL-13Rα2 mRNA expression was also found to be significantly increased in breast, pancreatic and prostate cancers and decreased in stomach cancer

3.2. Materials and Methods

All reagents were obtained from Sigma, unless otherwise stated.

3.2.1. Multiplex Real-time polymerase chain reaction (RT-PCR)

In this section, the primers and probes were selected using the mRNA sequences of IL-13α2, LHCGR, GnRHR and β-Actin from NCBI database. The sequences of primers and probes are shown in Table 3.2.1, which were synthesized by Eurofins Genomics (Eurofins MWG Operon, Germany). The multiplex qPCR was carried according to the manufacturer's protocol out using Quanti-Tect Multiplex PCR No ROX Kit (Qiagen. 204743). The multiplex qPCR was performed in a final volume of 10μl containing 400nM primer and 200nM probe, and using a Bio-Rad CFX 96 Real Time Detection System (Bio-Rad, Hercules, CA, USA). The data in this study was analysed using the ΔCT method of relative expression: the mean of

threshold cycles (Ct) for normal tissue was subtracted from the Ct's of the experimental samples (including individual data for normal tissue) (ΔCt). The fold change of this difference was calculated by $2^{\Delta\Delta Ct}$.

For clinical validation, the TissueScan Cancer cDNA Array was used (OriGene). Quantitative PCR was conducted on these samples using the same Quanti-Tect Multiplex reagent as mentioned above. List of Primers used for multiplex RT-PCR are listed in section 2.10.3

3.2.2. Statistical Analysis

The non-parametric Mann-Whitney statistical test was used to calculate statistical significance of the data. Statistical analyses were performed using GraphPad Prism (v5.0) software, with data shown as mean ± standard error of mean (SEM). Statistical significance was defined as a p-value of ≤ 0.05, signifying a 5% or lower probability of the data occurring by chance.

3.3. Results

3.3.1. Expression analysis of GnRHR in normal tissues and cancers

There have been a number of studies linking alteration in GnRHR gene expression to cancer (Engel et al, 2012a). The overexpression of GnRHR mRNA has been found in many tumours including that of ovarian, endometrial, prostate and breast, while its gene expression in healthy tissues is relatively low (Engel et al, 2012a). However, there is a dearth of data concerning the expression of GnRHR at mRNA level in cancers over a wide range of tissues. In order to rectify this deficit, the expression of GnRHR was analysed in wide range of normal tissues and cancers using an OriGene TissueScan Cancer qPCR array, which contain cDNA, pre-normalised to housekeeping gene β-actin expression, of 18 different cancers and corresponding normal tissues.

GnRHR mRNA expression was analysed in all normal tissues to begin with (Figure 3.3.). The lowest expression of GnRHR mRNA was found in kidney tissue and the highest expression was seen in stomach. Overall the expression of GnRHR mRNA in normal tissues was low. When compared to the expression levels in kidney, GnRHR mRNA levels were <2-fold higher in breast, cervix, endometrium, oesophagus, liver, lung, lymphatic tissue, prostate, and testis (low expression). The expression levels were found to be <10-fold higher in ovary, pancreas, thyroid, bladder, and uterus (moderate expression) and <400-fold higher in colon and stomach (high expression).

GnRHR mRNA expression in cancer tissues was then analysed and compared to that in corresponding normal tissues (Figure 3.4.). A large number of cancer tissues (breast, cervix, colon, endometrium, kidney, liver, lung, lymphoid tissue, ovary, pancreas prostate, testis, thyroid gland, urinary bladder, and uterus) showed elevated GnRHR mRNA levels. The highest up-regulation (>1000 fold) in GnRHR expression was found in lung, ovarian, and pancreatic cancer tissue. Tissues that shown moderate levels of GnRHR mRNA (>100 fold) were breast, colon, liver, prostate, testis and bladder cancer. Tissues that expressed relatively low levels of GnRHR mRNA (<100) were adrenal, cervix, endometrium, oesophageal, kidney, lymphoid, stomach, and thyroidal cancers. The lowest expression was found in oesophageal cancer (0.169 ± 0.07 SD fold that of corresponding normal tissue).

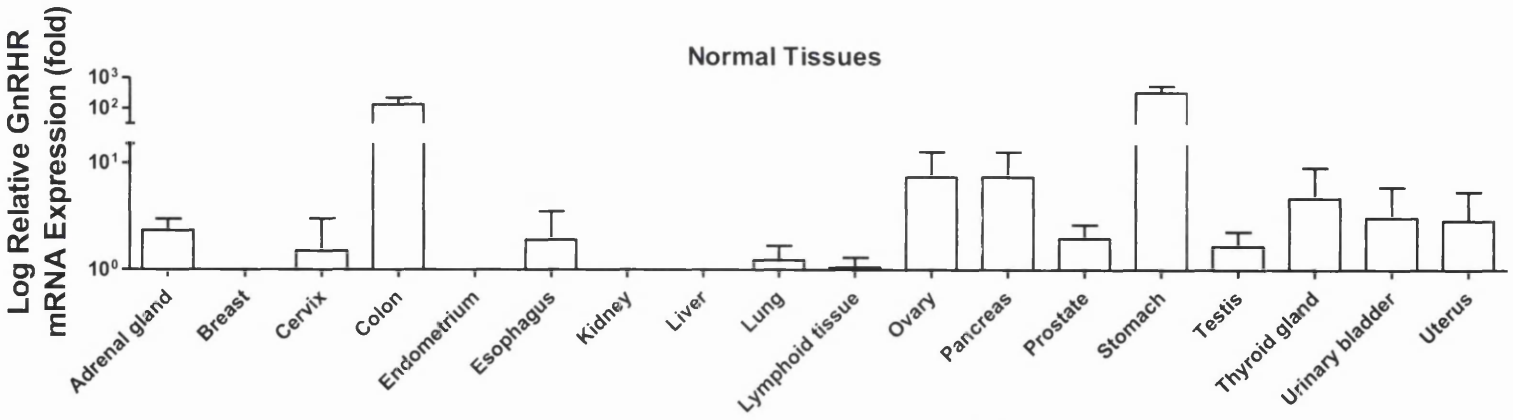

Tissue	Number of Samples	Mean Fold Change	SEM	p value	Average Ct
Adrenal gland	3	2.333	0.641	0.653	21.00
Breast	2	1.987	0.79	0.358	24.66
Cervix	2	1.5	1.5	0.795	32.67
Colon	7	127.7	88.49	0.004	16.38
Endometrium	2	1.76	0.44	0.753	27.84
Esophagus	2	1.905	1.625	0.963	25.72
Kidney	1	1	0	NA	49.00
Liver	1	1	0	NA	49.00
Lung	4	1.237	0.463	0.452	39.61
Lymphoid tissue	3	1.062	0.257	0.068	46.14
Ovary	3	7.76	5.1	0.409	26.31
Pancreas	3	7.443	5.212	0.406	26.58
Prostate	5	1.974	0.682	0.562	24.82
Stomach	4	316	201.3	0.345	10.16
Testis	6	1.672	0.628	0.505	29.31
Thyroid gland	3	4.7	4.4	0.602	16.43
Urinary bladder	2	3.09	2.92	0.773	15.86
Uterus	3	2.9	2.536	0.757	16.90

Figure 3.3. Expression of GnRHR in Human Tissues. The relative levels of GnRHR mRNA in 18 normal tissues cDNA array were assessed by qPCR using primers specific for *GnRHR* gene. After normalising the expression levels to β-*Actin,* GnRHR mRNA levels were calculated as folds relative to that in the lowest expressing tissue (Kidney). P-values given where fold change exceeded two fold. Data is shown as mean ± SEM (Error bars represent Standard Error of Mean). *P-value ≤0.05 was considered as statistically significant.

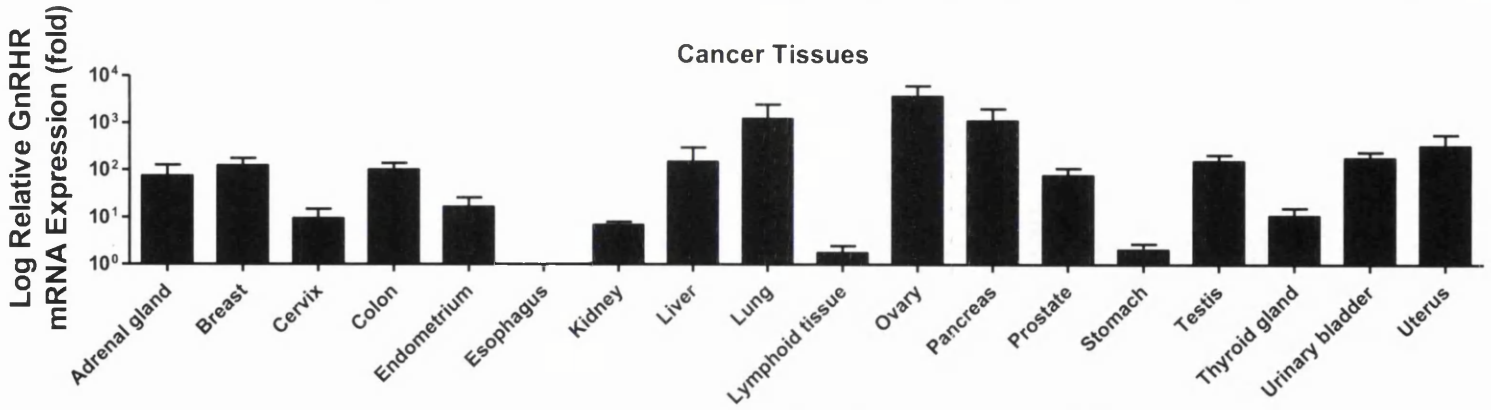

Tissue	Number of Samples	Mean Fold Change	SEM	p value	Average Ct
Adrenal gland	8	74.81	53.27	0.203	24.87
Breast	9	122.7	52.83	0.049	20.67
Cervix	8	9.426	5.454	0.128	35.67
Colon	13	101	38.39	0.022	19.38
Endometrium	17	16.56	9.369	0.097	30.84
Esophagus	18	0.169	0.065	NA	48.45
Kidney	11	6.816	1.199	0.04	40.64
Liver	22	150	148.7	0.323	21.34
Lung	12	1229	1222	0.337	13.64
Lymphoid tissue	26	1.757	0.716	0.222	49.14
Ovary	21	3645	2311	0.13	24.43
Pancreas	17	1096	905.2	0.244	21.75
Prostate	21	106.79	31.69	0.025	27.82
Stomach	14	2.049	0.697	NA	45.23
Testis	19	154.1	57.37	0.015	24.67
Thyroid gland	18	10.7	5.003	0.048	43.87
Urinary bladder	22	181.5	57.95	0.005	18.86
Uterus	2	320.1	235.7	0.404	13.23

Figure 3.4. Expression of GnRHR in Human cancers. The relative levels of GnRHR a cancer tissue cDNA array were analysed by qPCR. GnRHR mRNA levels in each cancer tissue were calculated relative to the corresponding normal tissue. P-values given where fold change exceeded two fold. Data is shown as mean $\pm$ SEM (Error bars represent Standard Error of Mean). *P-value ≤ 0.05 was considered as statistically significant.

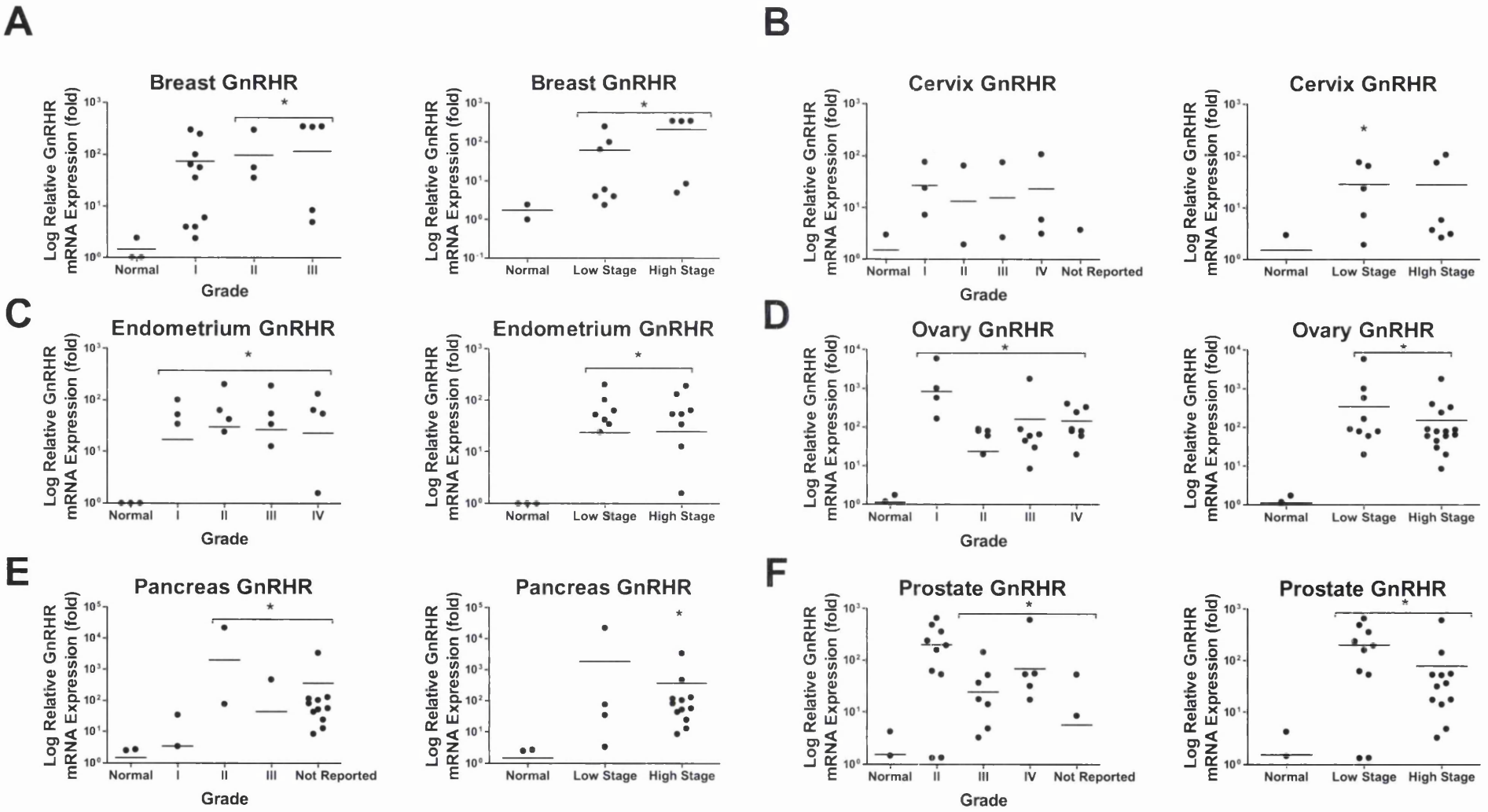

Figure 3.5. Expression of GnRHR associated with Grade of Human Tissues. GnRHR mRNA expression data separated by stage of cancer in breast (A), cervix (B), endometrium (C), ovary (D), pancreas (E), and prostate (F). The data is displayed as a dot plot with mean ± SEM (mean shown as —). GnRHR mRNA levels were calculated as folds in each stage relative to that in normal tissue. *P-value ≤0.05 was considered as statistically significant.

Cancer stage dependent alterations in GnRHR expression

The alternations in GnRHR mRNA expression in breast, cervical, endometrium, ovarian, pancreas, and prostate cancers were explored further by separating the expression data based on the stage of cancer (Figure 3.5. A-F). The results are displayed as dot plots.

In breast cancer, GnRHR expression showed a significate increase in both low and high stages of the cancer when compared to its expression in corresponding normal tissue (Figure 3.5. A). Statistical significance was found between the low and high stages of cancer (P=0.0.43 and 0.047 respectively). In addition, we divided the data further into four stages (I-III) of cancer and compared the results against each other. The results demonstrated statistical significance when compared to the different stages in stages II and III (P=0.045 and 0.048 respectively). However the results do show an increase in GnRHR expression in all three stages. This suggests that there is a strong connection between GnRHR expression and breast cancer. Our data is also in line with the studies that have been published before (Engel et al, 2012a; Li et al, 2014; Limonta et al, 2012).

In cervical cancer, GnRHR mRNA expression in both low and high stages showed an up-regulation (Figure 3.5. B). However only low stage of the cancer showed any statistical significance (p= 0.035). When the samples were further divided into stages of cancer, we can see an up-regulation in all four stages of cancer. However stages II and III are under-represented with only one data set.

In endometrial cancer, both low and high stages of cancers showed an up-regulation of GnRHR mRNA expression compared to normal tissue (Figure 3.5. C). A mean fold change observed was 23.59 in low stage and 24.78 in high stage; there was statistical significant difference in GnRHR mRNA expression between tumour and non-tumour tissues (P=0.041 and 0.036 respectively).

Ovarian cancer again showed an up-regulation of GnRHR mRNA expression in low and high stages when compared to the normal tissues (Figure 3.5. D).The expression in low stage of cancer showed a higher statistical significance than that in the high stage (P=0.034 and 0.043 respectively). When the samples were further divided into stages of cancer, stage I, II, III and IV showed any statistical significance [$P \leq 0.05$].

Pancreatic cancer showed an overall increase in GnRHR mRNA levels. Both the low and high stages of cancer showed increase in the expression of GnRHR. However, only the up-regulation in high stage of pancreatic cancer was statistically significant (Figure 3.5. E).The

lack of statistical significance between normal and low stage cancer may be due to the lack of enough samples in low stage cancer.

In prostate cancer, GnRHR showed up-regulation at mRNA level in both low and high stages of cancer when compared to that in normal tissues. The alterations in the gene expression of GnRHR in both stages were statistically significant [P =0.032] (Figure 3.5. F). However, the impact of stage IV cancers was minimal to this data set as there was only one tissue sample compared to seven tissue samples in stage III and eleven samples in stage II cancers. This meant that stage IV data set had no impact on statistical significance of high stage cancer results. However overall, GnRHR mRNA expression is up-regulated in prostate cancer.

Cancer Grade dependent alterations in GnRHR gene expression

Prostate and breast cancers can also be graded based on their histopathological assessments which correlate with the disease aggressiveness and patient outcome. Therefore the cancer grade dependent changes in the expression of GnRHR mRNA in prostate and breast cancer tissues were also explored.

The Gleason grading is the most common grading system for prostate cancer. This scoring is based on its gland architecture indicating the aggressiveness of the cancer (Figure 3.6. A). Overall there is no statistical connection between GnRHR mRNA expression and the Gleason score in this study.

The Nottingham grade is a well-established method in providing prognostic information of breast cancers, by grading its severity and the prognosis of cancers (Figure 3.6. B).The data was characterised by favourable and unfavourable prognosis. The 'moderately favourable' category showed no statistically significant difference in expression of GnRHR mRNA when compared to that in the 'unfavourable' category. However this could be explained by the limited number of data sets in the array.

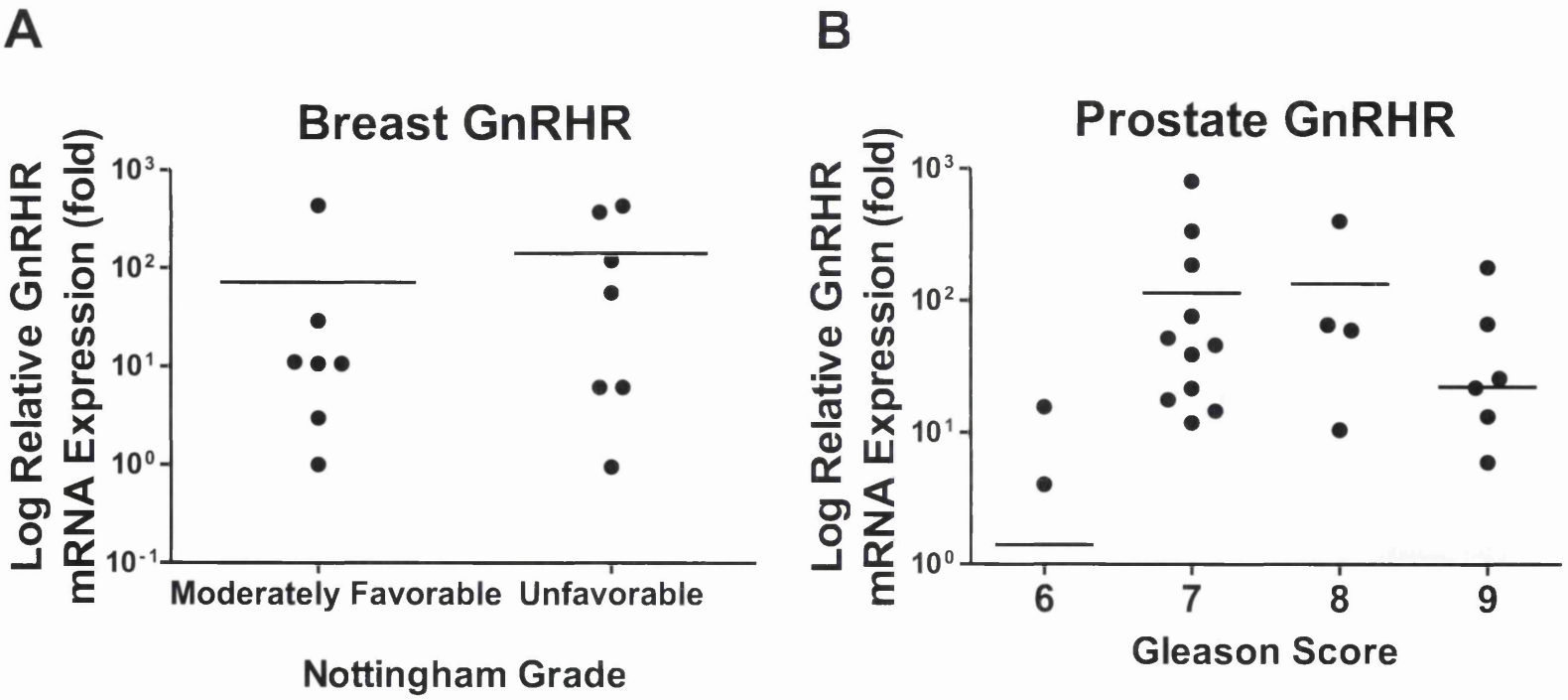

Figure 3.6. Expression of GnRHR associated with breast and prostate tissue sample scores. GnRHR mRNA expression data in breast cancer by Nottingham Grade (A) and in prostate cancer by Gleason score are. GnRHR mRNA levels were calculated relative to the each cancers representing normal tissue. Data is shown as mean ± SEM (Error bars represent Standard Error of Mean).

3.3.2. Expression analysis of LHCGR mRNA in normal tissues and cancers

The LHCGR gene expression has been shown to be up-regulated in a number of cancers, including breast, uterine, ovarian and prostate cancers (Ziecik et al, 2007). Here the gene expression of LHCGR was analysed globally using a TissueScan Cancer qPCR array.

As mentioned before for GnRHR, LHCGR expression was analysed first in all normal tissues (Figure 3.7.). The lowest expression of LHCGR mRNA was found in kidney, and the highest expression was in lymphatic tissue. Overall the LHCGR gene expression in normal tissues was low, however due to smaller sample size and full conclusion cannot be made. When compared to its expression in kidney, LHCGR mRNA expression levels were <10-fold in adrenal gland, breast, endometrium, oesophagus, kidney, liver, lung, pancreas, prostate, stomach, testis, thyroid, and bladder. Moderate expression (<70-fold) was found in cervix, colon, ovary, and uterus; and highest expression (<250-fold) of LHCGR mRNA expression was observed in lymphatic tissue. However no statistical significance was found in any of the samples.

LHCGR mRNA expression in cancer tissues again was compared to that of corresponding normal tissues (Figure 3.8.). A large number of cancer tissues (adrenal gland, breast, cervix, colon, kidney, liver, lymphoid tissue, ovary, pancreas prostate, stomach, testis, thyroid gland, urinary bladder, and uterus) showed elevated LHCGR mRNA expression. Highest up-regulation (>1,000 fold) in LHCGR expression was found in ovarian cancer tissue whereas the lowest increase (<1 fold) was found in kidney cancer tissues.

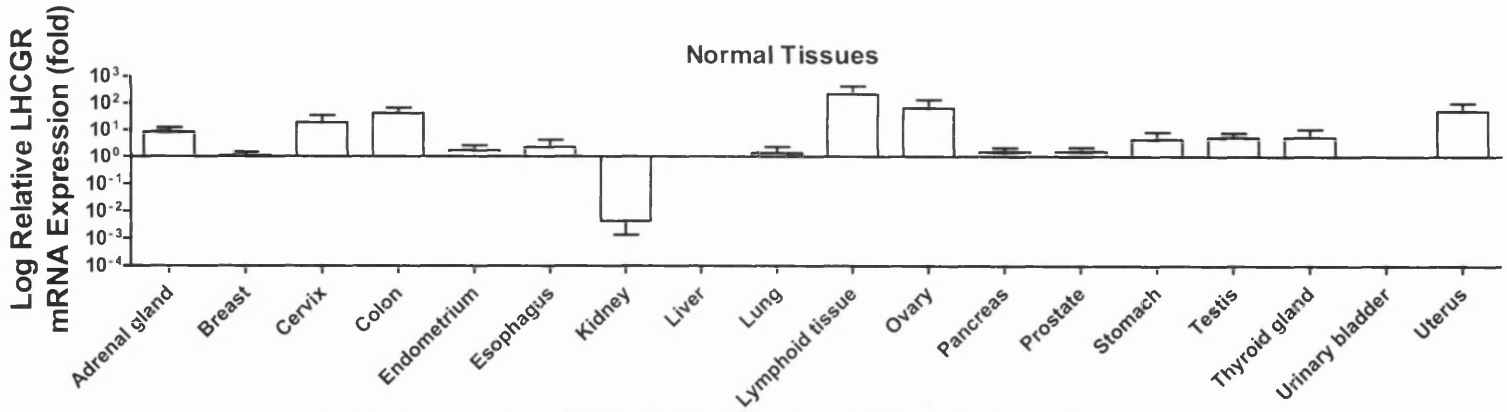

Tissue	Number of Samples	Mean Fold Change	SEM	p value	Average Ct
Adrenal gland	5	8.22	4.14	0.21	49.45
Breast	2	1.08	0.4	0.26	48.45
Cervix	4	18.54	17.54	0.42	43.32
Colon	7	41.44	26.52	0.19	35.65
Endometrium	3	1.7	1	0.79	48.87
Esophagus	2	2.24	2	0.92	45.25
Kidney	3	0.03	0.001	NA	49.84
Liver	1	1	0	NA	49.24
Lung	2	1.39	0.96	0.64	49.86
Lymphoid tissue	3	207.3	205.1	0.42	25.35
Ovary	3	64.69	63.78	0.43	29.79
Pancreas	4	1.49	0.63	0.48	47.43
Prostate	5	1.53	0.69	0.54	45.75
Stomach	4	4.38	3.8	0.58	48.42
Testis	5	5.15	2.59	0.29	45.87
Thyroid gland	3	5.33	5.08	0.58	46.76
Urinary bladder	1	1	0	NA	43.53
Uterus	3	47.17	47.07	0.44	43.46

Figure 3.7. Expression of LHCGR in Human Tissues. The relative levels of LHCGR mRNA in 18 normal tissues cDNA array were assessed by qPCR using primers specific for *LHCGR* gene. After normalising the expression levels to β-*Actin,* LHCGR mRNA levels were calculated as folds relative to that in the lowest expressing tissue (Kidney). P-values given where fold change exceeded two fold. Data is shown as mean ± SEM (Error bars represent Standard Error of Mean). *P-value ≤0.05 was considered as statistically significant.

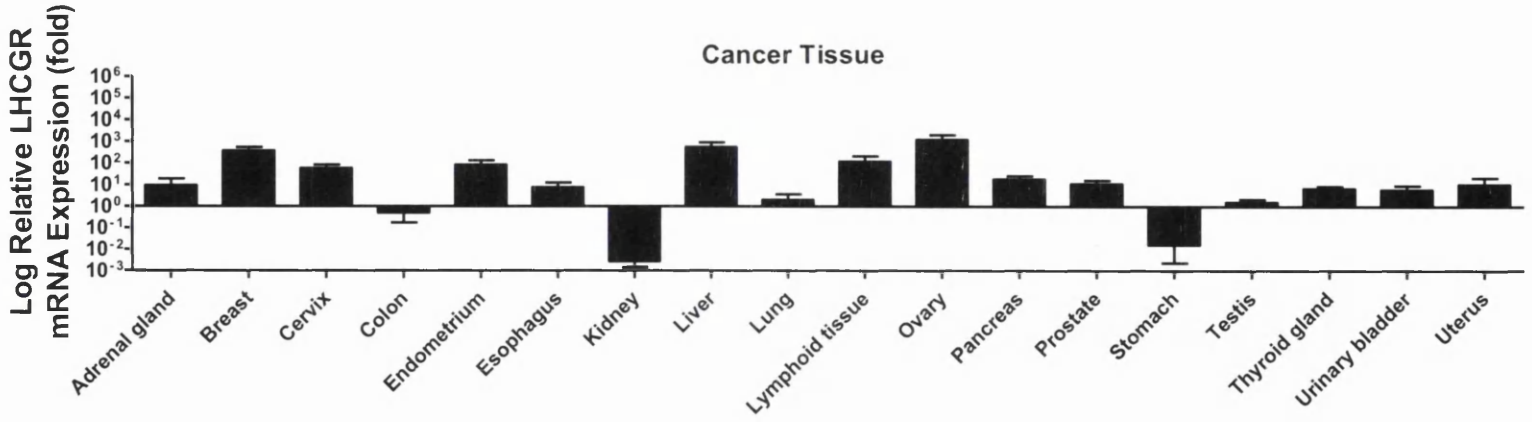

Tissue	Number of Samples	Mean Fold Change	SEM	p value	Average Ct
Adrenal gland	10	9.387	9.186	0.442	34.75
Breast	21	375.8	156.4	0.027	23.45
Cervix	9	57.69	24.65	0.054	47.43
Colon	12	0.484	0.315	0.001	23.76
Endometrium	14	83.2	51.1	0.136	29.24
Esophagus	19	7.577	4.924	0.272	48.65
Kidney	11	0.003	0.001	0	40.43
Liver	17	564.7	317.2	0.095	19.65
Lung	19	2.036	1.574	0.982	12.33
Lymphoid tissue	34	122	90.11	0.192	48.76
Ovary	20	1196	818.3	0.161	9.43
Pancreas	17	18.51	7.62	0.046	13.65
Prostate	21	11.54	4.5	0.047	26.43
Stomach	13	0.017	0.015	0	48.45
Testis	19	1.597	0.6	0.51	24.34
Thyroid gland	18	6.828	1.94	0.023	28.23
Urinary bladder	19	6.025	3.21	0.226	18.87
Uterus	2	10.73	10.68	0.564	16.24

Figure 3.8. Expression of LHCGR in Human cancers. The relative levels of LHCGR a cancer tissue cDNA array were analysed by qPCR. LHCGR mRNA levels in each cancer tissue were calculated relative to the corresponding normal tissue. P-values given where fold change exceeded two fold. Data is shown as mean ± SEM (Error bars represent Standard Error of Mean). *P-value ≤0.05 was considered as statistically significant.

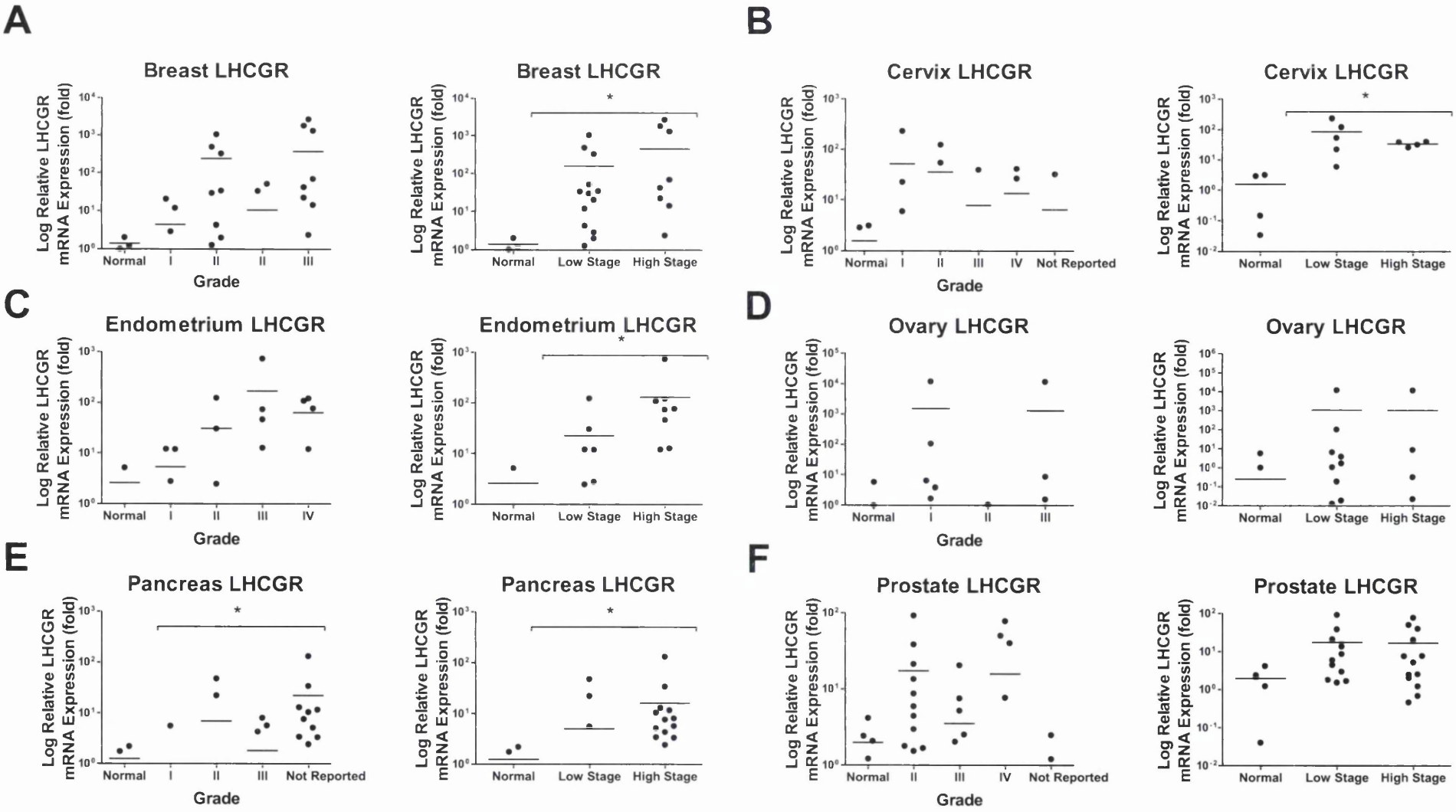

Figure 3.9. Expression of LHCGR associated with Grade of Human Tissues. LHCGR mRNA expression data separated by stage of cancer in breast (A), cervix (B), endometrium (C), ovary (D), pancreas (E), and prostate (F). The data is displayed as a dot plot with mean ± SEM (mean shown as —). LHCGR mRNA levels were calculated as folds in each stage relative to that in normal tissue. *P-value ≤0.05 was considered as statistically significant.

Cancer stage dependent alterations in LHCGR expression

Similar to the cancer stage dependent analysis of IL-13Rα2 mRNA expression, the changes in LHCGR mRNA expression in breast, cervical, endometrium, ovarian, pancreas, and prostate cancers were explored further by separating the expression data by stage of the cancer (Figure 3.9. A-F).

It has been well characterised that LHCGR is up-regulated in breast cancer (Lojun et al, 1997; Meduri et al, 1997). In this study the results were similar; we have seen overexpression of LHCGR mRNA in breast cancer tissues (Figure 3.9. A). There was a significant difference between high and low stages when compared to normal tissue [P = 0.045 and 0.048 respectively]. However by separating the expression data further into stages, we found no statistical significant difference between the groups.

In cervical cancer, both low and high stages showed an up-regulation of the LHCGR gene expression (Figure 3.9. B). When divided furtherer into stages of cancer, we saw statistical significant differences between the stages and the normal tissue in low and high stages [P = 0.045 and 0.035 respectively].

In endometrial cancer, both low and high stage cancers showed an up-regulation of LHCGR mRNA expression compared to normal tissue despite a mean fold change of >20 in low stage and >100 in high stages, statistical significance was found between the stages [P = 0.048 and 0.045 respectively] (Figure 3.9. C). However, the mean fold change increased as the cancer progressed. Between the samples there was too much variation.

Ovarian cancer again showed up-regulation of LHCGR mRNA expression, when compared to that in corresponding normal tissues (Figure 3.9. D). There have been a number of studies linking both low and high stages of ovarian cancer with alterations in the LHCGR gene expression (Gebauer et al, 2004a; Kuroda et al, 1998; Steinmeyer et al, 2003). Analysis of the LHCGR gene expression in low and high stages of ovarian cancer in this study has suggested an overall up-regulation of LHCGR mRNA expression compared to that in corresponding normal tissue. However no statistically significant difference between low and high stages was found. When the data separated further based on the stages of cancer, some individual data sets skewed the overall statistical analysis.

As with the expression in ovarian cancer, studies in pancreatic cancer have indicated high expression of LHCGR mRNA in cancer cells (Figure 3.9. E). When assessed the division between low and high stages of cancer, there were statistically significant differences

between them [$P \leq 0.05$]. However, only the alteration in LHCGR mRNA expression in low and high stage is statistically significant with p value 0.034. Separating the express data further showed no significant differences between the stages.

Finally prostate cancer overall showed an increase in the LHCGR gene expression compared to corresponding normal tissue, with a mean fold change of 11.5 (Figure 3.9. F). However separating the expression data between low and high stages, there is clearly no statistically significant difference between the two groups. When the expression data separated further based on the stage of cancer, the number of data results was limiting to draw any comparison. However stages I, II and III showed an increase in LHCGR gene expression. Stage IV had limited number of data sets so no conclusion was made.

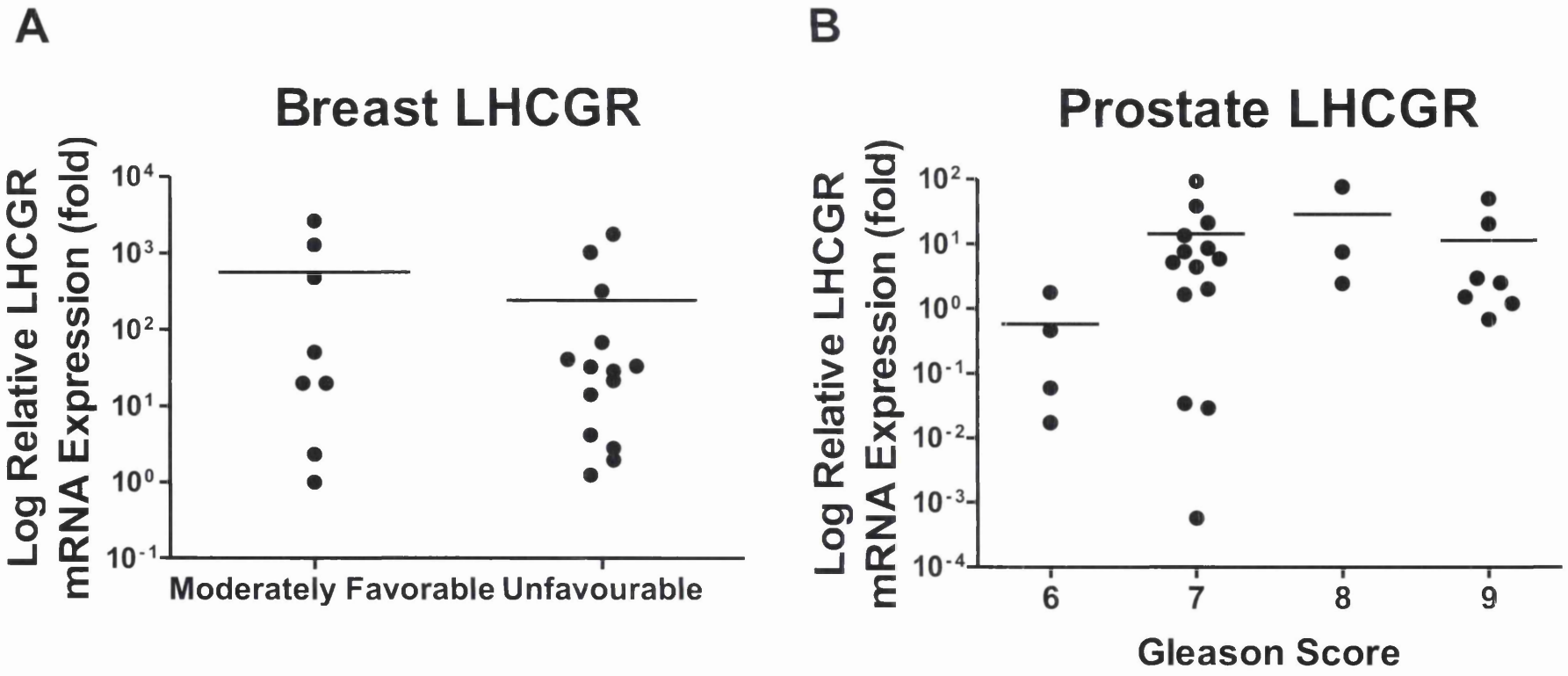

Figure 3.10. Expression of LHCGR associated with breast and prostate tissue sample scores. LHCGR mRNA expression data in breast cancer by Nottingham Grade (A) and in prostate cancer by Gleason score are. LHCGR mRNA levels were calculated relative to the each cancers representing normal tissue. Data is shown as mean ± SEM (Error bars represent Standard Error of Mean). *P-value ≤0.05 was considered as statistically significant.

Cancer Grade dependent alterations in LHCGR gene expression

The expression of LHCGR mRNA in breast cancer tissues was then separated based on the Nottingham grade (Figure 3.10. A). The LHCGR mRNA expression in 'moderately favourable' category is statistically not different from that in the 'unfavourable' category (p value= 0.38). This could be due to the limited number of data sets in the array. However data sets characterised as unfavourable are more compact than that of moderately favourable. Where the mean fold change for moderately favourable is 562.41± 335.8 and unfavourable is 243± 140.1.

Similarly there was no statistical connection between LHCGR mRNA expression and Gleason score in prostate cancer (Figure 3.10. B).

3.3.3. Expression analysis of IL-13Rα2mRNA in normal tissues and cancers

Previous studies have suggested an up-regulation of IL-13Rα2 expression in a cancers such as glioblastoma, kidney, ovarian, colon and pancreas (Shimamura et al, 2010). Like GnRHR and LHCGR genes expression, the expression of IL-13Rα2R mRNA was analysed globally (several cancers and corresponding normal tissues) in this study using a TissueScan Cancer qPCR array.

The IL-13Rα2 gene expression was first analysed in normal tissues (Figure 3.11.). IL-13Rα2 mRNA expression was found lowest in lymphoid gland, and the highest in stomach (1.01 ±0.01 and 9128±9109 fold change respectfully). Overall, the gene expression of IL-13Rα2 in normal tissues was low. When compared to its expression in lymphoid tissue, IL-13Rα2 mRNA expression levels were <2-fold higher in adrenal gland, breast, cervix, endometrium, liver, lymphoid tissue, ovary, pancreas, prostate, and uterus. IL-13Rα2 mRNA expression was observed at moderate levels (<10-fold) in oesophagus, kidney, lung, thyroid tissues and at higher levels (<1000-fold) in colon, stomach, testis, and bladder tissues.

IL-13Rα2 mRNA expression in cancer tissues was then analysed relative to that in corresponding normal tissues (Figure 3.12). A large number of cancer tissues (adrenal gland, breast, cervix, colon, kidney, liver, lymphoid tissue, ovary, pancreas prostate, testis, thyroid gland, urinary bladder, and uterus) showed elevated IL-13Rα2 mRNA expression. Highest up-regulation (>30,000 fold) in IL-13Rα2 expression was found in colon cancer tissue whereas the lowest increase (<30 fold) was found in stomach cancer tissues.

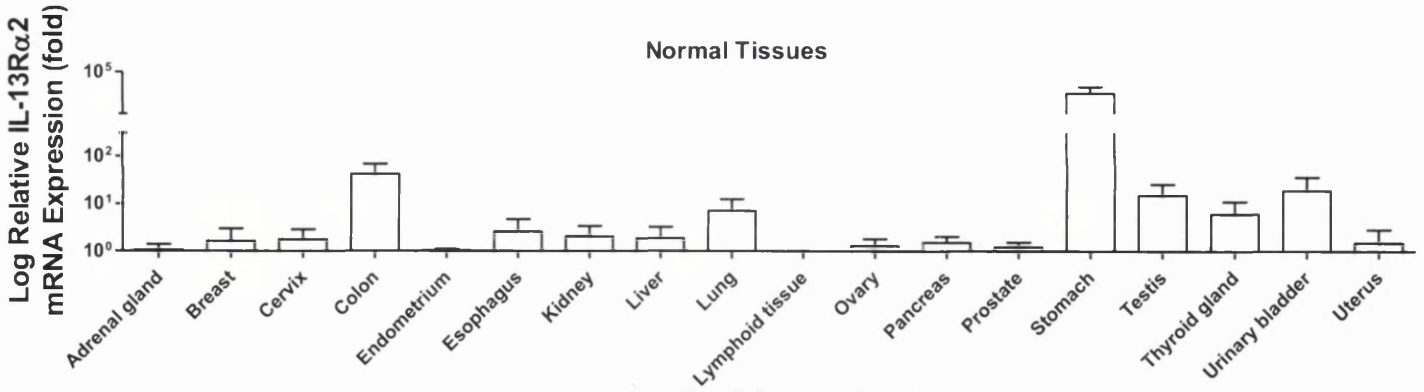

Tissue	Number of Samples	Mean Fold Change	SEM	p value	Average Ct
Adrenal gland	2	1.06	0.34	0.22	48.78
Breast	2	1.64	1.36	0.84	48.43
Cervix	4	1.75	1.11	0.84	48.67
Colon	7	41.44	26.52	0.19	41.34
Endometrium	2	1.1	0.1	0.12	47.87
Esophagus	3	2.59	2.1	0.81	47.23
Kidney	4	2.05	1.3	0.97	47.47
Liver	3	1.88	1.41	0.94	48.97
Lung	3	7.09	5.54	0.45	45.32
Lymphoid tissue	2	1.01	0.01	0.91	49.87
Ovary	3	1.31	0.5	0.3	49.64
Pancreas	4	1.55	0.5	0.43	48.98
Prostate	5	1.23	0.33	0.08	48.34
Stomach	4	9128	9109	0.39	9.83
Testis	6	14.96	11.14	0.3	37.78
Thyroid gland	3	6.06	5.08	0.51	39.23
Urinary bladder	2	18.58	18.55	0.54	42.78
Uterus	2	1.5	1.36	0.78	46.98

Figure 3.11. The expression of IL-13α2 in Human Tissues. The relative levels of IL-13α2 mRNA in 18 normal tissues cDNA array were assessed by qPCR using primers specific for *IL-13α2* gene. After normalising the expression levels to β-*Actin,* IL-13α2 mRNA levels were calculated as folds relative to that in the lowest expressing tissue (Lymphoid). P-values given where fold change exceeded two fold. Data is shown as mean ± SEM (Error bars represent Standard Error of Mean). *P-value ≤0.05 was considered as statistically significant.

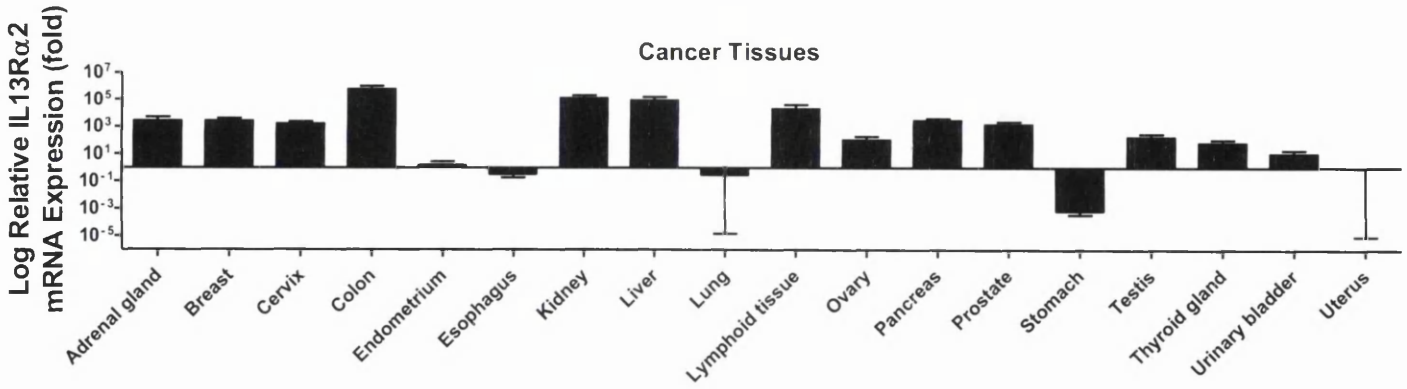

Tissue	Number of Samples	Mean Fold Change	SEM	p value	Average Ct
Adrenal gland	10	2721	2361	0.28	13.54
Breast	16	2604	1595	0.12	15.32
Cervix	9	1700	764.2	0.06	17.87
Colon	12	586719	402389	0.17	3.24
Endometrium	12	1.47	1.29	0.69	48.76
Esophagus	12	0.33	0.14	0.98	49.26
Kidney	18	129337	82120	0.13	3.64
Liver	17	89655	65743	0.19	4.34
Lung	17	0.31	0.31	0.76	49.87
Lymphoid tissue	33	22240	21651	0.31	3.23
Ovary	21	113.9	88.47	0.22	25.56
Pancreas	17	3173	1213	0.02	13.23
Prostate	21	1499	916.9	0.12	15.87
Stomach	14	0.000	0	0	50.92
Testis	19	174	118.3	0.16	30.49
Thyroid gland	17	67.62	43.34	0.15	38.22
Urinary bladder	22	10.71	7.99	0.29	40.76
Uterus	2	0.93	0.93	0.45	49.13

Figure 3.12. IL-13α2 mRNA expression in Human cancer tissues. The relative levels of IL-13α2 a cancer tissue cDNA array were analysed by qPCR. IL-13α2 mRNA levels in each cancer tissue were calculated relative to the corresponding normal tissue. P-values given where fold change exceeded two fold. Data is shown as mean ± SEM (Error bars represent Standard Error of Mean). *P-value ≤0.05 was considered as statistically significant.

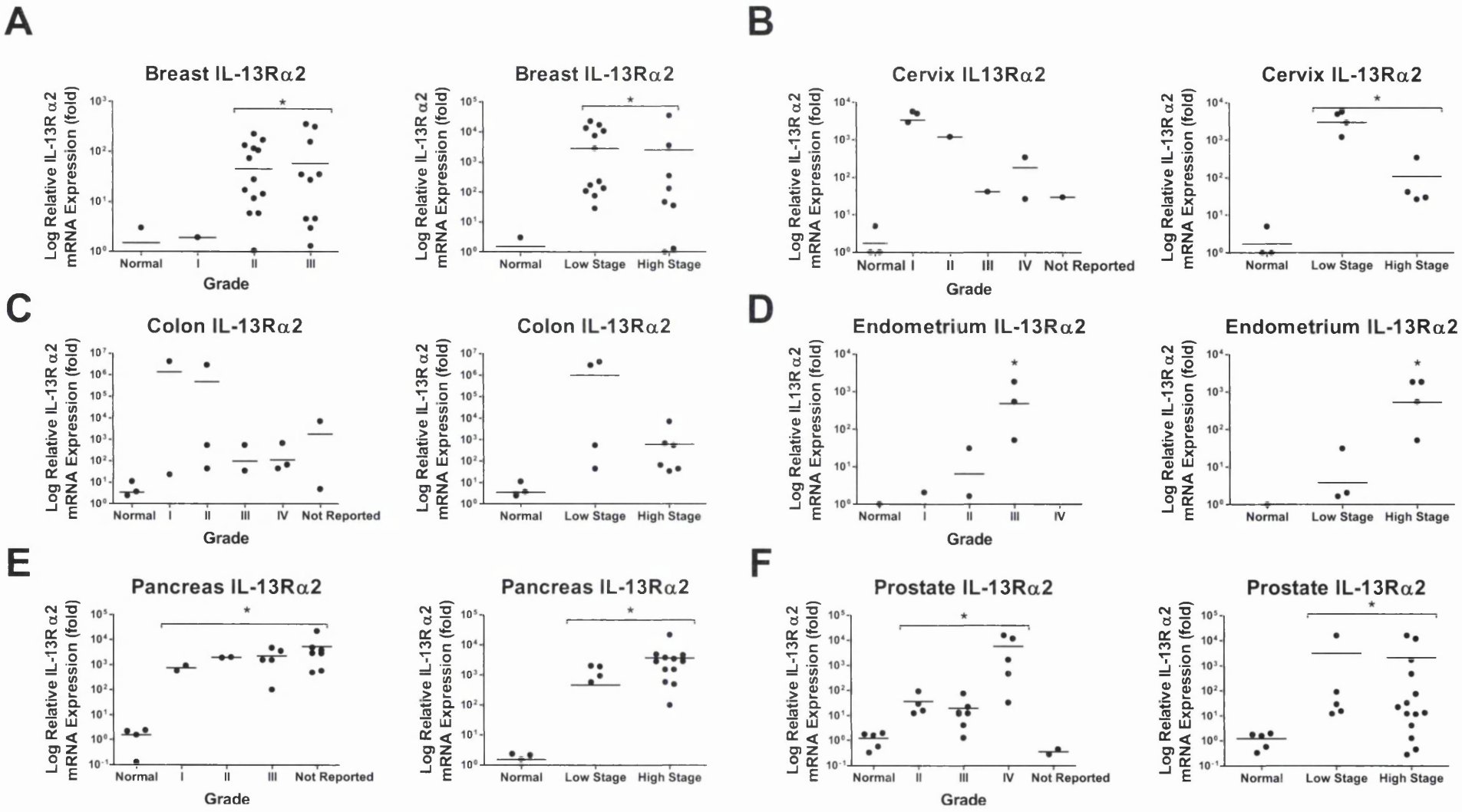

Figure 3.13. Cancer stage dependent expression of IL-13α2 mRNA. IL-13α2 mRNA expression data separated by stage of cancer in breast (A), cervix (B), colon (C), endometrium (D), pancreas (E), and prostate (F). The data is displayed as a dot plot with mean ± SEM (mean shown as —). IL-13α2 mRNA levels were calculated as folds in each stage relative to that in normal tissue. *P-value ≤0.05 was considered as statistically significant.

Cancer stage dependent alterations in IL-13Rα2 expression

Similar to the analysis of GnRHR and LHCGR genes expression, the expression of IL-13Rα2 mRNA in breast, cervical, colon, endometrium, pancreas and prostate cancers was explored further by separating the expression data by stage of cancer (Figure 3.13.A-F).

There have been reports associating alterations in IL-13Rα2 expression with breast cancer (Kawakami et al, 2004; Nakashima et al, 2010). Consistent with these studies, our results indicate that the expression of IL-13Rα2 mRNA is relatively high (>2600 ±1595 fold) in breast cancer tissues when compared to that in normal breast tissue (Figure 3.13.A). Furthermore, IL-13Rα2 mRNA expression was significantly up-regulated in both high stage and low stage of cancer. However when the expression data was separated into individual stages of cancer, only stages II and III were statistically significant different between the groups [P = 0.039 and 0.035 respectively]. The expression of IL-13Rα2 mRNA in stages II and III increased 45.67 ±15.29 and 58.62±28.68 respectfully compared to stage I and normal tissues giving a p value 0.048 and 0.045 respectively.

In cervical cancer, IL-13Rα2 expression in both low and high stages showed an up-regulation (Figure 3.13.B). When compared the expression of IL-13Rα2 mRNA between low and high stages of cancer, there were statistical significant difference between them [P = 0.034 and 0.046 respectively]. Separating the expression data based on the stages of cancer also showed no statistically significance difference between the groups, which could be due to limited number of samples.

Colon cancer showed an up-regulation in IL-13Rα2 mRNA expression when compared to normal tissues (Figure 3.13.C). The separation of the expression data between low and high stages showed no significant difference between the two groups [P = 0.085 and 0.055 respectively]. Some data sets also skewed the results, as IL-13Rα2 was highly expressed in some samples [P >0.05].

In endometrial cancer, there was significant difference between low and high stages cancer [P ≤0.05]. However the overall fold change in the expression was higher in endometrial cancer than that in the normal tissues but the p value was greater than 0.05. When the expression data separated based on the stages of cancer, there is a statistically significant difference between normal and stage III of endometrial cancer with a p value less than 0.05. Stage IV only had one data set, so no statistical analysis could be performed (Figure 3.13.D).

Pancreatic cancer showed up-regulation of IL-13Rα2 mRNA expression when compared to its normal tissue counterpart (Figure 3.13.E). When the expression data was separated based on low and high stages cancer, there was a statistical significant difference between the stages [P = 0.045 and 0.035 respectively]. Separating the expression data further showed a statistically significant difference between the stages of cancer compared to normal [P $\leq$0.05].

In prostate cancer, the IL-13Rα2 gene expression showed up-regulation when compared to that in normal tissue (Figure 3.13.F). There was a statistical significance when the expression between low and high stages of cancer was compared [P = 0.045 and 0.048 respectively]. The stage IV cancer showed an up-regulation in IL-13Rα2 mRNA expression. Stages II and III had more tissue samples also showed a statistical significant difference compared to normal [P $\leq$0.05]. The data also shows a statistically significant difference between normal and cancer tissues.

Cancer Grade dependent alterations in IL-13Rα2 expression

Prostate and breast cancers can also be graded based on their histopathological assessments which correlate with the disease aggressiveness and patient outcome. Therefore the cancer grade dependent changes in the expression of IL-13Rα2 mRNA in prostate and breast cancer tissues were also explored.

The Nottingham grade is a well-established method in providing prognostic information of breast cancers, by grading its severity and the prognosis of cancers .The expression of IL-13Rα2 mRNA in breast cancer tissues was separated based on the Nottingham grade (Figure 3.14.A). The 'moderately favourable' category showed statistically no significant difference in expression of IL-13Rα2 to that in the 'unfavourable' category with a p value of 0.154. This could be explained by the limited number of data sets in the array.

The Gleason grading is the most common grading system for prostate cancer. This scoring is based on its gland architecture indicating the aggressiveness of the cancer. There is no statistically significant connection between IL-13Rα2 expression and the Gleason score in prostate cancer tissue (Figure 3.14.B). This could be due to a limited number of samples in the array.

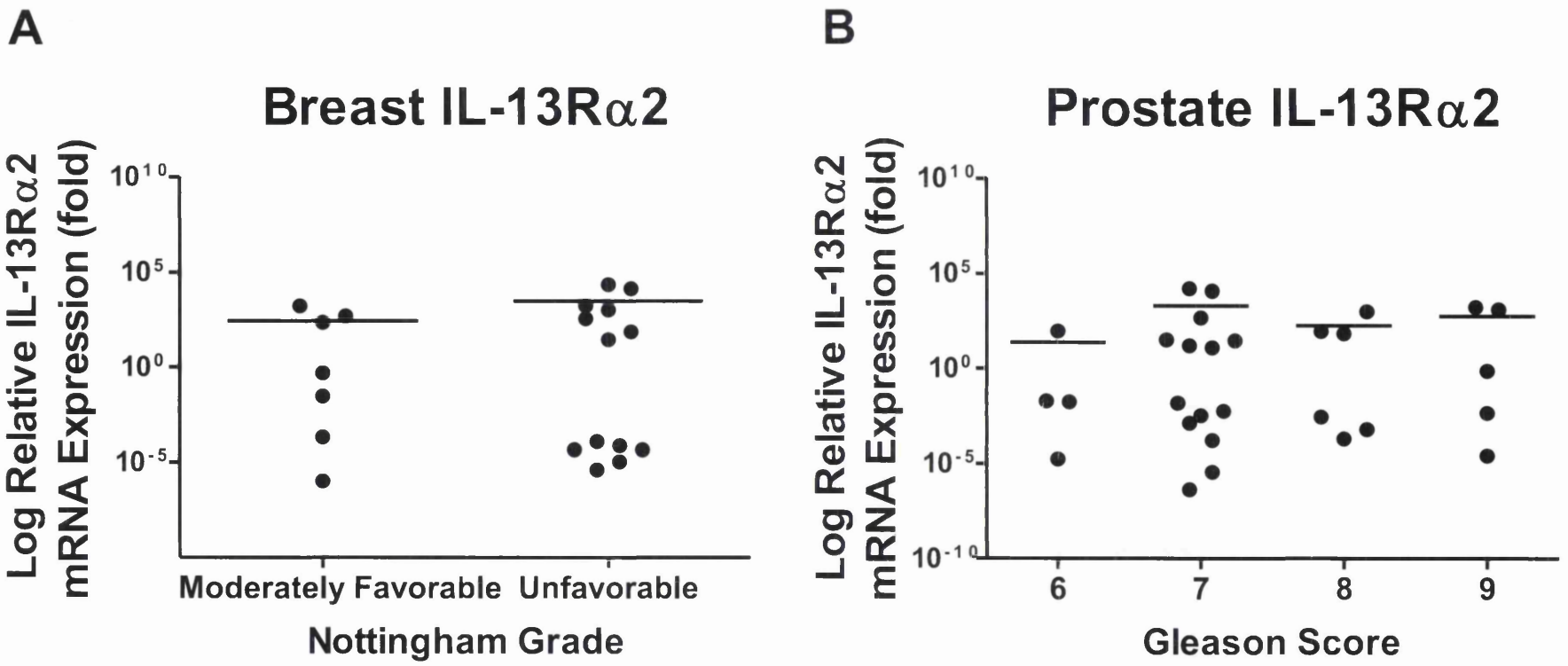

Figure 3.14. Cancer grade dependent expression of IL-13α2 in breast and prostate cancers. IL-13α2 mRNA expression data in breast cancer by Nottingham Grade (A) and in prostate cancer by Gleason score are. IL-13α2 mRNA levels were calculated relative to the each cancers representing normal tissue. The data is displayed as a dot plot with mean ± SEM (mean shown as —). *P-value ≤0.05 was considered as statistically significant.

3.4. Discussion

Although expression levels of these receptors have been reported, an overall view of these receptors gene expression in normal and cancer tissues has been lacking. In this chapter we measured the expression levels of GnRHR, LHCGR and IL-13Rα2 in 18 different cancer tissues samples. I have discussed below the alterations in the expression of each receptor and their implications.

3.4.1. GnRHR

GnRH regulates the release of follicular stimulating hormone (FSH) and LH from the pituitary gland, which in turn regulates gonadal functions (Bowen, 2004). The function of GnRH and its analogues are mediated by GnRHR, which is a GPCR expressed in the plasma membrane of the gonadotrophic cells (Ando et al, 2001). These cells are located in the pituitary gland. Once stimulated by GnRH, gonadotrophic cells synthesise and release gonadotropins (LH and FSH), into the blood circulation and then the gonadotropins regulate the reproductive processes in vertebrates (Schally et al, 2001).

Manipulation of the neuroendocrine cascade by GnRH inhibition leads to down regulation of the sex steroids levels and has been widely used in pharmacological castration, where ablation of androgen and estrogens is required (Schally et al, 2001). GnRH agonists cause pituitary desensitisation due to sustained stimulation of GnRHR whereas the GnRH antagonists compete with native GnRH in binding to GnRHR causing an immediate cessation of the release of the sex steroids (Schally et al, 2001). GnRH analogues are routinely used in the clinic for the treatment of cancers of the reproductive organs (breast and prostate carcinoma), central precocious puberty, in vitro fertilisation and many benign gynaecological disorders (Schally et al, 2001). In prostate and ovarian cancer cells, GnRH binding to its receptor causes the activation of $G_{\alpha i}$ protein (Kraus et al, 2001). It has been suggested that the $G_{\alpha i}$ protein activation is involved in the anti-proliferative effects. This is because the $G_{\alpha i}$ activation results in the activation of caspase and the trans-membrane transfer of phosphatidylserine to the outer membrane as well as JNK and p38 (Kraus et al, 2001).

At the mRNA level, there was a range of GnRHR expression across the array of cancers. On average, GnRHR expression appeared to be higher in cancer compared to its expression in corresponding normal tissue. GnRHR expression has also been reported to be up-regulated in non-hormonal related cancers, such as melanoma, pancreatic cancer, and glioblastoma. In this study, prostate and breast cancer showed increase in GnRHR expression. Furthermore,

GnRHR expression was significantly higher in stages II and III of breast cancer whereas in prostate cancer the expression levels in stage III and IV were higher; each having a [$P \leq 0.05$].

Buchholz et al in 2009 measured the expression of GnRHR protein in triple-negative breast cancer samples using immunohistochemistry (Buchholz et al, 2009). In that study, 17 samples tested and all were positive for GnRHR expression. However, the expression of GnRHR varied from very low to very high. Consistent with this study, our results in this chapter also showed up-regulation of GnRHR expression that varied from very low to very high. However in prostate cancer, we observed no difference in GnRHR mRNA levels between benign and malignant glands and no significant association of the expression with pathological grade or clinical stage and other clinic pathological parameters, including patient age, menopausal status, stage, tumour size, lymph node status, histological grade and prognosis. These results are consistent with previous studies at an mRNA level (Halmos et al, 2000; Straub et al, 2003; Tieva et al, 2001).

There is an overwhelming evidence to suggest that GnRH axis may have a paracrine role in the prostate gland and thereby it may play a role in regulating prostate carcinogenesis. The treatment of prostate cancer with GnRH analogs suggest anti-tumourigenic effect of GnRH in prostate cancer (Gnanapragasam et al, 2005). Gnanapragasam et al showed inhibition of both androgen-independent and dependent prostate cancers by a GnRH analog. In summary, this study provides further evidence that GnRHR expression is high in cancer cells and that the expression is not just limited to hormone dependent tumours.

3.4.2. LHCGR

Studies on LHCGR receptor have gathered a lot of interest. This is because mutations in LHCGR can cause diseases such as pseudohermaphroditism in males and primary amenorrhea in females (Shenker, 2002). The intracellular accumulation of cAMP via the mutation of LHCGR has been shown to result in tumour formation, Leydig cell hyperfunction and hyperplasia (Shenker 2002). The expression of LHCGR has been reported mainly in gonadal cells such as the testicular Leydig cells and the ovarian theca, granulose and luteal cells (Ascoli et al, 2002; Pakarainen et al, 2007). However there is evidence to indicate its expression in non-gonadal tissues such as human blood vessel, uterus and placenta (Singh et al, 1995; Zhang et al, 2001). Interestingly LHCGR is over expressed in tumours of breast, endometrial, ovary and prostate (Gebauer et al, 2003; Lenhard et al, 2012b; Noci et al, 2008; Tao et al, 1997b).

In this study, the expression of LHCGR has been found in both gonadal and nongonadal tissues. However LHCGR expression appeared to be higher in cancer compared to its corresponding normal tissue, indicating that LHCGR is useful as target for cancer diagnosis and therapeutic purposes. In 1983, Goldsmith et al reported the expression of LHCGR in fetal kidney but not in adult organ, suggesting LHCGR may promote organ growth and differentiation in the foetus (Cole, 2010; Goldsmith et al, 1983). Since all kidney tissue sampled in the tissue array are from patients that are above 35 years old, this could explain why our results showed a large down regulation in LHCGR expression in normal kidney. However, LHCGR expression was reduced further in kidney cancer.

In breast and prostate cancers, it is been reported that LHCGR is preferentially expressed in both hormone dependant and hormone independent tumours. Furthermore, LHCGR is a potential prognostic and diagnostic marker for cohorts of breast and prostate cancer patient with poor prognosis (Cole & Butler, 2008; Lenhard et al, 2011; Lenhard et al, 2012a). With use of the tissue cDNA array, we found in this study that over 70% of breast and 80% of prostate cancer tissues exhibit high levels of LHCGR and the alterations in LHCGR expression were found in both hormone dependant and independent cancers tissues. Altogether, this study suggests that LHCGR is frequently overexpressed in breast and prostate malignant tissues. LHCGR expression was significantly higher in both (low and high) stages of breast cancer [$P \leq 0.05$]. The same could be said for prostate cancer. Furthermore, we observed no difference in the expression of LHCGR mRNA between benign and malignant glands of prostate cancer and no significant association of the expression with pathological grade or clinical stage and other clinic pathological parameters, including patient age, menopausal status, stage, tumour size, lymph node status, histological grade and prognosis.

In the study by Meduri et al. (2003) 72% of breast tumour samples from 160 patients tested positive for LHCGR. They concluded that the status of LHCGR had no connection with lymph node invasion, tumour size, or progesterone receptor status. However, their findings also showed that LHCGR positive tumours were more frequent in premenopausal women (Meduri et al, 2003). Our results on LHCGR expression in breast cancer are in agreement with the findings of Meduri et al, concluding no direct link between the stages of breast cancer and the level of LHCGR expression..

The expression of LHCGR in prostate cancer exhibited a trend similar to that in breast cancer. Were there was no link between the stages of prostate cancer and the expression

levels of LHCGR. There are a number of studies which showed that the expression of LHCGR is prominent in prostate cancer. Tao et al showed that both benign prostatic hyperplasia (BPH) and prostate carcinomas express LHCGR (Tao et al, 1997a). Studies on the role of LHCGR in prostate cancer have found that the LHCGR expression is heterogeneous, and that the levels are lower in normal glands.

By using immunohistochemistry, LHCGR protein expression levels were found low in glioma, lymphoma and stomach cancer tissues (www.ProteinAtlas.org). Moderate levels were seen in breast, prostate, cervical, endometrial, carcinoid, head and neck, thyroid, lung, melanoma, skin, urothelial, renal, pancreatic and liver cancers. Highest levels were reported in colorectal, ovarian and testicular cancers. Consistent with this, our results in this study showed increase in LHCGR expression in breast, prostate, cervical, endometrial, pancreatic, thyroid, lung, colorectal, ovarian, testicular and liver cancers; together with low levels in lymphoma and stomach. In summary, this study suggests further evidence that LHCGR expression is high in some cancer cells

3.4.3. IL-13Rα2

A considerable amount of work has been done to analyse IL-13Rα2 expression in human glioblastoma cell lines and tumours. The receptor expression was found in ~75% of WHO grade IV glioblastoma multiforme (GBM) patients (Wykosky et al, 2008). There is little known about the expression of IL-13Rα2 in other cancers. In 2012, Barderas et al showed that the expression levels of IL-13Rα2 are high in human colon cancer compared to that in normal colon, indicating a link between IL-13Rα2 expression and progression of cancer (Barderas et al, 2012). This study also showed IL-13 activation of oncogenic signalling molecules such as phosphoinositide 3-kinase, AKT and SRC in highly metastatic colon cancer cells, indicating that the high expression of IL-13Rα2 plays a critical role in colon cancer invasion and metastasis (Barderas et al, 2012). Like in colon cancer, IL-13Rα2 showed overexpression in pancreatic cancer (Fujisawa et al, 2009). Fujisawa et al showed that IL-13Rα2 expression is high in metastatic pancreatic cancer. Similarly, Minn and colleagues reported higher levels of *IL-13Rα2* mRNA in lung metastasis compared with that in the parent breast cancer cells (Minn et al, 2005). He et al was able to show that prostate cancer with high tumorigenic and metastatic potential express high levels of IL-13Rα2. Using the prostate cell line model ARCaPM, they were able to target prostate cancer using an IL-13-conjugated cytotoxic drug (He et al, 2010).

With more and more data showing it as a prominent target for metastatic cancers, *IL-13Rα2* may serve as a new therapeutic target for prevention of invasion and metastasis of cancers such as pancreatic cancer, which is highly lethal and drug resistant. At the mRNA level, there was a range of IL-13Rα2 expression across the array of cancers studied here. On average, IL-13Rα2 expression appeared to be higher in cancer compared to that in corresponding normal tissue control. To date there are no studies reporting the expression of IL-13Rα2 in human stomach. However Wu et al reported high expression normal rat stomach tissues (Wu & Low, 2002). Consistent with this, our study in this chapter showed down regulation of IL-13Rα2 mRNA expression in stomach cancer [mean fold change of 0.0050±0.00053]

In this study, breast cancer showed higher expression of IL-13Rα2 when compared to that in normal corresponding tissue [$P \leq 0.05$]. Furthermore, IL-13Rα2 expression was significantly higher in the high stage of cancer. The same could be said for prostate cancer. We observed a difference in IL-13Rα2 mRNA levels between benign and malignant glands. However there is no significant association between alteration in IL-13Rα2 and pathological grade or clinical stage or other clinic pathological parameters, including patient age, menopausal status, stage, tumour size, lymph node status, histological grade and prognosis.

The expression analysis of IL-13Rα2, LHCGR, and GnRHR in an array of cancer and corresponding normal tissues is a very important for improving new strategies of prevention, diagnosis and therapy of hormone sensitive and insensitive cancers. We have demonstrated here that IL-13Ra2, LHCGR, and GnRHR are preferentially overexpressed in a number of cancers especially in breast and prostate carcinoma and that the expression levels are not associated with tumour grade. We found that mRNA levels for IL-13Rα2, LHCGR, and GnRHR in normal breast and prostate tissue are extremely low compared with those of other major human tissues. Based on these observations, we suggest that IL-13Rα2, LHCGR, and GnRHR could be used as potential targets to treat these cancers.

4. Membrane disrupting lytic peptide conjugates destroy prostate and breast cancer

4.1. Introduction

Cancer has become a worldwide problem, an estimated 14 million patients diagnosed with and approximately 8 million dying of cancer globally in 2008 (Jemal et al, 2011). In the United Kingdom (UK) 1 in 3 will develop some form of cancer during their lifetime (UK, 2009).

In developed countries, the incidence rate of cancer has increased and is likely to continue due to an increased aging population and changes to lifestyles. There is supporting evidence showing that breast cancer incidence rates in western countries have increased between the 1980s and 1990s due to changes in lifestyles such as increased use of post-menopausal hormone therapy. An increase in cancer rates due to changes in lifestyles could also explain why incidence rate for colorectal cancer is high, linking it to increase in obesity and also smoking (Jemal et al, 2011). However it is important to note that increases in number of cases could also be due to the development of effective and highly sensitive screening techniques.

Despite the development of new drugs and use of combinational therapies, mortality rates are still not improving. In 2009, 408,381 patients were diagnosed with cancer in the UK, resulting in 156,090 deaths; the highest mortality rate occurred due to lung cancer (UK, 2009). Between 1979 and 2008, incidence rates for cancer in the UK increased by 26% with a 13% increase in men and a 34% increase in women (UK, 2009). The second most common cause of cancer death in men is prostate cancer and breast cancer in women.

Current treatments such as hormonal therapy cannot cure cancer but only prolong patient's lives. Although hormonal therapy has shown to reduce tumour size, its usage can cause the disease to re-emerge and differentiate into a more aggressive form, making the treatment therapy ineffective (Pantel & Otte, 2001; Tammela, 2004). Chemotherapeutic drugs such as docetaxel, triptorelin and tamoxifen, are usually given when the disease starts to spread to secondary sites within the body or metastasize. Although these chemotherapeutic drugs are affective, there are non-specific and hence their usage can cause serious side effects by destroying healthy tissue and organs (Jang et al, 2003). Moreover, these drugs only destroy

rapidly dividing cells and therefore unable to target dormant cancer cells or slow growing tumours (Pantel & Otte, 2001).

Patients with an aggressive form of cancer are initially treated by removing cancerous tissue by surgery (for example prostatectomy for prostate cancer and mastectomy for breast cancer) (Meijers-Heijboer et al, 2001; Tan et al, 2011). These therapies are mostly systemic and palliative, which mean they can reduce effect on surrounding normal healthy tissues and relieve symptoms the patient's experience. Palliative treatments are designed to treat symptoms such as pain, nausea, breathlessness, insomnia and other physical systems caused by cancer or its treatments. Problems associated with current treatments such as chemotherapy and surgery clearly illustrate the need for developing therapeutic drugs that target primary tumours (dormant as well as actively growing) and their metastasis.

Targeted cancer therapy has made huge progress over the years. With the over or only expression of cell surface receptors in tumour cells, cellular uptake of drugs targeting those cell surface receptors can be highly specific in destroying cancers cells (Dharap et al, 2003). The development of monoclonal antibodies (mAbs) has shown the effectiveness of targeting cell surface receptors overexpressed in cancer cells. In fact several mAbs are now approved for clinical use and are very effective against numerous types of cancers. These include Erbitux® (cetuximab); a drug that treats inhibits metastatic colorectal cancer by binding to epidermal growth factor receptor (EGFR) (Mendelsohn & Baselga, 2003). Herceptin® (trastuzumab), a mAbs used against metastatic breast cancers overexpressing HER2 (Slamon et al, 2001). However, targeting the receptors with mAbs can be problematic, in some cases, due to the size of the antibodies (~150 kDa), penetration of the entire tumour mass by mAbs can be difficult. Additionally the Fc region of the antibody binds to the reticuloendothelial system, resulting in high uptake of cytotoxic drugs, or toxins into bone marrow, liver, and spleen, leading to severe toxicities (Hudson & Souriau, 2003; Todorovska et al, 2001).

Peptide based target therapy is an alternative, if not more effective, to mAbs based therapy against cancer. The peptide ligands, which target cell surface receptors, able to penetrate the entire tumour structure due to their small size. Moreover, they are chemically stable, easy to synthesize, and can be conjugated to a cytotoxic drug or a toxin. In some cases, substitution of natural L-amino acid with D-amino acid in the ligand can increase the peptide stability (Schally & Nagy, 1999; Sethi et al, 2014; Yang et al, 2012; Zelezetsky et al, 2005). It has been shown that altering the amino acid composition of a peptide drug results in increase in resistance to enzymatic degradation and thereby increase in stability of the peptide (Papo et

al, 2003). However, the effectiveness of peptide conjugated cytotoxic drugs or toxins, which rely on cellular uptake, can be limited by multidrug resistance (MDR) of tumour cells. For example, ovarian cancer may become resistant to treatment with the peptide conjugated cytotoxic drugs or toxins (Friedlander et al, 2013). Unlike cytotoxic drugs or toxins, the lytic peptides, membrane disrupting peptides, don't depend on cellular uptake and therefore they can overcome the MDR problems in peptide based target therapy. Consistent with this, the lytic peptides fused with ligands, which bind specifically to cancer cells, have shown to kill both drug resistant and drug sensitive tumour cells with equal potency (Johnstone et al, 2000).

Prostate cancer is one of the most common causes of cancer in men worldwide (Jemal et al, 2011). The prostate cancer will become metastatic in approximately 15% of people diagnosed with the disease and 30-50% of patients treated for the cancer (UK, 2009). Prostate cancer incidence increases with age more rapidly than any other type of cancer. In the initial stages of the disease, prostate cancer development and growth is dependent on androgens and can be suppressed by androgen ablation monotherapy (Meijers-Heijboer et al, 2001; Tan et al, 2011). Due to the emergence of androgen-independent prostate cancer, prostate tumours recur as hormone-refractory and highly metastatic for which no treatment is currently available (Meijers-Heijboer et al, 2001; Tan et al, 2011). Breast cancer is one on the most common malignancies in women. It continues to be a major problem and cause of death among women worldwide. Early stages of cancer can be curable with local or regional treatment; however the formation of metastases in most cases requires systemic treatment (Catz & Johnson, 2003). Current treatments include, hormonal therapy, chemotherapy, or both based on the extent of disease and tumour characteristics. However 30% of women with breast cancer will progress to locally advanced or metastatic disease. In this case any standard chemotherapy regimen will be inefficient in treating advanced and metastatic breast cancer (O'Regan & Jordan, 2001; Tammela, 2004).

In the past 20 years, several studies have indicated elevation of Luteinizing hormone/chorionic gonadotropin hormone receptor (LHCGR) as well as Gonadotropin-releasing hormone receptor (GnRHR) in prostate, breast and uterine cancers (Ji et al, 2002; Lojun et al, 1997; Tao et al, 1997b); and low expression in peripheral organs, making them potential drug target (Ziecik et al, 2007). Similarly interleukin-13 receptor α2 (IL-13Rα2) has been reported to be overexpressed in human tumours including brain, renal cell carcinoma, squamous cell carcinoma of head and neck, ovarian cell carcinoma, pancreatic, breast and prostate cancers (Fujisawa et al, 2009; Gonzalez-Moreno et al, 2005; Jarboe et al, 2007;

Kawakami et al, 2003; Kioi et al, 2006a; Kioi et al, 2006b; Puri et al, 1996; Zhao et al, 2014). Furthermore, IL-13Rα2 shown to play a prominent role in promoting cancer cell growth and tumour formation (He et al, 2010).There are a number of tumour-suppressor and other cancer related genes that have been identified to be inactivated by methylation of CpG islands sites in their promoter region. Histone deacetylation has also been found to be associated with transcriptional silencing through chromatin condensation (Hebbes et al, 1988; Jones & Laird, 1999; Momparler & Bovenzi, 2000; Monneret, 2007). There is increasing evidence to suggest that epigenetic alterations, such as the histone acetylation and promoter DNA methylation, play an important role in the regulation of gene expression of LHCGR, GnRHR and IL-13Rα2 (Fujisawa et al, 2011; Honrado et al, 2006; Schang et al, 2012). Trichostatin A (TSA), a histone deacetylase inhibitor, and 5-aza-2 deoxycytidine (5-Aza-dC), a DNA methyltransferase inhibitor, have demonstrated their potential in anticancer treatments.

The development a novel lytic peptide (Pep-1-Phor21) that specifically targets IL-13Rα2 is apparent. Pep-1-Phor21 peptide is composed of an IL-13Rα2 binding moiety, Pep-1, and a cell membrane disrupting peptide called Phor21 (Figure 4.0) (Pandya et al, 2012; Rivero-Muller et al, 2007). Pep-1 is a 9 amino acid peptide (CGEMGWVRC), which was first isolated by screening for IL-13Rα2 ligand using a heptapeptide phage's display library (Pandya et al, 2012). It not only specifically binds IL-13Rα2 with high affinity but also cross the blood brain barrier and hence it is also suitable to target brain cancers such as glioma (Pandya et al, 2012). The lytic peptide Hecate (a seven amino acid long peptide composed of mainly arginine and lysine residues) was shown to be effective in destroying prostate cancer xenografts in nude mice when conjugated to [D-Trp^6]GnRH ([D-Trp^6]GnRH-Hecate) (Hansel et al, 2007a; Rivero-Muller et al, 2007). Phor21 is a well characterised lytic peptide, which consists of three repeats of Hecate. A 15 amino acid segment (residues 81-95) of the beta chain of human chorionic gonadotropin in which the cysteine residues replaced by alanine's (βCG[ala]) has been shown to contain 70% of the binding capacity of entire hCG (Leuschner & Hansel, 2005; Morbeck et al, 1993). Previous studies using Phor21 conjugated to βCG(ala) (Phor21-βCG[ala]) showed a significant decrease in tumour size (Hansel et al, 2007a; Rivero-Muller et al, 2007). Phor21-βCG(ala) was able to destroy human breast cancer xenografts in nude mice at relatively low dosage, (0.2 mg/kg body weight) compared to tamoxifen, which effective dosage is 100 mg/kg body weight However, no such studies were carried out so far using Pep-1 conjugated to a lytic peptide (figure 4.0).

Since prostate and breast cancers are most common cancers in men and women respectively, we studied the effect of Pep-1-Phor21 on viability of prostate and breast cancer cells grown

in monolayers and compared it effects with that of Phor21-βCG(ala) and [D-Trp^6]GnRH-Phor21. In this study, we focused on:

1) Analysing the expression of IL-13Ra2, GnRH and LHCG receptors in prostate and breast cell lines.

2) Testing the efficacy of the lytic peptides [D-Trp^6] GnRH-Phor21 Pep-1-Phor21 and Phor21-βCG (ala) in killing prostate and breast cancer cells *in vitro* and the relationship between cell cytotoxicity and their representing receptor expression.

3) Determining whether we can increase the sensitivity of the cancer cells to the lytic peptide conjugates by up-regulating the receptors expression through epigenetic inhibitors or hormonal treatment.

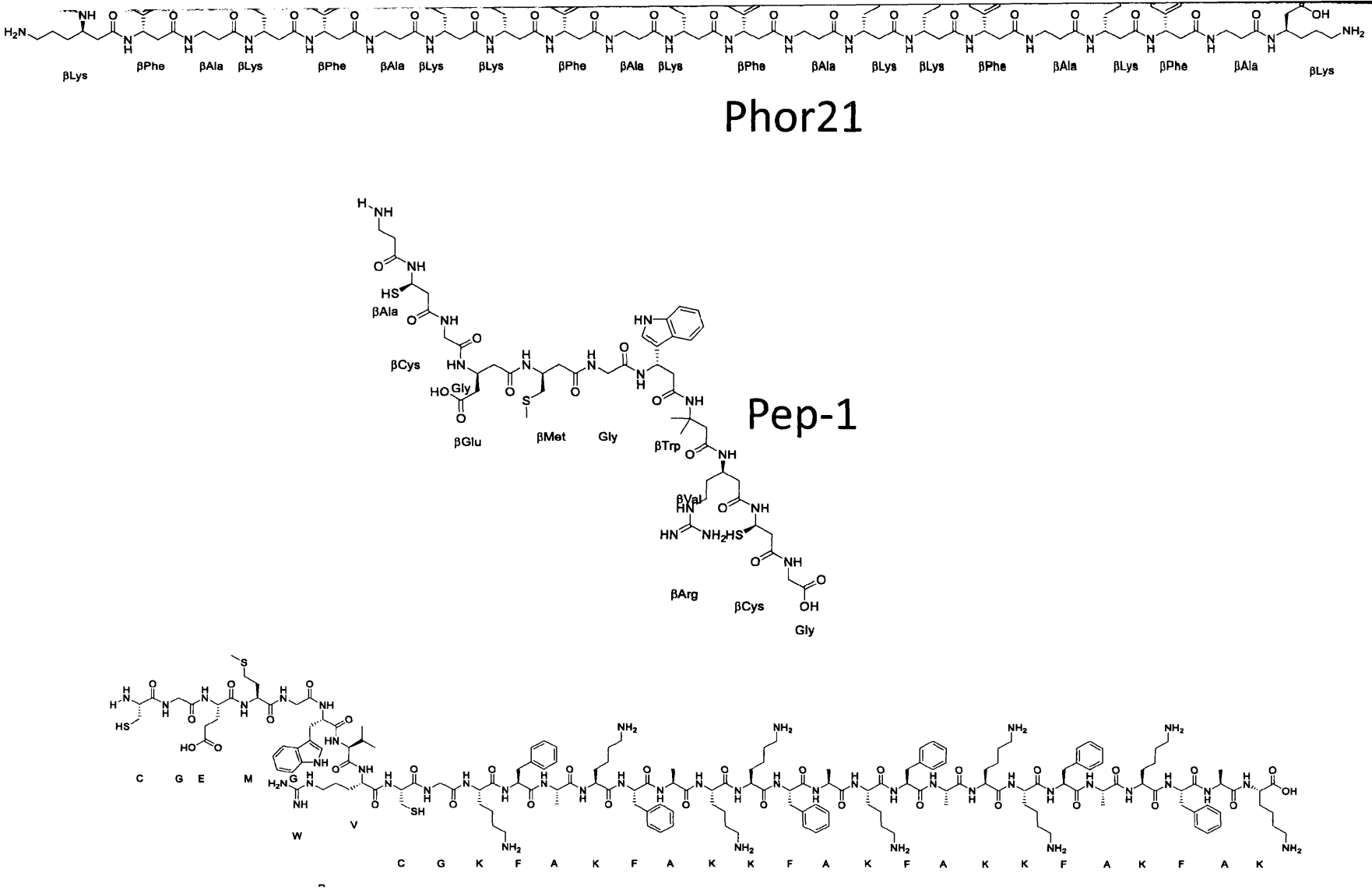

Figure 4.0 Molecular structure of Pep-1-Phor21. A) Phor21 a membrane disrupting peptide is linked to a **B**) IL-13Rα2 binding moiety, Pep-1 to form a lytic peptide conjugate **C**) Pep-1-Phor21

4.2. Materials and Methods

4.2.1. Antibodies and Other Reagents

The antibodies used in the experiments were: mouse monoclonal anti- IL-13Rα2 (sc-134363, Santa Cruz Biotechnology), rabbit polyclonal anti-LHCGR (Price et al, 2013), rabbit polyclonal anti-GnRHR (sc-13944, Santa Cruz Biotechnology) and horseradish peroxidases (HRP) conjugated secondary antibodies (GE Healthcare). Enhanced chemiluminescence (ECL) advanced reagent was obtained from GE Healthcare. Pep-1 (CGEMGWVRC), Pho21 (KFAKFAKKFAKFAKKFAKFAK), Pep-1-Phor21 (CGEMGWVRCKFAKFAKKFAKFAKKFAKFAK), βCG(ala) (SYAVALSAQAALARR), Phor21-βCG(ala) (KFAKFAKKFAKFAKKFAKFAKSYAVALSAQAALARR), [D-Trp^6]GnRH ([Pyr]-HWSY-*W-LRPG, *W = D-Trp) and [D-Trp^6]GnRH-Phor21 ([Pyr]-HWSY-*W-LRPGKFAKFAKKFAKFAKKFAKFAK) were synthesised by Thermo Fisher Scientific. Alamar Blue was obtained from Thermo Fisher Scientific. CellTox Green and ApoTox-Glo Triplex assay kits were purchased from Promega Corporation. Pharmacological inhibitors Trichostatin A (TSA) and 5-aza-2'-deoxycytidine (5-AZA) were from Tocris. JetPRIME transfecting reagent was from polyplus-transfection. Follicle stimulating hormone (FSH), Gonal-F, was from Merck-Serono. All other reagents, unless otherwise specified, were obtained from Sigma-Aldrich.

4.2.2. Cell Culture

Human breast cancer cell lines (MCF-7, MDA-MB 231) and non-tumour cell line (MCF-10A) were from American Type Culture Collection (ATCC) (Rockville). MCF-7 and MDA-MB 231 cells were cultured in Dulbecco's Modified Eagle's medium (DMEM) supplemented with 10% foetal bovine serum (FBS) and PSG (2mM L-glutamine, penicillin [100 μg/ml], and streptomycin [100 μg /ml]) (complete medium). MCF-10A cells were cultured in DMEM:Ham's F12 (50:50) (DMEM/F12) supplemented with 5% horse serum (HS), PSG, 20 ng/ml epidermal growth factor (EGF), 0.1 mg/ml cholera toxin (CT), 10 μg/ml insulin, 500 ng/ml hydrocortisone at 37°C/5% CO_2 in a humidified incubator.

Human prostate cancer cell lines (LNCaP, DU145 and PC3) and non-tumour epithelial cell line (PNT2) and Human Embryonic Kidney cell line (HEK293) were from ATTC (Rockville). Cells were cultured in RPMI1640 (PNT2, LNCaP, DU145 and PC3) or DMEM (HEK293) supplemented with 10% FBS and PSG (complete medium) at 37°C/5% CO_2 in a humidified incubator.

4.2.3. Cell Transfection

Cells were transfected with expression plasmid FLAG-IL13Rα2 (Daines et al, 2006) or Myc-LHCGR (Kanamarlapudi et al, 2012b) or an empty control plasmid (pcDNA3) using JetPRIME transfection reagent (Polyplus) according to the manufacturers' instructions. Briefly, 2-4 μg of plasmid DNA was diluted in 200 μl of JetPRIME buffer and the appropriate volume of JetPRIME transfection reagent (2 μl/μg DNA) was added to it, which then incubated at room temperature (RT) for 15 min. The DNA-JetPRIME mixture was added drop wise to the cells grown to 60-80 confluency in a 6 cm plate, gently rocked the cell culture plate to mix and incubated the culture plate at 37°C/5% CO_2 in a humidified incubator. 1 day after transfection, the medium was replaced. The cells were used for experimentation 2 days after transfection.

4.2.4. Immunoblotting

This was carried out as described in section 2.4.3. Briefly, proteins were separated using a SDS-PAGE gel electrophoresis and then transferred onto polyvinylidene fluoride (PDVF) membrane (Kanamarlapudi et al, 2012a). Membranes were blocked with TBST (Tris buffered saline [TBS] with 0.1% tween 20) containing 5% milk powder (blocking buffer) for 1 hour at room temperature. Membranes were then incubated with anti-IL-13Rα2 mouse monoclonal (diluted 1:500 in blocking buffer), anti-LHCGR rabbit polyclonal (diluted 1:500) or anti-GnRHR rabbit polyclonal (diluted 1:1000) overnight at 4°C. The membranes were then washed with TBST and then incubated with the HRP-conjugated anti-mouse or anti-rabbit secondary antibody (diluted 1:2500 in blocking buffer) for 1 hour at room temperature. Membranes were then developed using ECL select substrate and bands on the membrane were visualised using ChemiDocTM XRS system (Bio-Rad) (Davies et al, 2014). Blots were stripped of antibodies by incubating them in Western blot stripping buffer at RT for 15 min. The blots were then washed twice with water and once with TBST. The blots were blocked and re-probed using anti-alpha Tubulin mouse monoclonal (diluted 1:10,000) and HRP-conjugated anti-mouse secondary (diluted 1:2500 in blocking buffer) (Thompson & Kanamarlapudi, 2014).

4.2.5. Enzyme linked immunosorbent assay (ELISA)

Cell surface expression of IL-13Rα2 was assessed by ELISA using unpermeablised cells (Kanamarlapudi et al, 2012b). 60-80 % confluency of cells were plated into poly-L-lysine (0.1 mg/ml) coated wells of a 48-well plate and allowed them to adhere to the surface of

wells by incubating at 37°C/5% CO_2 in a humidified incubator. After 24h of incubation, cells were serum starved for 2 hours by incubating them in serum free medium at 37°C/5% CO_2 in a humidified incubator. Cells were then fixed with 4% (w/v) paraformaldehyde for 5 min, followed by a 45 minute incubation with blocking buffer (1% bovine serum albumin [BSA] made in TBS [1% BSA/TBS]). Cells were then incubated with anti-IL-13Rα2 mouse monoclonal (diluted 1:800 in 1% BSA/TBS) for 2 hours. Cells were washed 3 times with TBS and then incubated with HRP-conjugate anti-mouse IgG (diluted 1:5000 in 1% BSA/TBS) for 1 hour. Cells were washed 3 times and developed by incubating with 1-step Ultra TMB-ELISA substrate (Bio-Rad) for 15 min and the reaction was stopped by adding equal volume of 2M H_2SO_4 (sulphuric acid). Absorbance of the reaction mixture was read at 450nm using a microplate reader (Thompson & Kanamarlapudi, 2014).

4.2.6. Cell Viability Assay

Cell viability was assessed using alamar blue assay. 40,000 cells per well were plated into 96-well μclear half area black plate and incubated at 37°C/5% CO_2 in a humidified incubator. After 24 hours, the medium was replaced with complete medium containing 10% (v/v) alamar blue and increasing concentration of 0-120μM Phor21 or conjugated Phor21 and incubated the cells at 37°C/5% CO_2. The fluorescence of the medium was read after 30 min incubation (considered as zero) and every 3 hours afterwards. The fluorescence was assessed at 570nm (excitation) and 630nm (emission) using a microplate reader (POLAR star Omega).

4.2.7. Cytotoxicity Assay

Cell cytotoxicity was assessed using CellTox™ Green Cytotoxicity Assay (Promega). 40,000 cells per well were plated into 96-well μclear half area black plate and incubated at 37°C/5% CO_2 in a humidified incubator. After 24 hours, the medium was replaced with FSM containing 0.1% (v/v) CellTox Green Dye and a set concentration of Phor21 or conjugated Phor21 and incubated cells at 37°C/5% CO_2. The fluorescence of the medium was read after 30 min incubation (considered as zero) and every 3 hours afterwards. The fluorescence was assessed at 490nm (excitation) and 525nm (emission) using a microplate reader (POLAR star Omega) the overall results will be given as cell viability.

4.2.8. Cell viability, cytotoxicity and apoptosis assays

Cell viability, cytotoxicity and apoptosis of PC3 cells were determined by ApoTox-Glo ™ Triplex Assay (Promega), according to the manufacturer's protocol. 40,000 cells per well were plated into 96-well μclear half area black plate and incubated at 37°C/5% CO_2 in a

humidified incubator. After 24 hours, the medium was replaced with complete medium containing test compound. After 6 hours of incubation at 37°C/5% CO_2. Cell viability and cytotoxicity was determined by adding 10µl of glycylphenylalanyl-aminofluorocoumarin (GF-AFC) substrate and 10µl of bis-alanylalanyl-phenylalanyl-rhodamine 110 (bis-AAF-R110) substrate to 2 ml of assay buffer. 10µl of the cell viability and cytotoxicity reagent was added to each test well and controls. The plate was then placed in the incubator for 1 hour at 37°C/5% CO_2. Cell viability was measured at 400 nm (excitation) and 505 nm (emission). Cytotoxicity was measured at 485 nm (excitation) and 520 nm (emission). Apoptosis was determined by adding 10ml Caspase-Glo 3/7 buffer to Caspase-Glo 3/7 substrate to form Caspase-Glo 3/7 reagent. 50 µl of the reagent was added to all test wells and allowed to incubate for 30 min at room temperature, after luminescence was measured. All readings were taken using a microplate reader (POLAR star Omega).

4.2.9. Real-time PCR

In this section, the primers and probes were selected using the mRNA sequences of IL-13α2, LHCGR, GnRHR and β-Actin from NCBI database. The sequences of primers are shown in Table 4.1, which were synthesized by Oligo Architect sigma. The RT-PCR was carried according to the manufacturer's protocol out using SensiFAST SYBR & Fluorescein Kit (BIO-96020, Bioline). The RT-PCR was performed in a final volume of 10µl containing 250nM primer, and using a Bio-Rad CFX 96 Real Time Detection System (Bio-Rad, Hercules, CA, USA). The data in this study was analysed using the ΔCt method of relative expression: the mean of threshold cycles (Ct) for normal tissue was subtracted from the Ct's of the experimental samples (including individual data for normal tissue) (ΔCt). The fold change of this difference was calculated by $2^{\Delta\Delta Ct}$. List of Primers used in RT-PCR are shown in section 2.10.2.

4.2.10. Treatment of cells with Charcoal Treated Serum, Steroids and FSH

60% of confluent cells were plated in 6 cm plate and incubated at 37°C/5% CO_2. After 24 hours of plating, the medium was replaced with complete medium containing normal serum or charcoal treated serum. After 48 hours of incubation, indicated concentration of 17β-estradiol or FSH was added to the medium and incubated cells for an additional 48 hours. After which they were either extracted for RT-PCR and immunoblotting or plated for cytotoxic assays (Hansel et al, 2007b; Leuschner et al, 2003b; Leuschner et al, 2001).

4.2.11. TSA and 5-aza-dC treatment

Cells grown in complete medium to 80% confluency were treated with 0-100μM TSA or 5-aza-dC. For RT-PCR and immunoblotting 80% confluent cells were plated on 6cm plate. After 24 hours of treatment, the cells were extracted. For cytotoxic assays 80% confluent cells were plated onto 96-well μclear half area black plate and incubated at 37°C/5% CO_2 in a humidified incubator. After 24 hours, the medium was replaced with 0-100μM TSA or 5-aza-dC. After 24 hours of treatment, Phor21 or conjugated Phor21 was added to the cells and incubated the cells for additional 3 hours 37°C/5% CO_2 (Fujisawa et al, 2011; Takenouchi et al, 2011). After which they were either extracted for RT-PCR and immunoblotting or plated for cytotoxic assays

4.2.12. Statistical Analysis

Data were analysed using GraphPad prism program. All data are presented as means ± standard error of the mean (SEM) of three independent experiments. Statistical tests between controls and test values were performed using two-tailed unpaired Student's t-test. Statistical test between groups was performed using the Bonferroni's post-test after one-way or two-way analysis of variance (ANOVA), where $p > 0.05$ was considered as statistically not significant (n.s.) and $p < 0.05$, $p < 0.01$ and $p < 0.001$ were considered statistically significant (Thompson & Kanamarlapudi, 2014).

4.3. Results

4.3.1. Specificity of Pep-1-Phor21 and Phor21- βCG (ala) in targeting and killing their receptor expressing cells

HEK293 cells transfected with an empty expression plasmid (control) or expression plasmid IL-13Rα2 or LHCGR were used to assess Pep-1-Phor21 and Phor21-βCG(ala) specificity in targeting and killing IL-13Rα2 and LHCGR expressing cells respectively. The lysates of HEK293 cells transfected with these constructs were immunoblotted using either anti- IL-13Rα2 or anti- LHCGR (Figure 4.3.1 A-B) antibody to assess the expression of IL-13Rα2 and LHCGR. IL-13Rα2 expressed as ~50 kDa protein only in cells transfected with IL-13Rα2 plasmid but not in cells transfected with empty plasmid. Similarly LHCGR expressed as a 70kDa protein only in cells transfected with LHCGR plasmid.

HEK293 cells transfected with either empty vector, IL-13Rα2 or LHCGR plasmid were treated with 0-10μM Pep-1-Phor21 or Phor21-βCG (ala) peptide drug and assessed for toxicity using both cell viability (Alamar Blue; Figure 4.3.1B) and cytotoxicity (CellTox; Figure 4.3.1C) assays. Pep-1-Phor21 showed a dose-dependent cytotoxicity and loss of cell viability only in cells expressing IL-13Rα2 with a 50% inhibitory concentration (IC_{50}) of 0.037μM for Pep-1-Phor21 in both the methods. Similarly Pho21-βCG(ala) showed a dose-dependent cytotoxicity and loss of cell viability effect on LHCGR expressing cells with an IC_{50} of 0.04μM in both the methods. The lytic peptide (Phor21) alone showed no cytotoxicity or reduced cell viability of HEK293 cells expressing either IL-13Rα2 or LHCGR whereas Pep-1-Phor21 or Pho21-βCG (ala) had no effect on HEK293 cells expressing neither receptor. To confirm Pep-1-Phor21 and Phor21-βCG(ala) only target IL-13Rα2 and LHCGR, respectively, HEK293 cells expressing IL-13Rα2 were treated with Phor21-βCG (ala) and HEK293 cells expressing LHCGR were treated with Pep1-Phor21 and assessed cell viability (Figure 4.3.1D). Pep-1-Phor21 had no effect on cell viability of HEK293 cells expressing LHCGR whereas Phor21-βCG (ala) treated LHCGR expressing cells showed a significant decrease in cell viability (92.87 ± 8.08 % [$P > 0.05$] and 13.80 ± 0.62 % [$P < 0.0001$] respectively). HEK293 cells expressing IL-13Rα2 showed a significant decrease in cell viability when treated with Pep-1-Phor21 whereas Phor21-βCG (ala) had no effect on cell viability of IL-13Rα2 expressing cells (29.70 ± 2.76% [$P < 0.0001$] and 91.30±4.85% [$P > 0.05$] respectively). These results demonstrate that Pep-1-Phor21 and Phor21-βCG (ala) specifically target IL-13Rα2 and LHCGR respectively. These results also demonstrate that conjugated controls show no effect on the cell viability. The specificity of [D-Trp^6]GnRH-Phor21, the third lytic peptide conjugate used in this study, could not be tested due to lack of GnRHR expression plasmid. However, GnRH peptide conjugated to a lytic peptide is well characterised with respect to its specificity in targeting and killing GnRHR over-expressing cancer cells (Hansel et al, 2007b).

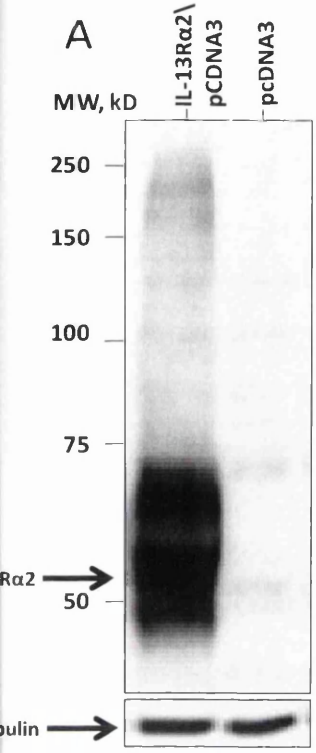

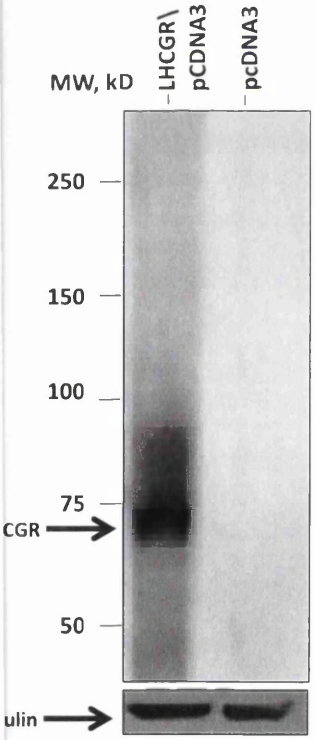

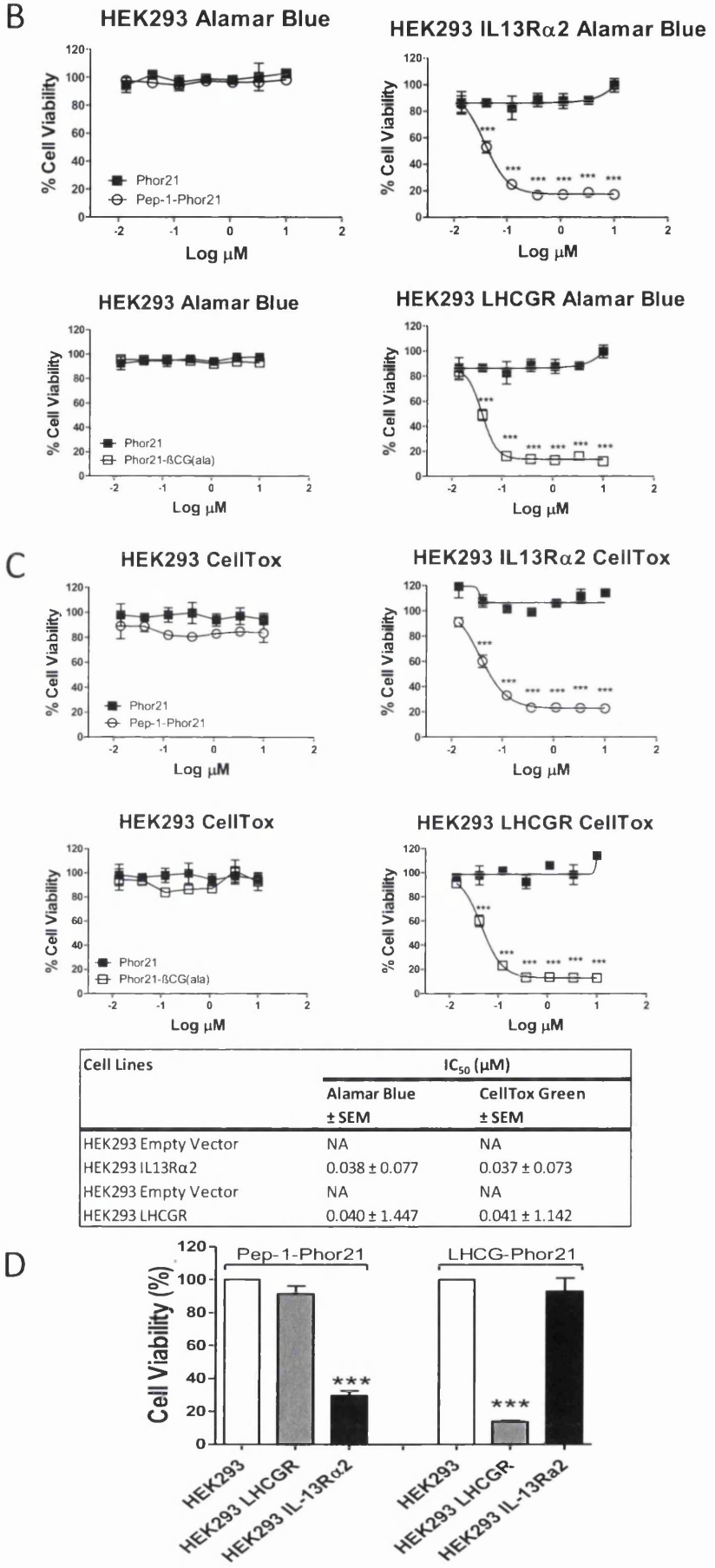

Cell Lines	IC_{50} (μM)	
	Alamar Blue ± SEM	CellTox Green ± SEM
HEK293 Empty Vector	NA	NA
HEK293 IL13Rα2	0.038 ± 0.077	0.037 ± 0.073
HEK293 Empty Vector	NA	NA
HEK293 LHCGR	0.040 ± 1.447	0.041 ± 1.142

Figure 4.3.1. Specificity of Pep-1-Phor21 and Phor21-βCG (ala) in targeting their receptors expressing cells. (**A**) Western blot analysis of IL-13Rα2 and LHCGR protein expression in HEK293 cells. The lysates of HEK293 cells transfected with IL-13Rα2 or LHCGR plasmid or empty plasmid were separated by SDS-PAGE, transferred onto PVDF membrane and probed using an anti-IL-13Rα2 or anti-LHCGR antibody. The lysates were also probed with an anti-α-tubulin antibody to ensure equal loading. HEK293 cells or HEK293 cells expressing IL-13Rα2 or LHCGR were incubated with 0-10μM of Pep-1-Phor21 or Phor21-βCG (ala) or Ph0or21 for 3h and measured their cytotoxicity by using alamar blue (**B**) and CellTox (**C**) assays. (**D**) The specificity of cytotoxicity effect of Pep-1-Phor21 (⊖) and Phor21-βCG(ala) (⊟) on HEK293 cells expressing IL-13Rα2 and LHCGR respectively. HEK293 cells expressing nothing or IL-13Rα2 or LHCGR were incubated with 0.5μM Pep-1-Phor21 or Phor21-βCG(ala) for 3h and their cytotoxicity was measured by CellTox assay. The data represent means ± SEM (error bars represent SEM) of three independent experiments (***, $P < 0.001$).

4.3.2. Expression of IL-13Rα2, LHCGR and GnRHR in prostate and breast cancer cell lines

IL-13Rα2

It has been shown previously that IL-13Rα2 can play a prominent role in promoting cancer cell growth and tumour formation (He et al, 2010). Furthermore, IL-13Rα2 has been shown to be overexpressed in several cancers including brain, renal cell carcinoma, squamous cell carcinoma of head and neck, ovarian cell carcinoma, pancreatic, breast and prostate cancers (Fujisawa et al, 2009; Gonzalez-Moreno et al, 2005; Jarboe et al, 2007; Kawakami et al, 2003; Kioi et al, 2006a; Kioi et al, 2006b; Puri et al, 1996; Zhao et al, 2014). Therefore the expression of IL-13Rα2 mRNA and protein was analysed in non-cancer cell line (HEK293) and prostate cancer cell lines (androgen dependent [LNCaP] and androgen independent with a high metastatic potential [DU145 and PC3]) by RT-PCR and immunoblotting respectively. IL-13Rα2 protein was expressed in prostate cancer cell lines but undetectable in HEK293 cells (Figure 4.2A-B). IL-13Rα2 protein expression was low but detectable in LNCaP cells and therefore IL-13Rα2 expression in LNCaP cells was used to compare with that in other prostate cancer cell lines to analyse relative expression in subsequent studies. When

compared to IL-13Rα2 protein expression in LNCaP cells, DU145 and PC3 cells expressed high levels of IL-13Rα2 protein (4.5 fold [$P \leq 0.05$] and 8.6 fold [$P \leq 0.01$] respectively). Consistent with this, DU145 and PC3 cells expressed high levels of IL-13Rα2 mRNA when compared to that in LNCaP cells (13.53 fold [$P \leq 0.05$] and 27.95 fold [$P \leq 0.05$] respectively). Since IL-13Rα2 protein functions mainly at the cell surface, we have also assessed its cell surface expression in the prostate cancer cell lines by ELISA (Figure 4.3.2D). IL-13Rα2 protein cell surface expression is relatively high in metastatic prostate cancer cell lines DU145 and PC3 (160.6% [$P \leq 0.05$] and 311.9% [$P \leq 0.01$] respectively). Together, these results suggest that IL-13Rα2 expression is high in metastatic prostate cancer cell lines.

The expression of IL-13Rα2 mRNA and protein was also analysed in a non-cancer breast cell line (MCF-10A) and the breast cancer cell lines (androgen dependent [MCF-7] and androgen independent with a high metastatic potential [MDA-MB 231]), by immunoblotting (Figure 4.3.2A-B) and RT-PCR (Figure 4.3.2C) respectively. The expression of IL-13Rα2 mRNA and protein was low in non-cancer cell line MCF-10A. Consistent with this, IL-13Rα2 cell surface expression was found to be very low (Figure 4.3.2D). Therefore expression of IL-13Rα2 in breast cancer cell lines was measured relative to that expressed in MCF-10A. MCF-7 showed no significant increase in the expression of IL-13Rα2 mRNA (4.678 fold [$P > 0.05$]) and protein (3.6 fold [$P \leq 0.05$]). IL-13Rα2 protein cell surface expression, assessed by ELISA, was also low (116.8% [$P > 0.05$]). However, MDA-MB 231 cells with a high metastatic potential showed a significant increase in the expression of IL-13Rα2 mRNA (18.85 fold [$P \leq 0.05$]) and protein (5.01 fold [$P \leq 0.01$]). Consistent with this, IL-13Rα2 protein cell surface expressions was also shown to be high in MDA-MB 231 cells (361.3% [$P \leq 0.001$]).

These results suggest that non-cancer HEK293 and breast epithelial cells and hormone dependent prostate and breast cancer cell lines express no or little IL-13Rα2whereas prostate and breast cancer cell lines with high metastatic potential express high levels of IL-13Rα2.

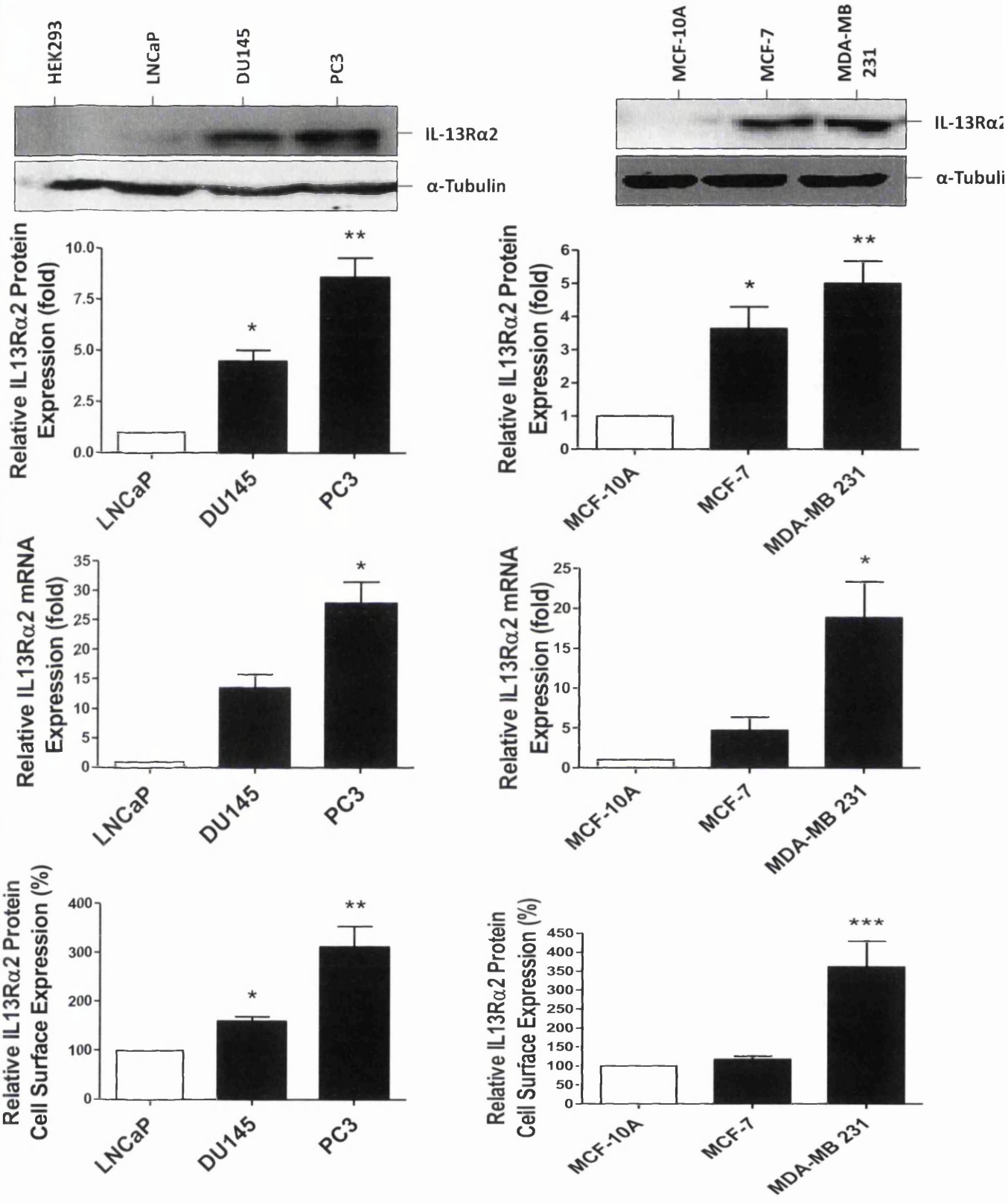
HEK293
LNCaP
DU145
PC3
IL-13Rα2
α-Tubulin
MCF-10A
MCF-7
MDA-MB 231
IL-13Rα2
α-Tubuli
Relative IL13Rα2 Protein Expression (fold)
Relative IL13Rα2 mRNA Expression (fold)
Relative IL13Rα2 Protein Cell Surface Expression (%)
LNCaP
DU145
PC3
MCF-10A
MCF-7
MDA-MB 231

Figure 4.3.2 Expression of IL-13Rα2 in prostate and breast cell lines. A) Western blot analysis of IL-13Rα2 protein expression in non-cancer cell lines (HEK293 and MCF-10A) and cancer cell lines (LNCaP, DU145, MCF-7 and MDA-MB 231). **B**) Quantification of IL-13Rα2 protein expression shown in **(A)** by densitometric analysis and normalising to housekeeping protein (α-Tubulin) expression. **C**) Real-time PCR (RT-PCR) analysis of IL-13Rα2 mRNA expression in non-cancer and cancer cell lines. **D**) Cell surface expression of IL-13Rα2 protein was assessed by subjecting un-permeablised cells to ELISA. All Western blots and RT-PCR values are normalised to housekeeping controls. The data are mean ± SEM values of three independent experiments (*P < 0.05, **P < 0.01and ***P < 0.001 compared with non-cancer cell line control).

LHCGR

LHCGR has previously been shown that LHCGR is over-expressed in a number of cancer cells, including breast and prostate cancer cells (Hansel, 2005; Leuschner & Hansel, 2005). Non-cancer cell lines (PNT-2 and MCF-10A) together with prostate cancer cell lines (LNCaP, DU145 and PC3) and breast cancer cell lines (MCF-7 and MDA-MB 231), were analysed for LHCGR protein and mRNA expression using immunoblotting (Figure 4.3.3 A-B) and RT-PCR (Figure 4.3.3. C) respectively. The expression of LHCGR mRNA and protein was low in non-cancer prostate (PNT-2) and breast (MCF-10A) cell lines. LHCGR expression in prostate cancer cell lines LNCaP, DU145 and PC3 increased when compared to that in PNT-2 at the protein (6.413 fold [$P \leq 0.05$], 5.973 fold and 6.614 fold [$P \leq 0.05$] respectively) and mRNA (9.715 fold [$P \leq 0.01$], 6.758 fold [$P \leq 0.01$] and 10.60 fold [$P \leq 0.01$] respectively) levels. The breast cancer cell lines MCF-7 and MDA-MB 231 also showed a significant increase in LHCGR expression compared to MCF-10A when assessed by RT-PCR (14.92 fold [$P > 0.001$] and 12.61 fold [$P \leq 0.01$] respectively) and immunoblotting (7.00 fold [$P \leq 0.001$] and 5.67 fold [$P \leq 0.01$] respectively). The cell surface expression of LHCGR was not assessed due to lack of anti- LHCGR antibody suitable for ELISA.

These results suggest that the non-cancer prostate (PNT-2) and breast (MCF-10A) cell lines express little or no LHCGR whereas prostate (LNCaP, Du145 and PC3) and breast (MCF-7 and MDA-MB 231) cancer cell lines express high levels of LHCGR.

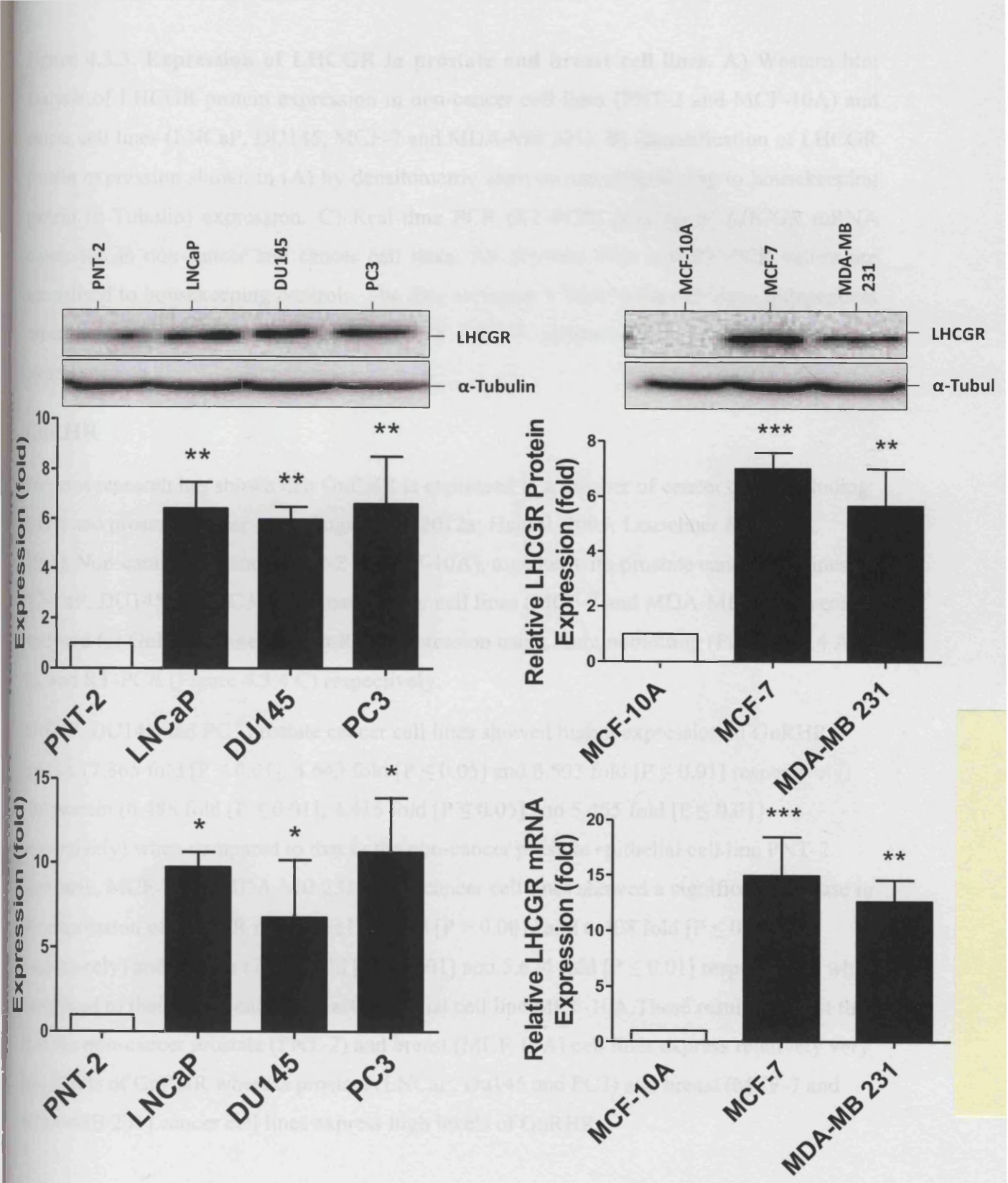
PNT-2
LNCaP
DU145
PC3
LHCGR
α-Tubulin
MCF-10A
MCF-7
MDA-MB 231
LHCGR
α-Tubul
Expression (fold)
Relative LHCGR Protein Expression (fold)
Expression (fold)
Relative LHCGR mRNA Expression (fold)

Figure 4.3.3. Expression of LHCGR in prostate and breast cell lines. A) Western blot analysis of LHCGR protein expression in non-cancer cell lines (PNT-2 and MCF-10A) and cancer cell lines (LNCaP, DU145, MCF-7 and MDA-MB 231). **B)** Quantification of LHCGR protein expression shown in **(A)** by densitometric analysis and normalising to housekeeping protein (α-Tubulin) expression. **C)** Real-time PCR (RT-PCR) analysis of *LHCGR* mRNA expression in non-cancer and cancer cell lines. All Western blots and RT-PCR values are normalised to housekeeping controls. The data are mean ± SEM values of three independent experiments (*P < 0.05, **P < 0.01and ***P < 0.001 compared with non-cancer cell line control).

GnRHR

Previous research has shown that GnRHR is expressed in a number of cancer cells, including breast and prostate cancer cells (Engel et al, 2012a; Hansel, 2005; Leuschner & Hansel, 2005). Non-cancer cell lines (PNT-2 and MF-10A), together with prostate cancer cell lines (LNCaP, DU145, and PC3) and breast cancer cell lines (MCF-7 and MDA-MB 231), were analysed for GnRHR protein and mRNA expression using immunoblotting (Figure 4.3.4 A-B), and RT-PCR (Figure 4.3.4 C) respectively.

LNCaP, DU145 and PC3 prostate cancer cell lines showed higher expression of GnRHR mRNA (7.865 fold [$P \leq 0.01$], 4.643 fold [$P \leq 0.05$] and 8.503 fold [$P \leq 0.01$] respectively) and protein (6.488 fold [$P \leq 0.01$], 4.415 fold [$P \leq 0.05$] and 5.455 fold [$P \leq 0.01$] respectively) when compared to that in the non-cancer prostate epithelial cell line PNT-2. Similarly, MCF-7 and MDA-MB 231 breast cancer cell lines showed a significant increase in the expression of GnRHR mRNA (11.84 fold [$P > 0.001$] and 6.408 fold [$P \leq 0.01$] respectively) and protein (7.482 fold [$P \leq 0.001$] and 5.624 fold [$P \leq 0.01$] respectively) when compared to that in non-cancer breast epithelial cell line MCF-10A.These results suggest that that the non-cancer prostate (PNT-2) and breast (MCF-10A) cell lines express relatively very low levels of GnRHR whereas prostate (LNCaP, Du145 and PC3) and breast (MCF-7 and MDA-MB 231) cancer cell lines express high levels of GnRHR.

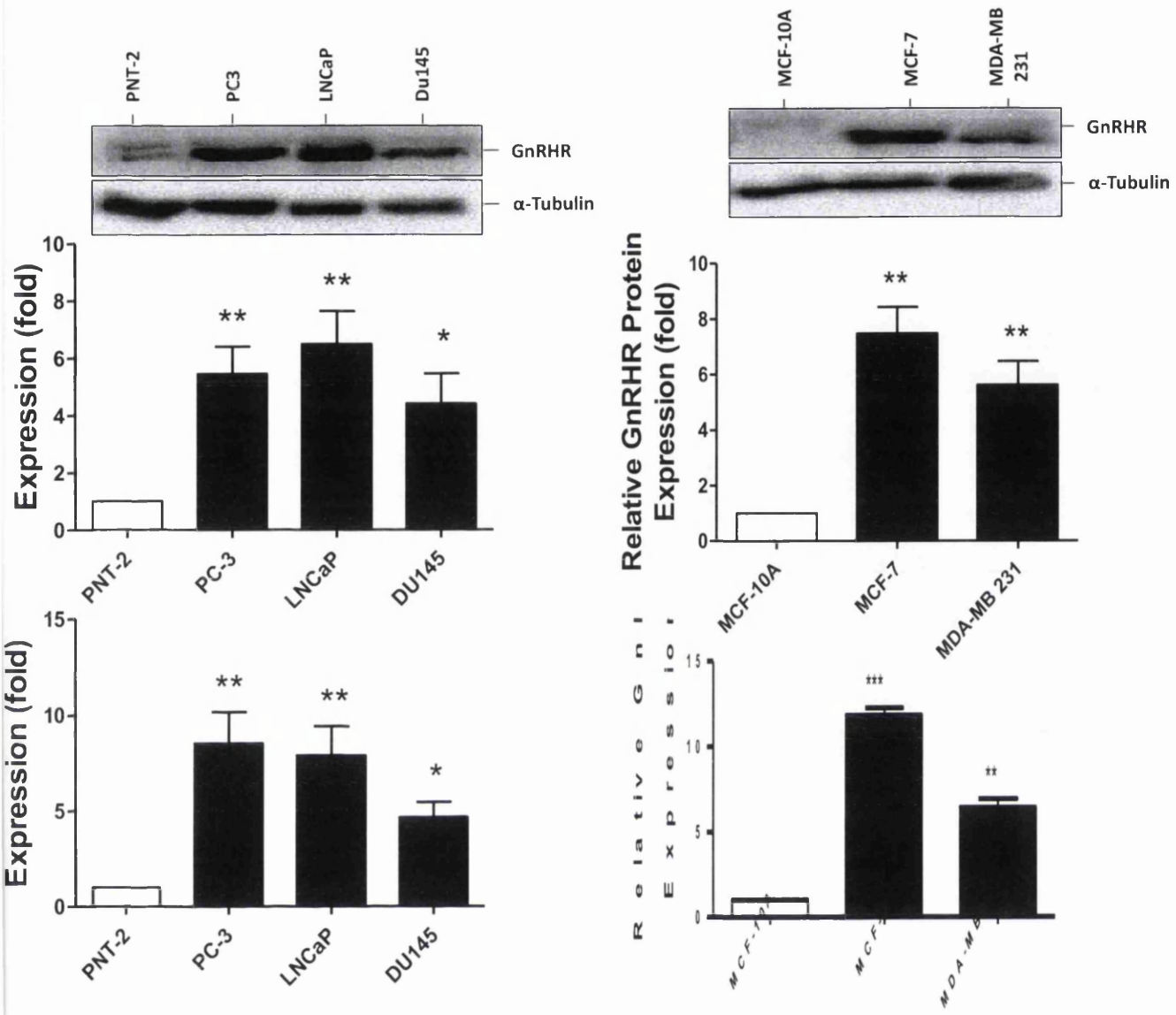
PNT-2
PC3
LNCaP
Du145
GnRHR
α-Tubulin
Expression (fold)
PNT-2
PC-3
LNCaP
DU145
MCF-10A
MCF-7
MDA-MB 231
Relative GnRHR Protein Expression (fold)

Figure 4.3.4 Expression of GnRHR in prostate and breast cell lines. A) Western blot analysis of GnRHR protein expression in non-cancer cell lines (PNT-2 and MCF-10A) and cancer cell lines (LNCaP, DU145, MCF-7 and MDA-MB 231). **B**) Quantification of GnRHR protein expression shown in **(A)** by densitometric analysis and normalising to housekeeping protein (α-Tubulin) expression. **C**) Real-time PCR (RT-PCR) analysis of *GnRHR* mRNA expression in non-cancer and cancer cell lines. All Western blots and RT-PCR values are normalised to housekeeping controls. The data are mean ± SEM values of three independent experiments (*P < 0.05, **P < 0.01and ***P < 0.001 compared with non-cancer cell line control.

4.3.3. The cytotoxic activity of Pep-1-Phor21, Phor21-βCG (ala) and [D-Trp^6]GnRH-Phor21 peptides on prostate and breast cancer cell lines

Pep-1-Phor21

The cytotoxic activity of Pep-1-Phor21 peptide on low IL-13Rα2 expressing prostate (LNCaP) and breast cell lines (MCF-10A and MCF-7), and high IL-13Rα2 expressing IL-13Rα2 prostate (DU145 and PC3) and breast (MDA-MB 231) cell lines was determined. Cells grown in a monolayer (2D culture) were incubated with 0-125 μM Pep-1, Phor21 or Pep-1-Phor21 for 3 hours and the viability of cells was assessed by using alamar blue assay (Figure 4.3.5.A). Prostate (DU145, and PC3) and breast (MDA-MB 231) cell lines with a high metastatic potential, which express relatively high levels of IL-13Rα2, were more sensitive to Pep-1-Phor21, which affected the viability of these cells in a dose dependent manner. The IC_{50} of Pep-1-Phor21 for these cell lines by was <13μM (Figure 4.3.5.B). In contrast, low IL-13Rα2 expressing prostate (LNCaP) and breast (MCF-10A and MCF-7) cell lines, showed little to no cell death in the presence of Pep-1-Phor21 and the IC_{50} of Pep-1-Phor21 for these cell lines was >50μM (Figure 4.3.5.B). However, ligand Pep-1 and the lytic peptide Phor21 showed little or no effect on the viability of both low IL-13Rα2 and high IL-13Rα2 expressing prostate and breast cell cancer lines used in this study.

The sensitivity of prostate and breast cancer cell lines to Pep-1-Phor21 peptide were further assessed by CellTox cytotoxicity assay (Figure 4.3.5C). Prostate (LNCaP [120μM], DU145 [24μM] and PC3 [10μM]) and breast (MCF-10A [120μM], MCF-7 [120μM] and MDA-MB231 [24μM]) cell lines were treated with Pep-1-Phor21, Pep-1 or Phor21 (concentration

used indicated next to each cell line) peptide for 3 hours before assessing the cytotoxicity of the peptide to the cells. The concentration of peptide used for each cell line was based on its IC_{50} in the alamar blue assay. Prostate (LNCaP) and breast (MCF-10A and MCF-7) cell lines with low IL-13Rα2 expression demonstrated no significant reduction in cell viability when incubated with the conjugated lytic peptide Pep-1-Phor21 (MCF-10A:100.19% [$P \geq 0.05$], MCF-7: 96.95% [$P \geq 0.05$], and LNCaP: 76.91% [$P \geq 0.05$]. However, the high IL-13Rα2 expressing prostate (DU145 and PC3) and breast (MDA-MB 231) cell lines incubated with the conjugated peptides showed a significant reduction in cell viability (DU145:35.19% [$P \leq 0.001$], PC3: 26.95% [$P \leq 0.001$], and MDA-MB231: 26.91% [$P \leq 0.001$]). The ligand Pep-1 and the lytic peptide Phor21 had no cytotoxic effect on any of these cell lines.

These results suggest that that prostate and breast cancer cells expressing high levels of IL-13Rα2 are more sensitive to Pep-1-Phor21, indicating a direct connection between the sensitivity of cells to Pep-1-Phor21 and the levels of IL-13Rα2 they express.

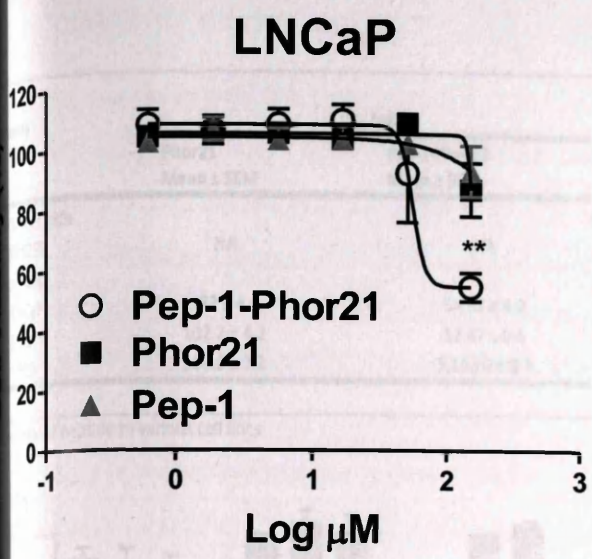
LNCaP
Pep-1-Phor21
Phor21
Pep-1
Log μM

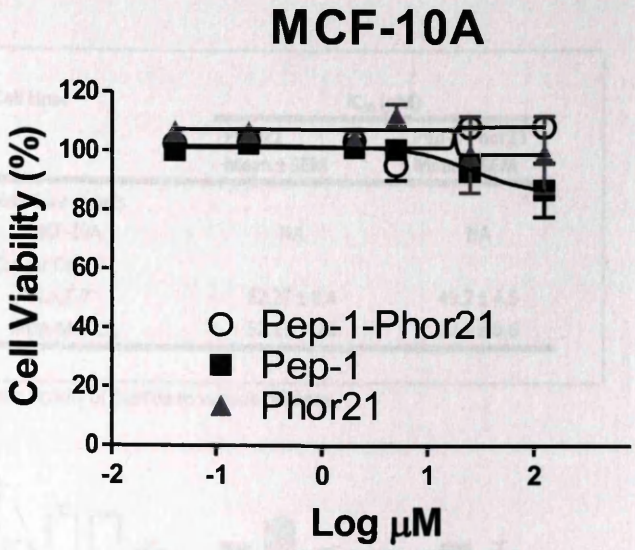
MCF-10A
Cell Viability (%)
Pep-1-Phor21
Pep-1
Phor21
Log μM

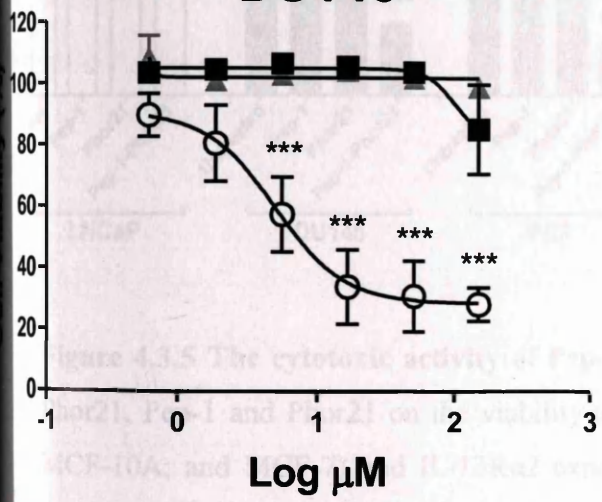
DU145
Log μM

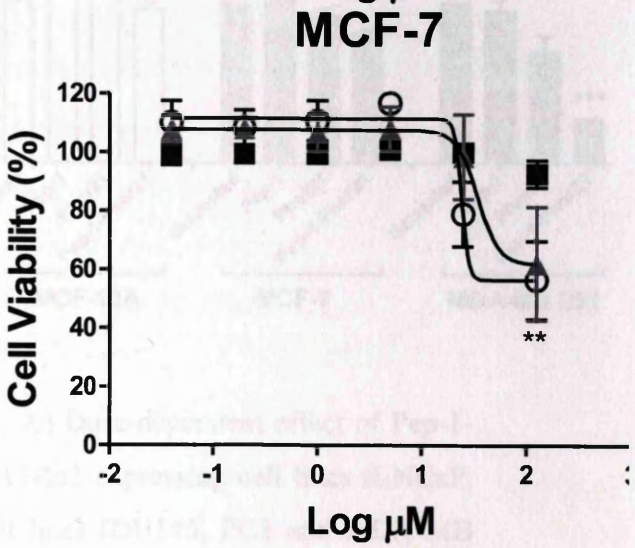
MCF-7
Cell Viability (%)
Log μM

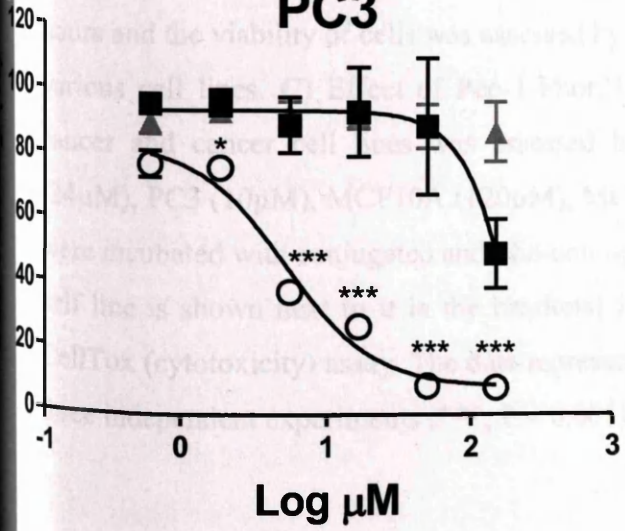
PC3
Log μM

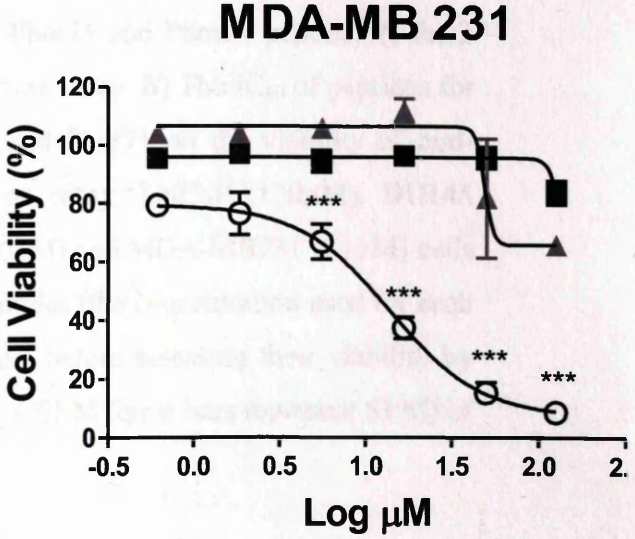
MDA-MB 231
Cell Viability (%)
Log μM

lines	IC_{50} (μM)	
	Phor21 Mean ± SEM	Pep-1-Phor21 Mean ± SEM
Cancer cells		
HEK293	NA	NA
er Cells		
LNCaP	153 ± 4.1	54.92 ± 4.0
DU145	102.2 ± 4.2	12.47 ± 0.6
PC3	156.0 ± 2.1	5.156.0 ± 0.4

ctivity of peptide to various cell lines

Cell Lines	IC_{50} (μM)	
	Phor21 Mean ± SEM	Pep-1-Phor21 Mean ± SEM
Non Cancer cells		
MCF-10A	NA	NA
Cancer Cells		
MCF-7	62.27 ± 8.4	49.7 ± 4.5
MDA-MD 231	52.17 ± 5.6	12.2 ± 0.6

Cytotoxic activity of peptide to various cell lines

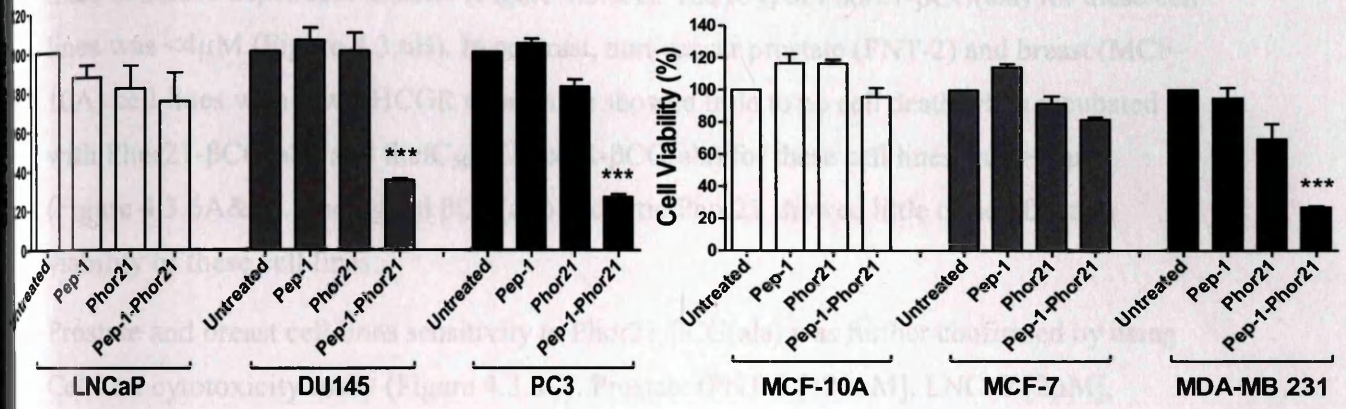

Figure 4.3.5 The cytotoxic activity of Pep-1-Phor21. A) Dose-dependent effect of Pep-1-Phor21, Pep-1 and Phor21 on the viability of non-IL-13Rα2 expressing cell lines (LNCaP, MCF-10A, and MCF-7) and IL-13Rα2 expressing cell lines (DU145, PC3 and MDA-MB 231). The cells were treated with 0-120 μM of Pep-1-Phor21 and Phor21 peptides () for 3 hours and the viability of cells was assessed by alamar blue assay. **B**) The IC_{50} of peptides for various cell lines. **C**) Effect of Pep-1-Phor21, Pep-1 and Phor21 on the viability of non-cancer and cancer cell lines was assessed by CellTox assay. LNCaP (120μM), DU145 (24μM), PC3 (10μM), MCF10A (120μM), MCF-7 (120μM) and MDA-MB231 (24μM) cells were incubated with conjugated and non-conjugated peptides (the concentration used for each cell line is shown next to it in the brackets) for 3 hours before assessing their viability by CellTox (cytotoxicity) assay. The data represent means ± SEM (error bars represent SEM) of three independent experiments (***, $P < 0.001$).

Phor21-βCG(ala)

We also assessed the cytotoxic effect of Phor21-βCG(ala) peptide on non-cancer prostate (PNT-2) and breast (MCF-10A), and cancer prostate (LNCaP, DU145 and PC3) and breast (MCF-7 and MDA-MB 231) cell lines. For this purpose, cells grown in a monolayer (2D culture) were incubated with 0-125 μM βCG(ala), Phor21 or Phor21-βCG(ala) for 3 hours and the viability of cells was assessed by using alamar blue assay. Prostate (LNCaP, DU145 and PC3) and breast (MCF-7 and MDA-MB 231) cancer cell lines with high LHCGR expression were more sensitive to Phor21-βCG(ala), which affected viability of these cell lines in a dose dependent manner (Figure 4.3.6A). The IC_{50} of Phor21-βCG(ala) for these cell lines was <4μM (Figure 4.3.6B). In contrast, non-cancer prostate (PNT-2) and breast (MCF-10A) cell lines with low LHCGR expression showed little to no cell death when incubated with Phor21-βCG(ala) and theIC_{50} of Phor21-βCG(ala) for these cell lines was >50μM (Figure 4.3.6A&B). The ligand βCG(ala) and lytic Phor21 showed little or no effect on viability of these cell lines.

Prostate and breast cell lines sensitivity to Phor21-βCG(ala) was further confirmed by using CellTox cytotoxicity assay (Figure 4.3.6C). Prostate (PNT-2 [120μM], LNCaP [2μM], DU145 [4μM] and PC3 [4μM]) and breast (MCF-10A [120μM], MCF-7 [2μM] and MDA-MB231 [6μM]) cell lines were incubated with βCG(ala), Phor21 or Phor21-βCG(ala) (concentration used indicated next to each cell line) peptide for 3 hours assessing the cytotoxicity of the peptide to the cells. The concentration of peptide used for each cell line was based on its IC_{50} in the alamar blue assay. The non-cancer prostate (PNT-2) and breast (MCF-10A) cell lines with low LHCGR expression showed no significant reduction in cell viability when treated with Phor21-βCG(ala) (MCF-10A:104.09% [$P \geq 0.05$], and PNT-2: 79.95% [$P \geq 0.05$]). However, Prostate (LNCaP, DU145 and PC3) and breast (MCF-7 and MDA-MB 231) cancer cell lines, which express high levels of LHCGR, demonstrated a significant loss in cell viability in the presence of Phor21-βCG(ala) (LNCaP: 23.15% [$P \leq 0.001$], DU145:20.13% [$P \leq 0.001$] PC3: 9.194% [$P \leq 0.001$], MCF-7: 20.16% [$P \leq 0.001$] and MDA-MB 231: 10.23% [$P \leq 0.001$]) . The ligand βCG(ala) and lytic peptide Phor21 had no cytotoxic effect in any of the cell lines used in this study. These result suggest that Phor21-βCG(ala) selectively kills prostate and breast cancer cells expressing high levels of LHCGR, indicating a direct connection between the sensitivity of cells to Phor21-βCG(ala) and the levels of LHCGR they express.

A

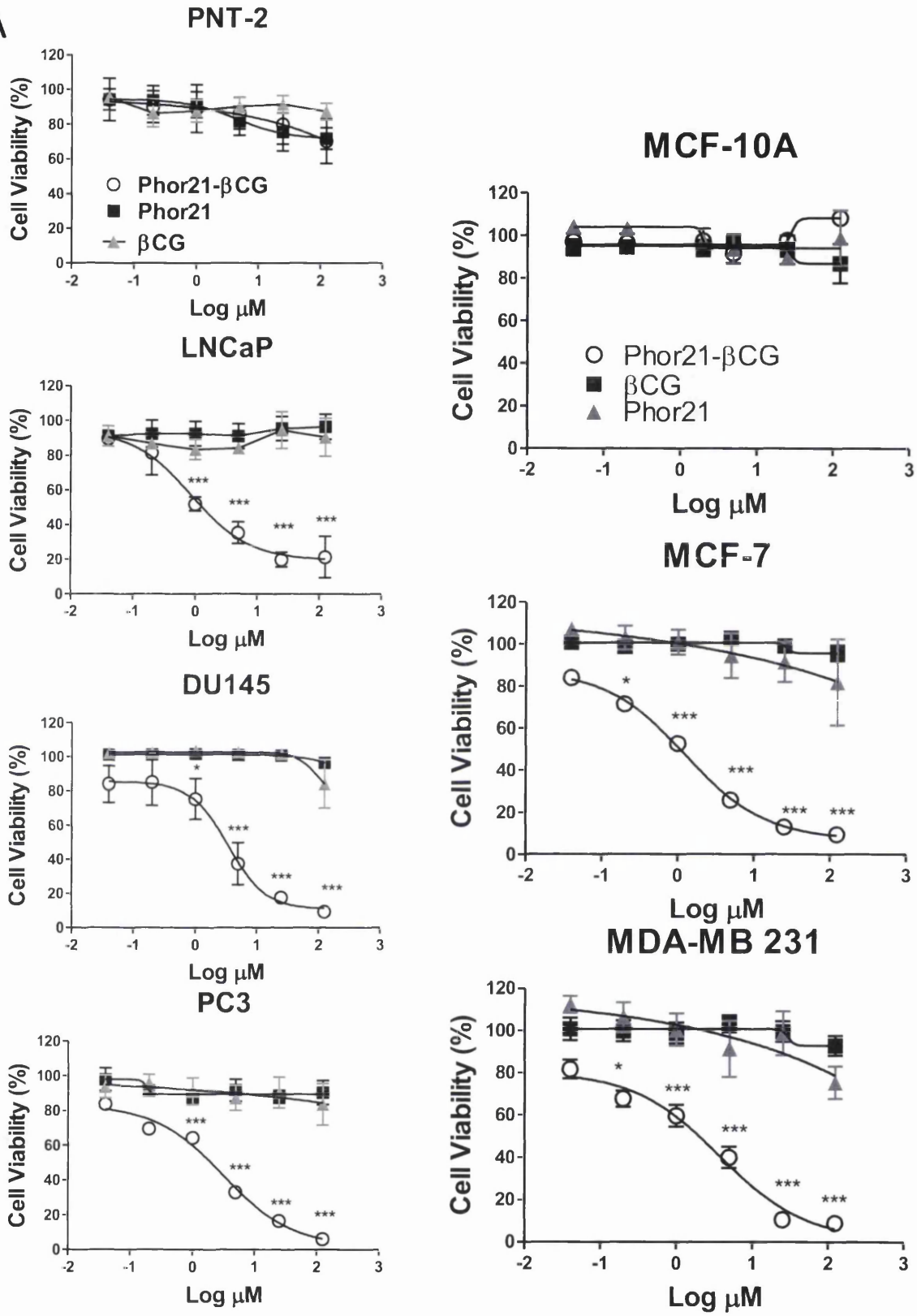
PNT-2
Cell Viability (%)
Log μM
Phor21-βCG
Phor21
βCG
LNCaP
DU145
PC3
MCF-10A
MCF-7
MDA-MB 231

ll Lines	IC_{50} (μM)	
	Phor21 Mean ± SEM	Phor21-ßCG(ala) Mean ± SEM
n Cancer cells		
PNT-2	NA	NA
ncer Cells		
LNCaP	NA	0.86 ± 7.6
DU145	98.76 ± 3.2	2.9 ± 0.32
PC3	NA	3.2 ± 0.15

c activity of peptide to various cell lines

Cell Lines	IC_{50} (μM)	
	Phor21 Mean ± SEM	Phor21-ßCG(ala) Mean ± SEM
Non Cancer cells		
MCF-10A	NA	NA
Cancer Cells		
MCF-7	NA	1.24 ± 2.28
MDA-MB 231	NA	3.72 ± 1.24

Cytotoxic activity of peptide to various cell lines

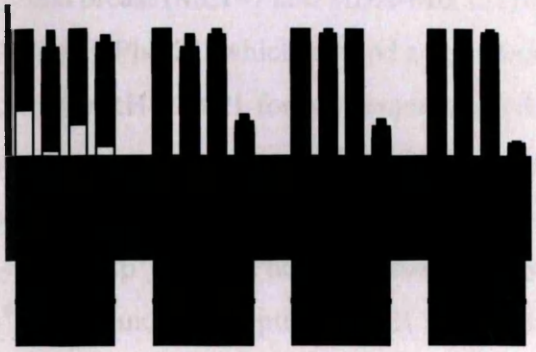

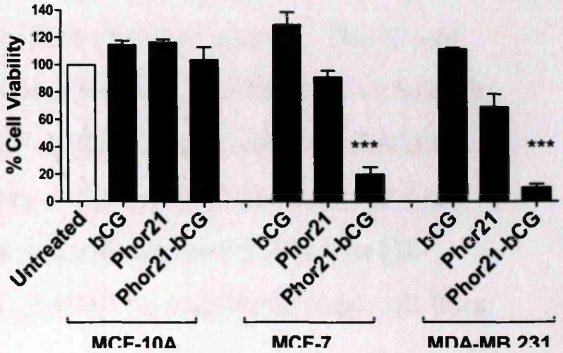

Figure 4.3.6 The cytotoxic activity of Phor21-βCG(ala). **A**) Dose-dependent effect Phor21-βCG(ala), βCG(ala) and Phor21 on the viability of non-LHCGR expressing cell lines (PNT-2 and MCF-10A) and LHCGR expressing cell lines (LNCaP, DU145, PC3, MCF-7 and MDA-MB 231). The cells were treated with 0-120 μM of Phor21-βCG(ala)and Phor21 peptides () for 3 hours and the viability of cells was assessed by alamar blue assay. **B**) The IC_{50} of peptides for various cell lines. **C**) Effect of effect Phor21-βCG(ala), βCG(ala) and Phor21 on the viability of non-cancer and cancer cell lines was assessed by CellTox assay. PNT-2 (120μM), LNCaP (2μM), DU145 (4μM), PC3 (4μM), MCF10A (120μM), MCF-7 (2μM) and MDA-MB231 (6μM) cells were incubated with conjugated and non-conjugated peptides (the concentration used for each cell line is shown next to it in the brackets) for 3 hours before assessing their viability by CellTox assay. The data represent means ± SEM (error bars represent SEM) of three independent experiments (***, $P < 0.001$).

[D-Trp^6]GnRH-Phor21

The cytotoxic activity of [D-Trp^6]GnRH-Phor21 peptide on low GnRHR expressing (PNT-2, and MCF-10A), and high GnRHR expressing (LNCaP, DU145, PC3, MCF-7 and MDA-MB 231) prostate and breast cell lines was determined. Cells grown in 2D were incubated with 0-125 μM, D-Trp^6]GnRH, Phor21 or D-Trp^6]GnRH-Phor21 for 3 hours and the viability of cells was assessed by using alamar blue assay (Figure 4.3.7A). Prostate (LNCaP, DU145 and PC3) and breast (MCF-7 and MDA-MB 231) cancer cell lines were more sensitive to [D-Trp^6]GnRH-Phor21, which showed a dose dependent effect on these cell lines. The IC_{50} of [D-Trp^6]GnRH-Phor21 for cells expressing relatively high levels of GnRHR was <3.5μM. In contrast, non-cancer prostate (PNT-2) and breast (MCF-10A) cell lines with low GnRHR expression showed little or no cell death in the presence of [D-Trp^6]GnRH-Phor21 and the IC_{50} of [D-Trp^6]GnRH-Phor21 for these cell lines was >50μM (Figure 4.3.7B). The [D-Trp^6]GnRH and lytic peptide Phor21 showed little or no effect on viability of these cell lines.

Prostate and breast cell lines sensitivity to [D-Trp^6]GnRH-Phor21 was further confirmed by using CellTox cytotoxicity assay (Figure 4.3.7C). Prostate cell lines (PNT-2 [120μM], , LNCaP [2μM], DU14[5 4μM] and PC3 [4μM]) and breast (MCF-10A [120μM], MCF-7 [2μM] and MDA-MB231 [4μM]) were incubated with [D-Trp^6]GnRH, Phor21 or [D-Trp^6]GnRH-Phor21 (concentration used indicated next to each cell line) peptide for 3 hours and assayed the cytotoxicity of cells to the peptide . The concentration of peptide used for each cell line was based on its IC_{50} in the alamar blue assay. Treatment of non-cancer prostate (PNT-2) and breast (MCF-10A) cell lines, which show low GnRHR expression, with [D-Trp^6]GnRH-Phor21 resulted in no significant reduction in their cell viability (MCF-10A:85.09% [$P \geq 0.05$], and PNT-2: 76.95% [$P \geq 0.05$]).. Treatment of prostate (LNCaP, DU145 and PC3) and breast (MCF-7 and MDA-MB 321) cancer cell lines, which express relatively high levels of GnRHR, resulted in significant reduction in cell viability (LNCaP: 18.82% [$P \leq 0.001$], DU145: 20.77% [$P \leq 0.001$], PC3: 10.87% [$P \leq 0.001$], MCF-7: 18.51% [$P \leq 0.001$] and MDA-MB 231: 10.56% [$P \leq 0.001$]). The ligand D-Trp^6]GnRH and lytic peptide Phor21 showed no cytotoxic effect in any of these cell lines.

These results suggest that [D-Trp^6]GnRH-Phor21 selectively kill prostate and breast cancer cells expressing relatively high levels of GnRHR, suggesting a direct connection between the sensitivity of cells to [D-Trp^6]GnRH-Phor21 and the levels of LHCGR they express.

A

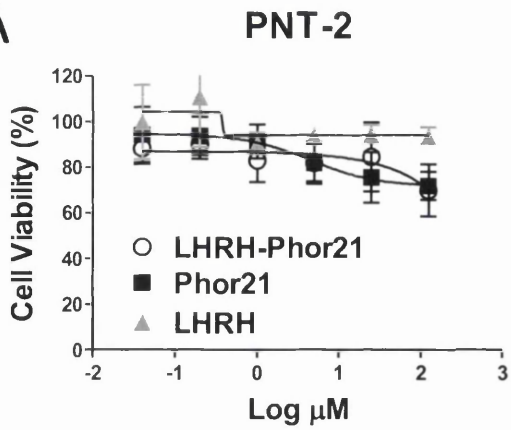
PNT-2
Cell Viability (%)
LHRH-Phor21
Phor21
LHRH
Log μM

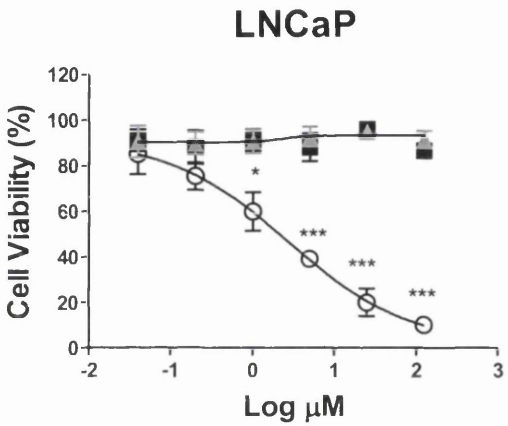
LNCaP
Cell Viability (%)
Log μM

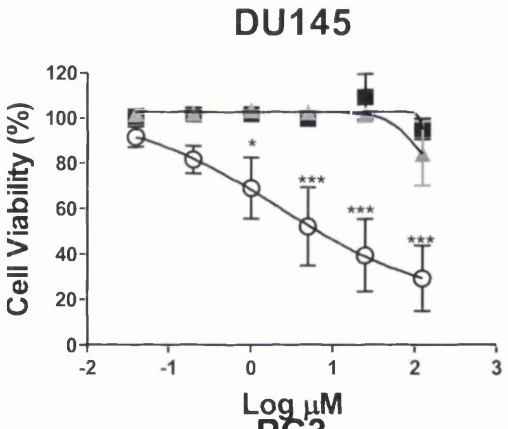
DU145
Cell Viability (%)
Log μM

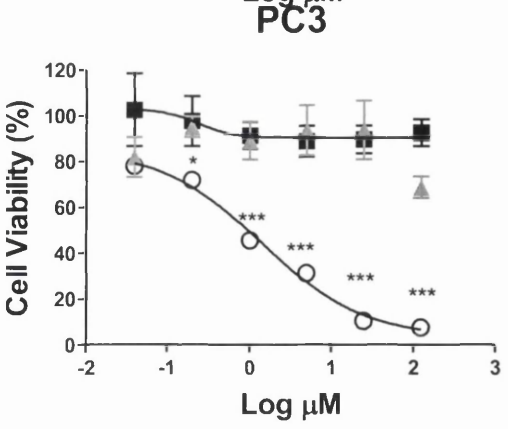
PC3
Cell Viability (%)
Log μM

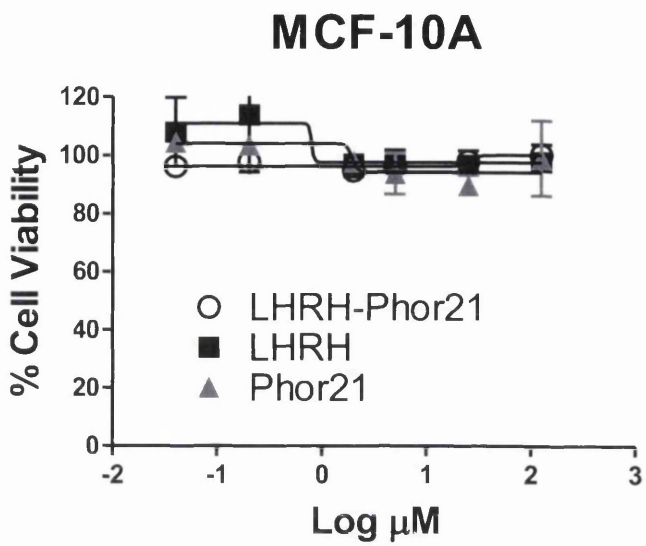
MCF-10A
% Cell Viability
LHRH-Phor21
LHRH
Phor21
Log μM

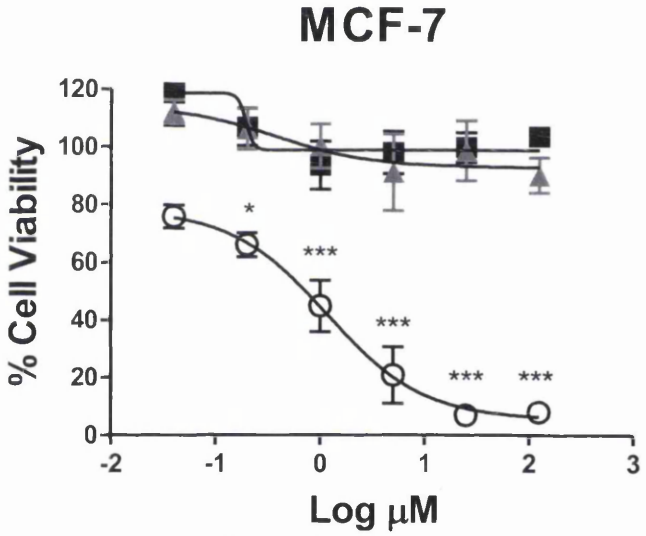
MCF-7
% Cell Viability
Log μM

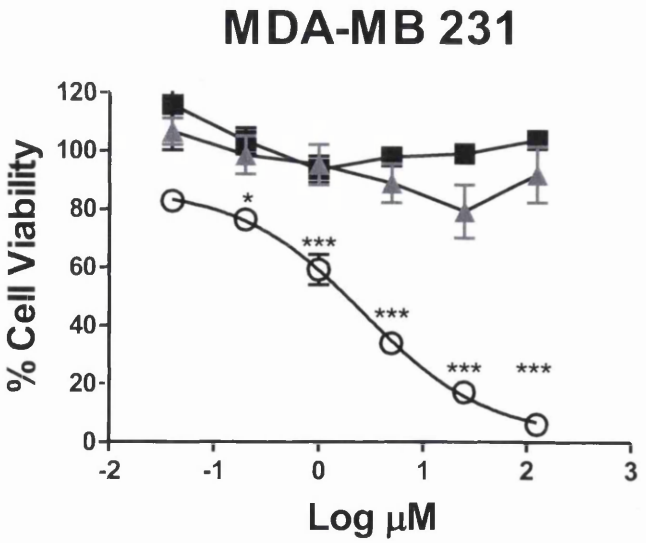
MDA-MB 231
% Cell Viability
Log μM

	IC_{50} (μM)	
	Phor21 Mean ± SEM	GnRH-Phor21 Mean ± SEM
ancer cells		
PNT-2	NA	NA
r Cells		
LNCaP	NA	2.8 ± 0.29
DU145	98.8 ± 3.2	2.3 ± 1.1
PC3	NA	3.1 ± 0.14

Cell Lines	IC_{50} (μM)	
	Phor21 Mean ± SEM	GnRH-Phor21 Mean ± SEM
Normal cells		
MCF-10A	NA	NA
Cancer Cells		
MCF-7	NA	1.7 ± 4.5
MDA-MD 231	NA	2.2 ± 0.6

tivity of peptide to various cell lines

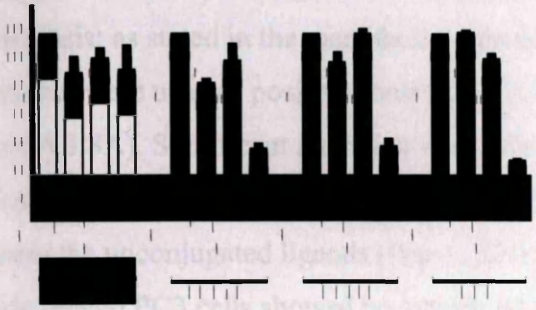

Cytotoxic activity of peptide to various cell lines

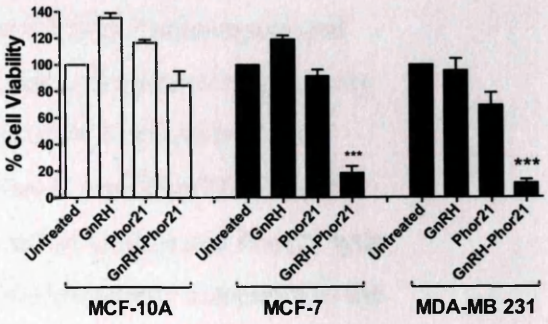

Figure 4.3.7 The cytotoxic activity of [D-Trp^6]GnRH-Phor21. **A**) Dose-dependent effect [D-Trp^6]GnRH-Phor21, [D-Trp^6] and Phor21 on the viability of non-GnRHR expressing cell lines (PNT-2 and MCF-10A) and GnRHR expressing cell lines (LNCaP, DU145, PC3, MCF-7 and MDA-MB 231). The cells were treated with 0-120 μM of [D-Trp^6]GnRH-Phor21and Phor21 peptides () for 3 hours and the viability of cells was assessed by alamar blue assay. **B**) The IC_{50} of peptides for various cell lines. **C**) Effect of effect [D-Trp^6]GnRH-Phor21, [D-Trp^6] and Phor21 on the viability of non-cancer and cancer cell lines was assessed by CellTox assay. PNT-2 (120μM), LNCaP (2μM), DU145 (4μM), PC3 (4μM), MCF10A (120μM), MCF-7 (2μM) and MDA-MB231 (4μM) cells were incubated with conjugated and non-conjugated peptides (the concentration used for each cell line is shown next to it in the brackets) for 3 hours before assessing their viability by CellTox assay. The data represent means ± SEM (error bars represent SEM) of three independent experiments (***, $P < 0.001$).

4.3.4. Characteristics of Pep-1-Phor21, Phor21-βCG(ala) and [D-Trp^6]GnRH-Phor21 using APOTOX GLO Triple assay.

To understand how Pep-1-Phor21, Phor21-βCG(ala) and [D-Trp^6]GnRH-Phor21 *in vitro* affect the viability of cancer cells, PC3 cells were incubated with ligand (Pep-1 or βCG(ala) or [D-Trp^6]GnRH) or lytic peptide Phor21 or Phor21 conjugated ligand (Pep-1-Phor21, Phor21-βCG(ala) or [D-Trp^6]GnRH-Phor21) for 6 hours and assessed cell viability, apoptosis and necrosis; as stated in the manufactures protocol (Figure 4.3.8A). Tunicamycin and Ionomycin were used as positive controls for cell apoptosis and cell necrosis respectively (Figure 4.3.8A). Significant reduction was found in viability of PC3 cells treated with Tunicamycin, Ionomycin, Pep-1-Phor21, [D-Trp^6]GnRH-Phor21, and Phor21-βCG(ala). Whereas the unconjugated ligands (Pep-1, [D-Trp^6]GnRH and βCG(ala)) and Phor21 lytic peptide treated PC3 cells showed no significant difference in cytotoxicity compared to the untreated control cells. PC3 cells incubated with Ionomycin, Pep-1-Phor21, [D-Trp^6]GnRH-Phor21 and Phor21-βCG(ala) exhibited significant necrosis (Figure 4.3.8B). The cell necrosis levels in PC3 cells incubated with these chemicals were approximately three fold more than that seen in PC3 cells treated with Tunicamycin, which induces cell death mainly through the apoptotic pathway. The PC3 cells treated with various peptides or chemical mentioned above were also assessed for apoptosis by measuring caspase-3/7 activity. The PC3 cells treated with Tunicamycin appeared to have a two-fold higher caspase-3 or caspase-7 activity compared to the untreated control cells. However, PC3 cells treated with Ionomycin, Pep-1-Phor21, [D-Trp^6]GnRH-Phor21, and Phor21-βCG(ala) showed a decrease in caspase-3/7 activity compared to untreated control cells (Figure 4.8 C). This indicates negative effect of cell necrosis on cell apoptosis. Together these results suggest that Pep-1-Phor21, [D-Trp^6]GnRH-Phor21 and Phor21-βCG(ala) lytic peptide conjugates reduce the viability of cancer cells mainly through cell necrosis (Figure 4.15).

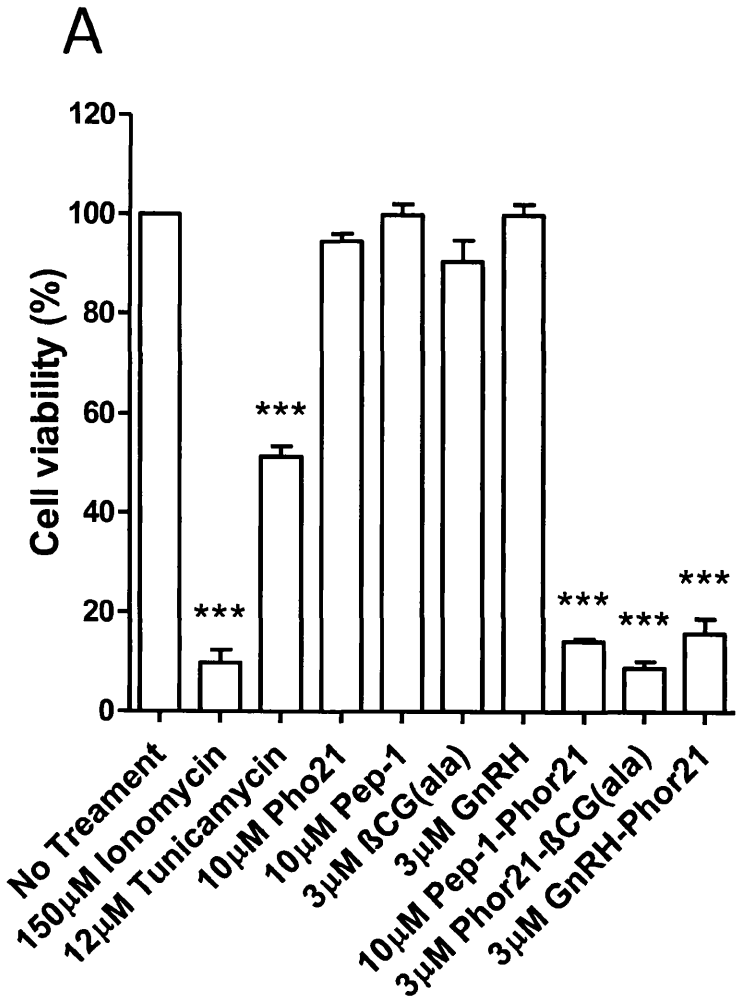
A
Cell viability (%)
120
100
80
60
40
20
0
***
***
***
***
***
No Treament
150µM Ionomycin
12µM Tunicamycin
10µM Pho21
10µM Pep-1
3µM ßCG(ala)
3µM GnRH
10µM Pep-1-Phor21
3µM Phor21-ßCG(ala)
3µM GnRH-Phor21

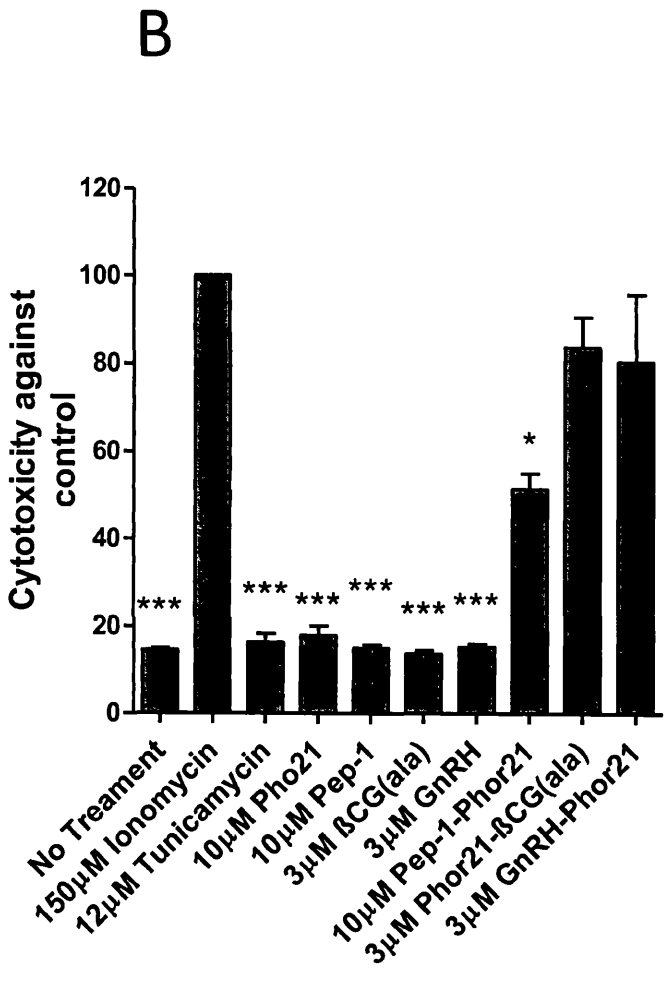
B
Cytotoxicity against control
120
100
80
60
40
20
0
***
***
***
***
***
***
*
No Treament
150µM Ionomycin
12µM Tunicamycin
10µM Pho21
10µM Pep-1
3µM ßCG(ala)
3µM GnRH
10µM Pep-1-Phor21
3µM Phor21-ßCG(ala)
3µM GnRH-Phor21

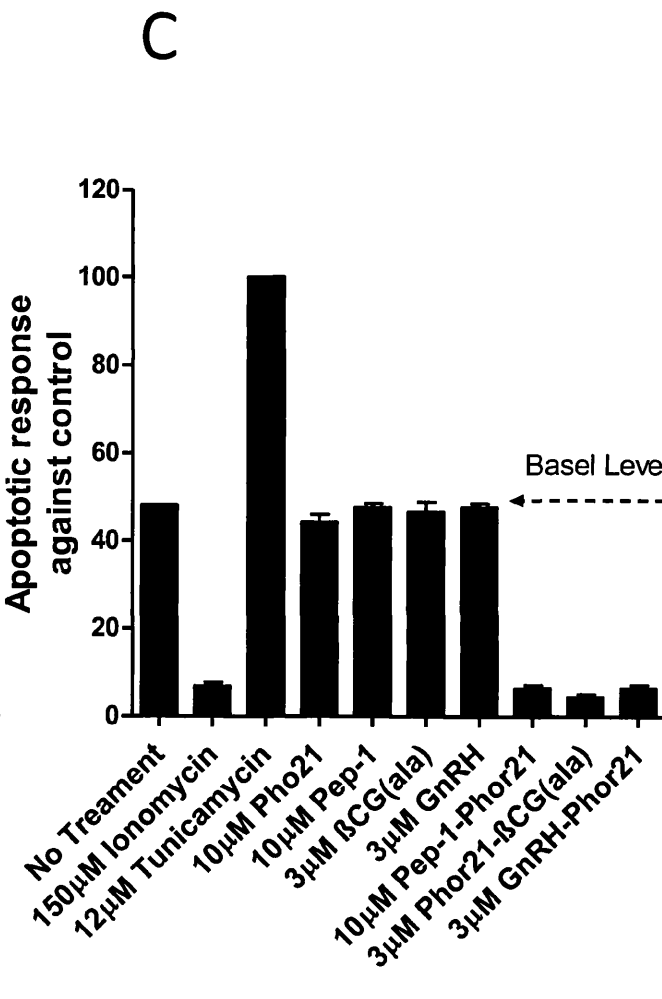
C
Apoptotic response against control
120
100
80
60
40
20
0
Basel Leve
No Treament
150µM Ionomycin
12µM Tunicamycin
10µM Pho21
10µM Pep-1
3µM ßCG(ala)
3µM GnRH
10µM Pep-1-Phor21
3µM Phor21-ßCG(ala)
3µM GnRH-Phor21

Figure 4.3.8. Characterisation of Pep-1-Phor21, GnRH-Phor21, and Phor21-βCG(ala) mode of action. PC-3 cells were treated with Pep-1, Phor21, [D-Trp^6] GnRH, βCG(ala),Tunicamycin (positive control for apoptosis), Ionomycin (positive control for necrosis [cytotoxicity]), Pep-1-Phor21, GnRH-Phor21, and Phor21-[D-Trp^6] for 6 hours and assessed the cell viability (**A**), necrosis (**B**) and apoptosis (**C**). Untreated in (**A**), Ionomycin treated in (**B**) and Tunicamycin treated in (**C**) considered as 100%. The data represent means ± SEM (error bars represent SEM) of three independent experiments in three different passages of the respective cell line (*, $P < 0.05$; **, $P < 0.01$; ***, $P < 0.001$).

4.3.5. Analysis of IL-13Rα2 protein, mRNA and cell surface expression in prostate and breast cell lines treated with TSA and 5-aza-dC

IL-13Rα2

The epigenetic regulation of IL-13Rα2 expression was assessed since there is one CpG site in the IL-13Rα2 promoter region and DNA methylation at this site was evaluated (Fujisawa et al, 2011). Cells were treated with a histone deacetylase inhibitor (TSA), and a DNA methyltransferase inhibitor (5-aza-dC,) to determine if they modulate IL-13Rα2 expression in prostate (Figure 4.9A) and breast (Figure 4.9B) cell lines. Cells treated with 0-10μM TSA or 5-aza-dC for 24 hours were assessed for IL-13Rα2 mRNA (by RT-PCR) and protein (total protein by immunoblotting and cell surface expressed protein by ELISA) HEK293 cells, a non-cancer cell line that have undetectable levels of IL-13Rα2, showed no significant difference between untreated or treated with TSA or 5-aza-dC in IL-13Rα2 protein expression (Figure 4.9.Ai). Interestingly LNCaP cancer cell lines, which normally have low levels of IL-13Rα2, had increased expression levels of IL-13Rα2 protein (Figure 4.9Ai&ii) and mRNA (Figure 4.9Aiii) and cell surface expression (Figure 4.9Aiv) when treated with TSA 5-aza-dC. This was assessed using immunoblotting (Figure 4.9.1 i-ii), cell surface ELISA (Figure 4.9.1 iv) and using the anti- IL-13Rα2 and mRNA analysis (Figure 4.9.1 iii) using IL-13Rα2 specific primers. Increase in the expression of IL-13Rα2 was also detected on the more aggressive cell lines DU145 and PC3 as the results below shows.

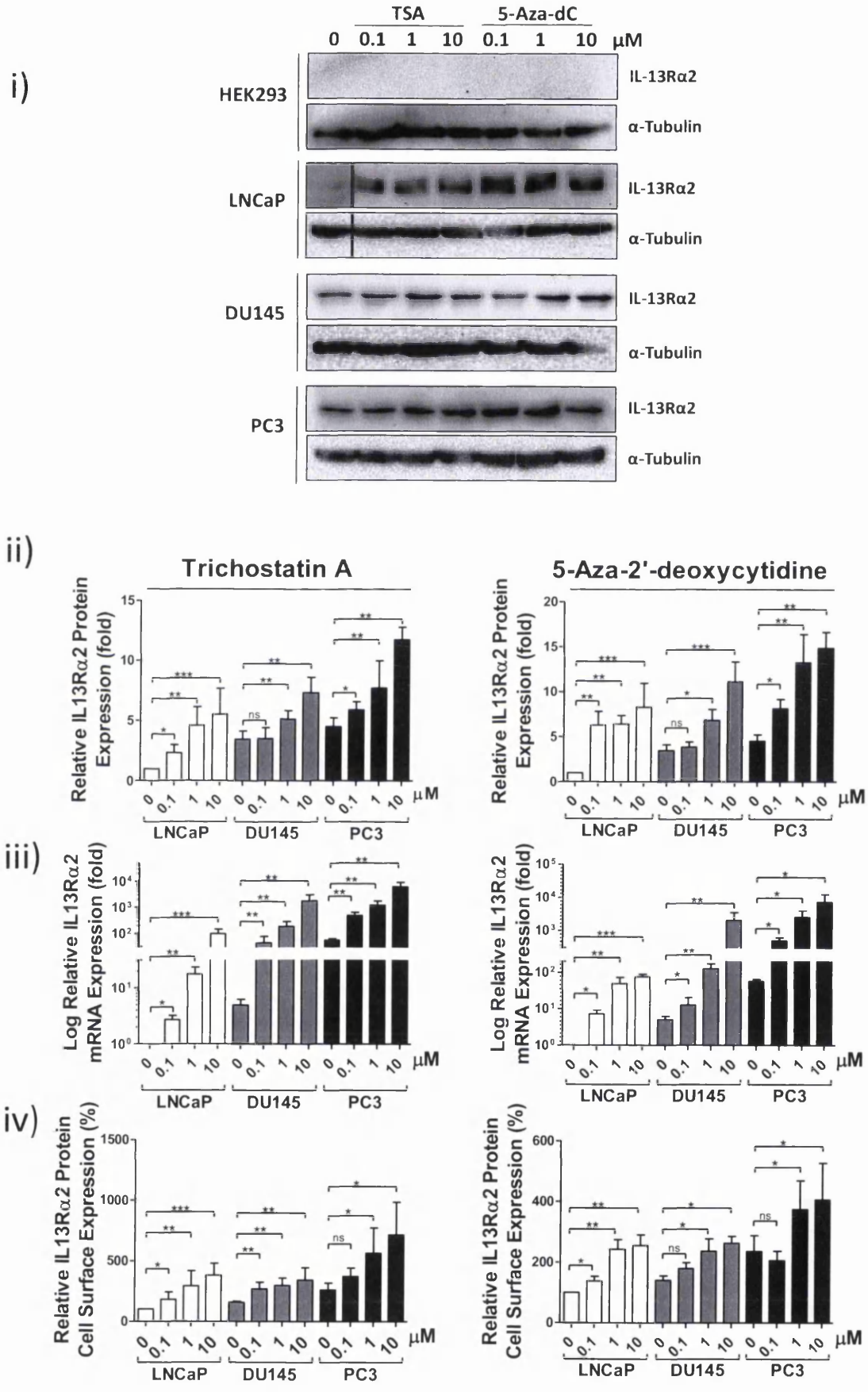
i)
TSA
5-Aza-dC
0 0.1 1 10 0.1 1 10 μM
HEK293
LNCaP
DU145
PC3
IL-13Rα2
α-Tubulin
ii)
Trichostatin A
5-Aza-2'-deoxycytidine
Relative IL13Rα2 Protein Expression (fold)
iii)
Log Relative IL13Rα2 mRNA Expression (fold)
iv)
Relative IL13Rα2 Protein Cell Surface Expression (%)
LNCaP
DU145
PC3
μM

Figure 4.9A. Analysis of IL-13Rα2 expression in prostate cancer cell lines treated with TSA and 5-aza-dC. Non-cancer cell lines (HEK293) and cancer cell lines (LNCaP, DU145, and PC-3) were treated with 0.1, 1, and 10μM of TSA or 5-aza-dC for 24 hours. **i)** Western blot analysis of IL-13Rα2 protein expression in non-cancer and cancer cell lines. **ii)** Quantification of IL-13Rα2 protein expression shown in **(i)** by densitometric analysis and normalising to house-keeping protein (α-Tubulin) expression. **iii)** RT-PCR analysis of IL-13Rα2 mRNA expression in non-cancer and cancer cell lines. **iv)** Cell surface expression of anti-IL-13Rα2 was assessed by subjecting un-permeablised cells to ELISA. All western blots, and RT-PCR values are normalised to housekeeping controls. The data are mean ± SEM (error bars represent SEM) values of three independent experiments. *P < 0.05, **P < 0.01 and ***P < 0.001, and compared with non-cancer cell line control.

With regards to breast cancer, the results demonstrated that MCF-10A, the non-cancer cell line with relatively low levels of IL-13Rα2, showed no significant changes in IL-13Rα2 expression even with TSA or 5-aza-dC treatment. Like LNCaP cell lines, MCF-7 cells have very little IL-13Rα2 expression. However upon TSA or 5-aza-dC treatment the expression IL-13Rα2 at protein (Figure 4.9.Bi-ii) and mRNA levels in MCF-7 increased significantly. IL-13Rα2 protein cell surface expression also increased in MCF-7 cells treated with TSA or 5-aza-dC (Figure 4.9.B iv) expression was also increased upon treatment with TSA or 5-aza-dC. MDA-MB 231 also showed an increase in IL-13Rα2 expression when treated with TSA or 5-aza-dC. The expression levels of IL-13Rα2 in prostate and breast cancer cell lines treated without or with TSA or 5-aza-dC are shown.

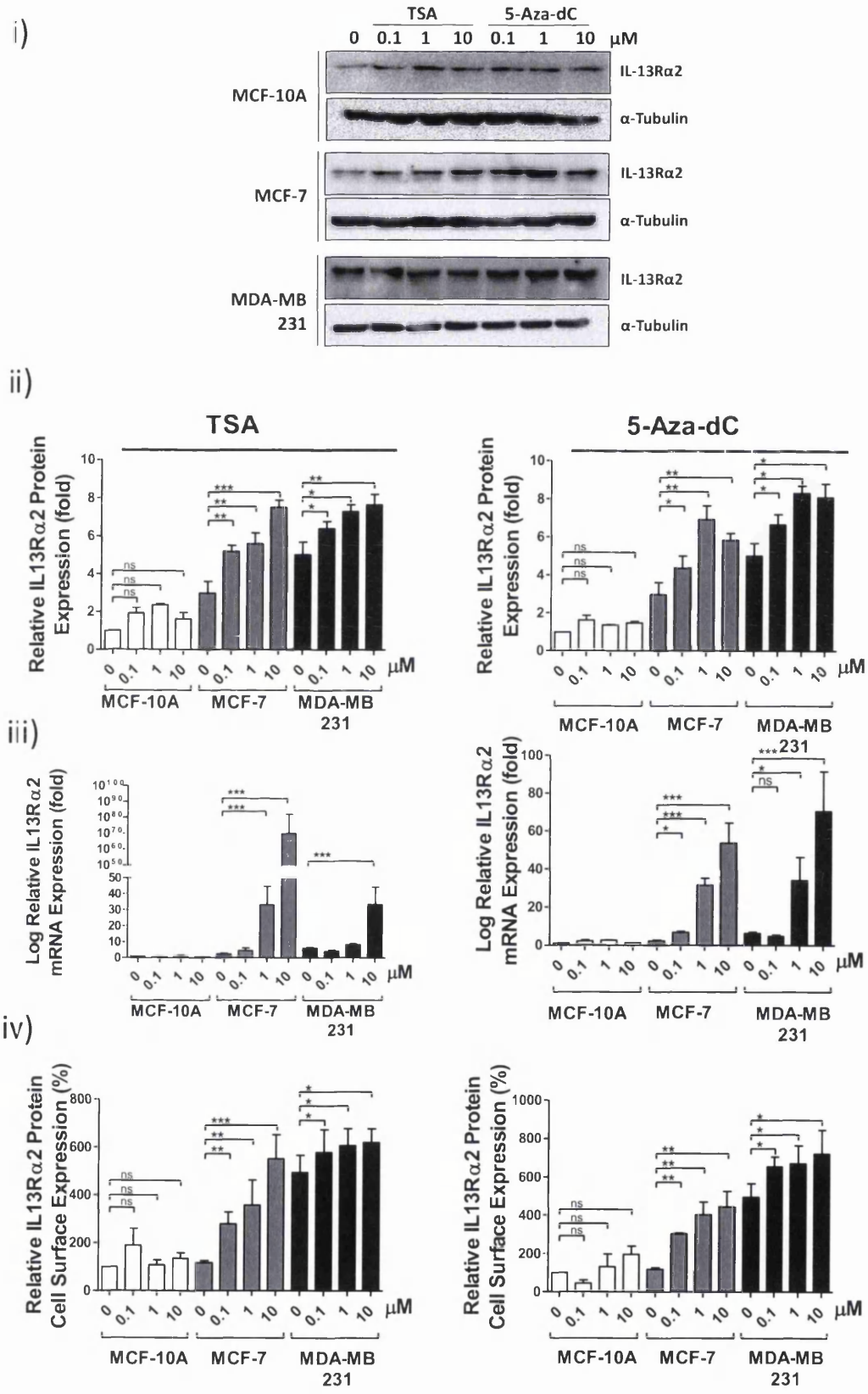
i)
TSA
5-Aza-dC
0 0.1 1 10 0.1 1 10 μM
MCF-10A
MCF-7
MDA-MB 231
IL-13Rα2
α-Tubulin
ii)
TSA
5-Aza-dC
Relative IL13Rα2 Protein Expression (fold)
iii)
Log Relative IL13Rα2 mRNA Expression (fold)
iv)
Relative IL13Rα2 Protein Cell Surface Expression (%)
MCF-10A
MCF-7
MDA-MB 231
μM

Figure 4.9.B Analysis of IL-13Rα2 expression in breast cancer cell lines treated with TSA and 5-aza-dC. Non-cancer cell lines (MCF-10A) and cancer cell lines (MCF-7 and MDA-MB 231) were treated with 0.1, 1, and 10μM of TSA or 5-aza-dC for 24 hours. **i)** Western blot analysis of IL-13Rα2 protein expression in non-cancer and cancer cell lines. **ii)** Quantification of IL-13Rα2 protein expression shown in **(i)** by densitometric analysis and normalising to house-keeping protein (α-Tubulin) expression. **iii)** RT-PCR analysis of IL-13Rα2 mRNA expression in non-cancer and cancer cell lines. **iv)**Cell surface expression of anti-IL-13Rα2 was assessed by subjecting un-permeablised cells to ELISA. All western blots and RT-PCR values are normalised to housekeeping controls. The data are mean ± SEM (error bars represent SEM) values of three independent experiments. *$P < 0.05$, **$P < 0.01$ and ***$P < 0.001$, and compared with non-cancer cell line control.

LHCGR

Next any epigenetic regulation of LHCGR expression in prostate (Figure 4.10.A) and breast (Figure 4.10.B) cell lines was determined by treating them with TSA or 5-aza-dC. PNT-2, a non-cancer cell line with low levels of LHCGR expression, cells showed no significant difference in LHCGR expression between any treatment and treatment with TSA or 5-aza-dC (Figure 4.10Ai-iii). However, LNCaP, DU145 and PC3 cell lines showed a decrease in the expression of LHCGR protein and mRNA (Figure 4.10.A i-iii) when treated with TSA or 5-aza-dC.

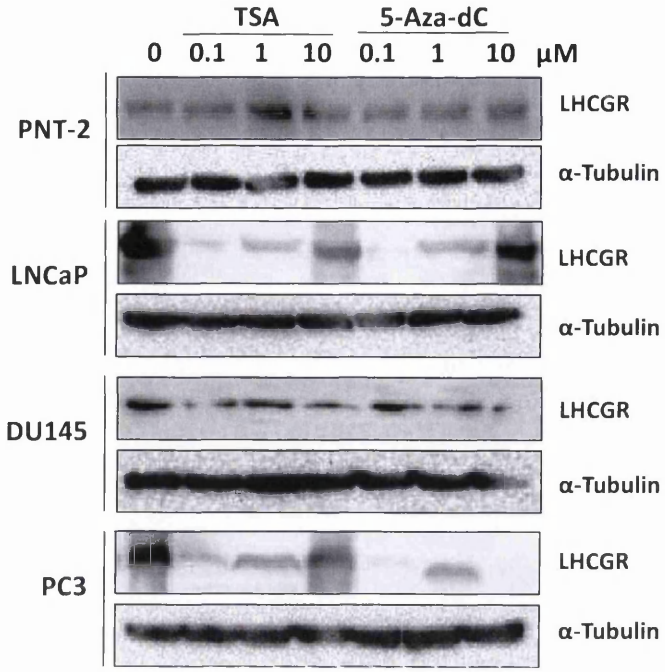
TSA
5-Aza-dC
0 0.1 1 10 0.1 1 10 μM
PNT-2
LNCaP
DU145
PC3
LHCGR
α-Tubulin

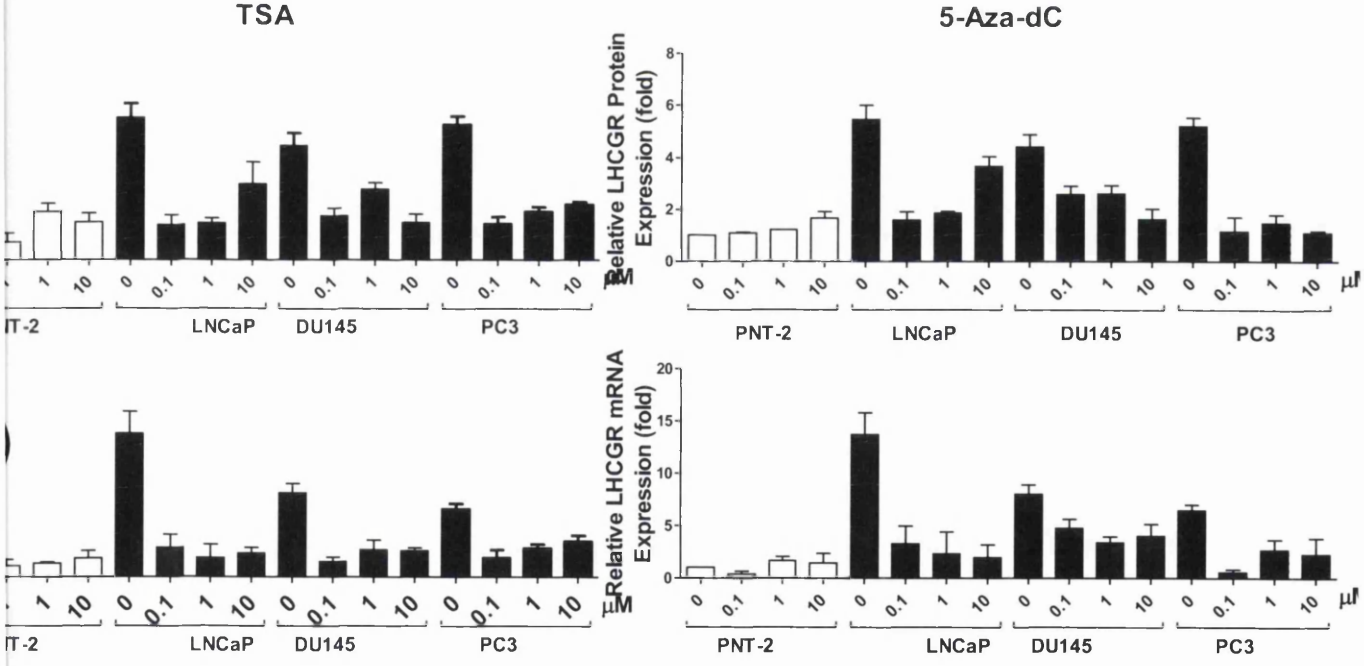
TSA
5-Aza-dC
Relative LHCGR Protein Expression (fold)
Relative LHCGR mRNA Expression (fold)
PNT-2
LNCaP
DU145
PC3
μM

Figure 4.10.A Analysis of LHCGR expression in prostate cancer cell lines treated with TSA and 5-aza-dC. Non-cancer cell lines (PNT-2) and cancer cell lines (LNCaP, DU145, and PC-3) were treated with 0.1, 1, and 10μM of TSA or 5-aza-dC for 24 hours. **i)** Western blot analysis of LHCGR protein expression in non-cancer and cancer cell lines. **ii)** Quantification of LHCGR protein expression shown in **(i)** by densitometric analysis and normalising to house-keeping protein (α-Tubulin) expression. **iii)** RT-PCR analysis of *LHCGR* mRNA expression in non-cancer and cancer cell lines. **iv)** Cell surface expression of anti-LHCGR was assessed by subjecting un-permeablised cells to ELISA. All western blots, and RT-PCR values are normalised to housekeeping controls. The data are mean ± SEM (error bars represent SEM) values of three independent experiments.

With regards to breast cancer, results demonstrated that MCF-10A, the non-cancer cell line, showed no significant changes in IL-13Rα2 expression even with TSA or 5-aza-dC treatment. Like the prostate cancer cells, MCF-7 and MDA-MB 231 show a reduction in the expression of LHCGR at protein and mRNA levels (Figure 4.10.Bi-iii)

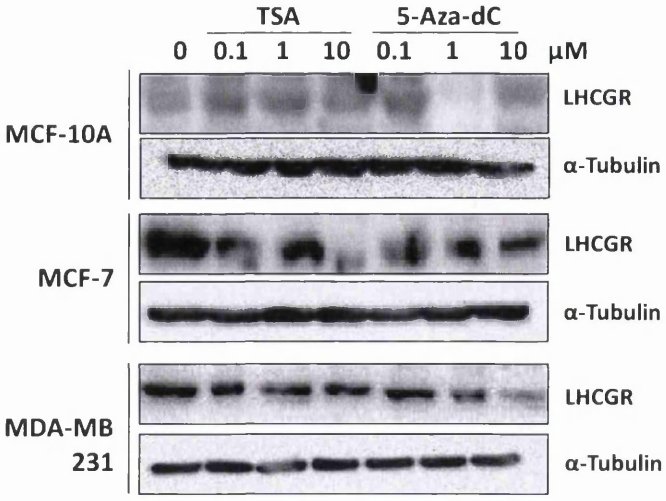
TSA
5-Aza-dC
0 0.1 1 10 0.1 1 10 μM
MCF-10A
LHCGR
α-Tubulin
MCF-7
LHCGR
α-Tubulin
MDA-MB 231
LHCGR
α-Tubulin

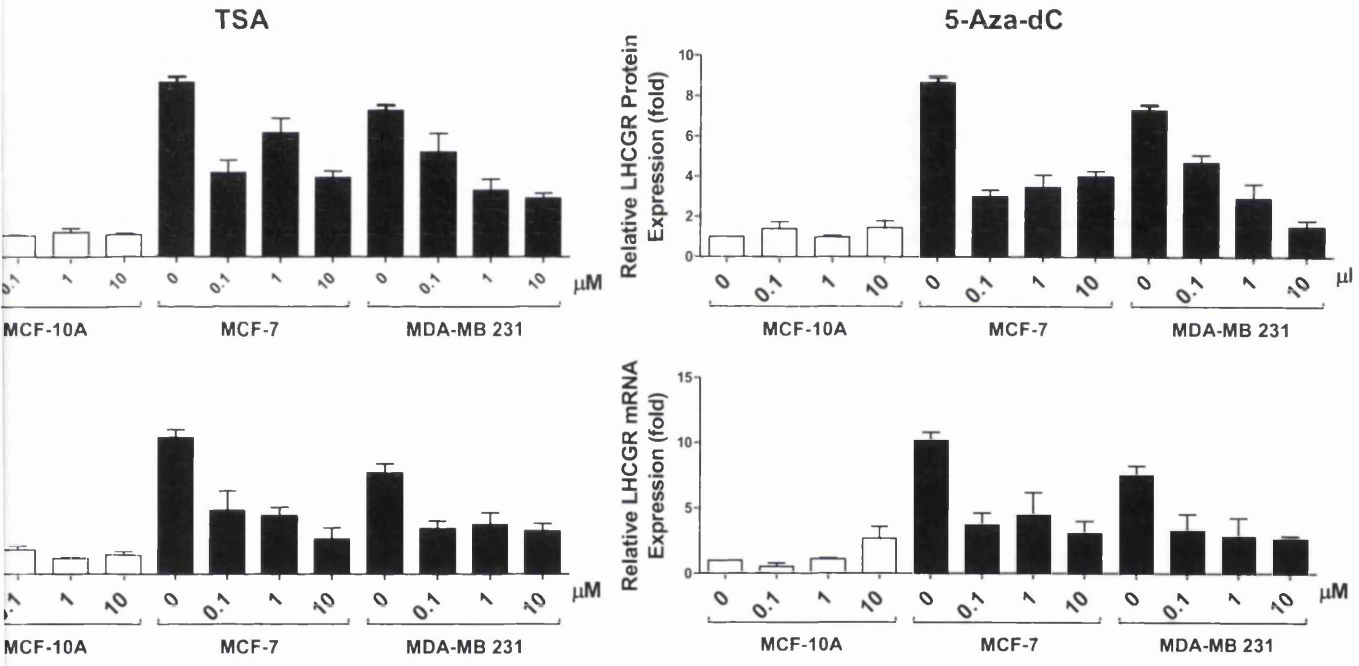
TSA
5-Aza-dC
Relative LHCGR Protein Expression (fold)
MCF-10A
MCF-7
MDA-MB 231
μM
Relative LHCGR mRNA Expression (fold)
MCF-10A
MCF-7
MDA-MB 231
μM

Figure 4.10.B Analysis of LHCGR expression in breast cancer cell lines treated with TSA and 5-aza-dC Non-cancer cell lines (MCF-10A) and cancer cell lines (MCF-7 and MDA-MB 231) were treated with 0.1, 1, and 10μM of TSA or 5-aza-dC for 24 hours. **i)** Western blot analysis of LHCGR protein expression in non-cancer and cancer cell lines. **ii)** Quantification of LHCGR protein expression shown in **(i)** by densitometric analysis and normalising to house-keeping protein (α-Tubulin) expression. **iii)** RT-PCR analysis of LHCGR mRNA expression in non-cancer and cancer cell lines. **iv)**Cell surface expression of anti-LHCGR was assessed by subjecting un-permeablised cells to ELISA. All western blots and RT-PCR values are normalised to housekeeping controls. The data are mean ± SEM (error bars represent SEM) values of three independent experiments.

GnRHR

Finally the epigenetic regulation of GnRHR expression following TSA or 5-aza-dC treatment in prostate (Figure 4.11A) and breast (Figure 4.11B) cell lines was assessed. PNT-2, a non-cancer cell line, showed no significant difference in GnRHR protein expression (Figure 4.11.A i-ii) between no treatment and treatment with TSA or 5-aza-*dC*. Interestingly treatment with 1 and 10μM of 5-aza-dC resulted in increased GnRHR protein expression in LNCaP cancer cell lines. DU145 showed a significant increase in GnRHR expression upon treatment with 1 and 10μM of TSA, similar results were also demonstrated in PC3 cells. PNT-2 showed no significant difference in GnRHR mRNA expression between any treatment and treatment with TSA or 5-aza-dC (Figure 4.11Aiii). However GnRHR mRNA showed a different expression pattern in prostate cancer cells treated with TSA or 5-aza-dC (Figure 4.11Aiii). LNCaP cells showed a significant increase in GnRHR mRNA expression with 1 and 10 μM of TSA or 5-aza-dC treatments. DU145 cells showed a significant increase in GnRHR mRNA expression with 1 and 10 μM of TSA or 0.1 -10 μM of 5-aza-dC treatments. Both TSA and 5-aza-dC 0.1-10 μM caused a significant increase in GnRHR mRNA expression in PC3 cells.

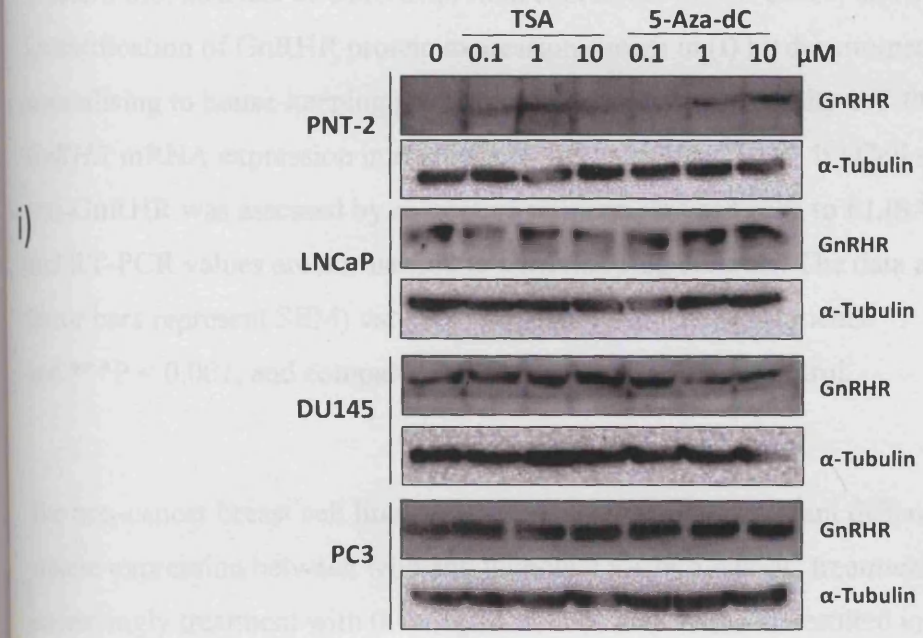
TSA
5-Aza-dC
0 0.1 1 10 0.1 1 10 μM
i)
PNT-2
LNCaP
DU145
PC3
GnRHR
α-Tubulin

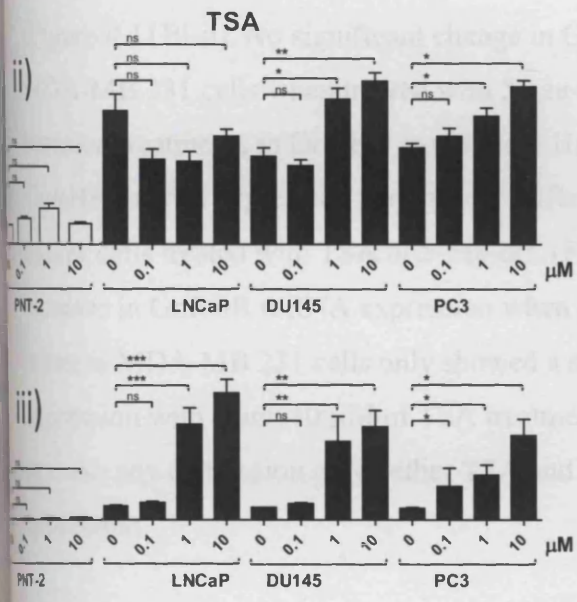
TSA
ii)
iii)
PNT-2
LNCaP
DU145
PC3
μM

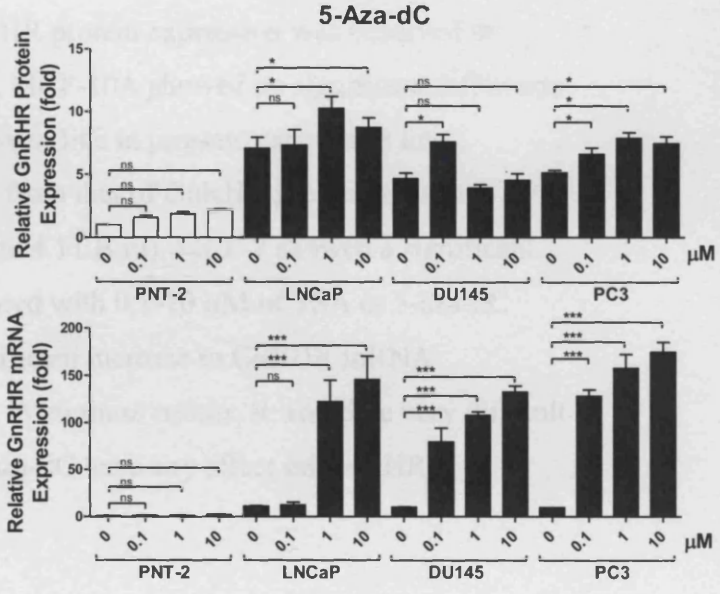
5-Aza-dC
Relative GnRHR Protein Expression (fold)
Relative GnRHR mRNA Expression (fold)
PNT-2
LNCaP
DU145
PC3
μM

Figure 4.11 A. A Analysis of GnRHR expression in prostate cancer cell lines treated with TSA and 5-aza-dC. Non-cancer cell lines (PNT-2) and cancer cell lines (LNCaP, DU145, and PC-3) were treated with 0.1, 1, and 10μM of TSA or 5-aza-dC for 24 hours. **i)** Western blot analysis of GnRHR protein expression in non-cancer and cancer cell lines. **ii)** Quantification of GnRHR protein expression shown in **(i)** by densitometric analysis and normalising to house-keeping protein (α-Tubulin) expression. **iii)** RT-PCR analysis of *GnRHR* mRNA expression in non-cancer and cancer cell lines. **iv)** Cell surface expression of anti-GnRHR was assessed by subjecting un-permeablised cells to ELISA. All western blots, and RT-PCR values are normalised to housekeeping controls. The data are mean ± SEM (error bars represent SEM) values of three independent experiments. *P < 0.05, **P < 0.01 and ***P < 0.001, and compared with non-cancer cell line control.

The non-cancer breast cell line, MCF-10A, showed no significant difference in GnRHR protein expression between with and without TSA or 5-aza-dC treatment (Figure 4.11B). Interestingly treatment with 0.1 -10μM of TSA and 5-aza-dC resulted in increased GnRHR protein expression in MCF-7 cancer cell line. MDA-MB 231 breast cancer cell line showed no significant change in GnRHR protein expression until treatment increased to 10 μM (Figure 4.11Bi-ii). No significant change in GnRHR protein expression was observed in MDA-MB 231 cells when treated with 5-aza-dC. MCF-10A showed no significant difference between treatments in GnRHR expression. However, like in prostate cancer cell lines, GnRHR mRNA expression pattern was different from that of GnRHR protein in breast cancer cells treated with TSA or 5-aza-dC. (Figure 4.11.B iii). MCF-7 showed a significant increase in GnRHR mRNA expression when treated with 0.1-10 μM of TSA or 5-aza-dC whereas MDA-MB 231 cells only showed a significant increase in GnRHR mRNA expression with 1 and 10 μM of TSA treatments. With these results, it would be very difficult to make any conclusion on whether TSA and 5-aza-dC have any effect on GnRHR expression.

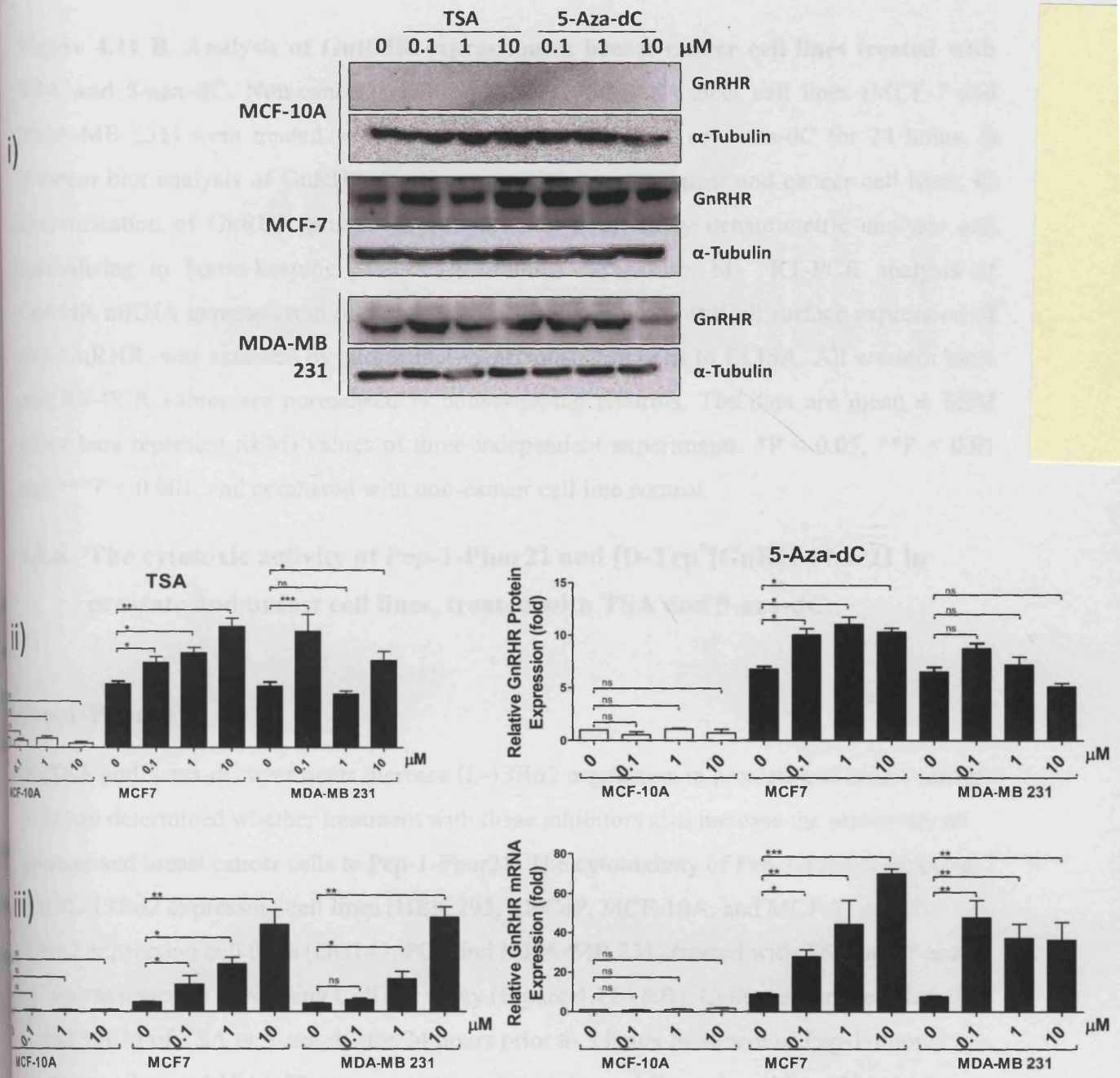
i)
TSA
5-Aza-dC
0 0.1 1 10 0.1 1 10 μM
MCF-10A
MCF-7
MDA-MB 231
GnRHR
α-Tubulin
ii)
TSA
5-Aza-dC
Relative GnRHR Protein Expression (fold)
MCF-10A
MCF7
MDA-MB 231
μM
iii)
Relative GnRHR mRNA Expression (fold)
ns

Figure 4.11 B. Analysis of GnRHR expression in breast cancer cell lines treated with TSA and 5-aza-dC. Non-cancer cell lines (MCF-10A) and cancer cell lines (MCF-7 and MDA-MB 231) were treated with 0.1, 1, and 10μM of TSA or 5-aza-dC for 24 hours. **i)** Western blot analysis of GnRHR protein expression in non-cancer and cancer cell lines. **ii)** Quantification of GnRHR protein expression shown in **(i)** by densitometric analysis and normalising to house-keeping protein (α-Tubulin) expression. **iii)** RT-PCR analysis of GnRHR mRNA expression in non-cancer and cancer cell lines. **iv)**Cell surface expression of anti-GnRHR was assessed by subjecting un-permeablised cells to ELISA. All western blots and RT-PCR values are normalised to housekeeping controls. The data are mean ± SEM (error bars represent SEM) values of three independent experiments. *P < 0.05, **P < 0.01 and ***P < 0.001, and compared with non-cancer cell line control.

4.3.6. The cytotoxic activity of Pep-1-Phor21 and [D-Trp^6]GnRH-Phor21 in prostate and breast cell lines, treated with TSA and 5-aza-dC.

Pep-1-Phor21

As TSA and 5-aza-dC treatments increase IL-13Rα2 expression in prostate and breast cancer cells, we determined whether treatment with these inhibitors also increase the sensitivity of prostate and breast cancer cells to Pep-1-Phor21. The cytotoxicity of Pep-1-Phor21 on no or low-IL-13Rα2 expressing cell lines (HEK 293, LNCaP, MCF-10A, and MCF-7) and IL-13Rα2 expressing cell lines (DU145, PC3 and MDA-MB 231) treated with TSA and 5-aza-dC was assessed *in vitro* using CellTox assay (Figure 4.12A&B). Cells were treated with 0.1, 1, and 10μM of TSA or 5-aza-dC for 24 hours prior to 3 hours treatment of Pep-1-Phor21 treatment (Figure 4.12A). The concentration of peptide used for each cell line (120μM for HEK293 cells, 20μM for LNCaP, 12μM for DU145, 5μM for PC3, 120μM for MCF-10A, 20μM for MCF-7 and 12μM for MDA-MB 231) was based on its IC_{50} in the alamar blue assay (Figure 14.), TSA and 5-aza-dC did not increase the sensitivity of non-cancer cell lines (HEK293 and MCF-10A) to Pep-1-Phor21. However TSA and 5-aza-dC significantly increased low IL-13Rα2 expressing cancer cell lines (LNCaP and MCF-7) sensitivity to Pep-1-Phor21. DU145, PC3 and MDA-MB 231 cell lines, which express high levels of IL13Rα2, also showed increased Pep-1-Phor21sensitivity when treated with TSA or 5-aza-dC. The results demonstrate that TSA and 5-aza-dC increase prostate and breast cancer cells sensitivity to Pep-1-Phor21.

HEK293 Pep-1-Phor21

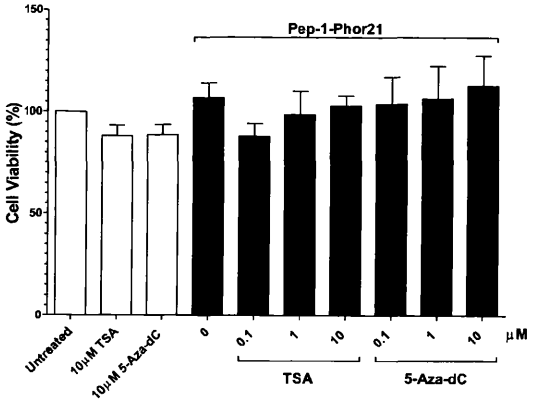

MCF-10A Pep-1-Phor21

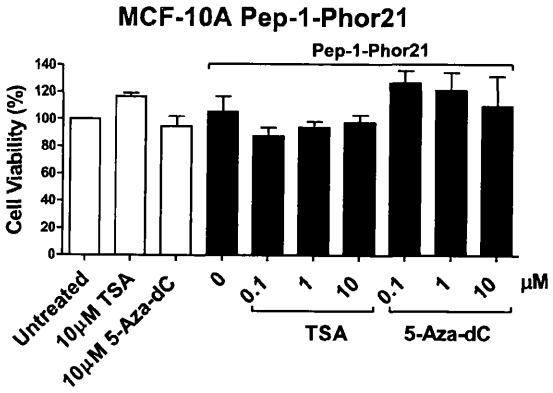

LNCaP Pep-1-Phor21

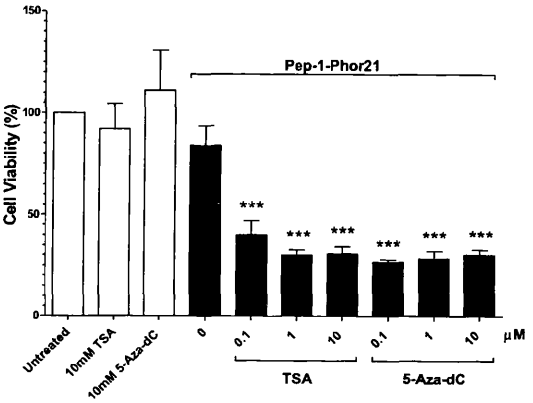

MCF-7 Pep-1-Phor21

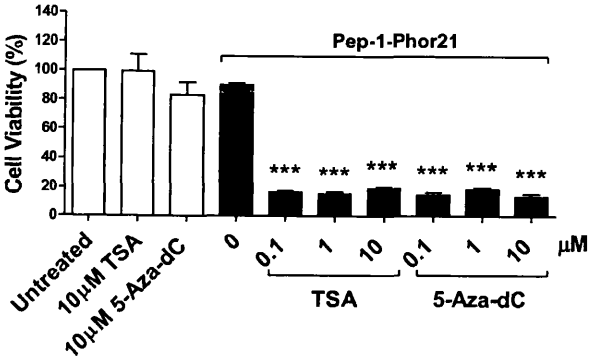

DU145 Pep-1-Phor21

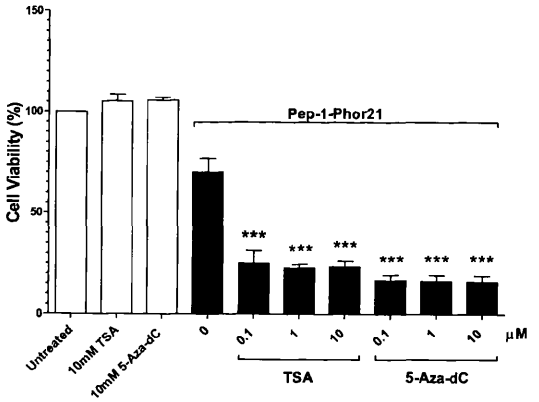

MDA-MB 231 Pep-1-Phor21

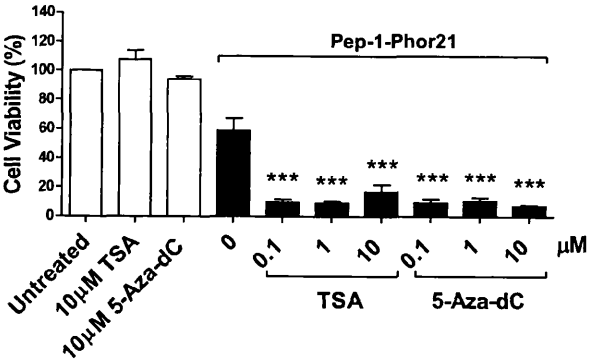

PC3 Pep-1-Phor21

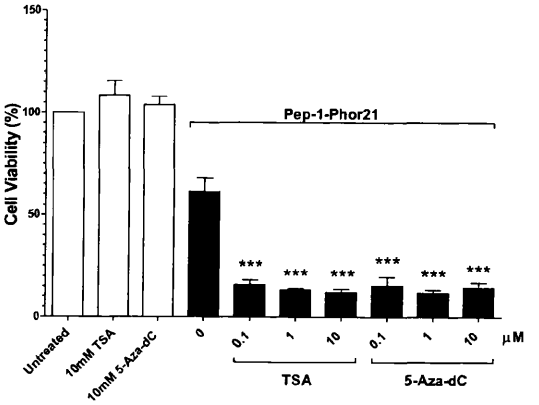

Figure 4.12A. Effect of Pep-1-Phor21 on prostate and breast cell lines treated with TSA or 5-aza-dC. Pep-1-Phor21 sensitivity of no or lowIL-13Rα2 expressing (HEK 293, LNCaP, MCF-10A, and MCF-7) and high IL-13Rα2 expressing (DU145, PC3 and MDA-MB 231) cell lines treated with 0.1, 1, and 10μM of TSA or 5-aza-dC for 24 hours was analysed by CellTox assay. HEK293 (120μM), LNCaP (20μM), DU145 (12μM), PC3 (5μM), MCF10A (120μM), MCF-7 (20μM) and MDA-MB231 (12μM) were incubated with the conjugated lytic peptide (the concentration used for each cell line is shown next to it in the brackets) for 3 hours before assessing their viability by CellTox assay. The data represent means ± SEM (error bars represent SEM) of data obtained from three independent experiments (***, $P < 0.001$).

[D-Trp^6]GnRH-Phor21

TSA and 5-aza-dC treatments increase GnRHR expression in prostate and breast cancer cells, we determined whether treatment with these inhibitors also increase the sensitivity of prostate and breast cancer cells to [D-Trp^6]GnRH-Phor21. The cytotoxicity of D-Trp^6]GnRH-Phor21on no or low-GnRHR expressing cell lines (PNT-2 and MCF-10A) and high GnRHR expressing cell lines (LNCaP,DU145, PC3, MCF-7 and MDA-MB 231) treated with TSA and 5-aza-dC was assessed *in vitro* using CellTox assay (Figure 4.12B). Cells were treated with 0.1, 1, and 10μM of TSA or 5-aza-dC for 24 hours prior to 3 hours treatment of Pep-1-Phor21 treatment (Figure 4.12B). The concentration of peptide used for each cell line (120μM for PNT-2 cells, 1μM for LNCaP, 1μM for DU145, 1μM for PC3, 120μM for MCF-10A, 1μM for MCF-7 and 1μM for MDA-MB 231) was based on its IC_{50} in the alamar blue assay (Figure 14.), TSA and 5-aza-dC did not increase the sensitivity of non-cancer cell lines (PNT-2 and MCF-10A) to [D-Trp^6]GnRH-Phor21. However TSA and 5-aza-dC significantly increased GnRHR expressing cancer cell lines (LNCaP,DU145, PC3, MCF-7 and MDA-MB 231) sensitivity to [D-Trp^6]GnRH-Phor21. The results demonstrate that TSA and 5-aza-dC increase prostate and breast cancer cells sensitivity to [D-Trp^6]GnRH-Phor21.Non-cancer normal cells showed no difference in sensitivity, based on cell viability results.

PNT-2 [D-Trp^6]GnRH-Phor21

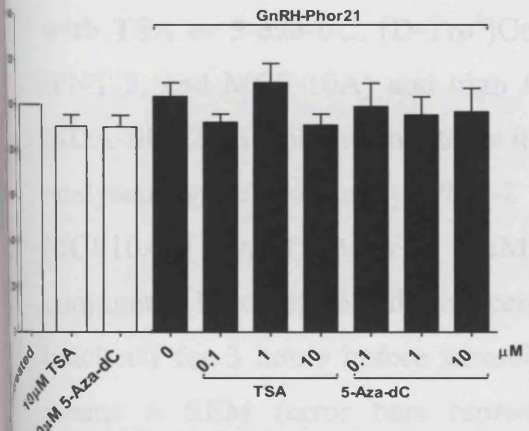

MCF-10A [D-Trp^6]GnRH-Phor21

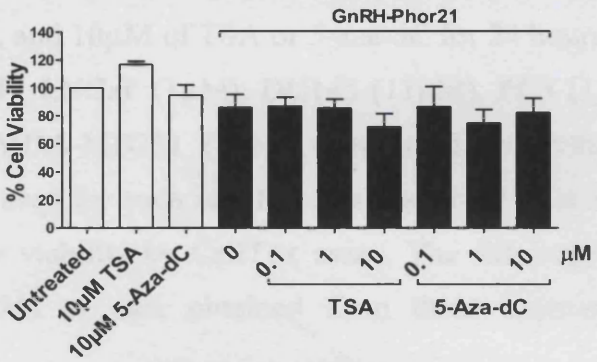

LNCaP [D-Trp^6]GnRH-Phor21

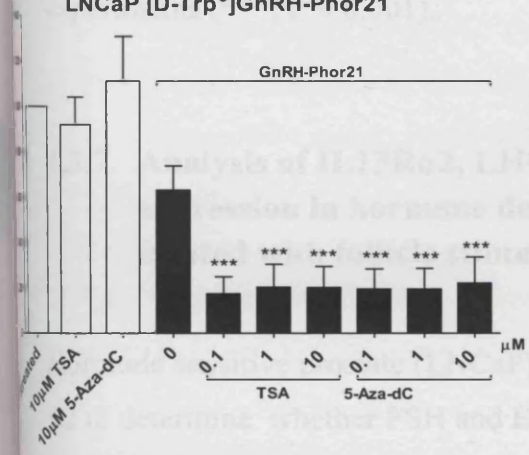

MCF-7 [D-Trp^6]GnRH-Phor21

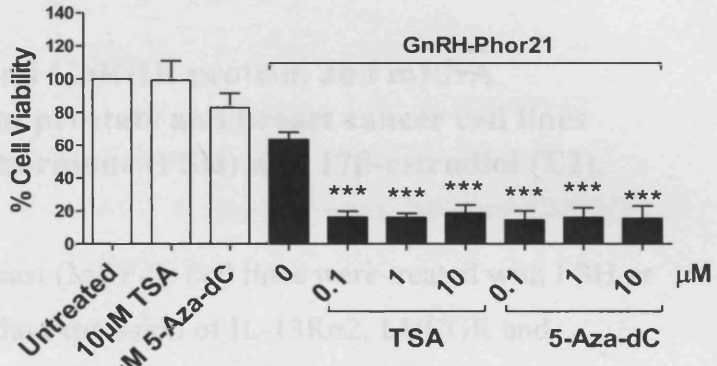

DU145 [D-Trp^6]GnRH-Phor21

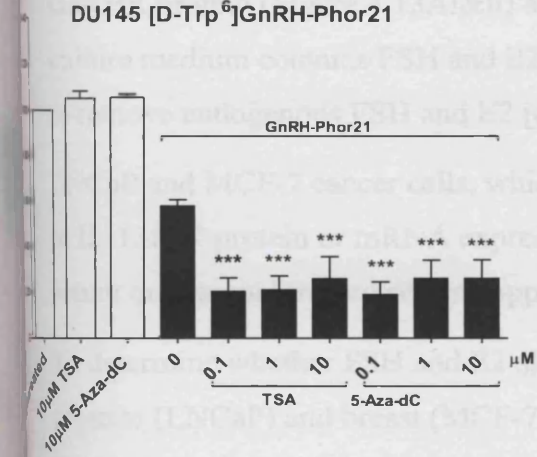

MDA-MB 231 [D-Trp^6]GnRH-Phor21

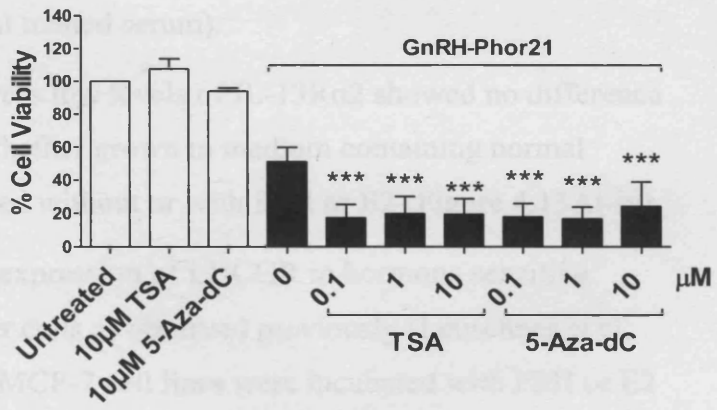

PC3 [D-Trp^6]GnRH-Phor21

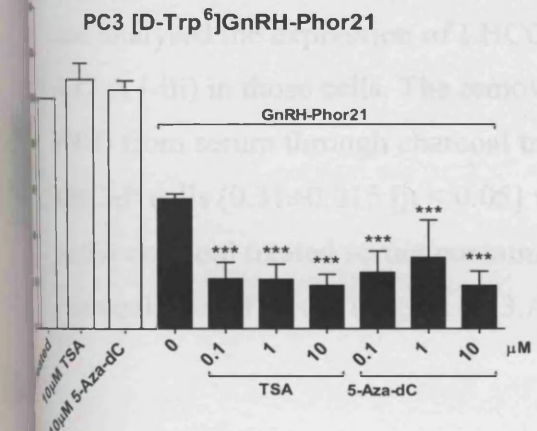

Figure 4.12.B. Effect of [D-Trp^6]GnRH-Phor21, on prostate and breast cell lines treated with TSA or 5-aza-dC. [D-Trp^6]GnRH-Phor21 sensitivity of no or low GnRHR expressing (PNT-2, and MCF-10A) and high GnRHR expressing (LNCaP, DU145, PC3, MCF-7 and MDA-MB 231) cell lines treated with 0.1, 1, and 10μM of TSA or 5-aza-dC for 24 hours was analysed by CellTox assay. PNT-2 (120μM), LNCaP (1μM), DU145 (11μM), PC3 (1μM), MCF10A (120μM), MCF-7 (1μM) and MDA-MB231 (1μM) were incubated with the conjugated lytic peptide (the concentration used for each cell line is shown next to it in the brackets) for 3 hours before assessing their viability by CellTox assay. The data represent means ± SEM (error bars represent SEM) of data obtained from three independent experiments (***, $P < 0.001$).

4.3.7. Analysis of IL13Rα2, LHCGR and GnRHR protein, and mRNA expression in hormone dependent prostate and breast cancer cell lines treated with follicle stimulating hormone (FSH) and 17β-estradiol (E2).

Hormone sensitive prostate (LNCaP) and breast (MCF-7) cell lines were treated with FSH or E2 to determine whether FSH and E2 alter the expression of IL-13Rα2, LHCGR and GnRHR protein (Figure 4.13Ai&ii) and mRNA (Figure 4.13Aiii). Bovine serum in the culture medium contains FSH and E2 and therefore serum incubated with activated charcoal to remove endogenous FSH and E2 (charcoal treated serum).

LNCaP and MCF-7 cancer cells, which express low levels of IL-13Rα2 showed no difference in IL-13Rα2 protein or mRNA expression whether grown in medium containing normal serum or charcoal treated serum supplemented without or with FSH or E2 (Figure 4.13Ai-iv).

To determine whether FSH and E2 alter the expression of LHCGR in hormone sensitive prostate (LNCaP) and breast (MCF-7) cancer cells as observed previously (Leuschner et al, 2003b; Leuschner et al, 2001), LNCaP and MCF-7 cell lines were incubated with FSH or E2 and analysed the expression of LHCGR protein (Figure 4.13Ai&ii) and mRNA (Figure 4.13.A i-iii) in those cells. The removal of steroids (including E2) and androgens (including FSH) from serum through charcoal treatment reduced the expression of LHCGR protein in LNCaP cells (0.31±0.015 [$p < 0.05$] vs growth in normal serum). The addition of FSH and E2 to the charcoal treated serum containing reversed the inhibition of LHCGR expression by charcoal treated serum (Figure 4.13.A iii). The addition of FSH and E2 to normal serum

containing medium also increased LHCGR protein and mRNA expression in LNCaP cell lines.

The hormone sensitive breast cancer cell line MCF-7 also showed reduction in the expression of LHCGR protein (0.57± 0.3 fold, $p < 0.05$) and mRNA (0.36±0.13 fold, $p < 0.05$)when the cells were cultured in charcoal treated serum containing medium (Figure 4.13.B i-iii). The addition of FSH or E2 to charcoal treated serum containing medium brought back LHCGR protein and mRNA to the levels seen in cells grown in normal serum containing medium. The addition of FSH in normal serum containing medium showed no effect on the expression of LHCGR protein (1.0 ± 0.064 fold change, $P>0.05$) or mRNA (Figure 4.13.B i-ii). However, the expression of LHCGR mRNA increased to 2.5 ±0.36 fold ($P<0.05$) by adding FSH to normal serum containing medium (Figure 4.13Biii). The addition of E2 to normal serum containing medium had a greater effect on the expression of LHCGR protein (2.8 ± 0.60 fold, $P<0.05$) and mRNA (4.4 ± 0.66 fold, $P<0.05$). FSH and E2 have also been shown to alter GnRHR expression in hormone sensitive prostate and breast cancer cells (Leuschner et al, 2003b; Leuschner et al, 2001). Therefore the effect of FSH or E2 on the expression GnRHR protein (Figure 4.13Ci&ii) and mRNA (Figure 4.13Ciii) was analysed in LNCaP and MCF-7 cell lines. The expression of GnRHR protein (0.097 ± 0.075, $p < 0.05$) and mRNA (0.25±0.15) reduced in LNCaP cells when they were cultured in charcoal treated serum containing medium. Adding FSH or E2 to the charcoal treated serum containing medium reversed the expression of GnRHR protein and mRNA to basal levels. Adding FSH to normal serum containing medium slightly increased the expression of GnRHR protein (1.6 ± 0.35 fold, $P<0.05$) and mRNA (4.1 ± 0.33 fold, $P<0.05$) in LNCaP cells. The addition of E2 to normal serum containing medium had also caused minimal increase in the expression of LHCGR protein (1.1 ± 0.028 fold) and mRNA (1.9 ± 0.32 fold). However these results suggest that there is no significant change in GnRHR expression in LNCaP cells when they are cultured in normal serum containing medium supplement with FSH or E2.

For breast cancer, the hormone sensitive cell line MCF-7 showed no significant reduction in the expression of GnRHR protein (1.1 ± 0.11 fold, $p > 0.05$) and mRNA (0.89 ±0.17 fold, $p > 0.05$) when the cells were cultured in charcoal treated serum containing medium. The addition of FSH to charcoal treated serum containing medium had no effect on the expression of GnRHR protein (1.0 ± 0.043 fold, $P>0.05$) and mRNA (1.4 ± 0.28fold $P>0.05$) (Figure 4.13Ci-iii). However, the addition of E2 to charcoal treated serum containing medium had slightly increased the expression GnRHR protein (1.9± 0.32fold, $P<0.05$) and mRNA (1.4± 0.34 fold, $P>0.05$). The addition of FSH to full serum containing medium increased the

expression of GnRHR protein (2.2 ± 0.58 fold, $P<0.05$) and mRNA (2.6 ± 0.30 fold, $P<0.05$) in MCF-7 cells. The addition of E2 to full serum containing medium increased the expression of GnRHR protein (2.9 ± 0.29 fold, $P<0.05$) and mRNA (4.9 ± 0.40 fold, $P<0.05$).

These results demonstrate that FSH and E2 have an effect on the expression of LHCGR and GnRHR but not IL-13Rα2 in hormone and androgen sensitive cell lines.

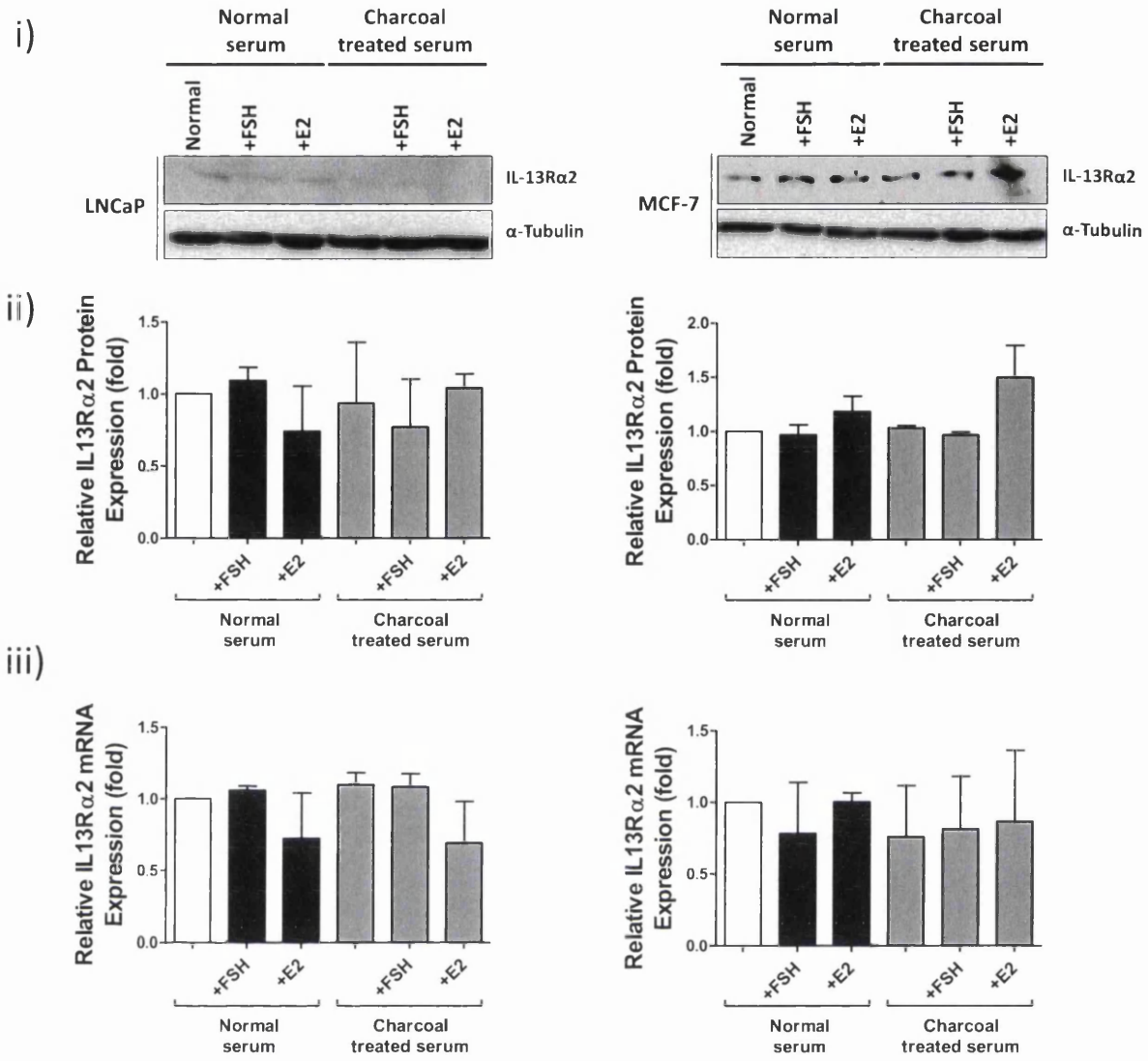

Figure 4.13.A Analysis of IL-13Rα2 expression in hormone dependent prostate and breast cancer cell lines treated with FSH and 17β-estradiol. Hormone dependent prostate and breast cancer cell lines (LNCaP and MCF-7 respectively) were cultured in charcoal treated media for 48 hours and FSH and 17β-estradiol for further 48 hours. **i)** Western blot analysis of IL-13Rα2 protein expression in non-cancer and cancer cell lines. **ii)** Quantification of IL-13Rα2 protein expression shown in **(i)** by densitometric analysis and normalising to house-keeping protein (α-Tubulin) expression. **iii)** RT-PCR analysis of IL-13Rα2 mRNA expression in non-cancer and cancer cell lines .All western blots, and RT-PCR values are normalised to housekeeping controls. The data are mean ± SEM (error bars represent SEM) values of three independent experiments. *P < 0.05, **P < 0.01 and ***P < 0.001, and compared with non-cancer cell line control.

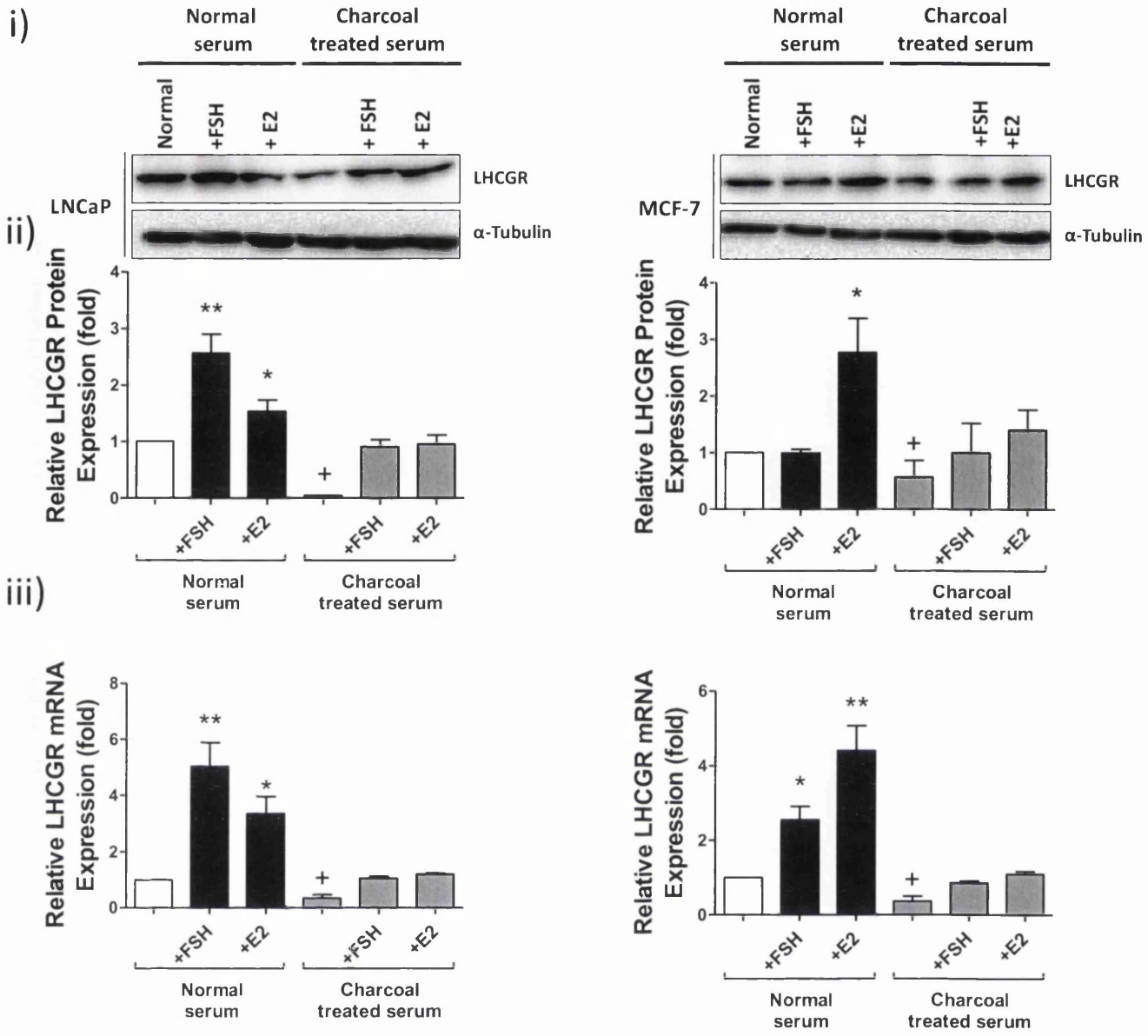

Figure 4.13.B Analysis of LHCGR expression in hormone dependent prostate and breast cancer cell lines treated with FSH and 17β-estradiol. Hormone dependent prostate and breast cancer cell lines (LNCaP and MCF-7 respectively) were cultured in charcoal treated media for 48 hours and FSH and 17β-estradiol for further 48 hours. **i)** Western blot analysis of LHCGR protein expression in non-cancer and cancer cell lines. **ii)** Quantification of LHCGR protein expression shown in **(i)** by densitometric analysis and normalising to house-keeping protein (α-Tubulin) expression. **iii)** RT-PCR analysis of *LHCGR* mRNA expression in non-cancer and cancer cell lines .All western blots, and RT-PCR values are normalised to housekeeping controls. The data are mean ± SEM (error bars represent SEM) values of three independent experiments. *P < 0.05, **P < 0.01 and ***P < 0.001, and compared with non-cancer cell line control.

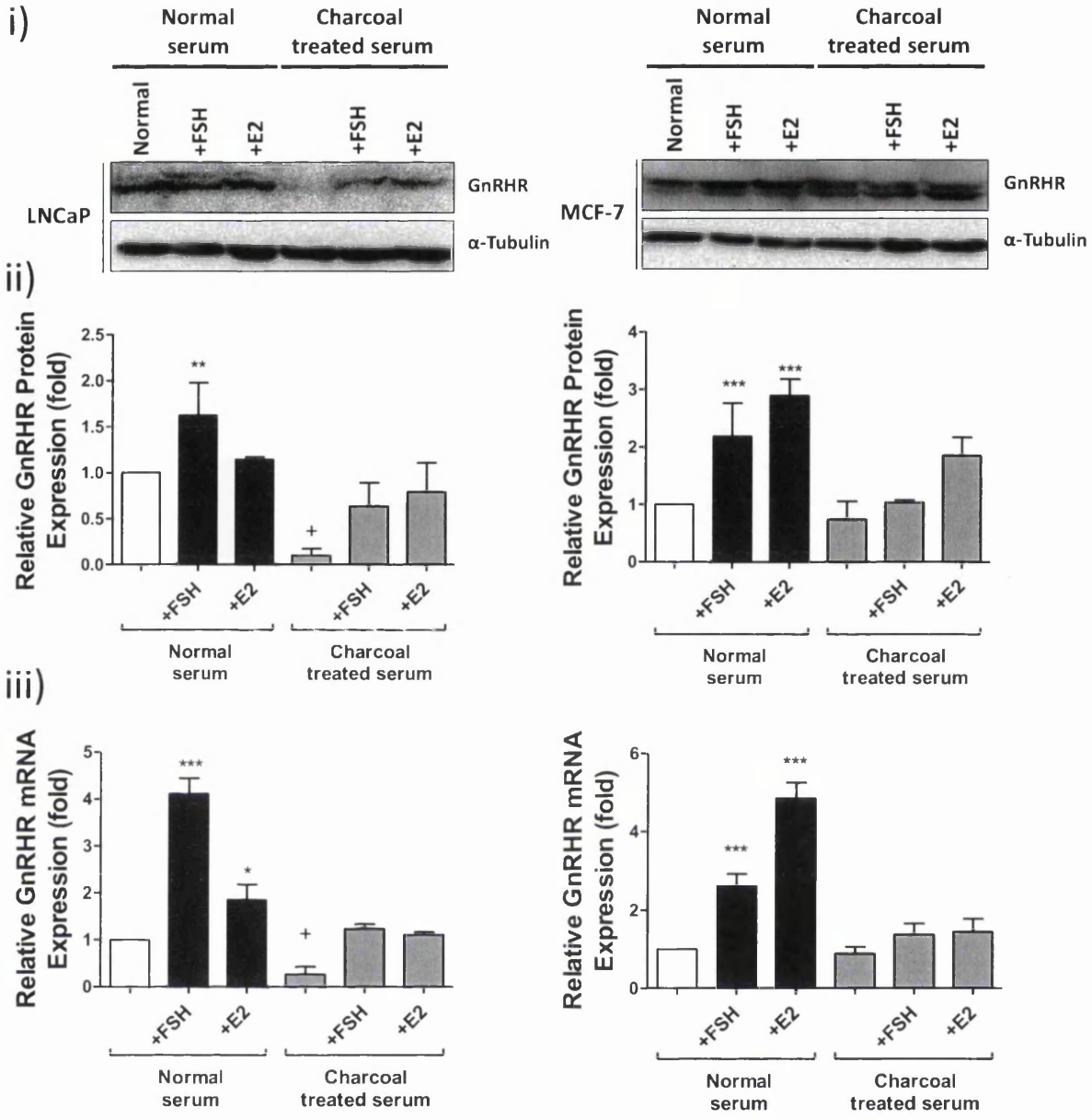

Figure 4.13.C Analysis of GnRHR expression in hormone dependent prostate and breast cancer cell lines treated with FSH and 17β-estradiol. Hormone dependent prostate and breast cancer cell lines (LNCaP and MCF-7 respectively) were cultured in charcoal treated media for 48 hours and FSH and 17β-estradiol for further 48 hours. **i**) Western blot analysis of GnRHR protein expression in non-cancer and cancer cell lines. **ii**) Quantification of GnRHR protein expression shown in (**i**) by densitometric analysis and normalising to house-keeping protein (α-Tubulin) expression. **iii**) RT-PCR analysis of *GnRHR* mRNA expression in non-cancer and cancer cell lines .All western blots, and RT-PCR values are normalised to housekeeping controls. The data are mean ± SEM (error bars represent SEM) values of three independent experiments. *P < 0.05, **P < 0.01 and ***P < 0.001, and compared with non-cancer cell line control.

4.3.8. The cytotoxic activity of Phor21-βCG(ala) and [D-Trp^6]GnRH-Phor21 on hormone dependent prostate and breast cancer cell lines treated with FSH and E2.

As FSH and E2 have a direct effect on the expression of LHCGR and GnRHR in hormone sensitive cell lines, we examined whether FSH or E2 treatment increase the sensitivity LNCaP and MCF-7 cell to Phor21-βCG(ala) and [D-Trp^6]GnRH-Phor21. For this purpose, LNCaP and MCF-7 cells cultured in normal serum or charcoal treated serum containing medium supplemented with none or FSH or E2 (17β-estradiol) were treated with Phor21-βCG(ala) or [D-Trp^6]GnRH-Phor21 and analysed the cytotoxicity of cells using CellTox assay (Figure 4.14A&B)FSH or E2 alone had no cytotoxic effect on both LNCaP and MCF-7 cells. LNCaP cells cultured in charcoal treated serum containing medium showed a reduction in sensitivity to Phor21-βCG(ala) and [D-Trp^6]GnRH-Phor21. However, the addition of 30ng/ml FSH or 5nM E2 to charcoal treated serum containing medium restored the sensitivity of LNCaP cells to Phor21-βCG(ala) and [D-Trp^6]GnRH-Phor21. The addition of 30ng/ml FSH or 5nM E2 to normal serum containing medium also increased LNCaP cells sensitivity to Phor21-βCG(ala) and [D-Trp^6]GnRH-Phor21. FSH and E2 had increased Phor21-βCG(ala) induced cytotoxicity of LNCaP cells (Figure 4.14A) by 19.56% ($P \leq 0.001$) and 19.67% ($P \leq 0.001$) respectfully, and [D-Trp^6]GnRH-Phor21 induced cytotoxicity (Figure 4.14B) by 22.36% ($P \leq 0.001$) and 14.48% ($P \leq 0.001$) respectfully).

MCF-7 cells also showed a reduction in sensitivity to Phor21-βCG(ala) and [D-Trp^6]GnRH-Phor21 when they were treated with charcoal treated serum containing medium. The sensitivity was completely restored with the addition of 30ng/ml FSH or 100nM E2. The addition of 30ng/ml FSH or 100nM E2 to normal serum containing medium also increased the sensitivity of MCF-7 cells to Phor21-βCG(ala) and [D-Trp^6]GnRH-Phor21. FSH and E2 had increased Phor21-βCG(ala) induced cytotoxicity of MCF-7 cells (Figure 4.14 A) by 22.36% ($P \leq 0.001$) and 14.48% ($P \leq 0.001$) respectfully, and [D-Trp^6]GnRH-Phor21 induced cytotoxicity of MCF-7 cells (Figure 4.14 B) by 19.73% ($P \leq 0.001$) and 17.57% ($P \leq 0.001$) respectfully.

These results suggested that FSH and E2 increase the sensitivity of LNCaP and MCF-7 cells to Phor21-βCG(ala) and [D-Trp^6]GnRH-Phor21.

A

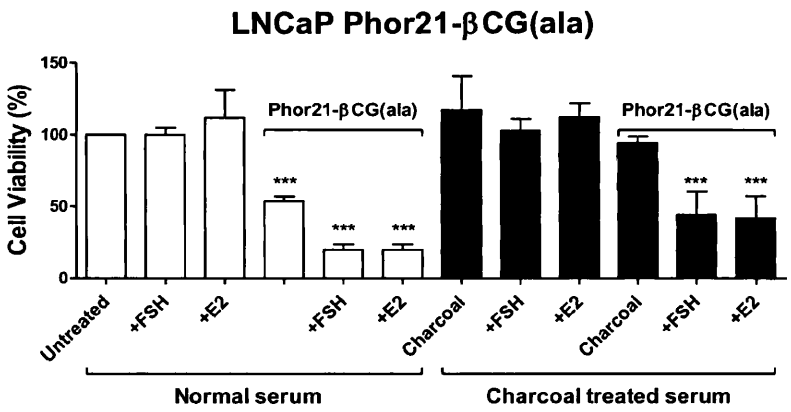
LNCaP Phor21-βCG(ala)
Cell Viability (%)
150
100
50
0
Phor21-βCG(ala)
Phor21-βCG(ala)
***
***
***
***
***
Untreated
+FSH
+E2
+FSH
+E2
Charcoal
+FSH
+E2
Charcoal
+FSH
+E2
Normal serum
Charcoal treated serum

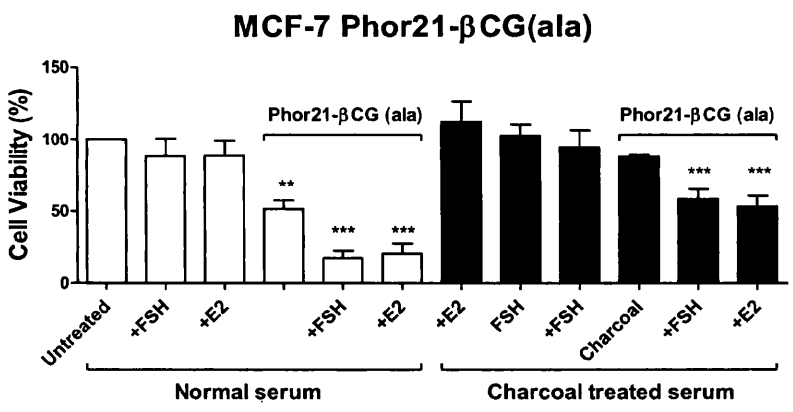
MCF-7 Phor21-βCG(ala)
Cell Viability (%)
150
100
50
0
Phor21-βCG (ala)
Phor21-βCG (ala)
**
***
***
***
***
Untreated
+FSH
+E2
+FSH
+E2
+E2
FSH
+FSH
Charcoal
+FSH
+E2
Normal serum
Charcoal treated serum

B

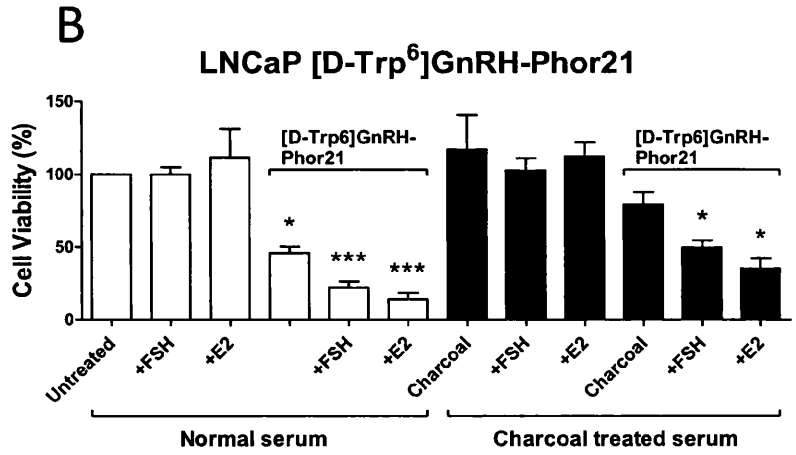
LNCaP [D-Trp6]GnRH-Phor21
Cell Viability (%)
150
100
50
0
[D-Trp6]GnRH-Phor21
[D-Trp6]GnRH-Phor21
*
***
***
*
*
*
Untreated
+FSH
+E2
+FSH
+E2
Charcoal
+FSH
+E2
Charcoal
+FSH
+E2
Normal serum
Charcoal treated serum

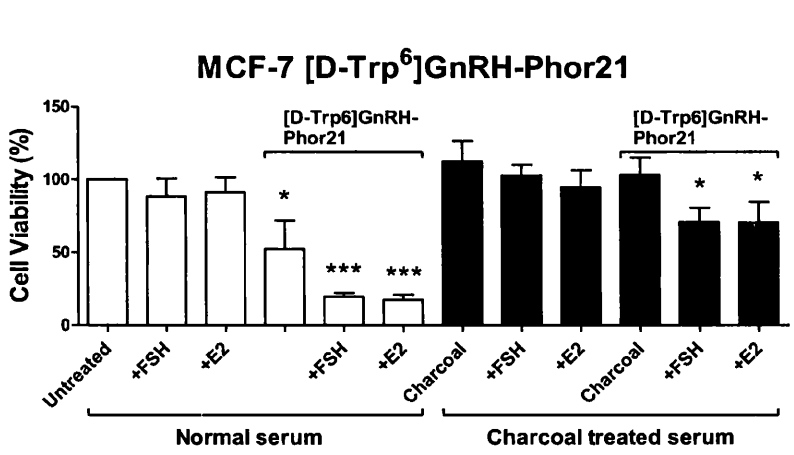
MCF-7 [D-Trp6]GnRH-Phor21
Cell Viability (%)
150
100
50
0
[D-Trp6]GnRH-Phor21
[D-Trp6]GnRH-Phor21
*
***
***
*
*
Untreated
+FSH
+E2
+FSH
+E2
Charcoal
+FSH
+E2
Charcoal
+FSH
+E2
Normal serum
Charcoal treated serum

Figure 4.14 Effect of Phor21-βCG(ala) and [D-Trp^6]GnRH-Phor21on hormone dependent prostate and breast cancer cell lines treated with FSH and 17β-estradiol. Phor21-βCG(ala) and [D-Trp^6]GnRH-Phor21sensitivity of hormone dependent prostate and breast cell lines (LNCaP and MCF-7 respectively) treated with 30ng/ml FSH with LNCaP and MCF-7. LNCaP with 5nM and MCF-7 100nM of E2 for 48 hours, then analysed by CellTox assay. Cells were cultured in charcoal treated media for 48 hours and treated with FSH and 17β-estradiol for further 48 hours. Treatment was initiated by addition of A) Phor21-βCG(ala) 1μM and B) GnRH-Phor21 1μM for 3 hours. The conjugated lytic peptide was incubated for 3 hours before assessing their viability by CellTox assay. The data represent means ± SEM (error bars represent SEM) of data obtained from three independent experiments (***, $P < 0.001$).

4.4. Discussion

The main treatments currently available for patients with prostate and breast cancers involve surgery, radiotherapy and chemotherapy, alone or in combination. Despite advances in treatment, survival rates and prognosis have improved but at very slow pace. Systemic chemotherapy is one of the effective ways to treat cancer. However patients who undergo this treatment have a high prevalence of co-morbidities and problematic lifestyle habits. These side effects could be overcome by using magic bullet based treatments. Paul Ehrlich first proposed the concept of a 'magic bullet'; meaning the search for agents that selectively target cancer cells (Bosch & Rosich, 2008). So the 'magic bullet' will have to be a treatment that acts for a short period of time, to minimise damage to healthy cells and selectively target tumour cells.

In the present study, we focused on analysing three cell surface receptors, IL-13Rα2, LHCGR and GnRHR, in targeting cancer cells. The result demonstrates that LHCGR and GnRHR are overexpressed in prostate and breast cancer cell lines. The overexpression of these two cell surface receptors in many cancers is well documented in a number of studies (Engel et al, 2012a; Hansel et al, 2007a; Hansel et al, 2007b; Jia et al, 2008; Pharmaceuticals, 2012). IL-13Rα2 has also been shown to be overexpressed in variety of malignancies; including brain tumours, ovarian cell carcinoma, pancreatic cancer, breast and prostate cancers(Fujisawa et al, 2009; Gonzalez-Moreno et al, 2005; Jarboe et al, 2007; Kawakami et al, 2003; Kioi et al, 2006a; Kioi et al, 2006b; Puri et al, 1996; Zhao et al, 2014). Therefore, IL-13Rα2 has gathered a lot of interest as a possible drug target for treating cancer. IL-13Rα2 is a very interesting target for glioblastoma multiforme (GBM); in fact a cytotoxic drug composed of IL-13 conjugated with a modified bacterial toxin (Pseudomonas exotoxin) is under clinical trials for GBM treatment (Madhankumar et al, 2004; Pandya et al, 2012). After different forms of mutated IL-13 were created to increase selectivity to IL-13Rα2, a peptide termed Pep-1, obtained through phage display library screening, was found to have high affinity and specific binding to IL-13Rα2 (Pandya et al, 2012). Pep-1 has a peptide sequence of CGEMGWVRC and has been shown to bind at a site different to that of IL-13 on IL-13Rα2 and therefore it's binding to IL-13Rα2is not inhibited by the native ligand cytokine IL-13 (Pandya et al, 2012).

Peptides used for drug development have several advantages. They are easily produced and affordable compared to protein based drugs. They can vary in sequence, producing a variety

of candidate peptides combining moieties for targeting and for toxicity can be tested in preclinical settings. EP-100 is a cancer drug, which is currently undergoing phase II trials (Pharmaceuticals, 2009). It is a conjugation between LHRH and the lytic peptide CLIP 71. In the phase I study, the maximum dose of EP-100, which is safe, against ovarian cancer has been determined as 5.2 mg/m^2. The drug is well tolerated, a maximum tolerated dose is 40 mg/m^2 (Pharmaceuticals, 2012).

We synthesised three lytic peptides Pep-1-Phor21, Phor21-βCG(ala), and [D-Trp6] GnRH-Phor21 that targets IL-13Rα2, LHCGR and GnRHR respectively. The cytotoxic activity of these peptides in prostate and breast cancer cell lines depends on the expression of the target receptors. Phor21-βCG(ala), and [D-Trp6] GnRH-Phor21 are lytic peptides have already been characterised and are shown to target and kill prostate and breast cancer; (Hansel, 2005; Leuschner & Hansel, 2005). This study confirms previous studies. Pep-1-Phor21 is a new lytic peptide conjugate that targets IL-13Rα2. The data presented in this chapter indicates that the more aggressive and metastatic prostate and breast cancer cells lines express more IL-13Rα2. Our results are in line with previous studies, which demonstrated that the expression of IL-13Rα2 is high in tumorigenic and metastatic prostate (such as PC3) and breast cancer (MDA-MB 231 and LM2) cells (He et al, 2010; Minn et al, 2005). These results indicate that IL-13Rα2 may be a potential target for metastatic cancers.

The characteristic action of the lytic peptides is necrotic. This was well characterised with Phor21-βCG(ala), and [D-Trp6] GnRH-Phor21 in previous studies by disrupting and diffusing in the target cell membrane causing necrosis, making it difficult for any cell to become resistant (Hancock & Diamond, 2000; Hansel, 2005; Leuschner & Hansel, 2005; Shai, 2002). Pep-1-Phor21 showed similar mode of action, as demonstrated in Figure 4.8A-C.

In this study, the in vitro cytotoxicity of Pep-1-Phor21, Phor21-βCG(ala), and [D-Trp6]GnRH-Phor21 peptides was examined in four prostate cell lines and three breast cell lines. Non-tumour cell lines (HEK293, PNT-2 and MCF-10A) exhibited low or undetectable levels of expression of IL-13Rα2, LHCGR and GnRHR, and thereby showed little or no sensitivity to Pep-1-Phor21, Phor21-βCG(ala), and [D-Trp6]GnRH-Phor21 lytic peptide conjugates. These results suggest that the cytotoxic effect of these lytic peptide conjugates correlates well with the levels of target receptor expression.

We also demonstrated that Histone deacetylation (TSA) and DNA methylation (5-aza-dC) inhibitors up-regulate the expression of IL-13Rα2 in prostate and breast cancer cell lines. We

therefore looked in this chapter whether TSA or 5-aza-dC could also enhance the sensitivity of prostate and breast cancer cells to Pep-1-Phor21 and [D-Trp6]GnRH-Phor21. We found that pre-treatment with TSA and 5-aza-dC increased the sensitivity of [D-Trp6]GnRH-Phor21 in all cancer cell lines. We also demonstrated that TSA and 5-aza-dC increase the sensitivity of low expressing IL-13Rα2 cancer cells to Pep-1-Phor21. The synergistic effect of Pep-1-Phor21 and Histone deacetylation or DNA methylation inhibitor on cancer cells is dose dependent and the synergy is specific for cancer cells. An additional advantage of such a combination is that it might help reduce the risk of toxicity observed in the surrounding normal tissues. Interestingly Pep-1-Phor21 showed no effect on non-tumour cells that are treated or untreated with TSA or 5-aza-dC, indicating that Pep-1-Phor21 is a potential therapeutic anti-cancer drug without effecting normal cells. The exact reason(s) for TSA and 5-aza-dC up-regulating IL-13Rα2 expression specifically in cancer cells is unknown. One possible reason is that TSA and 5-aza-dC induction of IL-13Rα2 requires AP-1/c-jun pathway, which could be inactivated in normal cells (Fujisawa et al, 2011).

The results obtained in this chapter also demonstrate that prostate and breast cancer can be targeted through LHCGR and GnRHR. The results also suggest that sensitivity of these cancer cells to Phor21-βCG(ala) and [D-Trp6]GnRH-Phor21 lytic peptide conjugates can be increased by pre-treating them with FSH and 17β-estradiol (E2), which was shown, in this study, to up-regulate LHCGR and GnRHR. Leuschner et al demonstrated that the lytic peptides Phor14-βLH and Hecate-βLH effect prostate tumours in animal models, more than 75% of all treated animals had no tumour cells (Leuschner et al, 2001). This study also showed a significant increase in sensitivity of prostate tumours to the lytic peptide conjugates when treated with FSH or E2. The same group also demonstrated a direct effect of E2 and FSH on LHCGR and GnRHR expression in breast cancer cell lines (Leuschner et al, 2003b). Tamoxifen, an antagonist for estrogen receptor, has been shown to reduce the effect of lytic peptides on hormone sensitive breast cancer cell lines expressing LHCGR and GnRHR (Leuschner et al, 2003b).

The overall results observed in the current study appear promising especially when comparing one treatment with combinational treatment. We employed a lytic peptide called Pep-1-Phor21, [D-Trp6]GnRH-Phor21 and Phor21-βCG (ala) in order to target cells expressing IL-13Rα2, GnRHR and LHCGR respectfully. Combining treatments with FSH, 17β-estradiol, TSA or 5-aza-dC induced syngeneic cell death when compared to the

efficacies of the lytic peptide treatments alone. Altogether, our results give evidence that this combination can be used for treating prostate and breast cancers.

5. Validation of cancer targeting lytic peptides using breast and prostate cancer cells grown as spheroids

5.1. Introduction

In terms of reaching clinical usage the success rate of putative therapeutic drugs is very low. It is estimated that only 5% of candidate drug compounds pass phase II clinical trials (Amiri-Kordestani & Fojo, 2012; Kola & Landis, 2004). A variety of in vitro models have been developed for the study of cancers based on two key factors:

1) The ability to easily monitor the cell number and viability
2) The ability to monitor the migration and invasion of the cell

A preclinical in vitro model must be inexpensive, suitable for high-throughput screening, and reflecting the in vivo environment.

Current in vitro cancer models are cell lines, which are derived from human cancerous tissues, grown in a 2-dimensional (2D) monolayer. This model is widely used and is an important tool for any drug testing. However whilst this model is useful for rapid, high throughput screening of new drugs against cancers , this usage is limited due to its inability to mimic key aspects of the *in vivo* environment of cancers (Khaitan & Dwarakanath, 2006; Minchinton & Tannock, 2006; Van Dyke & Jacks, 2002).

There are a number of *in vitro* cancer models available, one of which is cells grown in 3D spheroids. Multicellular tumour spheroid (MCTS) is a 3D model that formed through culturing of cancer cells in a non-adhesive environment, which mimics the physiological features of solid tumours (Fischbach et al, 2007).

It has been well established that cells in a 3D structure typically have lower sensitivity to cytotoxic drugs compared to cells grown in a 2D monolayer (Durand & Olive, 2001). A 3D model closely relates to solid tumours and therefore will provide a better understanding of the activity of anticancer drugs. One major requirement of any anticancer drug is the ability to penetrate solid tumours and still maintain its efficiency, a trait that cannot be detected in a monolayer model. Moreover, solid tumours are composed of proliferating and quiescent hypoxic cells (which are known to be drug resistant), whilst all monolayer cells are exponentially growing (Roberts et al, 2009). Reduced drug response in 3D environments was also demonstrated by growing cells in scaffolds like Matrigel, where the cell phenotype in the

3D environment is more representative of in the *in vivo* environment (Dhiman et al, 2005; Fischbach et al, 2007).

3D spheroid models are considered as the intermediary models between clinical trials and cancer cell lines grown as a monolayer (Hirschhaeuser et al, 2010; Rodday et al, 2011). It was shown that cancer cells were more likely to become resistant to antineoplastic agents when grown in a 3D model compared to a monolayer (Olive et al, 1993). There are studies showing a strong correlation between the sensitivity of in vitro grown spheroids and that of *in vivo* models (Kobayashi et al, 1993). This type of model has been used to study a range of different applications including: radiotherapy (Qvarnstrom et al, 2009), immunotherapy (MacDonald & Sordat, 1980), chemotherapy (Twentyman, 1980), drug resistance (Chen et al, 2009b), metastasis (Landry et al, 1981), gene expression (Chang & Hughes-Fulford, 2009), and extracellular matrix (ECM) (Hirschhaeuser et al, 2010).

In vitro 3D cancer models that mimic the parameters of *in vivo* microenvironments, such as cell–cell, cell–ECM interactions, can be very useful in identifying the therapeutic efficacy of many anticancer drugs (Ma et al, 2012). A 3D cell culture model has many advantages over 2D monolayer cell culture model. The first feature is the ability of 3D cell cultures to re-establish morphological, functional, and mass transport features of the corresponding tissue found *in vivo* (Hirschhaeuser et al, 2010). It was shown that 3D cell cultures can maintain some of the differentiation patterns found in animal models for a long period of time (Kunz-Schughart et al, 2004). These features are created and maintained by the tumour cell-derived ECM along with the cellular interactions, e.g. cell-cell and cell-matrix interactions (Hirschhaeuser et al, 2010). Secondly, 3D cell cultures can mimic many characteristics of the avascular tumour nodules, micro-metastases, or intravascular regions of large solid tumours (Hirschhaeuser et al, 2010). Diffusion gradients of various components (nutrients, drugs, nanoparticles etc.) can be studied using 3D cell cultures (Kunz-Schughart et al, 2004). Thirdly and most importantly, 3D cancer cell culture can reduce the use of animal models for testing anti-cancer drugs.

Overall, 3D cell culture is considered an alternative to 2D monolayer, which closely resembles the main features of solid tumours. However this is not a substitute for animal model derived information regarding the pharmacokinetics, pharmacodynamics and bioavailability of novel drugs (Khaitan & Dwarakanath, 2006). But 3D cell culture has shown real potential in validating novel drug compounds in high through put manner.

The purpose of this study is to develop an *in vitro* 3D tumour model for evaluating therapeutic efficiency of the lytic peptide conjugates used in the chapter 4. In this chapter, we demonstrated

- The formation of 3D cancer cell spheroids through a novel approach.
- Use of the cell spheroids to evaluate therapeutic efficiency of the lytic peptide drugs [D-Trp^6]GnRH-Phor21, Pep-1-Phor21, and Phor21-βCG(ala) in prostate and breast cancers.

5.2. Materials and Methods

Reagents, cell culture, RT-PCR, TSA and 5-aza-dC treatments, and CellTox assay were described in section 2.2

5.2.1. Generation of spheroids

HEK293, MCF-10A, MCF-7, MDA-MB 231, PNT-2, LNCaP, DU145 and PC3 cells were used in this study. Monolayer cells were detached with 1x Trypsin/EDTA (as described in section 4.2) to generate a single cell suspension. The cell suspension was diluted to 1x10^{5}cells/ml. 20µl of the diluted cells was seeded into each well of a Terasaki plate (Greiner bio-one), and the plates were incubated upside-down at 37°C/5% CO_2 in a humidified incubator to grow cells as spheroids. After 24 hours of incubation, the spheroids along with the medium were collected from 5 wells of the Terasaki plate, pooled and transferred into a single well of U-bottom surface repellent 96 well plates (CELLSTAR Greiner bio-one), incubated at 37°C/5% CO_2 in a humidified incubator for 1-4 days. For CellTox assays, spheroids incubated for 1 day in the U-bottom repellent plates were used. In some instances, cells (500-10,000/0.1ml) were seeded directly in U and F-bottom surface repellent plates and incubated at 37°C/5% CO_2 in a humidified incubator for 1-4 days. Cell spheroid formation was viewed using an inverted light microscope.

The viability of cells in spheroids was also assessed using LIVE/DEAD staining (Invitrogen). For this, single cell suspensions (1x10^5/ml) obtained by detaching monolayers cells through 1X Trypsin/EDTA treatment (as described above) were stained green by incubating with the fluorescent vital membrane dye Vybrant DiO (Molecular Probes; 1:200 dil.) for 10 minutes at 37°C/5% CO_2 in a humidified incubator. The labelled cells were washed once by centrifuging at 350xg for 5 minutes and re-suspending the cell pellet in fresh full serum medium (FSM) to

obtain the same cell density. The fluorescently labelled cells were seeded into wells of a Terasaki plate and incubated as described above to generate spheroids. Matrigel (Reconstituted basement membrane; BD Biosciences) was thawed on ice overnight and mixed with equal volume of ice cold FSM and 30µl pipetted into each well of a 96-well black plate with clear flat bottom (Greiner bio-one) and incubated at 37°C/5% CO_2 in a humidified incubator for 24 hours for solidification of Matrigel. The DiO stained spheroids grown in the wells of the Terasaki plate for 24 hours were pipetted into the Matrigel and incubated for 3 hours without or with test compound. Then the samples were incubated in phenol red-free DMEM containing 2 µM ethidium homodimer I at room temperature for 40 minutes. The wells containing spheroids in Matrigel were washed three times with phenol red-free DMEM and immediately imaged in the same medium using confocal microscopy LSM 510 microscope (Carl Zeiss, Inc).

5.2.2. Statistical Analysis

The data were analysed using GraphPad prism program. All data are presented as means ± standard error of the mean (SEM) of three independent experiments. Statistical tests between controls and test values were performed using two-tailed unpaired Student's t-test. Statistical tests between groups are performed using Bonferroni's post-test after one-way or two-way analysis of variance (ANOVA), where $p > 0.05$ was considered as statistically significant not significant (n.s.) and $p < 0.05$, $p < 0.01$ and $p < 0.001$ were considered as statistically significant (Thompson & Kanamarlapudi, 2014).

5.3. Results

5.3.1. Optimisation of conditions for spheroid formation of cancer cells

The conditions required for spheroid generation were investigated by seeding MDA-MB-231 breast cancer cells at different cell density (500-10,000 per well) in different culture plates (F-bottom [Figure 5.1] or U-bottom [Fig 5.2] cell repellent 96-well plates or Terasaki 60-well plates [Fig 5.3]). These cells were incubated for 1-4 days at 37°C/5% CO_2 in a humidified incubator and visualised cells by light microscopy every day. Terasaki plates were incubated up-side down to form a hanging drop of medium with MDA-MB 231 cells. Spheroids were formed only in Terasaki plates and the optimal conditions for formation of spheroids in these plates were 2000 cells per well and 24h incubation. F-bottom cell repellent plates caused the

cells to form 2D culture by adhering to bottom surface of the plate (Fig 5.1). In some conditions, the cells did from small clusters or irregularly shaped aggregates in U-bottom cell repellent plates (Figure 5.2). However the irregularly shaped aggregates showed poor adhesive strength. In contrast, the spheroids formed in Terasaki plates by seeding 2000 cells per well and 1 day incubation of plates yielded a compact spheroid structure that had a central dense core (Figure 5.3). Adding more than 2000 cells per well didn't increase spheroids size or number whereas incubation of the plates for more than 1 day resulted in disappearance of formed spheroids. Therefore in all subsequent assays, 2000 cells per well and 24h incubation in Terasaki plates were used to generate spheroids. Terasaki plate wells are small and can hold only 20µl of medium. For scaling up spheroids required for further analysis, we pooled spheroids formed in 3-4 wells of Terasaki plate, transferred them into one well of F- or U-bottom cell repellent plate, incubated the plates at 37°C/5% CO_2 in a humidified incubator for 1-4 days and visualised spheroids everyday using a light microscope (Figure 5.4. The spheroids transferred into F-bottom wells dissociated and attached to the bottom surface of the plate within 2 days of incubation and died and detached from the surface on 4th day of incubation. However, the spheroids transferred into U-bottom wells of cell repellent plate maintained spheroidal structure for 4 days (Figure 5.4). .

The viability of cells in spheroids generated in Terasaki plates were assessed quantitatively by CellTox assay and qualitatively by Live/Dead staining assay (Figure 5.5A). For CellTox assay, the spheroids generated in Terasaki plates were transferred into U-bottom cell repellent wells and incubating the plates for 1 day at 37°C/5% CO_2 in a humidified incubator for maintaining spheroidal structure. For Live/Dead staining assay, the spheroids generated in Terasaki plates were transferred into 50% Matrigel (basement membrane extract) in wells of F-bottom 96-well black plates and incubated for 1 day at 37°C/5% CO_2 in a humidified incubator for maintaining spheroidal structure. However, when the cells were seeded directly with Matrigel into wells of F-bottom 96-well black plates, we didn't see spheroid formation (Figure 5.5B), indicating that Matrigel is suitable for maintaining spheroidal structure but not generating spheroids.

We next determined whether in vitro generated spheroids of MDA-MB 231 show sensitivity to the lytic peptide conjugates described in Chapter 4 by using CellTox and Live/Dead staining assays. For CellTox green assay, the spheroids generated using Terasaki plates and maintained in U-bottom plate were treated with optimal concentration (determined for 2D culture) of βCG(ala), lytic peptide Phor21 and ligand conjugated lytic peptide Phor21-

βCG(ala) for 3 hours at 37°C/5% CO_2 in a humidified incubator. As expected, βCG(ala) and Phor21 showed no effect on spheroid integrity (assessed by viewing under light microscope) or cell viability in the spheroids (assessed by CellTox assay) (Figure 5.6). However Phor21-βCG(ala) treatment not only affected spheroid integrity (spheroid structure had disappeared) but also reduced cell viability in the spheroids by ~67%. In fact, Phor21-βCG(ala) had reduced cell viability of spheroids by ~55% within 1.5 hour of the treatment but had a little effect on the spheroids integrity. Therefore in all subsequent studies using CellTox assay, we treated spheroids with lytic peptides for 3 hours.

After evaluating the cell viability quantitatively by CellTox assay, we assessed qualitatively the effect of Phor21-βCG (ala) on MDA-MB 231 spheroids maintained in Matrigel by Live/Dead assay (Figure 5.7). Three hours after treating with Phor21-βCG (ala), almost 80% of cells in the spheroids were positive for EthD-1 staining, confirming cell death. The untreated control together with unconjugated controls βCG (ala) and Phor21 treated spheroids were more compact and showed low number dead cells.

Together, these results suggest that cancer cells grown in vitro in 3D culture (spheroids) are sensitive, like those grown in monolayers, to the lytic peptide conjugates.

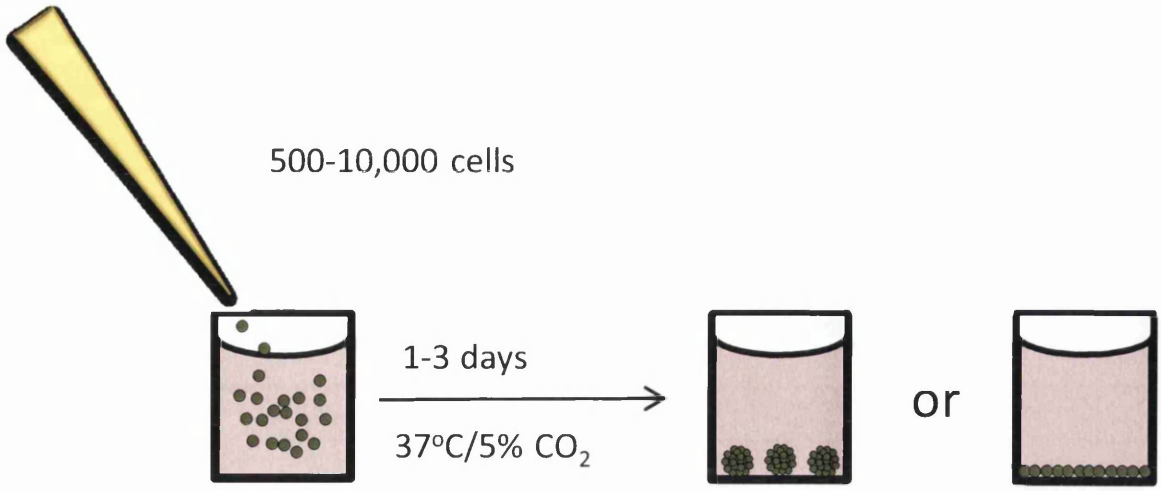
500-10,000 cells
1-3 days
37°C/5% CO_2
or

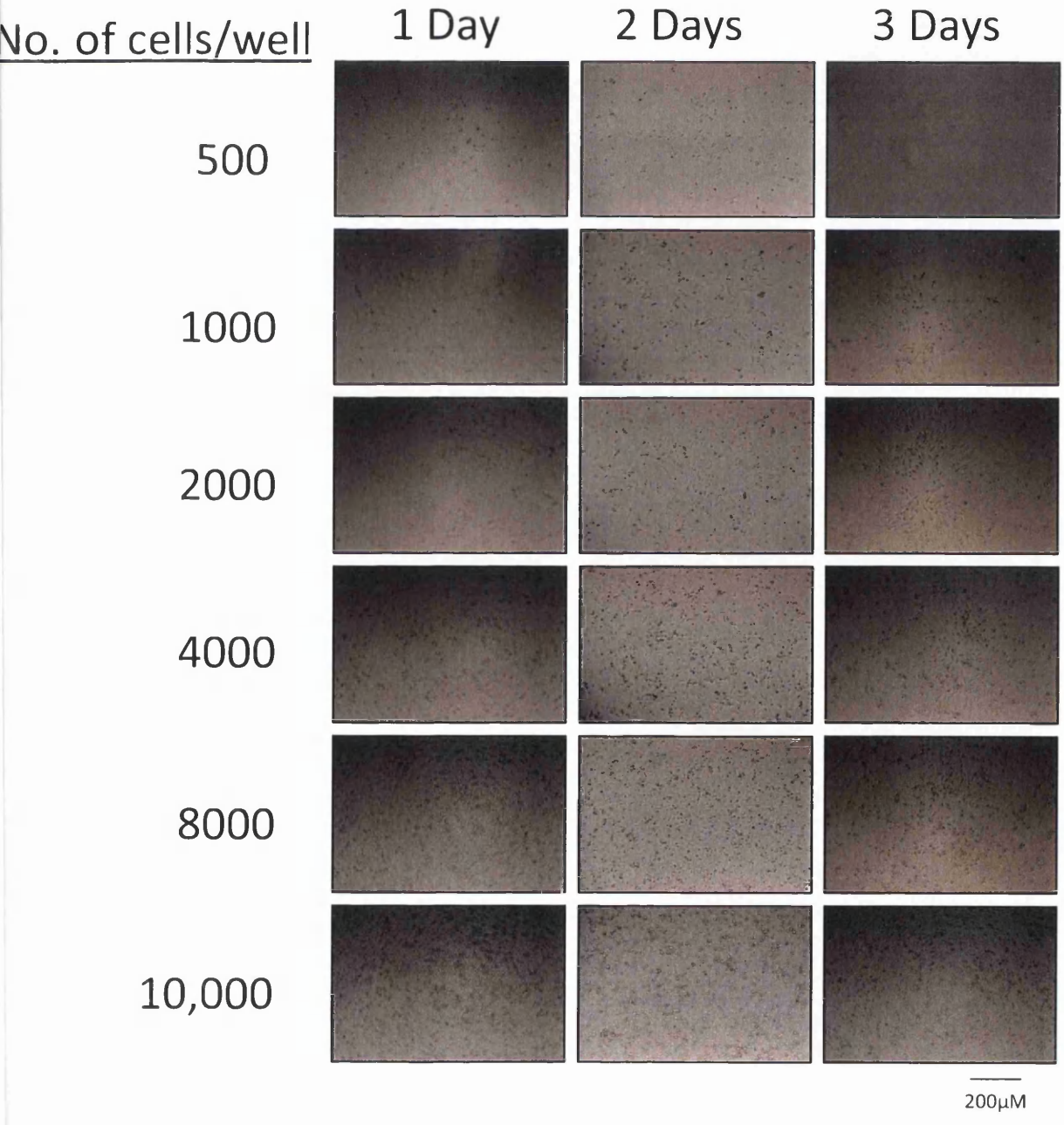
No. of cells/well
1 Day
2 Days
3 Days
500
1000
2000
4000
8000
10,000
200μM

Figure 5.1. Effect of cell density and incubation time on MDA-MB 231 cell spheroid formation in F bottom cell repellent plates. ***Upper panel.*** Schematic view of the procedure. ***Lower panel.*** 500-20,000 MDA-MB 231 cells in 0.1ml medium were seeded per well of F-bottom surface repellent plate, incubated 1-3 days at 37C/5% CO_2 and visualised spheroid formation by inverted light microscope.

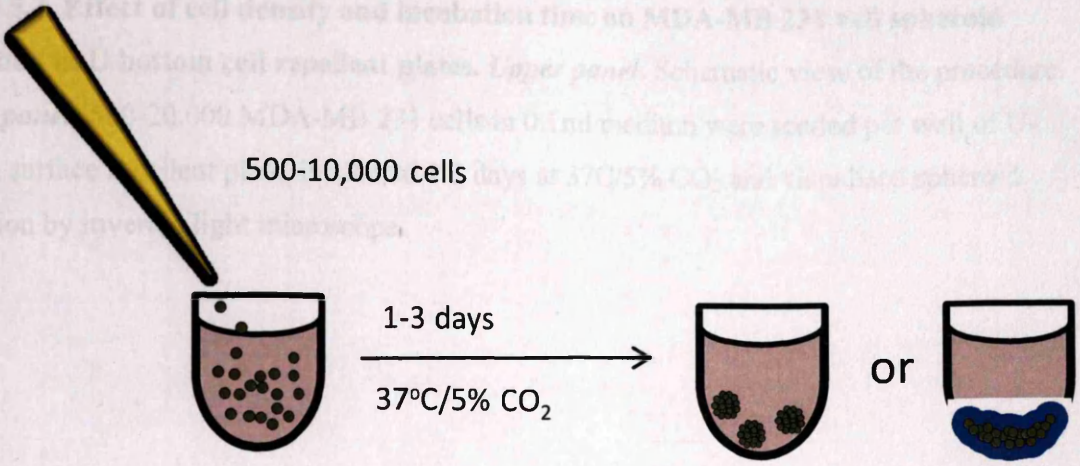
500-10,000 cells
1-3 days
37°C/5% CO_2
or

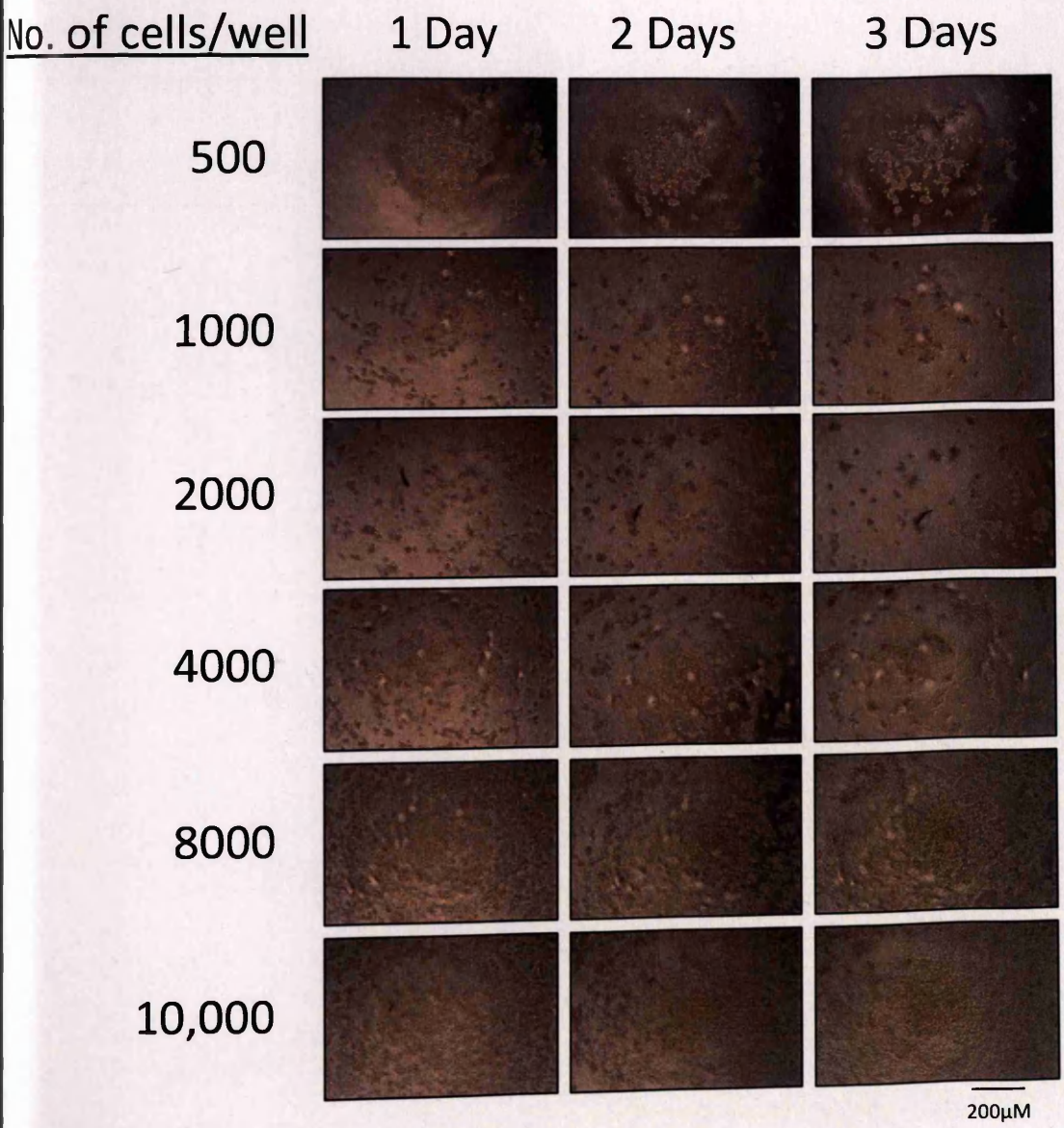
No. of cells/well
1 Day
2 Days
3 Days
500
1000
2000
4000
8000
10,000
200μM

Figure 5.2. Effect of cell density and incubation time on MDA-MB 231 cell spheroid formation in U bottom cell repellent plates. ***Upper panel.*** Schematic view of the procedure. ***Lower panel.*** 500-20,000 MDA-MB 231 cells in 0.1ml medium were seeded per well of U-bottom surface repellent plate, incubated 1-3 days at 37C/5% CO_2 and visualised spheroid formation by inverted light microscope.

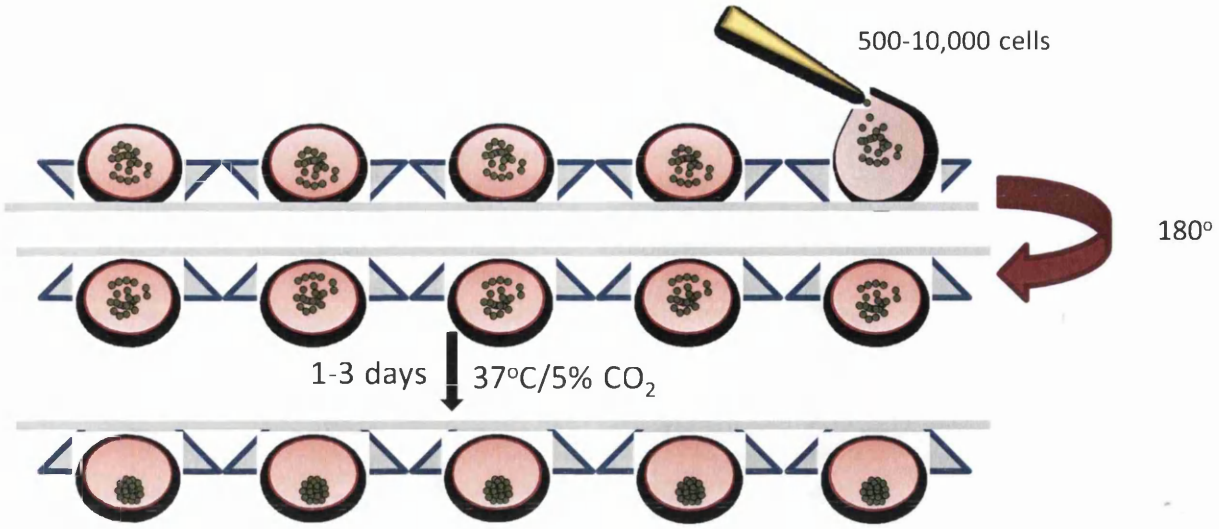
500-10,000 cells
180°
1-3 days
37°C/5% CO_2

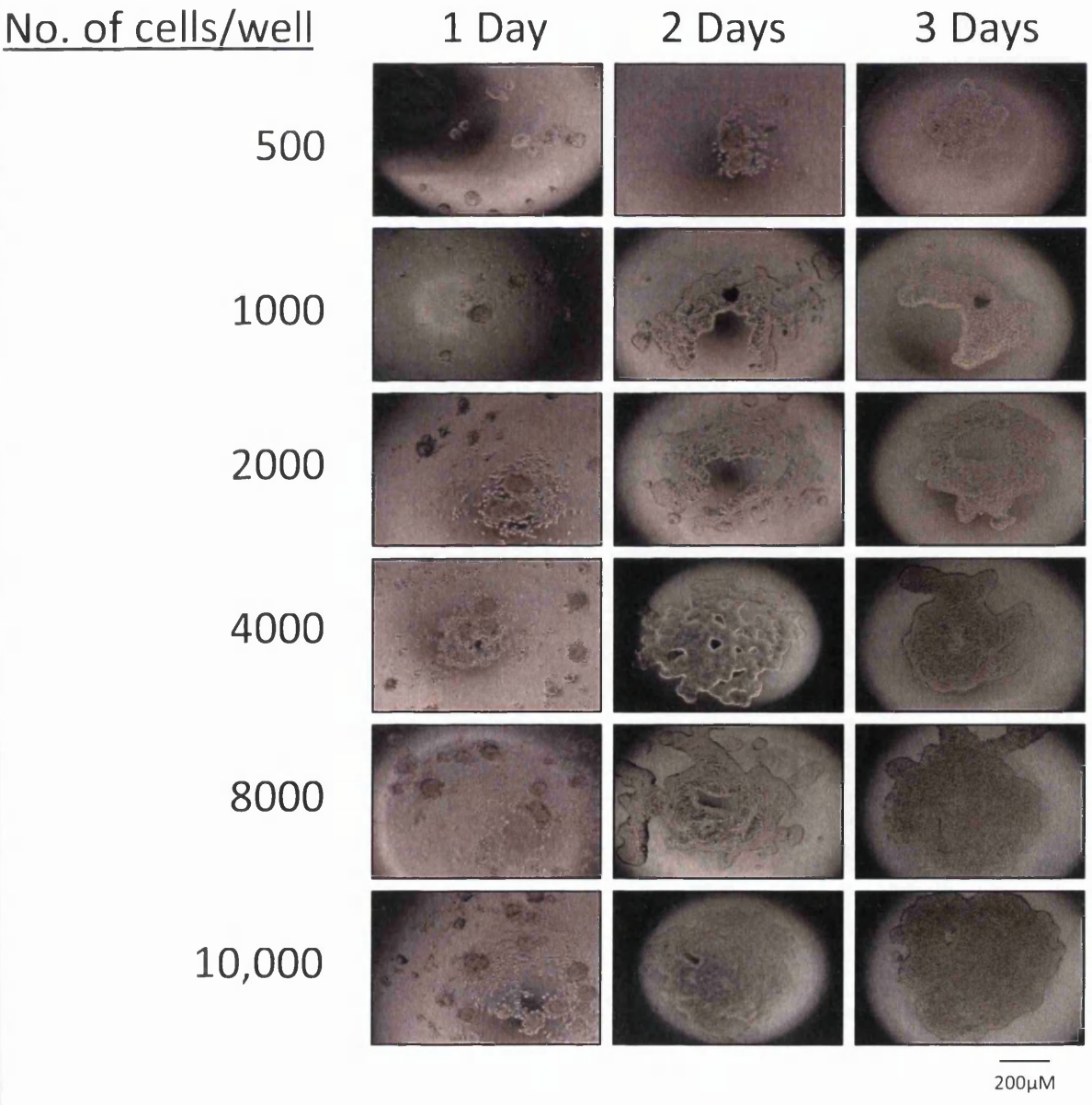
No. of cells/well
1 Day
2 Days
3 Days
500
1000
2000
4000
8000
10,000
200µM

Figure 5.3. Effect of cell density and incubation time on MDA-MB 231 cell spheroid formation in Terasaki plate. ***Upper panel.*** Schematic view of the procedure. ***Lower panel.*** 500-20,000 MDA-MB 231 cells in 0.02ml medium were seeded per well of Terasaki plate, incubated 1-3 days at 37C/5% CO_2 and visualised spheroid formation by inverted light microscope.

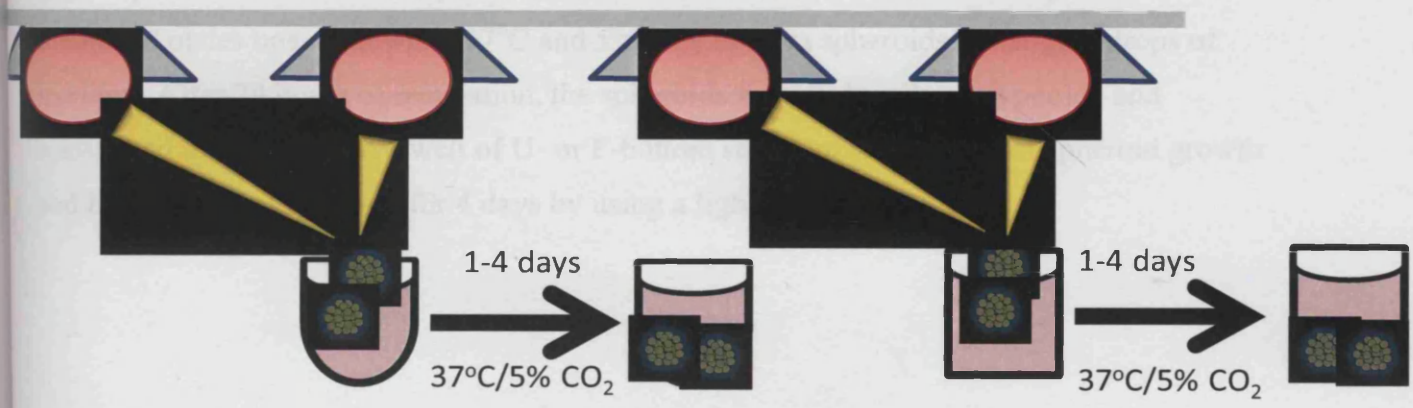
1-4 days
37°C/5% CO_2
1-4 days
37°C/5% CO_2

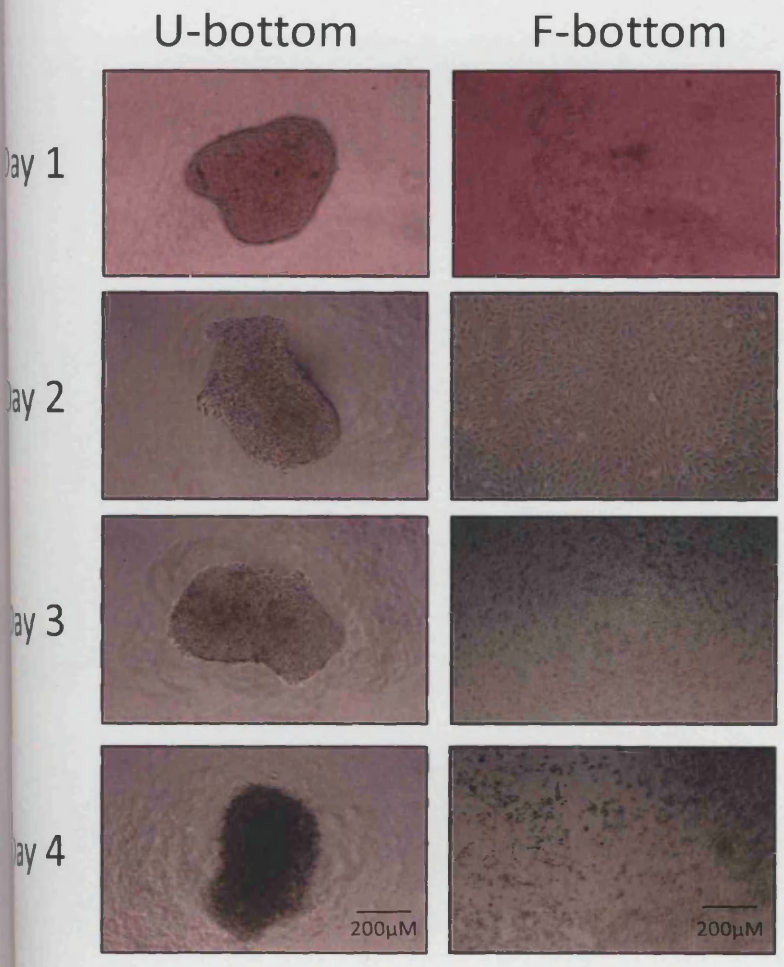
U-bottom
F-bottom
Day 1
Day 2
Day 3
Day 4
200µM
200µM

Figure 5.4. Analysis of MDA-MB 231 spheroid grown in hanging drop and transferred to F- or U-bottom surface repellent plates . ***Upper panel,*** Schematic view of the procedure. **Lower panel,** 2000 cells in 20µl medium were seeded into wells a Terasaki plate and incubated plates upside down at 37°C and 5% CO_2 to form spheroids in hanging drops of medium. After 24 hours of incubation, the spheroids from 3-4 wells were pooled and transferred into either into a well of U- or F-bottom repellent 96-well plate. Spheroid growth and integrity was visualised for 4 days by using a light microscope.

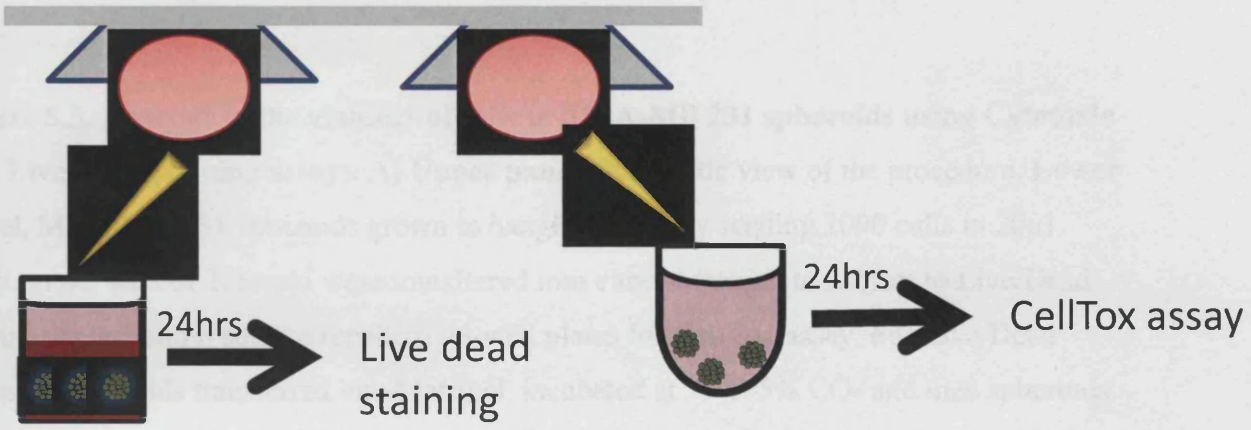
24hrs
Live dead staining
24hrs
CellTox assay

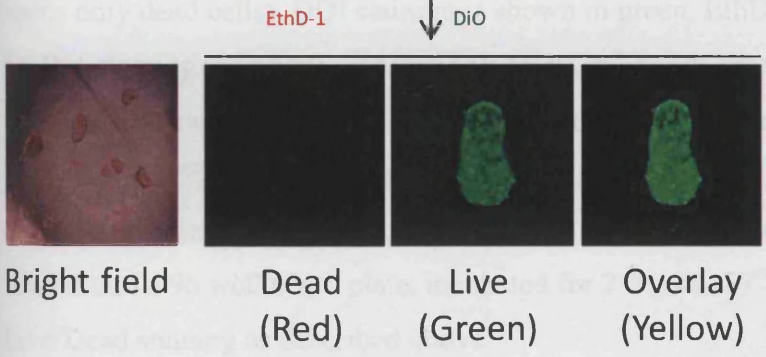
EthD-1
DiO
Bright field
Dead (Red)
Live (Green)
Overlay (Yellow)

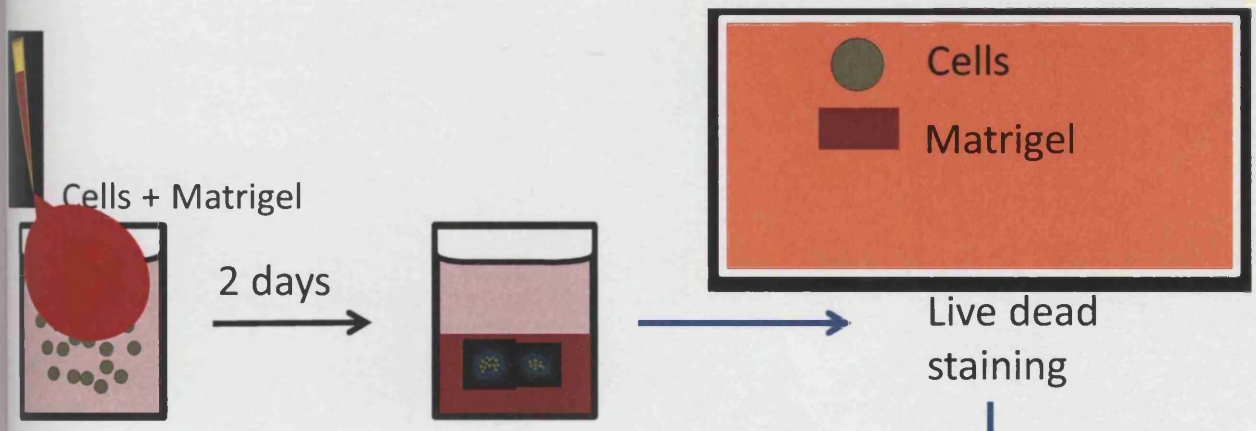
Cells
Matrigel
Cells + Matrigel
2 days
Live dead staining


Bright field
Dead (Red)
Live (Green)
Overlay (Yellow)

Figure 5.5. Analysis of the viability of cells in MDA-MB 231 spheroids using Cytotoxic and Live/Dead staining assays. A) Upper panel, Schematic view of the procedure. **Lower panel,** MDA-MB-231 spheroids grown in hanging drops by seeding 2000 cells in 20µl medium per well of Terasaki were transferred into either Matrigel to subject to Live/Dead staining or U-bottom surface repellent 96-well plates for CellTox assay. For Live/Dead staining, spheroids transferred into Matrigel, incubated at 37°C/5% CO_2 and then spheroids were stained using Live/Dead staining kit (DOI stains both live and dead cells where EthD-1 stains only dead cells). DOI staining is shown in green, EthD-1 in red and overlay of DOI and EthD-1 staining in yellow. For CellTox assay, spheroids grown in hanging drop of 3-4 wells were pooled, transferred into a well of U-bottom surface repellent plate, incubated for 24 hours at 37°C/5% CO_2 and then subjected to CellTox assay. **B)** ***Upper panel,*** schematic view of the procedure. **Lower panel,** MDA-MB 231 (2000 cells/well) were diluted in Matrigel and seeded into a 96 well black plate, incubated for 2 days at 37°C/5% CO_2 and then subjected to Live/Dead staining as described above.

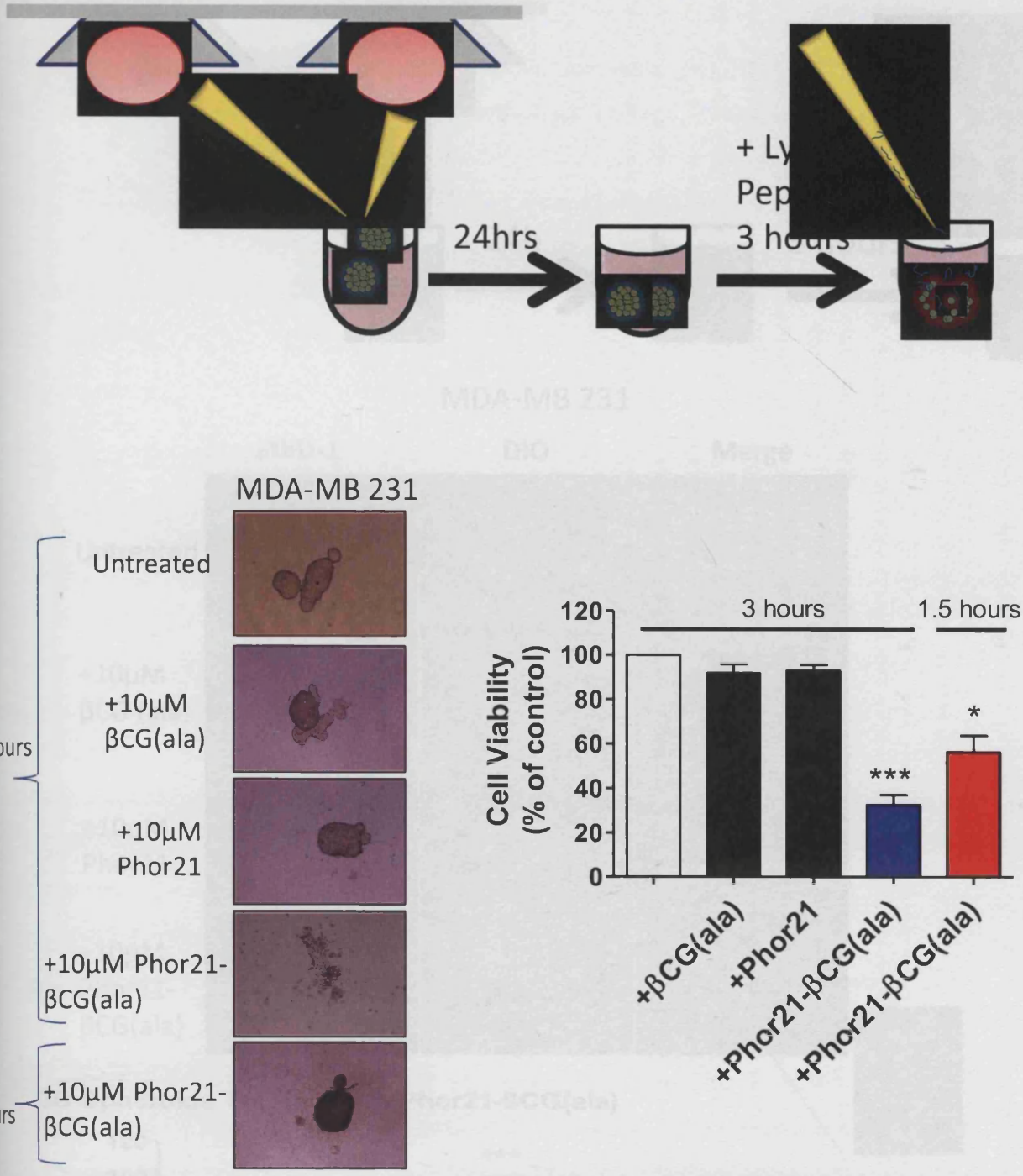

Figure 5.6 Effect of the lytic peptide conjugate on cell viability of MDA-MB 231 spheroids assessed by CellTox assay. Upper panel, Schematic view of the procedure. **Lower panel,** Spheroids generated in Terasaki plates were transferred into U-Bottom surface repellent plates, incubated at 37°C/5% CO_2 and then treated without or with 10μM βCG(ala), Phor21 or Phor21-βCG(ala) for 3 hours and analysed cell viability of spheroids using CellTox assay. Data represent means ± SEM (error bars represent SEM) of three independent experiments (***, $P < 0.001$).

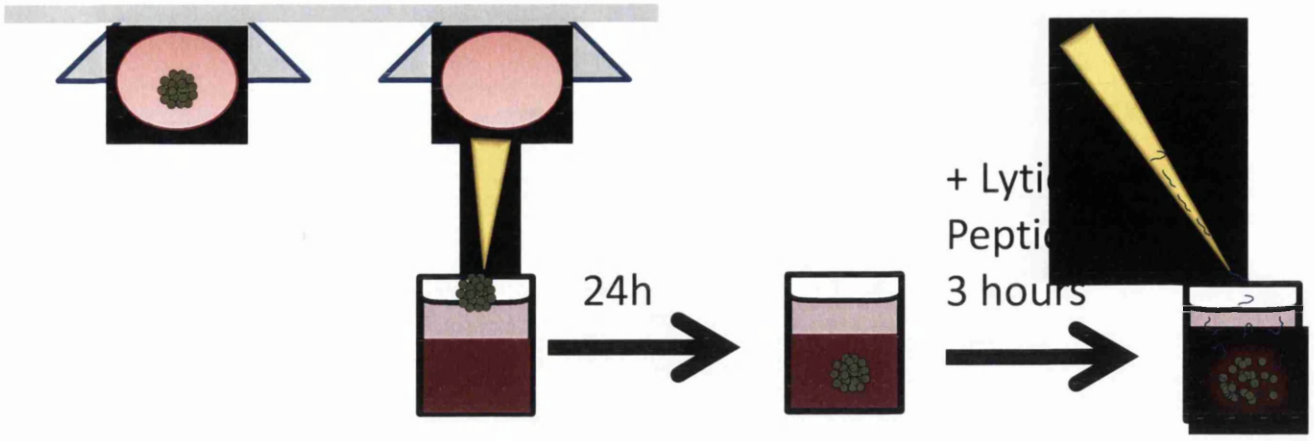

MDA-MB 231

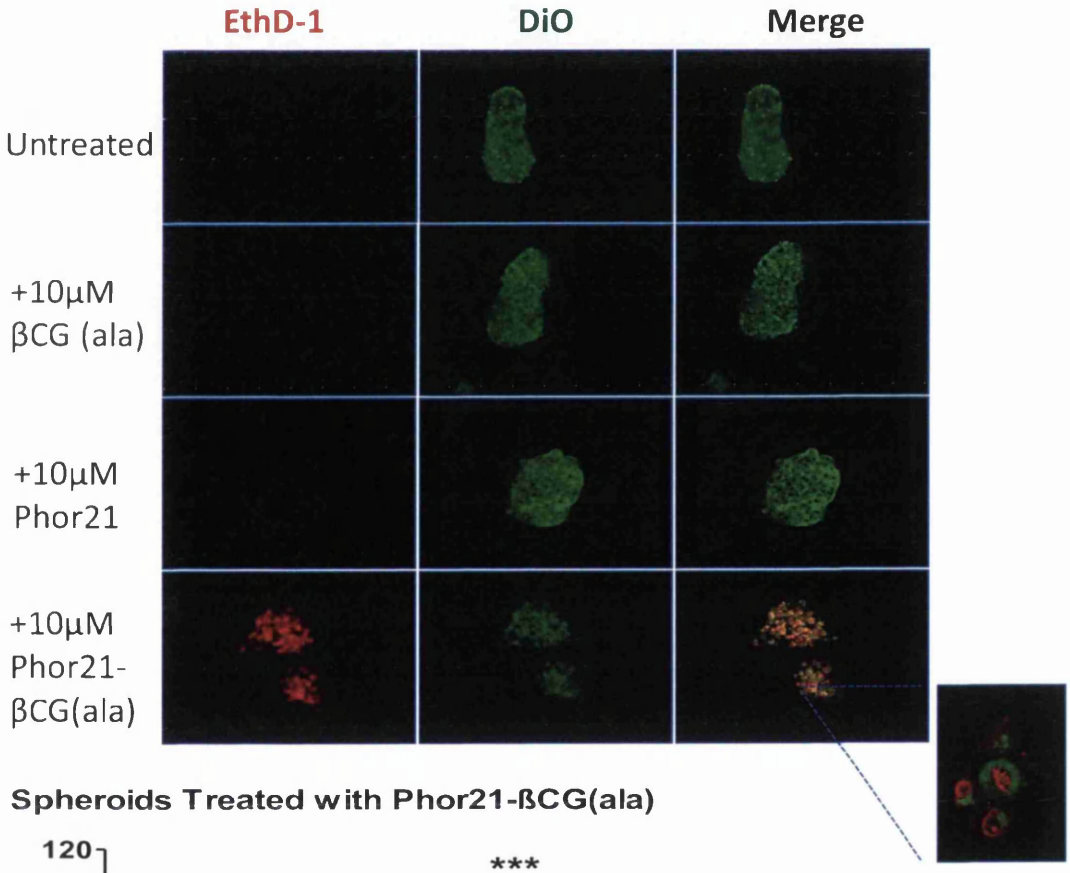

3D Spheroids Treated with Phor21-ßCG(ala)

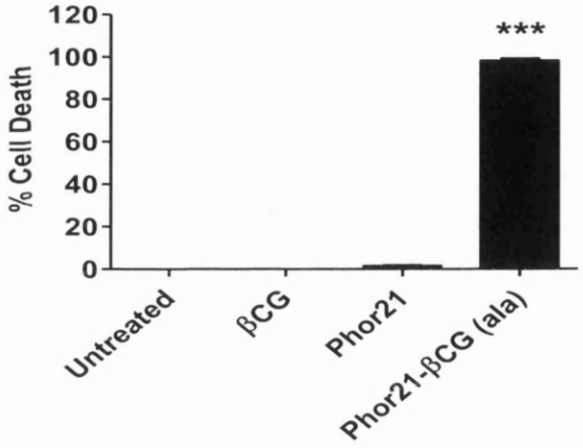

Figure 5.7. Effect of the lytic peptide conjugate on cell viability of MDA-MB 231 spheroids assessed by Live/Dead staining assay. Upper panel, Schematic view of the procedure. **Lower panel,** Spheroids generated in Terasaki plates were transferred into Matrigel, incubated at 37°C/5% CO_2 for 24 hours, treated without or with 10μM βCG(ala), Phor21 or Phor21-βCG(ala) for 3 hours and then subjected spheroids to Live/Dead staining. Data represent means ± SEM (error bars represent SEM) of three independent experiments (***, $P < 0.001$).

5.3.2. *IL-13Rα2*, *LHCGR* and *GnRHR* mRNAs expression in 3D cultured prostate and breast cancer cells

There is strong evidence to indicate that cells grown in a 3D cell model can induce different gene expression patterns as compared to cells grown in 2D culture (Dolznig et al, 2011). 3D spheroid can have similar characteristics to that of the native cancer tissue. The cells become hypoxic in the inner core of the spheroid, which is also known as the necrotic core. This can cause differences in proliferation rates, the differences in the uptake of oxygen and nutrients and also cause the accumulation of waste products (Cottin et al, 2010; Hirschhaeuser et al, 2010). These different physical and chemical properties can modify the cell behaviour and functions and also alter the gene expression profile. The expression of IL-13Rα2, LHCGR and GnRHR mRNAs was analysed in 3D cultured prostate and breast cancer cells to determine whether a 3D environment would have an effect on the receptor expression (Figure 5.8).

The expression of *IL-13Rα2* mRNA in 3D cultured non-cancer cell line (HEK293) and prostate cancer cell lines (androgen dependent [LNCaP] and androgen independent with a high metastatic potential [DU145 and PC3]) by RT-PCR. *IL-13Rα2* mRNA was expressed in prostate cancer cell lines but undetectable in HEK293 cells (Figure 5.8i). *IL-13Rα2* mRNA expression was low but detectable in LNCaP cells and therefore IL-13Rα2 expression in LNCaP cells was used to compare with that in other prostate cancer cell lines to analyse relative expression in subsequent studies. When compared to *IL-13Rα2* mRNA expression in LNCaP cells, DU145 and PC3 cells expressed high levels of *IL-13Rα2* mRNA. LNCaP spheroids demonstrated a down-regulation of *IL-13Rα2* expression (0.043 fold [$P \leq 0.05$])

when compared to LNCaP cells grown in a 2D monolayer. When compared to the expression of *IL-13Rα2* mRNA in DU145 and PC3 spheroids to that in cells grown in 2D monolayers, a significant reduction was observed (4.3 fold [$P \leq 0.05$] and 10.3fold [$P \leq 0.05$] respectively). Together, these results suggest that IL-13Rα2 expression is high in metastatic prostate cancer cell lines but lowered in 3D cultured cells compared to that in 2D cultured cells.

The expression of IL-13Rα2 mRNA was also analysed in 3D cultured non-cancer breast cell line (MCF-10A) and the breast cancer cell lines (androgen dependent [MCF-7] and androgen independent with a high metastatic potential [MDA-MB 231]) by RT-PCR (Figure 5.8i). The expression of *IL-13Rα2* mRNA was low in non-cancer cell line MCF-10A. Therefore expression of IL-13Rα2 in breast cancer cell lines was measured relative to that expressed in MCF-10A. MCF-7 showed no significant change in the expression of *IL-13Rα2* mRNA (2.6 fold [$P > 0.05$]) MDA-MB 231 cells with a high metastatic potential showed a significant increase in the expression of *IL-13Rα2* mRNA (8.7 fold [$P \leq 0.05$]). Like in 3D cultured prostate cancer cells, the expression of *IL-13Rα2* mRNA in MDA-MB 231 cells cultured in 3D spheroids was significantly reduced when compared that in 2D cultured cells .

These results suggest that 3D cultured non-cancer HEK293 and breast epithelial cells and hormone dependent prostate and breast cancer cell lines express no or little IL-13Rα2 whereas prostate and breast cancer cell lines with high metastatic potential express high levels of IL-13Rα2. Furthermore, when compared to its expression in 2D monolayers, the expression of *IL-13Rα2* mRNA shown to be down regulated in 3D cultured prostate and breast cancer cells.

The results show that the non-cancer prostate (PNT-2) and breast (MCF-10A) cell spheroids express very little to no *LHCGR* and *GnRHR* mRNA. The results also show that the expression of *LHCGR* and *GnRHR* mRNA in prostate and breast cancer spheroids is relatively higher but not significantly different from that seen in 2D cultured cells (Figure 5.8ii &iii).

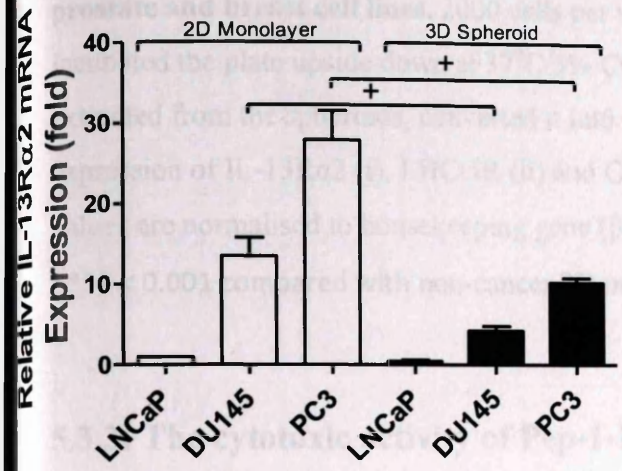
Relative IL-13Rα2 mRNA Expression (fold)
2D Monolayer
3D Spheroid
+
+
40
30
20
10
0
LNCaP
DU145
PC3
LNCaP
DU145
PC3

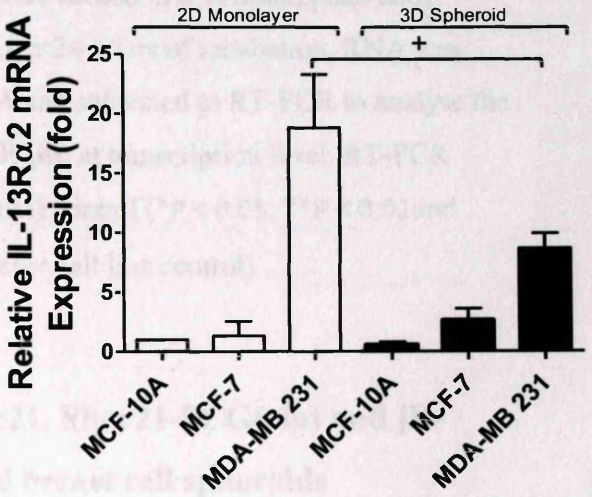
Relative IL-13Rα2 mRNA Expression (fold)
2D Monolayer
3D Spheroid
+
25
20
15
10
5
0
MCF-10A
MCF-7
MDA-MB 231
MCF-10A
MCF-7
MDA-MB 231

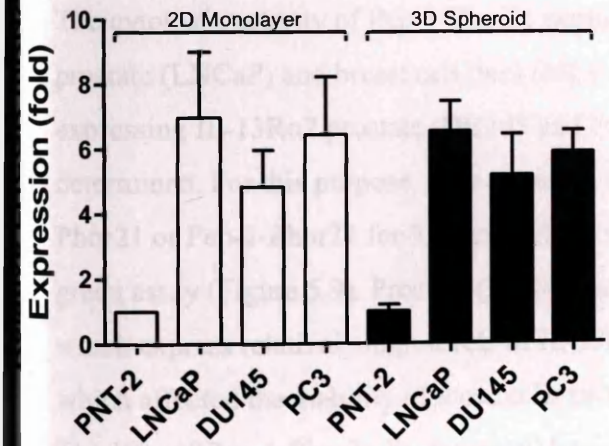
Expression (fold)
2D Monolayer
3D Spheroid
10
8
6
4
2
0
PNT-2
LNCaP
DU145
PC3
PNT-2
LNCaP
DU145
PC3

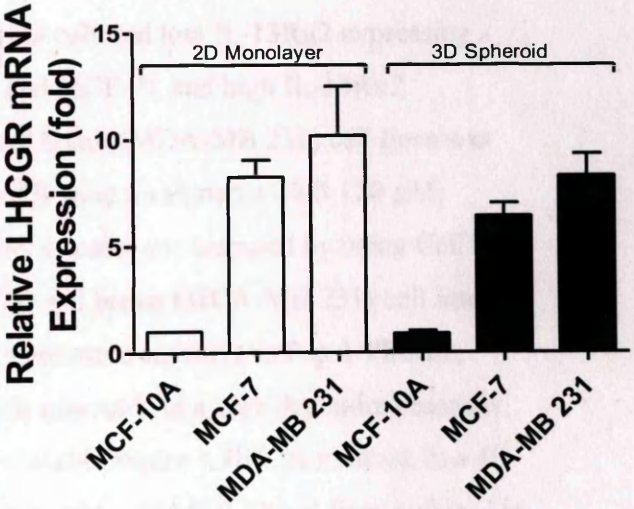
Relative LHCGR mRNA Expression (fold)
2D Monolayer
3D Spheroid
15
10
5
0
MCF-10A
MCF-7
MDA-MB 231
MCF-10A
MCF-7
MDA-MB 231

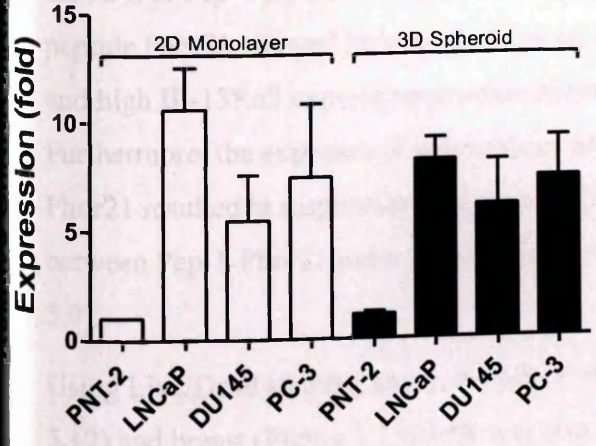
Expression (fold)
2D Monolayer
3D Spheroid
15
10
5
0
PNT-2
LNCaP
DU145
PC-3
PNT-2
LNCaP
DU145
PC-3

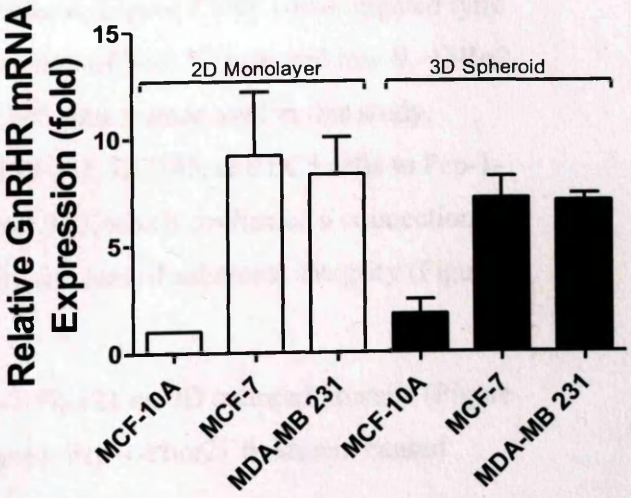
Relative GnRHR mRNA Expression (fold)
2D Monolayer
3D Spheroid
15
10
5
0
MCF-10A
MCF-7
MDA-MB 231
MCF-10A
MCF-7
MDA-MB 231

Figure 5.8. Expression of IL-13Rα2, LHCGR, and GnRHR mRNAs in 3D cultured prostate and breast cell lines. 2000 cells per well were seeded in a Terasaki plate and incubated the plate upside down at 37°C/5% CO_2. After 24 hours of incubation, RNA was extracted from the spheroids, converted it into cDNA and subjected to RT-PCR to analyse the expression of IL-13Rα2 (**i**), LHCGR (**ii**) and GnRHR (**iii**) at transcription level. RT-PCR values are normalised to housekeeping gene (β-tubulin) control (*P < 0.05, **P < 0.01and ***P < 0.001 compared with non-cancer 2D monolayer cell line control).

5.3.3. The cytotoxic activity of Pep-1-Phor21, Phor21-βCG(ala) and [D-Trp^6]GnRH-Phor21 on prostate and breast cell spheroids

Pep-1-Phor21

The cytotoxic activity of Pep-1-Phor21 peptide on 3D cultured low IL-13Rα2 expressing prostate (LNCaP) and breast cell lines (MCF-10A and MCF-7), and high IL-13Rα2 expressing IL-13Rα2 prostate (DU145 and PC3) and breast (MDA-MB 231) cell lines was determined. For this purpose, cells grown in spheroids were incubated with 0-120 μM, Phor21 or Pep-1-Phor21 for 3 hours and the viability of cells was assessed by using CellTox green assay (Figure 5.9). Prostate (DU145, and PC3) and breast (MDA-MB 231) cell lines, which express relatively high levels of IL-13Rα2, were more sensitive to Pep-1-Phor21, which affected the viability of these cells cultured in spheroids in a dose dependent manner. The IC_{50} of Pep-1-Phor21 for these cell lines was <30μM (Figure 4.9B). In contrast, low IL-13Rα2 expressing prostate (LNCaP) and breast (MCF-10A and MCF-7) cell lines cultured in 3D spheroids showed little to no loss in cell viability in the presence of Pep-1-Phor21 and the IC_{50} of Pep-1-Phor21 for these cell lines was >60μM (Figure 5.9B). Unconjugated lytic peptide Phor21 showed little or no effect on the viability of both 3D cultured low IL-13Rα2 and high IL-13Rα2 expressing prostate and breast cell cancer lines used in this study. Furthermore, the exposure of spheroids of MDA-MB 231, DU145, and PC3 cells to Pep-1-Phor21 resulted in dispersion of spheroids (Figure 5.9A), which confirmed a connection between Pep-1-Phor21 induced loss of cell viability and loss of spheroids integrity (Figure 5.9).

Using Live/Dead staining assay, the effect of Pep-1-Phor21 on 3D cultured prostate (Figure 5.12) and breast (Figure 5.13) cells was also analysed. Pep-1-Phor21 treatment caused

significant cell death (stained by EthD-1 [red] whereas both live and dead cells are stained by green dye [DiO]) in spheroids of prostate and breast cancer cells with relatively high IL-13Rα2 expression. This correlated with the results gained with the CellTox assay (Figure 5.9).

These results suggest that 3D cultured prostate and breast cancer cells with high levels of IL-13Rα2 are more sensitive to Pep-1-Phor21, indicating a direct connection between the sensitivity of cells in spheroids to Pep-1-Phor21 and the levels of IL-13Rα2 they express.

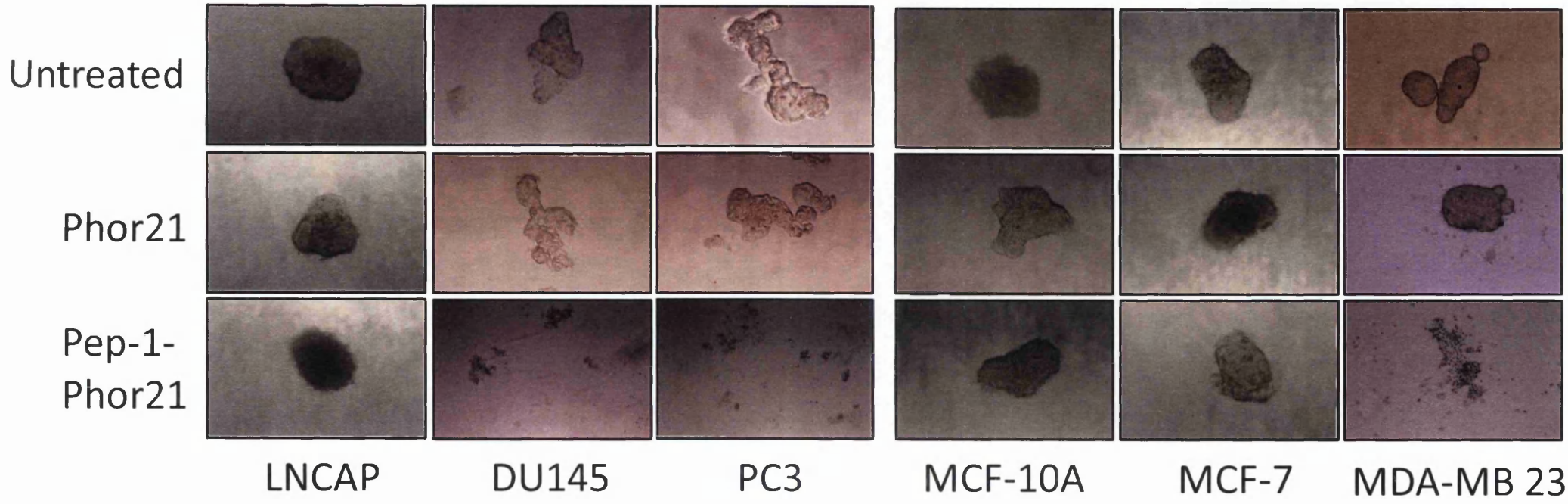
Untreated
Phor21
Pep-1-
Phor21
LNCAP
DU145
PC3
MCF-10A
MCF-7
MDA-MB 231

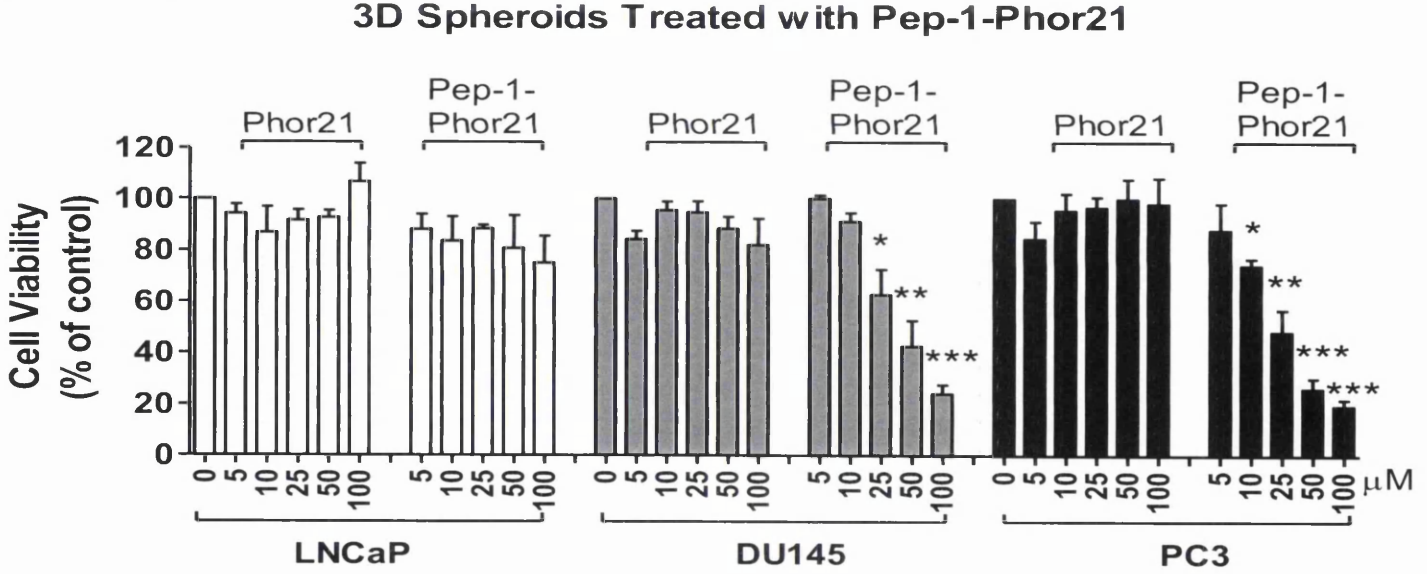
3D Spheroids Treated with Pep-1-Phor21
Cell Viability (% of control)
Phor21
Pep-1-Phor21
0 5 10 25 50 100 μM
LNCaP
DU145
PC3

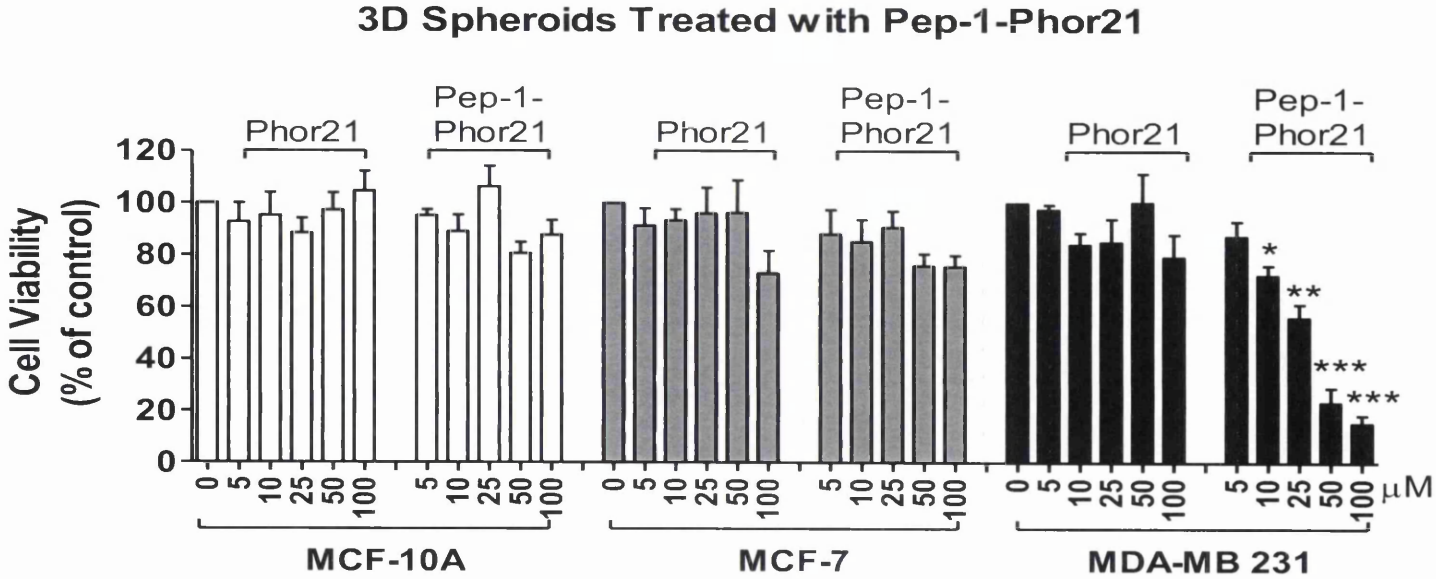
3D Spheroids Treated with Pep-1-Phor21
Cell Viability (% of control)
Phor21
Pep-1-Phor21
0 5 10 25 50 100 μM
MCF-10A
MCF-7
MDA-MB 231

Figure 5.9. Effect of Pep-1-Phor21 on cell viability of 3D cultured prostate and breast cancer cells. Dose-dependent effect of Pep-1-Phor21 and Phor21 on the viability of 3D cultured non-IL-13Rα2 expressing cell lines (LNCaP, MCF-10A, and MCF-7) and IL-13Rα2 expressing cell lines (DU145, PC3 and MDA-MB 231). The spheroids grown in hanging drops were transferred into U-bottom surface repellent plates, incubated at 37°C/5% CO_2 for 24 hours and then treated spheroids with 0-120 μM of Pep-1-Phor21 and Phor21 peptides for 3 hours and then the viability of cells in spheroids was assessed by CellTox assay. The data represent means ± SEM (error bars represent SEM) of three independent experiments (***, $P < 0.001$).

Phor21-βCG(ala)

We also assessed the cytotoxic effect of Phor21-βCG(ala) peptide on non-cancer prostate (PNT-2) and breast (MCF-10A), and cancer prostate (LNCaP, DU145 and PC3) and breast (MCF-7 and MDA-MB 231) cell lines (Figure 5.10B). For this purpose, cells grown as spheroids (3D culture) were incubated with 0-125 μM of Phor21 or Phor21-βCG(ala) for 3hours and the viability of cells was assessed by using CellTox green assay. Prostate (LNCaP, DU145 and PC3) and breast (MCF-7 and MDA-MB 231) cancer cell lines with high LHCGR expression were more sensitive to Phor21-βCG(ala), which affected viability of these cells grown as spheroids in a dose dependent manner (Figure 4.6A). The IC_{50} of Phor21-βCG(ala) for these cell lines was <12μM (Figure 5.10B). In contrast, non-cancer prostate (PNT-2) and breast (MCF-10A) cell lines with low LHCGR expression showed little to no loss in cell viability when incubated with Phor21-βCG(ala) and theIC_{50} of Phor21-βCG(ala) for these cell lines was >50μM (Figure 5.10B). The ligand βCG(ala) and lytic Phor21 showed little or no effect on viability of these cell lines. Microscopic observations confirmed reduction in the integrity of the spheroids treated with Phor21-βCG(ala) (Figure 5.10A).

The effect of Phor21-βCG(ala) on 3D cultured prostate (Figure 5.12) and breast cell lines (Figure 5.13) was also analysed by Live/Dead staining assay Phor21-βCG(ala) had little effect on cell viability of 3D cultured PNT-2 and MCF-10A, with low LHCGR expression, . However, prostate and breast cancer cell spheroids, which has high LHCGR expression, showed significant cell death when treated with Phor21-βCG(ala). These results are in agreement with the CellTox assay results. Prostate and breast cell spheroids with high LHCGR expression are more sensitive to Phor21-βCG(ala) .

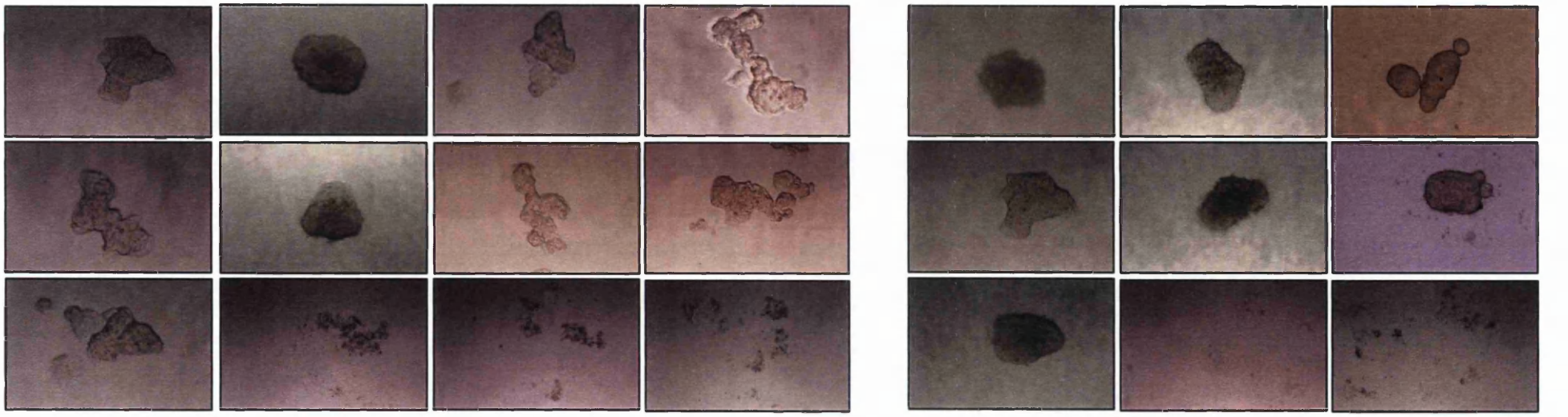
PNT-2
LNCAP
DU145
PC3
MCF-10A
MCF-7
MDA-MB 231

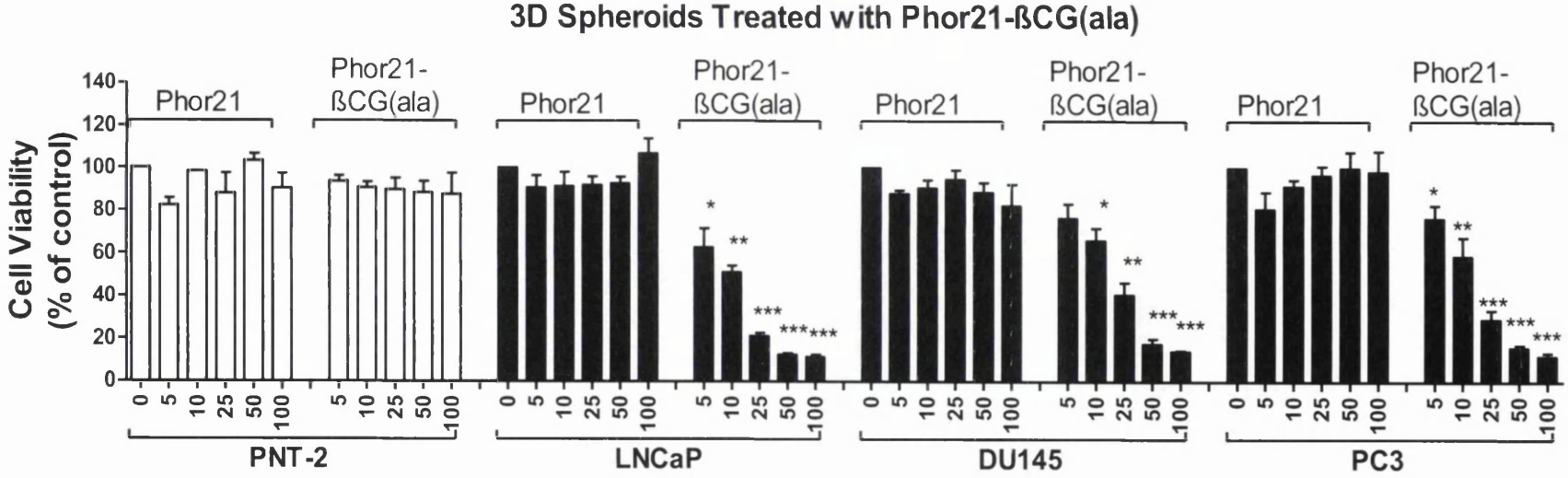
3D Spheroids Treated with Phor21-ßCG(ala)
Cell Viability (% of control)
Phor21
Phor21-ßCG(ala)
PNT-2
LNCaP
DU145
PC3

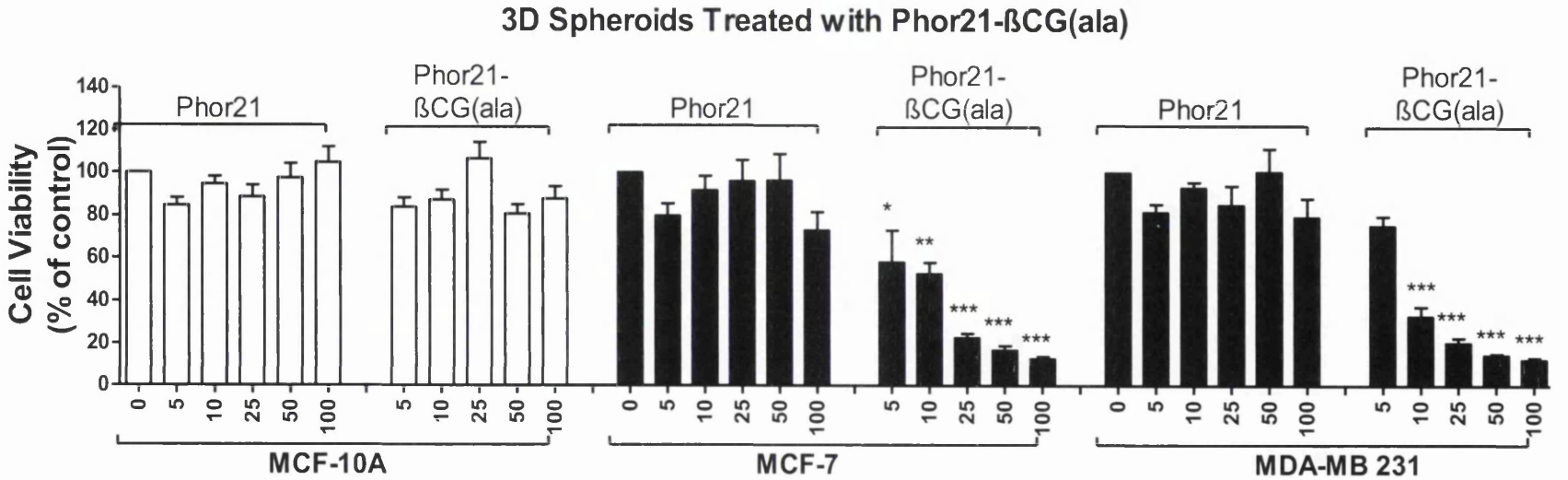
3D Spheroids Treated with Phor21-ßCG(ala)
Cell Viability (% of control)
Phor21
Phor21-ßCG(ala)
MCF-10A
MCF-7
MDA-MB 231

Figure 5.10. Effect of Phor21-βCG(ala) on cell viability of 3D cultured prostate and breast cancer cells. Dose-dependent effect of Phor21-βCG(ala) and Phor21 on the viability of 3D cultured non-LHCGR expressing cell lines (PNT-2 and, MCF-10A) and LHCGR expressing cell lines (DU145, PC3, MCF-7 and MDA-MB 231). The spheroids grown in hanging drops were transferred into U-bottom surface repellent plates, incubated at 37°C/5% CO_2 for 24 hours and then treated spheroids with 0-120 μM of Phor21-βCG(ala) and Phor21 peptides for 3 hours and then the viability of cells in spheroids was assessed by CellTox assay. The data represent means ± SEM (error bars represent SEM) of three independent experiments (***, $P < 0.001$).

[D-Trp^6]GnRH-Phor21

The cytotoxic activity of [D-Trp^6]GnRH-Phor21 peptide on low GnRHR expressing (PNT-2, and MCF-10A), and high GnRHR expressing (LNCaP, DU145, PC3, MCF-7 and MDA-MB 231) prostate and breast cell lines was determined (Figure 5.11). Cells grown in 3D spheroids were incubated with 0-125 μM, Phor21 or D-Trp^6]GnRH-Phor21 for 3 hours and the viability of cells was assessed by using CellTox green assay (Figure 5.11B). Prostate (LNCaP, DU145 and PC3) and breast (MCF-7 and MDA-MB 231) cancer cells grown as spheroids were more sensitive to [D-Trp^6]GnRH-Phor21, which showed a dose dependent effect on these cell lines. The IC_{50} of [D-Trp^6]GnRH-Phor21 for cells expressing relatively high levels of GnRHR was <12μM. In contrast, non-cancer prostate (PNT-2) and breast (MCF-10A) cell spheroids with low GnRHR expression showed little or no loss in cell viability in the presence of [D-Trp^6]GnRH-Phor21 and the IC_{50} of [D-Trp^6]GnRH-Phor21 for these cell lines was >50μM (Figure 5.11A). The lytic peptide Phor21 showed little or no effect on viability of these cell lines. Microscopic observations confirmed connection between loss of cell viability and integrity of the spheroids treated with [D-Trp^6]GnRH-Phor21. Breast (MCF-7 and MDA-MB 231) and prostate (LNCaP, DU145 and PC3) cell spheroids seemed dispersed once treated with [D-Trp^6]GnRH-Phor21 (Figure 5.11A).

The response of 3D cultured prostate (Figure 5.12) and breast (Figure 5.13) cells to [D-Trp^6]GnRH-Phor21 was also analysed by using Live/Dead assay. [D-Trp^6]GnRH-Phor21 showed little effect of cell viability of PNT-2 and MCF-10A cell spheroids. However, prostate and breast cells (MDA-MB 231), cells with high GnRHR expression exhibited high cell death when treated with [D-Trp^6]GnRH-Phor21.These results correlated with that of CellTox assay.

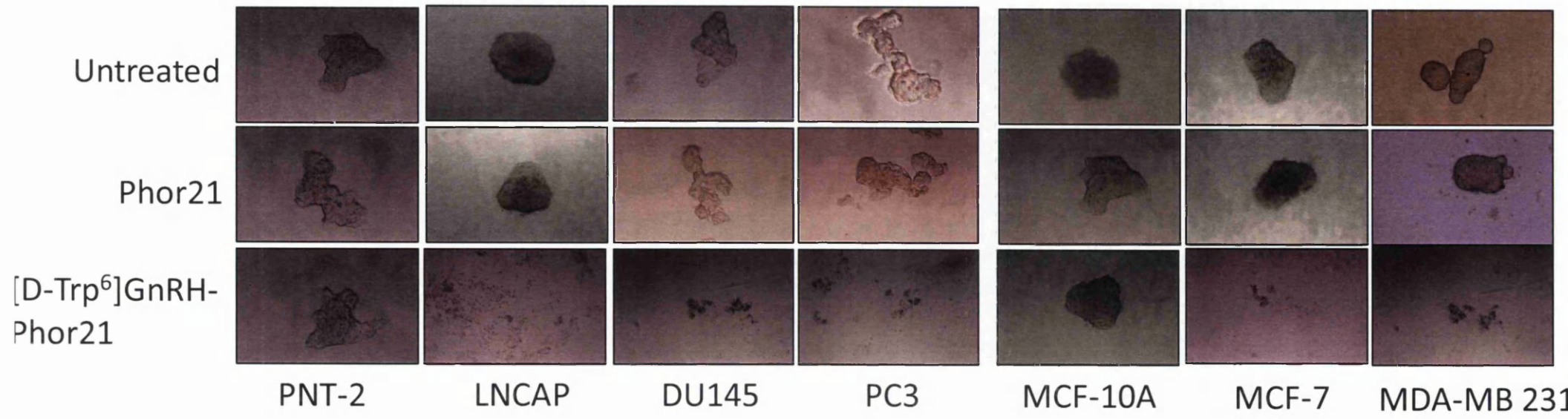
Untreated
Phor21
[D-Trp6]GnRH-Phor21
PNT-2
LNCAP
DU145
PC3
MCF-10A
MCF-7
MDA-MB 231

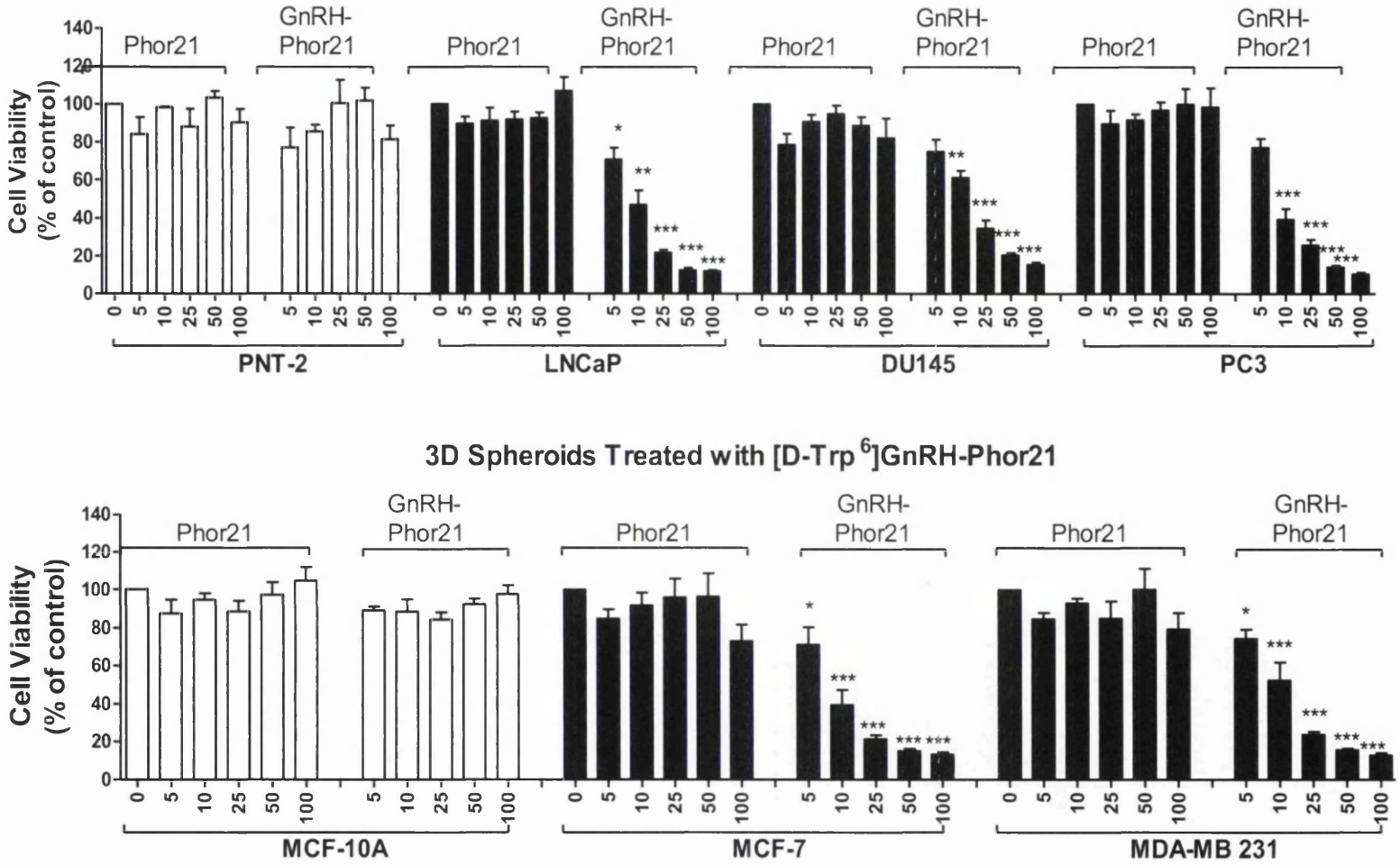
3D Spheroids Treated with [D-Trp 6]GnRH-Phor21
Cell Viability (% of control)
Phor21
GnRH-Phor21
PNT-2
LNCaP
DU145
PC3
3D Spheroids Treated with [D-Trp 6]GnRH-Phor21
Cell Viability (% of control)
Phor21
GnRH-Phor21
MCF-10A
MCF-7
MDA-MB 231

Figure 5.11. Effect of [D-Trp^6]GnRH-Phor21 on cell viability of 3D cultured prostate and breast cancer cells. Dose-dependent effect of [D-Trp^6]GnRH-Phor21 and Phor21 on the viability of 3D cultured non-GnRHR expressing cell lines (PNT-2 and, MCF-10A) and GnRHR expressing cell lines (DU145, PC3, MCF-7 and MDA-MB 231). The spheroids grown in hanging drops were transferred into U-bottom surface repellent plates, incubated at 37°C/5% CO_2 for 24 hours and then treated spheroids with 0-120 μM of [D-Trp^6]GnRH-Phor21 and Phor21 peptides for 3 hours and then the viability of cells in spheroids was assessed by CellTox assay. The data represent means ± SEM (error bars represent SEM) of three independent experiments (***, $P < 0.001$).

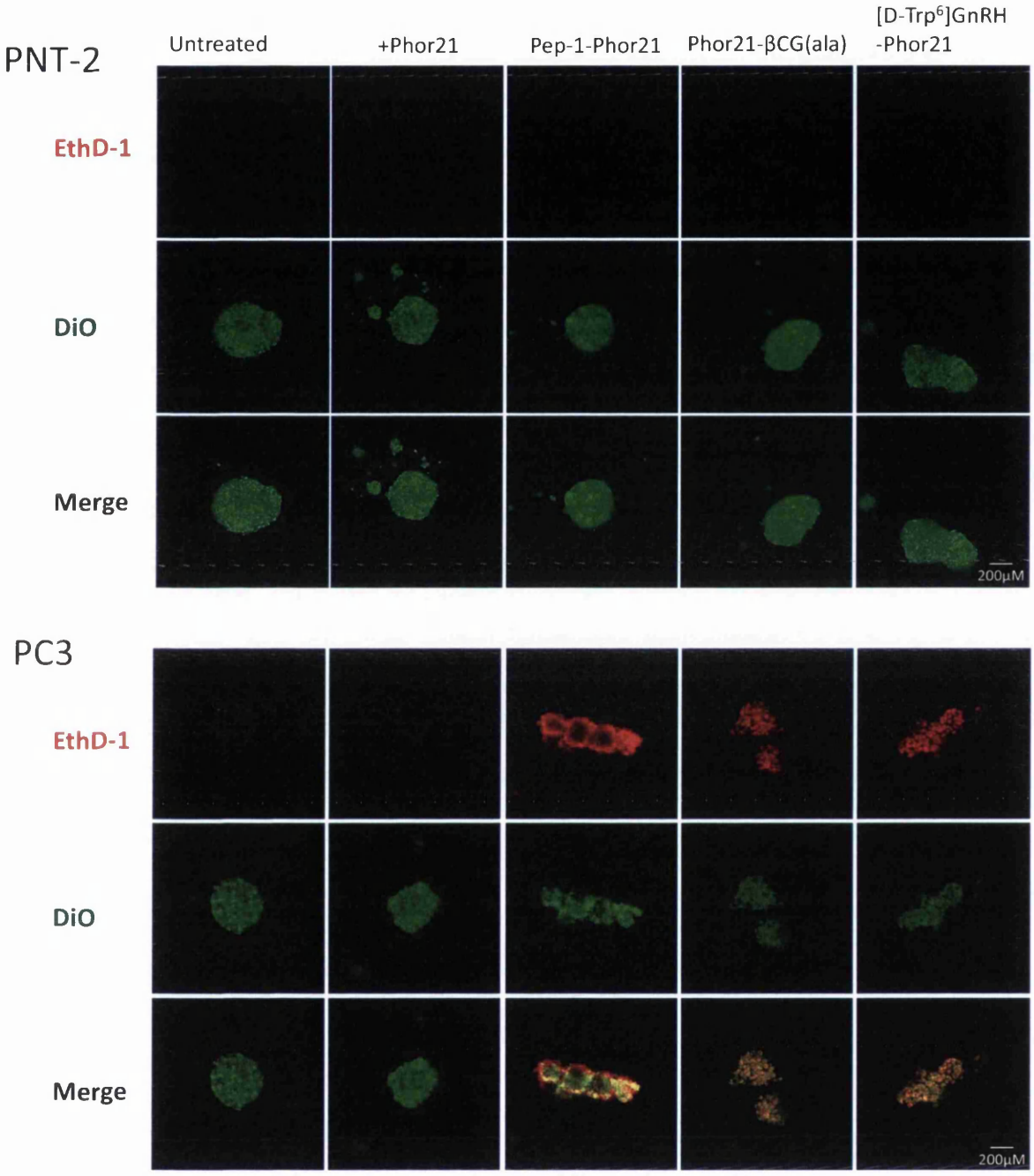

Figure 5.12 Effect of the lytic peptide conjugates on 3D cultured prostate cancer cells assessed by Live/Dead staining. The spheroids of prostate non-cancer (PNT-2) and cancer cells (PC3) grown in hanging drops were transferred into Matrigel, incubated at 37°C/5% CO_2 for 24 hours, treated without or with the lytic peptides (Phor21 120μM, 50 μM Pep-1-Phor21, 25 μM Phor21-βCG(ala) and 25 μM[D-Trp^6]GnRH-Phor21) for 3 hours and then the viability of cells was assessed using Live/Dead staining (DIO stains both live and dead cells where EthD-1 stains only dead cells). DOI staining is shown in green, EthD-1 in red and overlay of DOI and EthD-1 staining in yellow.

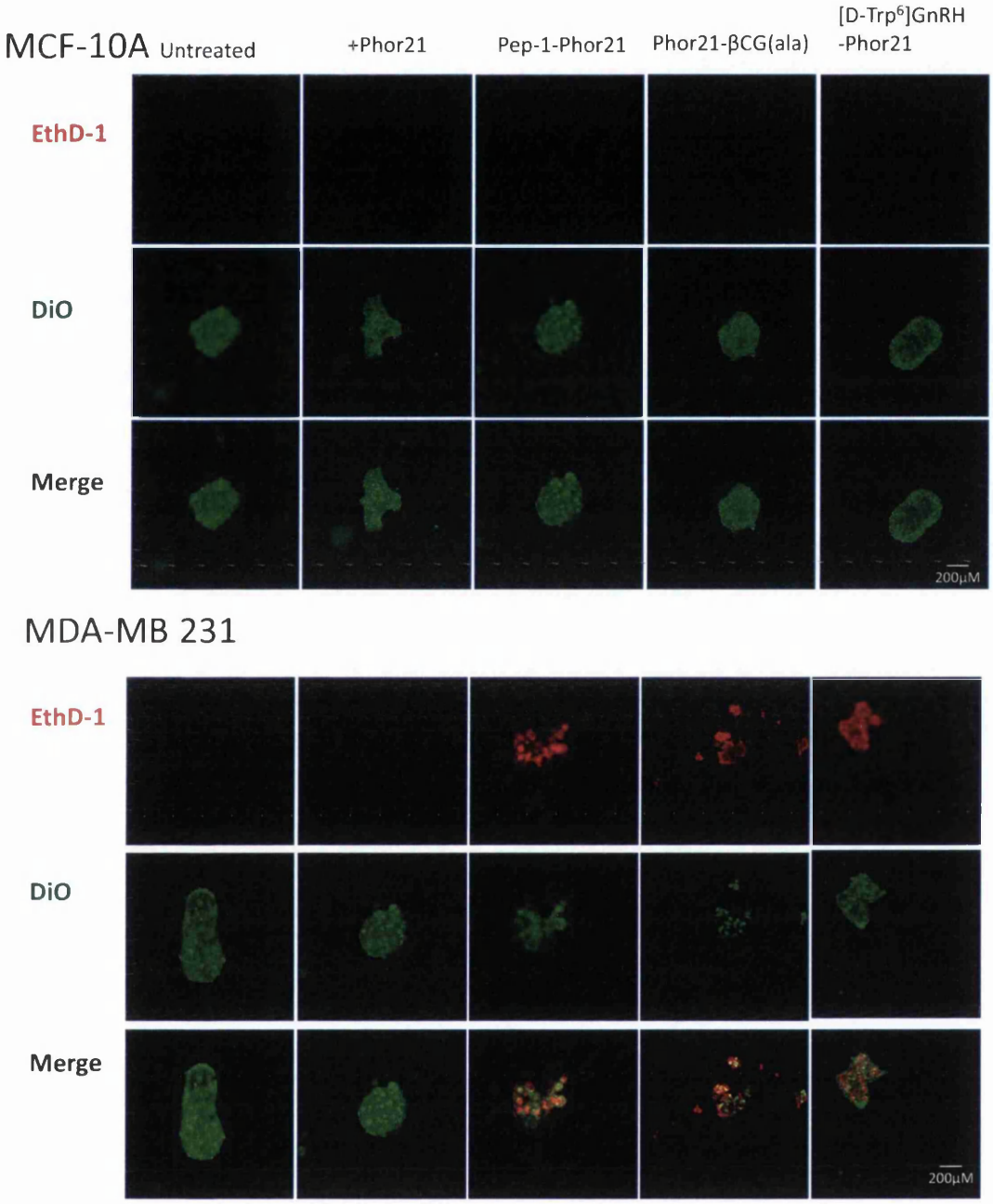

Figure 5.13 Effect of the lytic peptide conjugates on 3D cultured breast cancer cells assessed by Live/Dead staining. The spheroids of breast non-cancer (MCF-10A) and cancer cells (MDA-MB 231) grown in hanging drops were transferred into Matrigel, incubated at 37°C/5% CO_2 for 24 hours, treated without or with the lytic (Phor21 120μM, 50 μM Pep-1-Phor21, 25 μM Phor21-βCG(ala) and 25 μM[D-Trp^6]GnRH-Phor21) for 3 hours and then the viability of cells was assessed using Live/Dead staining (DIO stains both live and dead cells where EthD-1 stains only dead cells). DOI staining is shown in green, EthD-1 in red and overlay of DOI and EthD-1 staining in yellow.

IL-13Rα2, LHCGR and GnRHR mRNA expression in 3D cultured prostate and breast cell lines treated with TSA and 5-aza-dC

IL-13Rα2

Since Trichostatin A (TSA) or 5-aza-2'-deoxycytidine (5-aza-dC) treatment shown to alter IL-13Rα2 expression in prostate and breast cancer cells grown in vitro in 2D culture (section 4.3.5) we investigated whether they also alter the expression of IL-13Rα2 in prostate and breast cell spheroids. For this, the expression of IL-13Rα2 mRNA in prostate and breast cell spheroids treated with 0-10μM TSA or 5-aza-dC for 24 hours was assessed for by RT-PCR (Figure 5.14). LNCaP cancer cell spheroids, which normally have low levels of IL-13Rα2, showed increased expression levels of IL-13Rα2 mRNA; which was significate with 10μM of either TSA or 5-aza-dC treatment. However the increase was not as much as seen in TSA or 5-aza-dC treated cells grown in 2D culture. Increase in the expression of IL-13Rα2 was also detected in the more aggressive cancer cell lines (DU145 and PC3) when grown as spheroids and treated with TSA or 5-aza-dC.

With regards to breast cancer, the results demonstrated that MCF-10A (the non-cancer cell line) cell spheroids with relatively low levels of IL-13Rα2 showed no significant changes in IL-13Rα2 expression even with TSA or 5-aza-dC treatment. Like LNCaP cell line, MCF-7 cells have very little IL-13Rα2 expression. However, the expression of *IL-13Rα2* at mRNA level in MCF-7 cell spheroids increased significantly with 10μM of TSA or 5-aza-dC treatment (67.20 fold [P of $\leq$0.001] and 27.62 fold [P of $\leq$0.001] respectively) (Figure 5.14.). MDA-MB 231 cells also displayed increased *IL-13Rα2* gene expression but only when treated with 5-aza-dC at 10μM. Treatment with TSA showed no significant effect on *IL-13Rα2* mRNA in MDA-MB 231 cell spheroids. However, treatment of MDA-MB 231 cells in 2D culture with just 0.1μM of TSA or 5-aza-dC significantly increased *IL-13Rα2* mRNA expression. This highlights the existence of differences in the gene expression between 2D and 3D cultured cells.

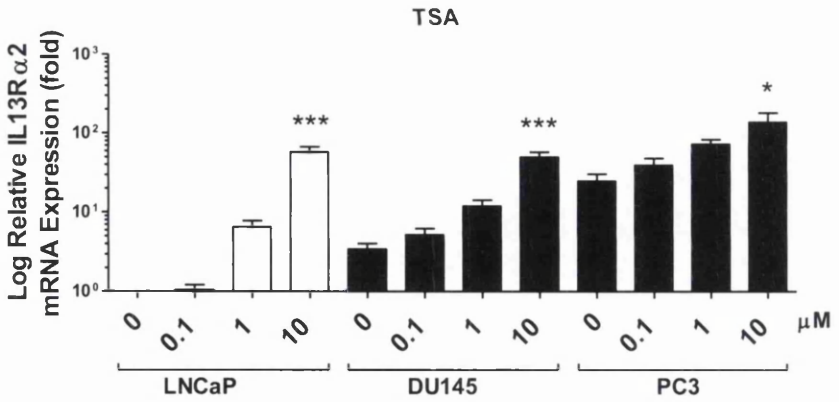
TSA
Log Relative IL13Rα2 mRNA Expression (fold)
10^3
10^2
10^1
10^0
***
***
*
0 0.1 1 10 0 0.1 1 10 0 0.1 1 10 µM
LNCaP
DU145
PC3

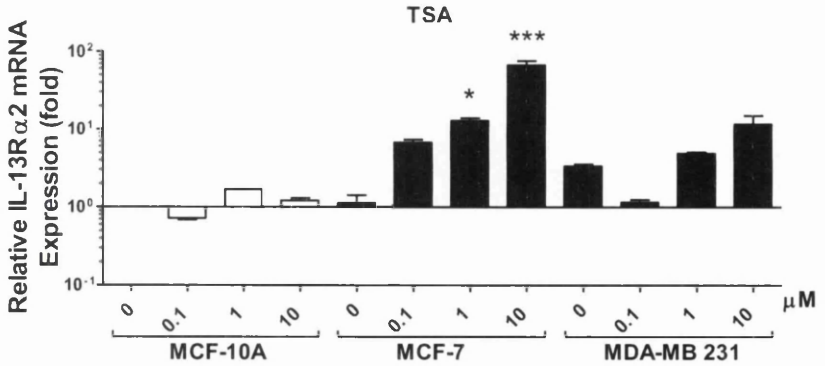
TSA
Relative IL-13Rα2 mRNA Expression (fold)
10^2
10^1
10^0
10^{-1}
*
***
0 0.1 1 10 0 0.1 1 10 0 0.1 1 10 µM
MCF-10A
MCF-7
MDA-MB 231

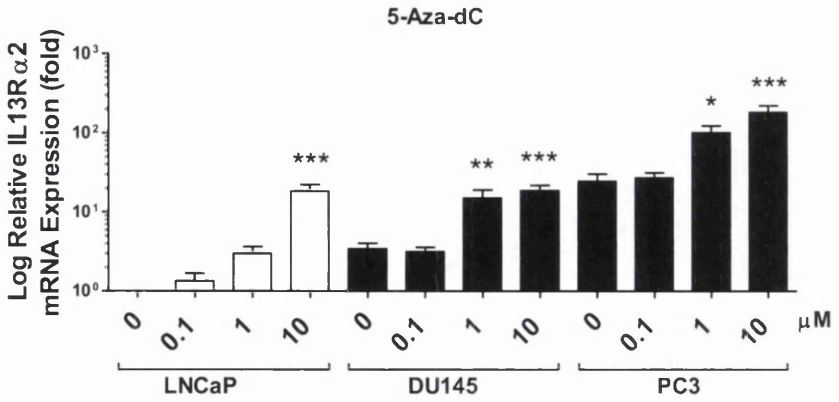
5-Aza-dC
Log Relative IL13Rα2 mRNA Expression (fold)
10^3
10^2
10^1
10^0
***
**
***
*
***
0 0.1 1 10 0 0.1 1 10 0 0.1 1 10 µM
LNCaP
DU145
PC3

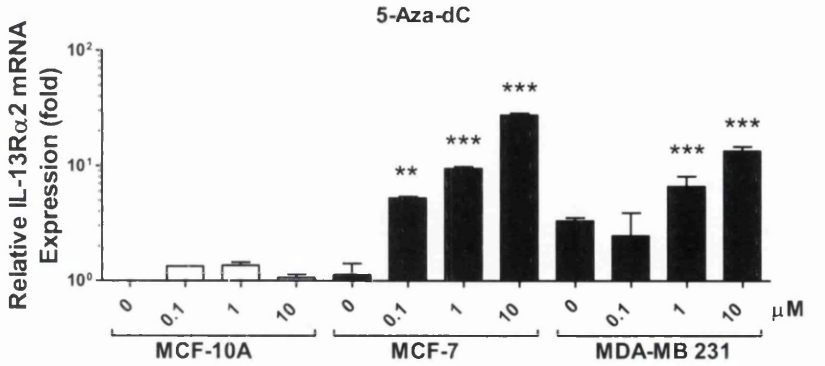
5-Aza-dC
Relative IL-13Rα2 mRNA Expression (fold)
10^2
10^1
10^0
**
***
***
***
***
0 0.1 1 10 0 0.1 1 10 0 0.1 1 10 µM
MCF-10A
MCF-7
MDA-MB 231

Figure 5.14. Analysis of IL-13Rα2 mRNA expression in 3D prostate and breast cell lines treated with TSA and 5-aza-dC by qRT-PCR. RT-PCR analysis of IL-13Rα2 mRNA expression in various prostate and breast cell lines treated with 0.1, 1, and 10μM of TSA and 5-aza-dC for 24 hours. The data are mean ± SEM (error bars represent SEM) values of three independent experiments. All RT-PCR values are normalized to housekeeping controls (*P < 0.05, **P < 0.01and ***P < 0.001 compared with non-cancer cell line control).

LHCGR

Trichostatin A (TSA) or 5-aza-2'-deoxycytidine (5-aza-dC) treatment was than tested to show if there is any alterations in LHCGR expression in prostate and breast cell spheroids. .For this, the expression of LHCGR mRNA in prostate and breast cell spheroids treated with 0-10μM TSA or 5-aza-dC for 24 hours was assessed for by RT-PCR (Figure 5.14). PNT-2, a non-cancer cell line with low levels of LHCGR expression, cells showed no significant difference in LHCGR expression between any treatment and treatment with TSA or 5-aza-dC (Figure 5.15). In a 2D monolayer there was no significant change in normal and cancer cells (SECTION). In both cases TSA and 5-aza-dC increased in LHCGR in mRNA expression in prostate and breast cancer cell lines. Prostate cancer cells LNCaP spheroid cells increased LHCGR expression once treated with 10μM of either TSA or 5-aza-dC. When compared to normal cell line PNT-2, the fold change in LNCaP increase from normal state 6.97 fold changes to 19.56 and 19.09 with 10μM TSA or 5-aza-dC respectively ($P \leq 0.001$). DU145 and PC3 cell lines also increased expression once treated with 10μM of either TSA or 5-aza-dC.

With regards to breast cancer, the results demonstrated that MCF-10A (the non-cancer cell line) cell spheroids with relatively low levels of IL-13Rα2 showed no significant changes in IL-13Rα2 expression even with TSA or 5-aza-dC treatment. LHCGR expression increased significantly in breast cancer cell lines MCF-7 with 10μM of either TSA or 5-aza-dC. Compared to MCF-10A cell lines LHCGR expression in MCF-7 increased from 8.25 fold to 19.37 fold ($P \leq 0.001$) and 20.38 fold ($P \leq 0.001$) once treated with TSA and 5-aza-dC respectively. MDA-MB 231 cells also displayed increased gene expression, but only when treated with 10μM of either TSA or 5-aza-dC (Figure 5.15).

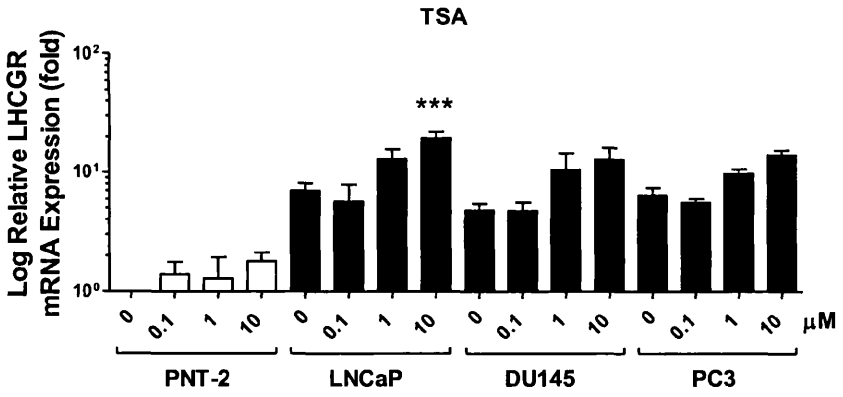
TSA
Log Relative LHCGR mRNA Expression (fold)
10^2
10^1
10^0
***
0 0.1 1 10 0 0.1 1 10 0 0.1 1 10 0 0.1 1 10 µM
PNT-2
LNCaP
DU145
PC3

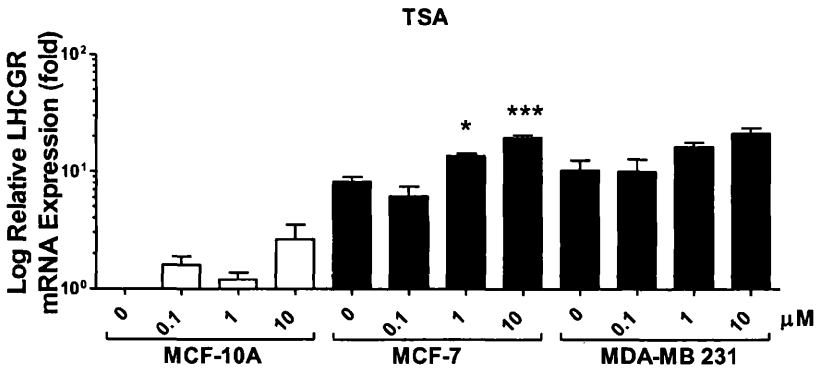
TSA
Log Relative LHCGR mRNA Expression (fold)
10^2
10^1
10^0
*
***
0 0.1 1 10 0 0.1 1 10 0 0.1 1 10 µM
MCF-10A
MCF-7
MDA-MB 231

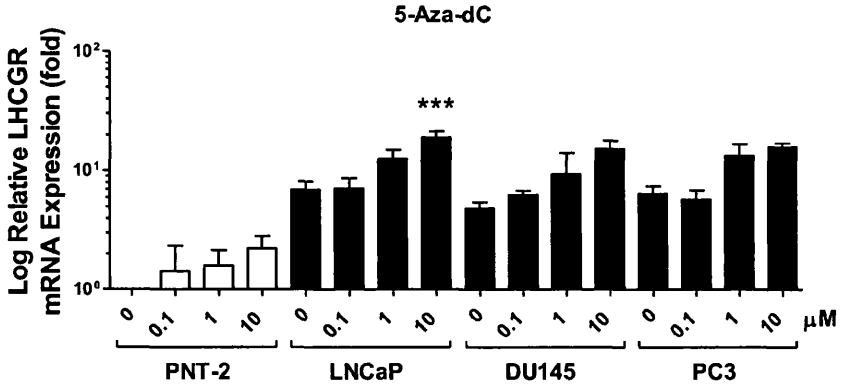
5-Aza-dC
Log Relative LHCGR mRNA Expression (fold)
10^2
10^1
10^0
***
0 0.1 1 10 0 0.1 1 10 0 0.1 1 10 0 0.1 1 10 µM
PNT-2
LNCaP
DU145
PC3

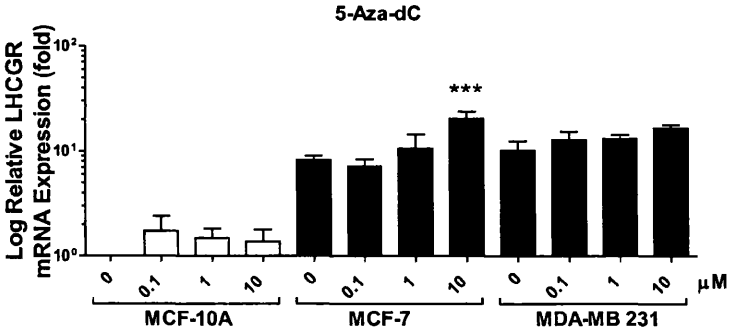
5-Aza-dC
Log Relative LHCGR mRNA Expression (fold)
10^2
10^1
10^0
***
0 0.1 1 10 0 0.1 1 10 0 0.1 1 10 µM
MCF-10A
MCF-7
MDA-MB 231

Figure 5.15. Analysis of LHCGR mRNA expression in 3D prostate and breast cell lines treated with TSA and 5-aza-dC by qRT-PCR. RT-PCR analysis of LHCGR mRNA expression in various prostate and breast cell lines treated with 0.1, 1, and 10μM of TSA and 5-aza-dC for 24 hours. The data are mean ± SEM (error bars represent SEM) values of three independent experiments. All RT-PCR values are normalized to housekeeping controls (*P < 0.05, **P < 0.01and ***P < 0.001 compared with non-cancer cell line control).

GnRHR

Finally the epigenetic regulation of GnRHR expression following TSA or 5-aza-dC treatment in prostate and breast cell lines was assessed (Figure 5.16). PNT-2, a non-cancer cell line, showed no significant difference in GnRHR mRNA expression (Figure 5.16) between any treatment and treatment with TSA or 5-aza-dC. LNCaP, DU145 and PC3 spheroids also showed no significant difference.

With regard to breast cancer, results demonstrated that MCF-10A, the normal cell lines showed no significant changes in GnRHR expression, even with TSA and 5-aza-dC treatment. Like the prostate cancer cells, MCF-7 and MDA-MB 231 show no significant increase in GnRHR expression (Figure 5.16).

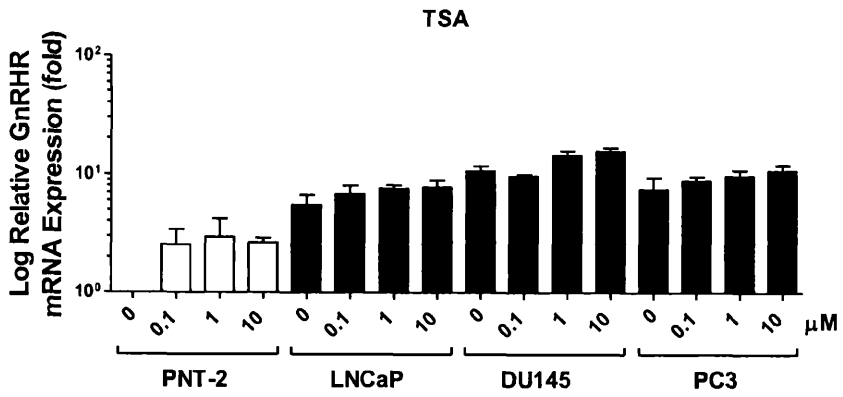
TSA
Log Relative GnRHR mRNA Expression (fold)
10^2
10^1
10^0
0 0.1 1 10 0 0.1 1 10 0 0.1 1 10 0 0.1 1 10 µM
PNT-2
LNCaP
DU145
PC3

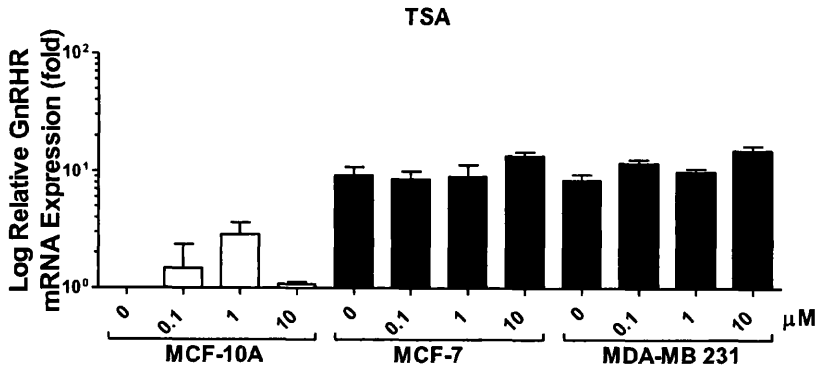
TSA
Log Relative GnRHR mRNA Expression (fold)
10^2
10^1
10^0
0 0.1 1 10 0 0.1 1 10 0 0.1 1 10 µM
MCF-10A
MCF-7
MDA-MB 231

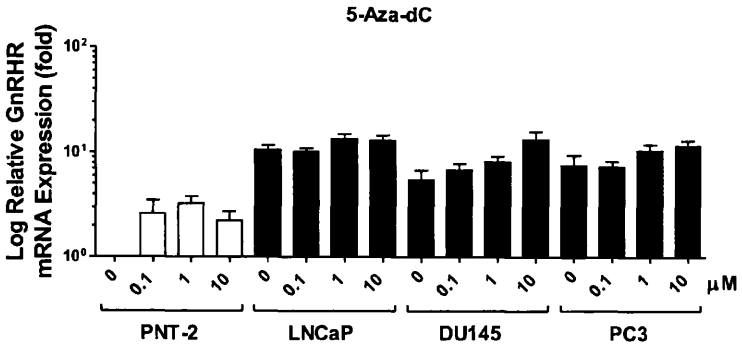
5-Aza-dC
Log Relative GnRHR mRNA Expression (fold)
10^2
10^1
10^0
0 0.1 1 10 0 0.1 1 10 0 0.1 1 10 0 0.1 1 10 µM
PNT-2
LNCaP
DU145
PC3

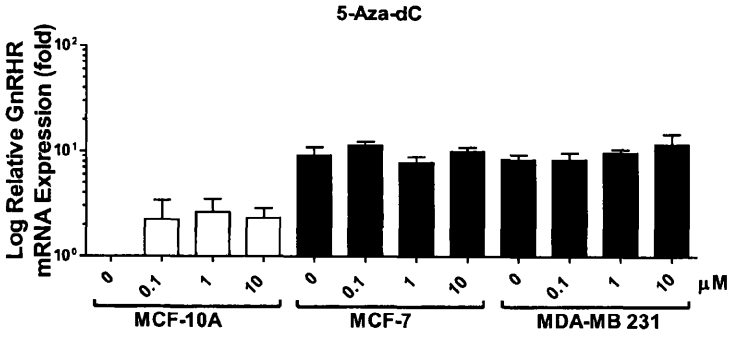
5-Aza-dC
Log Relative GnRHR mRNA Expression (fold)
10^2
10^1
10^0
0 0.1 1 10 0 0.1 1 10 0 0.1 1 10 µM
MCF-10A
MCF-7
MDA-MB 231

Figure 5.16. Analysis of GnRHR mRNA expression in 3D prostate and breast cell lines treated with TSA and 5-aza-dC by RT-PCR. RT-PCR analysis of GnRHR mRNA expression in various prostate and breast cell lines treated with 0.1, 1, and 10μM of TSA and 5-aza-dC for 24 hours. The data are mean ± SEM (error bars represent SEM) values of three independent experiments. All RT-PCR values are normalized to housekeeping controls (*P < 0.05, **P < 0.01and ***P < 0.001 compared with non-cancer cell line control).

5.3.4. The cytotoxic activity of Pep-1-Phor21, Phor21-βCG(ala) and [D-Trp^6]GnRH-Phor21 on prostate and breast cell spheroids treated with TSA and 5-aza-dC

Pep-1-Phor21

As TSA and 5-aza-dC treatments increase IL-13Rα2 expression in prostate and breast cancer cells grown in 3D culture, the effect of TSA or 5-aza-dC treatment on sensitivity of prostate and breast cancer cells to Pep-1-Phor21 was determined. The cytotoxicity of Pep-1-Phor21 on no or low-IL-13Rα2 expressing cell lines (HEK 293, LNCaP, MCF-10A, and MCF-7) and high IL-13Rα2 expressing cell lines (DU145, PC3 and MDA-MB 231) treated with TSA and 5-aza-dC was assessed *in vitro* using CellTox assay (Figure 5.17). Cell spheroids were treated with 0.1, 1, and 10μM of TSA or 5-aza-dC for 24 hours prior to 3 hours incubation with Pep-1-Phor21. The concentration of peptide used for each cell line (120μM for HEK293 cells, 30μM for LNCaP, 18μM for DU145,10μM for PC3, 120μM for MCF-10A, 30μM for MCF-7 and 18μM for MDA-MB 231) was based on its IC_{50} in the CellTox assay (Figure 5.14). The treatment with TSA or 5-aza-dC did not increase the sensitivity of non-cancer cell lines (HEK293 and MCF-10A) to Pep-1-Phor21. However TSA or 5-aza-dC treatment significantly increased low IL-13Rα2 expressing cancer cell lines (LNCaP and MCF-7) sensitivity to Pep-1-Phor21. DU145, PC3 and MDA-MB 231 cell lines, which express high levels of IL13Rα2, grown as spheroids also showed increased Pep-1-Phor21sensitivity when treated with TSA or 5-aza-dC. The results demonstrated that TSA and 5-aza-dC increase prostate and breast cancer cell spheroids sensitivity to Pep-1-Phor21.

HEK293 Spheroid Treated with Pep-1-Phor21

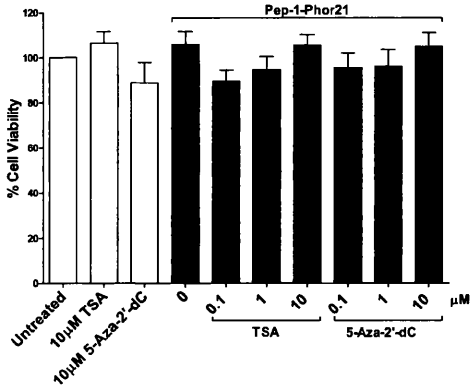

MCF-10A Spheroids Treated with Pep-1-Phor21

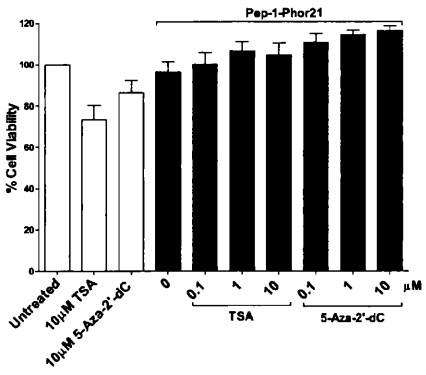

LNCaP Spheroid Treated with Pep-1-Phor21

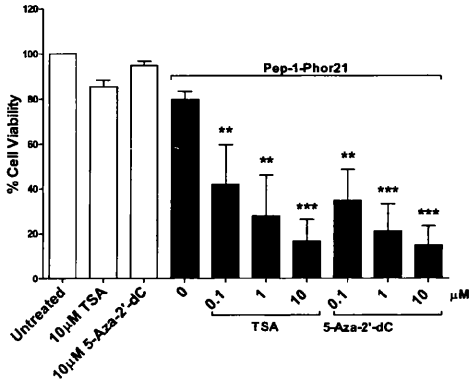

MCF-7 Spheroids Treated with Pep-1-Phor21

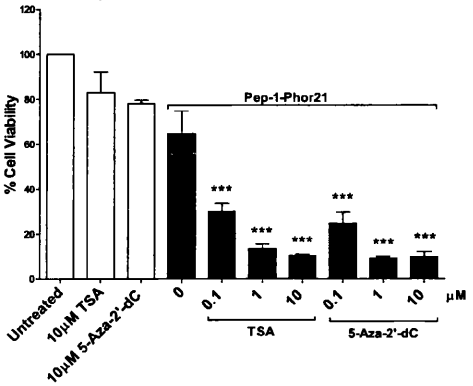

DU145 Spheroids Treated with Pep-1-Phor21

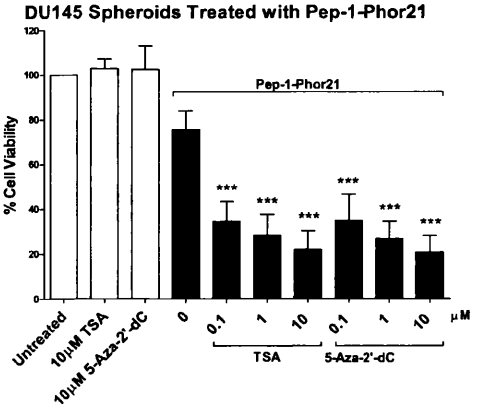

MDA-MB 231 Spheroids Treated with Pep-1-Phor21

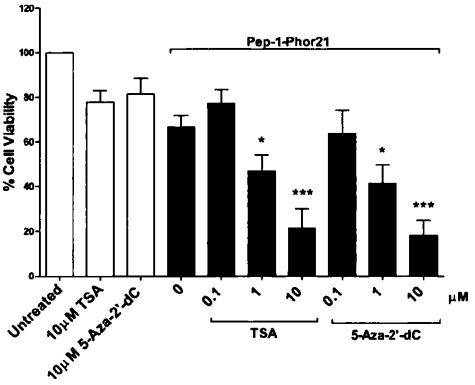

PC3 Spheroid Treated with Pep-1-Phor21

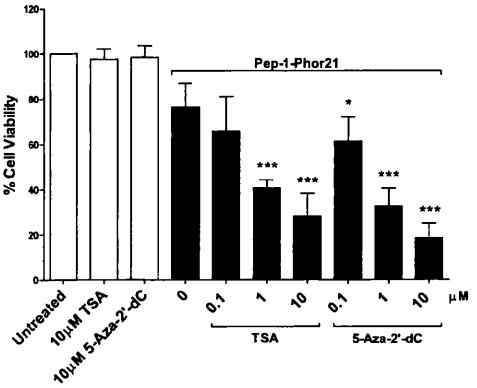

Figure 5.17. Effect of Pep-1-Phor21 on cell viability of 3D cultured prostate and breast cell lines treated with TSA or 5-aza-dC. A) Pep-1-Phor21 sensitivity of 3D cultured no or low IL-13Rα2 expressing (HEK 293, LNCaP, MCF-10A, and MCF-7) and high IL-13Rα2 expressing (DU145, PC3 and MDA-MB 231) cell lines treated with 0.1, 1, and 10μM of TSA or 5-aza-dC for 24 hours was analysed by CellTox assay. HEK293 (120μM), LNCaP (30μM), DU145 (18μM), PC3 (10μM), MCF10A (120μM), MCF-7 (30μM) and MDA-MB231 (18μM) cell spheroids were incubated with the conjugated lytic peptide (the concentration used for each cell line is shown next to it in the brackets) for 3 hours before assessing their cell viability by CellTox assay. The data represent means ± SEM (error bars represent SEM) of data obtained from three independent experiments (***, $P < 0.001$).

Phor21-βCG(ala)

Since the *LHCGR* mRNA expression increased with TSA or 5-aza-dC treatment of prostate and breast cancer cells grown in 3D culture, the Phor21-βCG(ala) sensitivity of prostate and breast cancer cells treated with TSA or 5-aza-dC was determined. The cytotoxicity of Phor21-βCG(ala) on no or low-LHCGR expressing cell lines (PNT-2 and MCF-10A) and LHCGR expressing cell lines (LNCaP,DU145, PC3, MCF-7 and MDA-MB 231) treated with TSA or 5-aza-dC was assessed *in vitro* using CellTox assay (Figure 5.18). Cell spheroids were treated with 0.1, 1, and 10μM of TSA or 5-aza-dC for 24 hours prior to 3 hours treatment of Phor21-βCG(ala) treatment. The concentration of peptide used for each cell line (120μM for PNT-2 cells, 5μM for LNCaP, 5μM for DU145,5μM for PC3, 120μM for MCF-10A, 5μM for MCF-7 and 5μM for MDA-MB 231) was based on its IC_{50} in the CellTox assay (Figure 5.15). The treatment with TSA or 5-aza-dC did not increase the sensitivity of non-cancer cell lines (PNT-2 and MCF-10A) to Phor21-βCG(ala). However TSA or 5-aza-dC treatment significantly increased low LHCGR expressing cancer cell lines (LNCaP, DU145, PC3, MCF-7 and MDA-MB 231) sensitivity to Phor21-βCG(ala) (Figure 5.18). The results demonstrated that TSA and 5-aza-dC increase prostate and breast cancer cell spheroids sensitivity to Phor21-βCG(ala).

HEK293 Spheroid Treated with Pep-1-Phor21

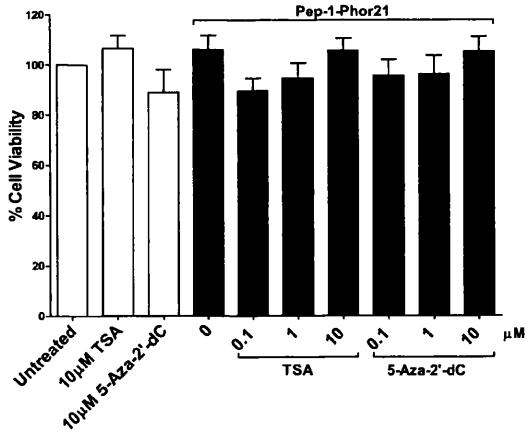

MCF-10A Spheroids Treated with Pep-1-Phor21

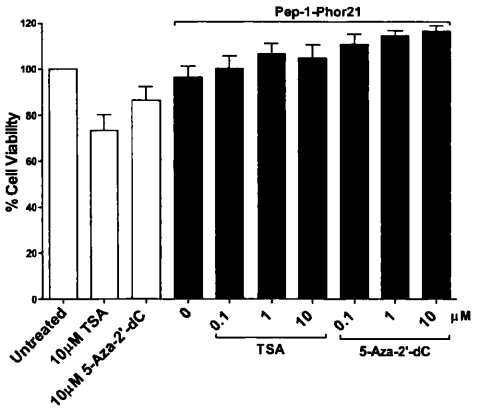

LNCaP Spheroid Treated with Pep-1-Phor21

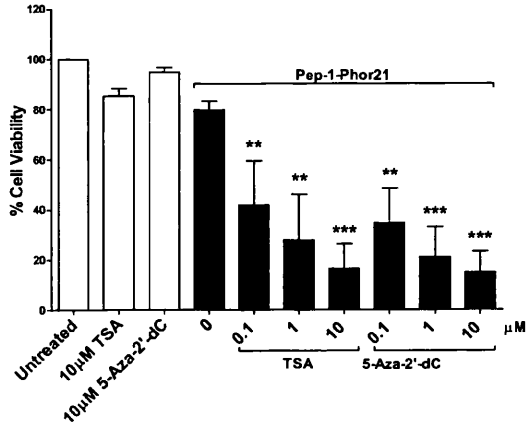

MCF-7 Spheroids Treated with Pep-1-Phor21

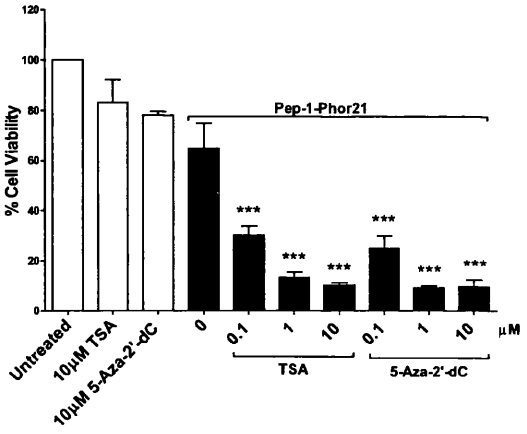

DU145 Spheroids Treated with Pep-1-Phor21

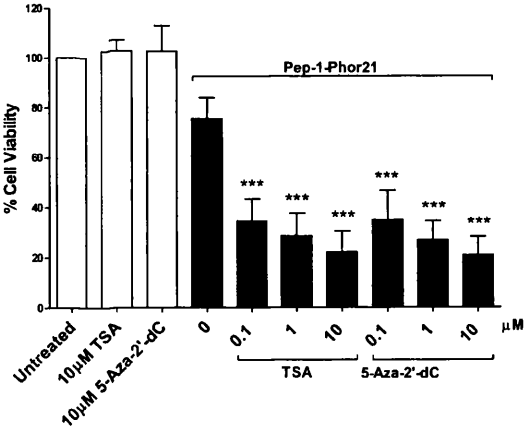

MDA-MB 231 Spheroids Treated with Pep-1-Phor21

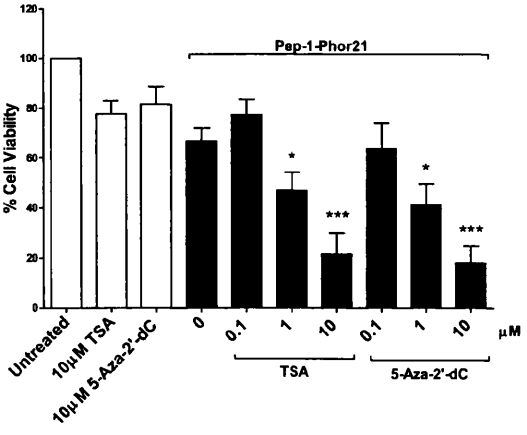

PC3 Spheroid Treated with Pep-1-Phor21

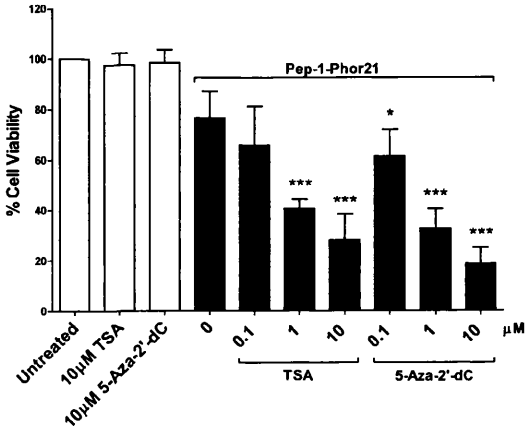

Figure 5.18. Effect of Phor21-βCG(ala) on cell viability of 3D cultured prostate and breast cell lines treated with TSA or 5-aza-dC. Phor21-βCG(ala) sensitivity of 3D cultured no or low LHCGR expressing (PNT-2 and MCF-10A) and high LHCGR expressing (LNCaP, DU145, PC3, MCF-7 and MDA-MB 231) cell lines treated with 0.1, 1, and 10μM of TSA or 5-aza-dC for 24 hours was analysed by CellTox assay. PNT-2 (120μM), LNCaP (5μM), DU145 (5μM), PC3 (5μM), MCF10A (120μM), MCF-7 (5μM) and MDA-MB231 (5μM) cell spheroids were incubated with the conjugated lytic peptide (the concentration used for each cell line is shown next to it in the brackets) for 3 hours before assessing their cell viability by CellTox assay. The data represent means ± SEM (error bars represent SEM) of data obtained from three independent experiments (***, $P < 0.001$).

[D-Trp^6]GnRH-Phor21

As the *GnRHR* mRNA expression increased with TSA or 5-aza-dC treatment in prostate and breast cancer cells grown as a 3D spheroids, the [D-Trp^6]GnRH-Phor21sensitivity of prostate and breast cancer cells treated with TSA and 5-aza-dC was determined. The cytotoxicity of [D-Trp^6]GnRH-Phor21 on no or low-GNRHR expressing cell lines (PNT-2 and MCF-10A) and GnRHR expressing cell lines (LNCaP,DU145, PC3, MCF-7 and MDA-MB 231) treated with TSA or 5-aza-dC was assessed *in vitro* using CellTox assay (Figure 5.19). Cells were incubated with 0.1, 1, and 10μM of TSA or 5-aza-dC for 24 hours prior to 3 hours of [D-Trp^6]GnRH-Phor21 treatment (Figure 5.19). The concentration of peptide used for each cell line (120μM for PNT-2 cells, 5μM for LNCaP, 5μM for DU145,5μM for PC3, 120μM for MCF-10A, 5μM for MCF-7 and 5μM for MDA-MB 231) was based on its IC_{50} in the CellTox assay (Figure 5.16). TSA or 5-aza-dC treatment did not increase the sensitivity of non-cancer cell lines (PNT-2 and MCF-10A) to [D-Trp^6]GnRH-Phor21. However TSA or 5-aza-dC treatment did not significantly increased low GnRHR expressing cancer cell lines (LNCaP,DU145, PC3, MCF-7 and MDA-MB 231) sensitivity to [D-Trp^6]GnRH-Phor21. The results demonstrated that TSA and 5-aza-dC did not increase prostate and breast cancer cell spheroids sensitivity to [D-Trp^6]GnRH-Phor21; opposite to the results obtained in 2D monolayer

PNT-2 Spheroid Treated with [D-Trp6]GnRH-Phor21

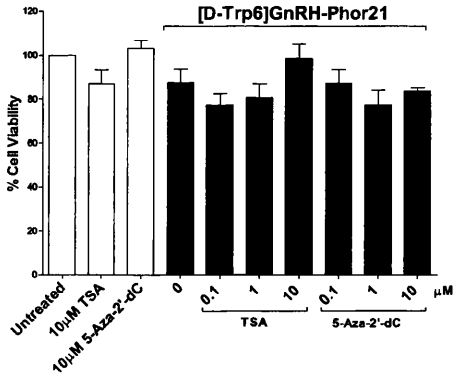

MCF-10A Spheroids Treated with [D-Trp6]GnRH-Phor21

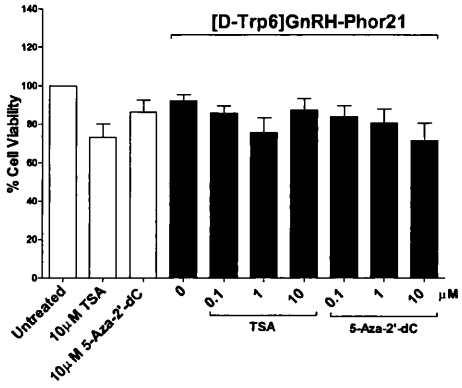

LNCaP Spheroid Treated with [D-Trp6]GnRH-Phor21

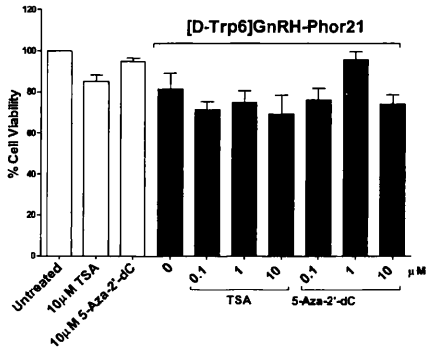

MCF-7 Spheroids Treated with [D-Trp6]GnRH-Phor21

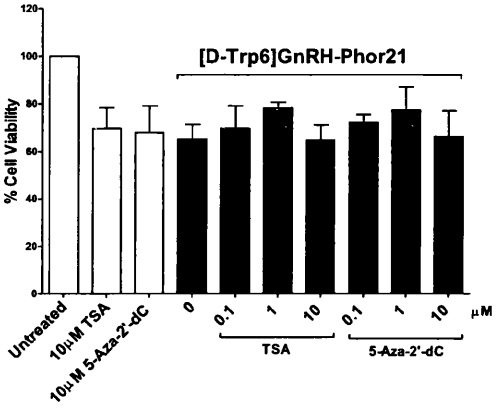

DU145 Spheroids Treated with [D-Trp6]GnRH-Phor21

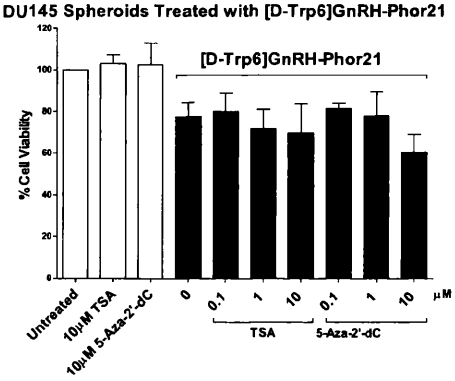

MDA-MB 231 Spheroids Treated with [D-Trp6]GnRH-Phor21

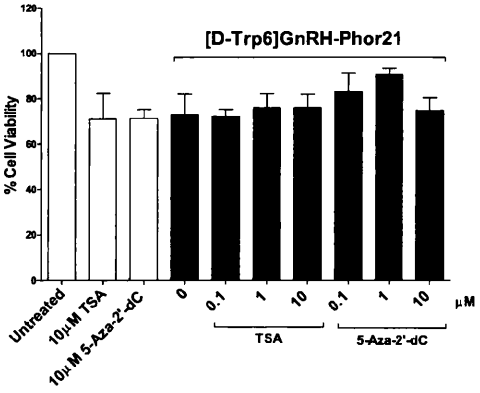

PC3 Spheroid Treated with [D-Trp6]GnRH-Phor21

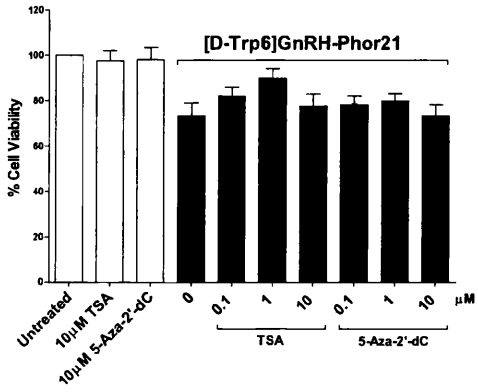

Figure 5.19. Effect of [D-Trp^6]GnRH-Phor21 on cell viability of 3D cultured prostate and breast cell lines treated with TSA or 5-aza-dC. [D-Trp^6]GnRH-Phor21 sensitivity of 3D cultured no or low GnRHR expressing (PNT-2 and MCF-10A) and high GnRHR expressing (LNCaP, DU145, PC3, MCF-7 and MDA-MB 231) cell lines treated with 0.1, 1, and 10μM of TSA or 5-aza-dC for 24 hours was analysed by CellTox assay. PNT-2 (120μM), LNCaP (5μM), DU145 (5μM), PC3 (5μM), MCF10A (120μM), MCF-7 (5μM) and MDA-MB231 (5μM) cell spheroids were incubated with the conjugated lytic peptide (the concentration used for each cell line is shown next to it in the brackets) for 3 hours before assessing their cell viability by CellTox assay. The data represent means ± SEM (error bars represent SEM) of data obtained from three independent experiments (***, $P < 0.001$).

5.4. Discussion

The requirement for the development of a new cell model that improves our understanding of drug development is apparent. Recent developments in 3D cell model cultures have focused on methods that avoid cell surface attachment and incorporate cell-cell attachment. Most 3D cell models are based on cellular aggregation on agarose-coated flat-bottomed plates (Friedrich et al, 2009; Li et al, 2011), poly-Hema-coated round-bottomed or V-bottomed plates (Ivascu & Kubbies, 2006) or even hanging drops (Del Duca et al, 2004).

Here the results demonstrate a novel method for the quick generation of cell spheroids and quantitative analysis of tumour spheroid growth in a high throughput format. This method of in vitro cell spheroid generation can be easily established in any laboratory without specialized equipment and negates the need to purchase preformed spheroids from commercial sources. We have established an image based method (Live/Dead staining assay) and a quantifiable CellTox assay to study the effect of lytic peptides on in vitro grown spheroids (3D tumour model). By using conventional microscopy or confocal microscopy, we were able to qualitatively characterise the morphology of prostate and breast cancer cell line spheroids. Using the hanging drop method, 3D spheroids were produced by gravity by seeding 500-10,000 cell per well of a Terasaki plate and incubating the plate at 37°C/5% CO_2. Spheroids formed within one day of incubation and minimal number cells seeded to obtain maximum number of spheroids was calculated as 2,000 cells per well. In conventional monolayer culture, the cell shape is mainly governed by the affinity of the cells for the substratum, which affects surface morphology. So a perfect selection/choice of substratum is

needed in monolayer culture to maintain differentiated cellular functions for each cell type. But in spheroid culture, no particular cell shape is dictated or imposed on the cell. The hanging drop system enables the spheroid formation without any force besides gravity.

The size of the spheroid using this assay is reproducible and can be adjustable for any particular experiment. Lower cell numbers are required for analysing cell proliferation in long term toxicity studies whereas higher number of cells required for short term toxicity studies. If a drug activity is potent and rapid, a short term endpoint assays will be required. Spheroids formed in a hanging drop method can be harvested and transferred into different conditions e.g. the reduction of serum, the exposure to drugs, induction and other activity studies as shown in our functional assay study.

In pilot studies we compared three different techniques for generating spheroids (hanging drop, Matrigel and surface repellent plates). We found that use of surface repellent plates (U- and F-bottom 96-well plates) is the least time consuming but, instead of forming of spheroids, the cells attached to the surface in the F-Bottom plates and formed small clusters or irregularly shaped aggregates in the U-Bottom plates. Cells cultured in Matrigel did form 3D structures; however the structure of spheroids was un-uniformed and less compact, mimicking a monolayer. Hanging drop method was a quick and easy method that generated the most reproducible spheroids. By generating the spheroids first using the hanging drop method and maintaining integrity of those spheroids by transferring them into surface repellent U-bottom 96-well plate, we were able to quantitatively assess the lytic peptide conjugates sensitivity on 3D spheroids in high throughput format. We also qualitatively assayed the lytic peptide effect on prostate and breast cancer cell spheroids by Live/Dead staining of Terasaki plate originated spheroids transferred into Matrigel. One of the biggest issues regarding drug efficiency is the microenvironment around the tumour cells. Tumour cells in extracellular matrix (ECM) have been reported to become drug resistant, enhancing tumour survival (Dalton, 1999; Doillon et al, 2004). In one case, prostate cancer PC3 cells have been shown to be resistant to doxorubicin and paclitaxel induced apoptosis, one of the main reasons for this resistance is the inability of the drugs to transport through the ECM (Doillon et al, 2004). In the present study we have demonstrated that Phor21-βCG(ala), Pep-1-Phor21 and [D-Trp^{6}]GnRH-Phor21 lytic peptides drugs are able to traffic through ECM and kill cells expressing their representing receptors. Altogether, the 3D model along with the additional functional assay developed in this chapter can play an important role in the preclinical oncology drug development.

IL-13Rα2, LHCGR and GnRHR expression was demonstrated to be slightly reduced in cells grown as multicellular spheroids, relative to 2D monolayer cultures. Cooper et al. found that intermittent hypoxia in breast tumours was associated with reduced levels of Estrogen receptor (ERα) expression (Cooper et al, 2004). Since it has been shown that the central layers of multicellular spheroids are hypoxic (le Roux et al, 2008; Rofstad et al, 1996), the reduction in *LHCGR*, *GnRHR* and more so in *IL-13Rα2* expression could be due to lack of oxygen. This is supported by a previous report, which suggested that hypoxia down regulates ERα mRNA expression in cerebral cortex and a reduced response to oestrogen is found in breast cancer cells exposed to hypoxia (Kurebayashi et al, 2001; Westberry et al, 2008). Liu *et al.* demonstrated that *IL-13Rα2* mRNA expression in glioblastoma cells is dependent on oxygenation status of cells and under hypoxic conditions the expression was decreased (Liu et al, 2009). This could explain why we saw a reduction in *IL-13Rα2* expression.

Finally, we demonstrated a short term functional assay with lytic peptides. Concentration dependent cytotoxicity effects were assessed in our study for prostate and breast cell lines in each of the three cultivation systems. The IC_{50} values of lytic peptides for 2D cultured prostate and breast cancer were mentioned in chapter 4. The IC_{50} values of lytic peptides on prostate and breast cancer cell spheroids indicated an influence of the extracellular matrix or reduction of the target receptor expression. In this study, we developed a quick and easy method to generate spheroids and evaluated the penetration and efficacy of lytic peptides on spheroids by using CellTox and Live/Dead staining assays. For example, prostate and breast cancer cell spheroids incubated with Phor21-βCG(ala), but not Phor21, showed greater staining with EthD-1 (stains only dead cells), and cytotoxicity in CellTox assay. Furthermore, the spheroids incubated with the lytic peptide conjugate showed EthD-1 staining throughout the spheroid, indicating deep penetration of the lytic peptide conjugate in the spheroid. This observation is important because it shows that lytic peptide can not only selectively kill cancer cells but also can access these cells deep inside tumours. As stated in chapter 4, the mode of action of the lytic peptides is cell necrosis and they do so by targeting their receptors on the cell surface membrane, thus preventing any drug resistance.

Our data also demonstrated that pre-treating prostate and breast cancer cell spheroids with TSA or 5-aza-dC enhances their sensitivity to Pep-1-Phor21 Results also showed that pre-treatments with TSA or 5-aza-dC does not sensitize non-cancer cell lines; leading to the conclusion that they may be potential anticancer drugs. The promoter region for human *IL-13Rα2* has been reported to contain only one CpG dinucleotide site, which exhibits a similar

acetylation status pattern in normal and cancer cells. However *IL-13Rα2* mRNA expression is not up regulated in normal epithelial cells. One possible explanation by Fujisawa *et al.*, was that normal epithelial cells show no c-jun activity indicating that TSA activation was dependent on AP-1/c-jun pathway (Fujisawa et al, 2011).

What is also noticeable is that TSA and 5-aza-dC increased the expression of LHCGR. This was further confirmed with increased sensitivity of TSA or 5-aza-dC treated prostate and breast cancer cell spheroids to Phor21-βCG(ala). This was surprising as we didn't observe any increase in LHCGR expression by TSA and 5-aza-dC treatment in 2D monolayer model. Flanagan *et al.* demonstrated an increased methylation of the *LHCGR* in breast cancer tissues samples. They concluded that the *LHCGR* gene can be regulated by DNA methylation and histone modifications (Flanagan et al, 2010). They observed an increase in methylation of the receptor in BRCA2 positive tumours. They also showed that *BRCA1* positive tumours had increased *LHCGR* expression and were more invasive breast tumours (Honrado et al, 2006). This result is consistent with that of ours. In our study also *LHCGR* expression had increased upon treatment of MCF cell spheroids with either TSA or 5-aza-dC. Zhang *et al.* also showed that treating with TSA or 5-aza-dC could have an effect on the expression of the *LHCGR* gene (Zhang et al, 2005).

It is important to remember that the vast majority of chemotherapeutic agents are screened for cytotoxic effects on cancer cells grown in monolayer cultures, which do not represent the critical mechanisms of drug resistance associated with the tumour microenvironment. The tumour microenvironment can also induce or suppress certain number of genes. Therefore monolayer models poorly predict a drug's therapeutic efficacy *in vivo* (Johnson et al, 2001; Mikhail et al, 2013). Nestor *et al.* recently published a paper highlighting the reprogramming of epigenetic and transcriptional states in mouse embryonic fibroblast (MEFS) in a monolayer cell culture. They demonstrated significant difference in epigenetic and transcriptional status between *in vitro* and *in vivo* models (Nestor et al, 2015). They concluded, perhaps a 3D model will be an *in vitro* 2D substitute with *in vivo* cellular morphologies. This could be one of the reasons why we see TSA or 5-aza-dC having an effect *GnRHR* expression in 2D cultured cells and not in 3D cultured cells. Our study adds to the global realisation that 2D monolayer cell line cultures of human cancer diseases can be a poor model for truly understanding *in vivo* biology. This was emphasised further in a recent study, in which Gillet *et al.* demonstrated multi-drug resistance genes in ovarian cancer

showed no connection between the expression found in primary ovarian cancer samples and their established cancer cell lines (Gillet et al, 2011).

3D models in drug discovery, especially in anticancer therapeutics, have proven to be more closely valuable and relevant over the years. The idea of *in vitro* assay that mimics more closely *in vivo* studies is highly attractive. Multicellular spheroids reflect many properties of solid tumours, including cell-cell interactions, ECM, and because tumours are heterogeneous, tight junctions between different cell types are important as it limits drug penetration (Minchinton & Tannock, 2006).

We provide a comprehensive suite of simple, reproducible 3D tumour spheroid models that recapitulate *in vivo* some of the key hallmarks of cancer, and at the same time can provide a dynamic, automated, quantitative cytotoxicity and qualitative imaging and analysis compatible with high-throughput preclinical studies. We provide evidence that our methods have the potential to enhance target selection through rapid functional screening assays and the effective triaging of drug candidates prior to *in vivo* studies.

6. General Discussion and Conclusions

The main aim of this project was to explore the effect of lytic peptides on breast and prostate cancer cells, in both 2D and 3D environment. In the United Kingdom (UK) 1 in 3 will develop some form of cancer during their lifetime (UK, 2009). Despite the development of new drugs and use of combinational therapies, mortality rates are still not improving. In 2009, 408,381 patients were diagnosed with cancer in the UK resulting in 156,090 deaths; the highest mortality rate occurring due to lung cancer (UK, 2009). Between 1979 and 2008, incidence rates for cancer in the UK increased by 26% with a 13% increase in men and a 34% increase in women respectively (UK, 2009). The second most common cause of cancer death in men is prostate cancer, and breast cancer in women respectively (UK, 2009).

One of the biggest issues related to cancer is the advances, in screening for early detection, aggressive therapy for localised diseases, and treatment for metastatic state; especially in prostate and breast cancers. Treatment of breast cancer depends on the disease stage and the pathologic feature, such as the receptor status and tumour grade. Stage IV breast cancer falls under advanced or metastatic disease that represents tumour spreading outside the breast or site of origin and onto the adjacent lymph nodes. Patients with the more aggressive or advanced stages of breast cancers have an approximately 2 years survival rate after diagnosis.

Breast cancer can be treated with chemotherapy agents, however an important factor that needs to be considered is that any reduction in tumour size may not be correlated to any improvements in progression free or overall survival. However, these patients fall under the group that are treated for localised disease. These patients prognosis is dependent on the number of axillary lymph nodes involved, the size of the primary tumour, and the pathologic features of the primary tumour

The early stages of prostate cancer, is normally characterised as an androgen-dependent disease that depends on the androgen receptor (AR) for growth and progression. Prostate cancer cells that are androgen dependent usually reflect the properties of the normal prostate gland, making androgen deprivation therapy very effective, as the first line of treatment therapy. However resistance, to androgen deprivation can develop over time and prostate cancer cells undergo recurrent growth despite low levels of circulating androgen. High

mortality is usually associated with cancer cells that have relapsed or recurred. High mortality can also be associated with the spread of cancer cells to other parts of the body. This is called castration-resistant prostate cancer, were the high mortality rate is due to the ineffectiveness of the androgen deprivation drugs.

Metastatic cancer treatment cannot be mediated through surgery in combination with radiotherapy or the appropriate chemotherapy treatment, making the prognosis for curing the patients very difficult. To date there are number of treatment regimes, that have applied one or a combination of agents, such as mAbs and even signal transduction inhibitors. These have proven beneficial for inhibiting or even reducing the size of the primary tumours and or metastases. However, these treatments are limited due to their toxicity in the patients. A large number of anticancer drugs act by killing rapidly dividing cells; a characteristic of many cancer cells. However to normal cells that rapidly divide such as the bone marrow, digestive tract and hair follicles they can also exhibit toxicity.

An alternative approach to conventional chemotherapy is clearly needed and the future is targeted therapy. This new approach has gathered a lot of interest for treating cancer. A new wave of drugs has been the development from mAbs that directly target tumour associated antigens. Several examples such as trastuzumab (Herceptin) used to treat HER2/neu breast cancer, also panitumumab (Vectibix®) which targets EGFR for treating colon cancer. As stated in **Chapter 4** histone deacetylase (HDAC) inhibitors that inhibit the proliferation of tumour cells by inducing cell cycle arrest, differentiation and or apoptosis have shown promising results. Vorinostat, an HDAC inhibitor that was first drug approved by the FDA, for the treatment of T cell lymphoma (Mann et al, 2007).

In the last decade, many new targeted drugs have been approved by the US Food and Drug Administration (FDA) for cancer treatment. Pfizer recently have been given a granted approval by the FDA for a drug called palbociclib (IBRANCE®). Palbociclib is a small molecule that inhibits cyclin-dependent kinases (CDKs) 4 and 6 in estrogen receptor (ER)-positive and human epidermal growth factor receptor 2 (HER2)-negative advanced breast cancers. The drug reduces cell proliferation by blocking the transition from G1 to S phase. During clinical trials patients were given orally 125mg of palbociclib, 21 consecutive days followed by 7 days off treatment to comprise a complete cycle of 28 days. Patients can also be treated with letrozole (Femara®) which is a drug already used to treat (ER)-positive breast cancer. By combining palbociclib and letrozole, it was found that the overall response rate was 55.4% (Finn et al, 2015).

Xtandi (enzalutamide) was approved in 2012 by the FDA, for treatment of patients with metastatic castration-resistant prostate cancer. The recommended dosage is 160mg and administered orally. This drug targets and inhibits androgen receptor binding to the ligand-binding domain of the receptor. Repose rate was significantly higher compared to the placebo (53.1%) (Althaus & Kibel, 2015; Froehner & Wirth, 2014; Saad, 2013).

The targeting of cell surface receptors that are specifically or over expressed in cancer cells has painted a new insight in anti-cancer therapy. The Gonadotropin-releasing hormone receptor (GnRHR), luteinizing hormone/choriogonadotropin receptor (LHCGR) and Interleukin-13 receptor alpha 2(IL-13Rα2), have been shown to be overexpressed in human tumours. In **Chapter 3** GnRHR, LHCGR and IL-13Rα2 have been identified as potential diagnostic and therapeutic targets. Although alterations in these receptor expression have been linked to cancer in few tissues, it is unknown whether changes in their expression are widespread or not (Hapgood et al, 2005; Iles et al, 2010; Zhou et al, 2013). In this chapter, we analysed the expression of these receptors at mRNA level in cancers and corresponding normal controls from 18 different tissues using quantitative PCR. The results indicated an up-regulation of GnRHR, LHCGR and IL-13Ra2 in several cancer types, relative to their representing normal tissue. GnRHR mRNA expression was found to be significantly increased in breast, pancreatic and prostate cancer whereas LHCGR gene expression was increased in breast, endometrial and prostate cancer and decreased in kidney cancer. IL-13Rα2 mRNA expression was also found to be significantly increased in breast, pancreatic and prostate cancers and decreased in stomach cancer. The alterations in these receptors expression at mRNA levels were explored further by separating the expression data by stage of cancer. The data revealed that the overexpression of GnRHR, LHCGR and IL-13Ra2 in a broad spectrum of human cancers indicates their potential use for targeting for diagnosis and treatment purposes.

Current methods for treating cancer involve radiation therapy and chemotherapy. However one major limitation to these therapies is the development of resistance. It is also increasingly becoming clear that cancer cells are heterogeneous and their signalling pathway varies between different populations, which can limit the potential of the cancer treatments. To overcome these limitations, anticancer treatments involving various combinations of drugs have been developed. However in some cases, combinational treatments have resulted in high toxicity.

Another innovative anticancer strategy is to develop drugs that target cell surface receptors. IL-13, GnRH and βCG binds, respectively, to cell surface receptors IL-13Rα2, GnRHR, and LHCGR, which are overexpressed in several cancers. IL-13Rα2 specific ligand (Pep-1) fused cytotoxin has recently been used to target glioblastoma whereas GnRH and βCG fused cytotoxin have been characterised for targeting prostate and breast cancers. Although IL-13Rα2 is overexpressed in breast and prostate cancers, it has not yet been assessed as a target for treatment of those cancers. In **Chapter 4** the aim of the study was to assess alterations in expression of GnRHR, LHCGR and IL-13Rα2 expression in prostate and breast cancer cell lines. We than demonstrated that specific ligands conjugated to membrane disrupting lytic peptide were able to target cell lines that were over-expressing these receptors. These lytic peptides are generally short with 14-40 amino acids, containing cationic and hydrophobic residues, and in the membrane environment, they are able to form amphipathic secondary structures that can disrupt negatively charged membranes, promoting rapid cell death and reduce the risk of any resistance. They do not rely on cellular uptake; they are able to overcome problems of multidrug resistance. However lytic peptides on their own have limited specificity in targeting cancer cells. For this purpose, we analysed the expression of GnRHR, LHCGR and IL-13Rα2 at mRNA and protein levels in prostate and breast cancer cells. We also generated Pep-1, GnRH and βCG(ala) peptides conjugated covalently to a membrane disrupting lytic peptide (Phor21) and assessed their effect on prostate and breast cell lines that over-express their respective receptors. Pandya et al was the first group to develop and test Pep-1 peptide. The ability to bind to IL-13Rα2 to a different site to that of the native ligand and not be inhibited has gathered a lot of interest, especially for targeting malignant primary brain tumours (Pandya et al, 2012). To date there are no known peptide drugs for IL-13Rα2 that use lytic peptides.

There are a number of studies that conjugated the native ligand IL-13 to a bacterial cytotoxin called *Pseudomonas* exotoxin. There are several problems in using protein based toxins, one of which is activation of the immune response leading to the generation of antibodies, especially when the toxin is of non-human origin (Baker et al, 2010). Also due to their relatively large molecular size, the ligand or antibody-conjugated toxins are unable to penetrate the whole tumour. The lytic peptides immune response is generally low or no repose at all also due to their relatively small size (14-40 amino acids). Since the lytic peptides are relatively small, they are also able to penetrate further into tissues (Bogacki et al, 2008; McGregor, 2008). Using, immunoblotting and real time PCR (RT-PCR) and enzyme-

linked immunosorbent assay (ELISA), to measure the expression, we found IL-13Rα2, GnRHR and LHCGR are over expressed in prostate and breast cancer cell lines. Also treatment with 5-azadC and TSA increased IL-13Rα2 and GnRHR expression in these cancer cells. Treatment with 17β-estradiol and FSH also increased LHCGR and GnRHR expression. When measuring the cytotoxicity the lytic peptide drugs GnRH-Phor21, Pep-1-Phor21, and Phor21-βCG(ala) conjugates selectively killed prostate and breast cancer cells *in vitro* and their toxicity depends on the expression levels of their respective receptors at the cell surface. The effectiveness of the lytic peptides also increased with 5-azadC, TSA, 17β-estradiol and FSH. Combining treatments induced syngeneic cell death when compared to the efficacies of the treatments alone.

We then focused our efforts on to three dimensional (3D) models. There are a number of studies that have stated the similarities between *in vitro* 3D tumour cell cultures and their representing tissue samples in an *in vivo* microenvironment, with respect to gene expression, signalling pathway activity and drug sensitivity. However, most current 3D model cultures are limited by size, cultivation time, and the accessibility for higher throughput screening. To address this, in **Chapter 5** we have developed a quick, easy and reproducible 3D tumour model to validate Phor21-βCG(ala), [D-Trp^6]GnRH-Phor21 and Pep-1-Phor21 lytic peptides cancer targeting ability. We assessed the expression of GnRHR, LHCGR and IL-13Rα2 in prostate and breast cancer cells grown in a 3D model. Then epigenetic regulation of IL-13Rα2, GnRHR and LHCGR expression was studied by treating the cells with DNA-methyltransferase inhibitor 5-AZA-2-deoxycytidine (5-azadC) and histone-deacetylase inhibitor Trichostatin A (TSA). The effect of these lytic peptides on prostate and breast cancer cells grown as spheroids was assessed qualitatively using live/dead staining and quantitatively using CellTox assay. Using the new 3D model that we developed, we have demonstrated for the first time that lytic peptide drugs can penetrate into cancer spheroids and selectively kill cancer cells expressing the receptor of interest. We have also demonstrated for the first time that combined therapy of 5-azadC or TSA and Pep-1-Phor21, and Phor21-βCG(ala) increases its cytotoxic efficacy against prostate and breast cancer. *In vitro* 3D cell cultures have progressed over the years, assisting in the development of new anticancer drugs. The use of synthetic matrices like Matrigel can be adapted for co-culturing with other cells e.g. non-cancer cells or even fibroblast cells, to further investigate the action of any drug in a tumour environment (Xu et al, 2014).

Based on our results, future studies investigating the role of other receptors in cancer can yield new drug targets. Our results demonstrated that conjugating a lytic peptide to a ligand can specifically bind to its receptor and bind, and kills that cell. The use of lytic peptides in clinical treatments has many advantages. Including that they can mass produced at a low cost and can be sequenced to improve on their delivery to the tumors while maintaining a low profile of toxic effects.

There are a number of new drugs that are currently being developed that target specific receptors. The first anticancer drug-GnRH derivative bioconjugate was first developed in 1996 by Nagy et al for which they developed a drug called AN-152, which consisted of the GnRH-1 derivative [D-^{6}Lys]-GnRH-I as a targeting moiety and a doxorubicin drug as the anticancer drug (Nagy et al, 1996). However there are number of isoforms of GnRH-1, for example GnRH-III (Glp-His-Trp-Ser-His-Asp-Trp-Lys-Pro-Gly-NH_2). This was first isolated from the brain of the sea lamprey (*Petromyzon marinus*) (Sower et al, 1993). This isoform was found to have insignificant effect of the production and release of luteinizing hormone (LH) and follicle-stimulating hormone (FSH). This isoform is a very interesting targeting moiety, because not only it can bind to the receptor with high affinity, but it can also carry more than one chemotherapeutic agent, increasing its potency compared to a monofunctional compound. It is possible to conjugate two anticancer drugs that work in a synergistic or in a stabilisation fashion. Leurs et al designed a bifunctional targeting moiety by replacing the Ser residue with a Lys; [^{4}Lys]-GnRH-III (Glp-His-Trp-Lys-His-Asp-Trp-Lys-Pro-Gly-NH_2) (Leurs et al, 2012). From this they were able to conjugate two chemotherapeutic agents' methotrexate (MTX) and daunorubicin on position 4 and 8 respectively (GnRH-III [^{4}Lys (MTX), ^{8}Lys (Dau = Aoa)]) (Leurs et al, 2012). The same group also conjugated novel short-chain fatty acid (SCFA) that can act as a chemopreventive agent by slowing cell growth and activating apoptosis. By adding SCFA's on position 4, they found that nBu and iBu (Figure 6.1) enhanced the cytotoxic effect on human breast MCF-7 and human colon HT-29 cancer cell lines *in vitro* (Hegedus et al, 2012).

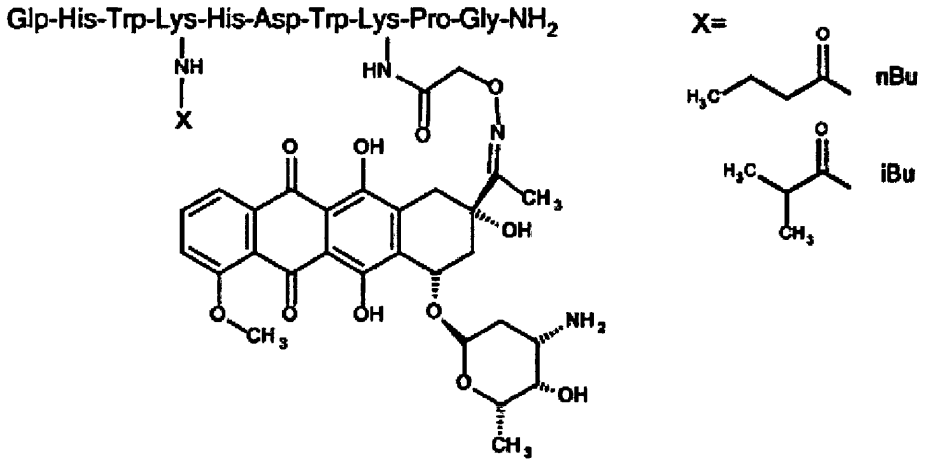

Figure 6.1. Structure representation of GnRH-III [^{8}Lys(Dau = Aoa)] and two short-chain fatty acid. Taken and adapted from (Hegedus et al, 2012).

Claudin-4 is an integral constituent of tight junctions and one of the most intensely studied candidates for drug targets in epithelial cancers. Claudin-4 has been shown to be upregulated in a number of cancers, including pancreatic cancer. There have been a number of studies that have targeted claudin-4 expressing cancer cells using C-terminal 30 amino acids of *Clostridium perfringens* enterotoxin (Cpe30). Ling et al demonstrated that a small peptide called Cpe17 that is 17 amino acid long can bind to claudin-4 with high affinity (Ling et al, 2008). Kakutani et al genetically prepared a novel claudin-4-targeting molecule by fusion of C-CPE and diphtheria toxin fragment A (DTA). They found that DTA-C-CPE was toxic specifically to claudin-4 expressing cells (Kakutani et al, 2010). The issue with using protein is the ability to emit a high immune response and one obstacle is that fact that most developed countries have immunisation programmes against diphtheria, this will result in the neutralization of diphtheria-toxin-based immunotoxins (Frankel, 2004; Kawamoto et al, 2011; Li et al, 2002). In addition, the molecular size of the fusion protein is greater than that of lytic peptides, which could prevent and lower the efficiency of penetrating the target site (Frankel, 2004; Kawamoto et al, 2011). To date no one has ever conjugated Cpe30 to a lytic peptide.

LHCGR has been shown to be a good candidate for targeting cancers. Over-expression of LHCGR has been identified in multiple cancers and their metastases. This can be exploited in designing the LHCGR targeting of nanoparticles for cancer treatment. Targeting of LHCGR in malignant cells and tumours by nanoparticles conjugated with βCG (LHCGR ligand)

would increase their uptake through the activation of tumour specific signal transduction cascades, which will improve specificity and efficiency of the conjugate. These characteristics have opened a new area of research into targeted imaging and treatment. With the development of 3D cell culture platforms, research can now have a better understanding of cancer cells and enhance anticancer drug screening and testing standards.

Naturally occurring phospholipid ethers (PLE) have been shown to accumulate in the membranes of cancer cells, but not normal cells. In fact this phospholipid had been associated with a broad spectrum of cancers whereas LHCGR expression is limited in some cancers. By designing a lytic peptide that only targets phospholipid ethers; we would potentially have a "wonder anticancer drug". Dave et al showed that a 20 amino acid Alamethicin was able to bind and disrupt ether-linked phospholipid membranes (Dave et al, 2005). In another study, a group successfully target phospholipid ethers with alkylphosphocholine (APC) analogs. They tagged an iodine isotope and found selective uptake and prolonged retention in both primary and metastatic malignant tumours (Weichert et al, 2014). They also concluded that this can target a broad spectrum of solid tumours (Davies et al, 2014).

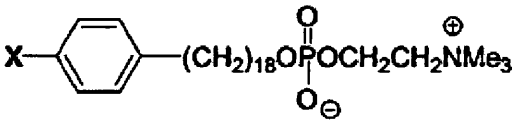

Figure 6.2 Alakylphosphocholine (APC) analog. APC analog could be tagged to a radioactive compound and a lytic peptide as a target that detect and kills cancer cells.

Although peptide base conjugated drugs have gained prominence over the years, they are yet to be clinically approved. One such example is Zoptarelin DOX (AN152 or AEZS108), developed by Aeterna Zentaris, they conjugated doxorubicin to D-Lys^6 side chain of the GnRH-R agonist [D-Lys^6]-GnRH. It is currently undergoing phase III trials, comparing AN-152 to doxorubicin as a second line of therapy for endometrial cancer patients (Engel et al, 2012a; Nagy et al, 1996). As mentioned before EP100, developed by Esperance Pharmaceuticals is a lytic peptide base that contains peptide LHRH analog conjugated to a disrupting cell membrane peptide called CLIP71. This drug has recently finished phase II trials with the combination of EP100 and paclitaxel to treat ovarian cancer (Curtis et al,

2014). Over the coming years we could see more and more peptide base conjugated drugs in preclinical and clinical development, the key aspects to these drugs success is the potent and specific and safe targeting. This is a future development that is still emerging and is gaining strength

In conclusion: The results from the studies described in this thesis encourage the further development of targeted therapies for the locoregional and systemic treatment of prostate and breast cancer. Lytic peptide drugs appear to be a valuable addition to the treatment of patients who can no longer be treated by surgery or radiotherapy, and combination with systemic therapies is interesting and needs further investigation. The selection of target receptors with strict tumour-selective expression needs attention to enable the use of lytic peptides conjugates for therapy. Unacceptable toxicities due to cross reactivity should be anticipated. Despite challenges that have limited broader use of anticancer drugs, advances including new technologies for spheroid formation, culture, and analysis that have been highlighted, suggest that use of spheroids to be an important step in *in vitro* studies for drug delivery and efficacy, providing readouts that better predict results in patients than standard 2D cultures. The results from the cytotoxicity studies for the selective targeting of tumour spheroids can pave the way for clinical studies. The development of next-generation highly specific anticancer drugs opens new avenues for multi-targeted therapies.

Bibliography

Abbott A (2003) Cell culture: biology's new dimension. *Nature* **424:** 870-872

Adams CW, Allison DE, Flagella K, Presta L, Clarke J, Dybdal N, McKeever K, Sliwkowski MX (2006) Humanization of a recombinant monoclonal antibody to produce a therapeutic HER dimerization inhibitor, pertuzumab. *Cancer immunology, immunotherapy : CII* **55:** 717-727

Aguilar-Rojas A, Huerta-Reyes M (2009) Human gonadotropin-releasing hormone receptor-activated cellular functions and signaling pathways in extra-pituitary tissues and cancer cells (Review). *Oncology reports* **22:** 981-990

Aina OH, Liu R, Sutcliffe JL, Marik J, Pan CX, Lam KS (2007) From combinatorial chemistry to cancer-targeting peptides. *Molecular pharmaceutics* **4:** 631-651

Alanine A, Nettekoven M, Roberts E, Thomas AW (2003) Lead generation--enhancing the success of drug discovery by investing in the hit to lead process. *Combinatorial chemistry & high throughput screening* **6:** 51-66

Althaus A, Kibel A (2015) Re: Enzalutamide in Metastatic Prostate Cancer Before Chemotherapy. *European urology* **67:** 174-174

Amiri-Kordestani L, Fojo T (2012) Why Do Phase III Clinical Trials in Oncology Fail so Often? *Journal of the National Cancer Institute* **104:** 568-569

Anders CK, Hsu DS, Broadwater G, Acharya CR, Foekens JA, Zhang Y, Wang Y, Marcom PK, Marks JR, Febbo PG, Nevins JR, Potti A, Blackwell KL (2008) Young Age at Diagnosis Correlates With Worse Prognosis and Defines a Subset of Breast Cancers With Shared Patterns of Gene Expression. *Journal of Clinical Oncology* **26:** 3324-3330

Ando H, Hew CL, Urano A (2001) Signal transduction pathways and transcription factors involved in the gonadotropin-releasing hormone-stimulated gonadotropin subunit gene expression. *Comp Biochem Physiol B Biochem Mol Biol* **129:** 525-532

Andrews A-L, Nasir T, Bucchieri F, Holloway JW, Holgate ST, Davies DE (2006) IL-13 receptor α 2: A regulator of IL-13 and IL-4 signal transduction in primary human fibroblasts. *Journal of Allergy and Clinical Immunology* **118:** 858-865

Andrews AL, Holloway JW, Puddicombe SM, Holgate ST, Davies DE (2002) Kinetic analysis of the interleukin-13 receptor complex. *The Journal of biological chemistry* **277:** 46073-46078

Arlt M (2005) Hit-to-Lead. Enhancing lead generation to accelerate quality compounds into lead optimization. 18-19 July 2005, London, UK. *IDrugs : the investigational drugs journal* **8:** 716-718

Arora KK, Sakai A, Catt KJ (1995) Effects of second intracellular loop mutations on signal transduction and internalization of the gonadotropin-releasing hormone receptor. *The Journal of biological chemistry* **270:** 22820-22826

Arrondeau J, Cottu P, Aerio (2012) Pertuzumab plus trastuzumab plus docetaxel for metastatic breast cancer. *Oncologie* **14:** 351-352

Ascoli M, Fanelli F, Segaloff DL (2002) The lutropin/choriogonadotropin receptor, a 2002 perspective. *Endocr Rev* **23:** 141-174

Ausbacher D, Svineng G, Hansen T, Strom MB (2012) Anticancer mechanisms of action of two small amphipathic beta(2,2)-amino acid derivatives derived from antimicrobial peptides. *Biochim Biophys Acta* **1818:** 2917-2925

Baker MP, Reynolds HM, Lumicisi B, Bryson CJ (2010) Immunogenicity of protein therapeutics: The key causes, consequences and challenges. *Self/nonself* **1:** 314-322

Balis FM (2002) Evolution of Anticancer Drug Discovery and the Role of Cell-Based Screening. *Journal of the National Cancer Institute* **94:** 78-79

Barderas R, Bartolomé RA, Fernandez-Aceñero MJ, Torres S, Casal JI (2012) High Expression of IL-13 Receptor α2 in Colorectal Cancer Is Associated with Invasion, Liver Metastasis, and Poor Prognosis. *Cancer Res* **72:** 2780-2790

Baselga J, Cortes J, Kim SB, Im SA, Hegg R, Im YH, Roman L, Pedrini JL, Pienkowski T, Knott A, Clark E, Benyunes MC, Ross G, Swain SM, Grp CS (2012) Pertuzumab plus Trastuzumab plus Docetaxel for Metastatic Breast Cancer. *New Engl J Med* **366:** 109-119

Basler JW, Thompson IM (1998) Lest we abandon digital rectal examination as a screening test for prostate cancer. *Journal of the National Cancer Institute* **90:** 1761-1763

Bates RC, Edwards NS, Yates JD (2000) Spheroids and cell survival. *Critical reviews in oncology/hematology* **36:** 61-74

Bauer KR, Brown M, Cress RD, Parise CA, Caggiano V (2007) Descriptive analysis of estrogen receptor (ER)-negative, progesterone receptor (PR)-negative, and HER2-negative invasive breast cancer, the so-called triple-negative phenotype: a population-based study from the California cancer Registry. *Cancer* **109:** 1721-1728

Baum M, Buzdar A, Cuzick J, Forbes J, Houghton J, Howell A, Sahmoud T, Group AT (2003) Anastrozole alone or in combination with tamoxifen versus tamoxifen alone for adjuvant treatment of postmenopausal women with early-stage breast cancer: results of the ATAC (Arimidex, Tamoxifen Alone or in Combination) trial efficacy and safety update analyses. *Cancer* **98:** 1802-1810

Bedecarrats GY, Kaiser UB (2003) Differential regulation of gonadotropin subunit gene promoter activity by pulsatile gonadotropin-releasing hormone (GnRH) in perifused L beta T2 cells: role of GnRH receptor concentration. *Endocrinology* **144:** 1802-1811

Ben-Efraim I, Bach D, Shai Y (1993) Spectroscopic and functional characterization of the putative transmembrane segment of the minK potassium channel. *Biochemistry* **32:** 2371-2377

Ben-Yehudah A, Lorberboum-Galski H (2004) Targeted cancer therapy with gonadotropin-releasing hormone chimeric proteins. *Expert review of anticancer therapy* **4:** 151-161

Benedettini E, Nguyen P, Loda M (2008) The pathogenesis of prostate cancer: from molecular to metabolic alterations. *Diagnostic histopathology* **14:** 195-201

Bernardi R, Lowery A, Thompson P, Blaney S, West J (2008) Immunonanoshells for targeted photothermal ablation in medulloblastoma and glioma: an in vitro evaluation using human cell lines. *J Neurooncol* **86:** 165-172

Beuschlein F, Looyenga BD, Bleasdale SE, Mutch C, Bavers DL, Parlow AF, Nilson JH, Hammer GD (2003) Activin Induces x-Zone Apoptosis That Inhibits Luteinizing Hormone-Dependent Adrenocortical Tumor Formation in Inhibin-Deficient Mice. *Molecular and Cellular Biology* **23:** 3951-3964

Bignold LP, Coghlan BL, Jersmann HP (2006) Cancer morphology, carcinogenesis and genetic instability: a background. *EXS*: 1-24

Bigsby RM, Li A (1994) Differentially regulated immediate early genes in the rat uterus. *Endocrinology* **134:** 1820-1826

Bilici A, Arslan C, Altundag K (2012) Promising therapeutic options in triple-negative breast cancer. *Journal of BUON : official journal of the Balkan Union of Oncology* **17:** 209-222

Bleicher KH, Bohm HJ, Muller K, Alanine AI (2003) Hit and lead generation: beyond high-throughput screening. *Nature reviews Drug discovery* **2:** 369-378

Bodek G, Rahman NA, Zaleska M, Soliymani R, Lankinen H, Hansel W, Huhtaniemi I, Ziecik AJ (2003) A novel approach of targeted ablation of mammary carcinoma cells through luteinizing hormone receptors using Hecate-CGbeta conjugate. *Breast Cancer Res Treat* **79:** 1-10

Bogacki M, Enright FM, Todd WJ, Hansel W (2008) Immune response to lytic peptides conjugated to a betaCG fragment in treated BALB/C mice. *Reproductive biology* **8:** 135-147

Bolla M, Gonzalez D, Warde P, Dubois JB, Mirimanoff RO, Storme G, Bernier J, Kuten A, Sternberg C, Gil T, Collette L, Pierart M (1997) Improved survival in patients with locally advanced prostate cancer treated with radiotherapy and goserelin. *N Engl J Med* **337:** 295-300

Bosch F, Rosich L (2008) The contributions of Paul Ehrlich to pharmacology: a tribute on the occasion of the centenary of his Nobel Prize. *Pharmacology* **82:** 171-179

Bowen R (2004) Gonadotropins: Luteinizing and Follicle Stimulating Hormones. *http://wwwvivocolostateedu*

Brannon-Peppas L, Blanchette JO (2004a) Nanoparticle and targeted systems for cancer therapy. *Advanced Drug Delivery Reviews* **56:** 1649-1659

Brannon-Peppas L, Blanchette JO (2004b) Nanoparticle and targeted systems for cancer therapy. *Adv Drug Deliv Rev* **56:** 1649-1659

Brigger I, Dubernet C, Couvreur P (2002) Nanoparticles in cancer therapy and diagnosis. *Advanced Drug Delivery Reviews* **54:** 631-651

Buchholz S, Seitz S, Schally AV, Engel JB, Rick FG, Szalontay L, Hohla F, Krishan A, Papadia A, Gaiser T, Brockhoff G, Ortmann O, Diedrich K, Koster F (2009) Triple-negative breast cancers express receptors for luteinizing hormone-releasing hormone (LHRH) and respond to LHRH antagonist cetrorelix with growth inhibition. *International journal of oncology* **35:** 789-796

Burstein HJ, Polyak K, Wong JS, Lester SC, Kaelin CM (2004) Ductal carcinoma in situ of the breast. *N Engl J Med* **350:** 1430-1441

cancer.org (2011) Chemotherapy Principles: An In-depth Discussion.

Casarini L, Lispi M, Longobardi S, Milosa F, La Marca A, Tagliasacchi D, Pignatti E, Simoni M (2012) LH and hCG action on the same receptor results in quantitatively and qualitatively different intracellular signalling. *PLoS One* **7:** e46682

Catz SD, Johnson JL (2003) BCL-2 in prostate cancer: a minireview. *Apoptosis* **8:** 29-37

Cetin B, Benekli M, Turker I, Koral L, Ulas A, Dane F, Oksuzoglu B, Kaplan MA, Koca D, Boruban C, Yilmaz B, Sevinc A, Berk V, Uncu D, Harputluoglu H, Coskun U, Buyukberber S (2014) Lapatinib plus capecitabine for HER2-positive advanced breast cancer: a multicentre study of Anatolian Society of Medical Oncology (ASMO). *Journal of chemotherapy* **26:** 300-305

Cha J, Lim J, Zheng Y, Tan S, Ang YL, Oon J, Ang MW, Ling J, Bode M, Lee SS (2012) Process automation toward ultra-high-throughput screening of combinatorial one-bead-one-compound (OBOC) peptide libraries. *Journal of laboratory automation* **17:** 186-200

Chang TT, Hughes-Fulford M (2009) Monolayer and spheroid culture of human liver hepatocellular carcinoma cell line cells demonstrate distinct global gene expression patterns and functional phenotypes. *Tissue engineering Part A* **15:** 559-567

Chen JG, Xu XN, Underhfll CB, Yang SM, Wang LP, Chen YX, Hong SG, Creswell K, Zhang LR (2005) Tachyplesin activates the classic complement pathway to kill tumor cells. *Cancer Res* **65:** 4614-4622

Chen JY, Lin WJ, Lin TL (2009a) A fish antimicrobial peptide, tilapia hepcidin TH2-3, shows potent antitumor activity against human fibrosarcoma cells. *Peptides* **30:** 1636-1642

Chen Y, Xu X, Hong S, Chen J, Liu N, Underhill CB, Creswell K, Zhang L (2001) RGD-Tachyplesin inhibits tumor growth. *Cancer Res* **61:** 2434-2438

Chen YY, Wang ZX, Chang PA, Li JJ, Pan F, Yang L, Bian ZH, Zou L, He JM, Liang HJ (2009b) Knockdown of focal adhesion kinase reverses colon carcinoma multicellular resistance. *Cancer science* **100:** 1708-1713

Cho CF, Behnam Azad B, Luyt LG, Lewis JD (2013) High-throughput screening of one-bead-one-compound peptide libraries using intact cells. *ACS combinatorial science* **15:** 393-400

Choi J, Smitz J (2014) Luteinizing hormone and human chorionic gonadotropin: origins of difference. *Molecular and cellular endocrinology* **383:** 203-213

Clarke M, Collins R, Darby S, Davies C, Elphinstone P, Evans E, Godwin J, Gray R, Hicks C, James S, MacKinnon E, McGale P, McHugh T, Peto R, Taylor C, Wang Y, Early Breast Cancer Trialists' Collaborative G (2005) Effects of radiotherapy and of differences in the extent of surgery for early breast cancer on local recurrence and 15-year survival: an overview of the randomised trials. *Lancet* **366:** 2087-2106

Clynes RA, Towers TL, Presta LG, Ravetch JV (2000) Inhibitory Fc receptors modulate in vivo cytotoxicity against tumor targets. *Nature medicine* **6:** 443-446

Coates AS, Colleoni M, Goldhirsch A (2012) Is Adjuvant Chemotherapy Useful for Women With Luminal A Breast Cancer? *Journal of Clinical Oncology* **30:** 1260-1263

Cole LA (2009) New discoveries on the biology and detection of human chorionic gonadotropin. *Reprod Biol Endocrinol* **7:** 8

Cole LA (2010) Biological functions of hCG and hCG-related molecules. *Reprod Biol Endocrinol* **8:** 102

Cole LA, Butler SA (2008) Hyperglycosylated human chorionic gonadotropin and human chorionic gonadotropin free beta-subunit - Tumor markers and tumor promoters. *J Reprod Med* **53:** 499-512

Cooper C, Liu GY, Niu YL, Santos S, Murphy LC, Watson PH (2004) Intermittent hypoxia induces proteasome-dependent down-regulation of estrogen receptor alpha in human breast carcinoma. *Clinical Cancer Research* **10:** 8720-8727

Cottin S, Ghani K, de Campos-Lima PO, Caruso M (2010) Gemcitabine intercellular diffusion mediated by gap junctions: new implications for cancer therapy. *Molecular cancer* **9:** 141

Cukierman E, Pankov R, Stevens DR, Yamada KM (2001) Taking cell-matrix adhesions to the third dimension. *Science* **294:** 1708-1712

Curtis C, Shah SP, Chin S-F, Turashvili G, Rueda OM, Dunning MJ, Speed D, Lynch AG, Samarajiwa S, Yuan Y, Graf S, Ha G, Haffari G, Bashashati A, Russell R, McKinney S, Langerod A, Green A, Provenzano E, Wishart G, Pinder S, Watson P, Markowetz F, Murphy L, Ellis I, Purushotham A, Borresen-Dale A-L, Brenton JD, Tavare S, Caldas C, Aparicio S (2012) The genomic and transcriptomic architecture of 2,000 breast tumours reveals novel subgroups. *Nature* **486:** 346-352

Curtis KK, Sarantopoulos J, Northfelt DW, Weiss GJ, Barnhart KM, Whisnant JK, Leuschner C, Alila H, Borad MJ, Ramanathan RK (2014) Novel LHRH-receptor-targeted cytolytic peptide, EP-100: first-in-human phase I study in patients with advanced LHRH-receptor-expressing solid tumors. *Cancer Chemoth Pharm* **73:** 931-941

Daines MO, Tabata Y, Walker BA, Chen WG, Warrier MR, Basu S, Hershey GKK (2006) Level of expression of IL-13R alpha 2 impacts receptor distribution and IL-13 signaling. *J Immunol* **176:** 7495-7501

Dalton WS (1999) The tumor microenvironment as a determinant of drug response and resistance. *Drug Resist Update* **2:** 285-288

Datta K, Muders M, Zhang H, Tindall DJ (2010) Mechanism of lymph node metastasis in prostate cancer. *Future oncology* **6:** 823-836

Dave PC, Billington E, Pan YL, Straus SK (2005) Interaction of alamethicin with ether-linked phospholipid bilayers: oriented circular dichroism, 31P solid-state NMR, and differential scanning calorimetry studies. *Biophysical journal* **89:** 2434-2442

Davies JCB, Tamaddon-Jahromi S, Jannoo R, Kanamarlapudi V (2014) Cytohesin 2/ARF6 regulates preadipocyte migration through the activation of ERK1/2. *Biochemical Pharmacology* **92:** 651-660

Debinski W, Obiri NI, Powers SK, Pastan I, Puri RK (1995) Human glioma cells overexpress receptors for interleukin 13 and are extremely sensitive to a novel chimeric protein composed of interleukin 13 and pseudomonas exotoxin. *Clinical Cancer Research* **1:** 1253-1258

Del Duca D, Werbowetski T, Del Maestro RF (2004) Spheroid preparation from hanging drops: characterization of a model of brain tumor invasion. *J Neurooncol* **67:** 295-303

Delena M, Brambilla C, Morabito A, Bonadonna G (1975) Adriamycin Plus Vincristine Compared to and Combined with Cyclophosphamide, Methotrexate, and 5-Fluorouracil for Advanced Breast-Cancer. *Cancer* **35:** 1108-1115

Demir A, Cecen K, Karadag MA, Kocaaslan R, Turkeri L (2014) The course of metastatic prostate cancer under treatment. *SpringerPlus* **3:** 725

Dent R, Trudeau M, Pritchard KI, Hanna WM, Kahn HK, Sawka CA, Lickley LA, Rawlinson E, Sun P, Narod SA (2007) Triple-negative breast cancer: clinical features and patterns of recurrence. *Clinical cancer research : an official journal of the American Association for Cancer Research* **13:** 4429-4434

Dharap SS, Qiu B, Williams GC, Sinko P, Stein S, Minko T (2003) Molecular targeting of drug delivery systems to ovarian cancer by BH3 and LHRH peptides. *J Control Release* **91:** 61-73

Dharap SS, Wang Y, Chandna P, Khandare JJ, Qiu B, Gunaseelan S, Sinko PJ, Stein S, Farmanfarmaian A, Minko T (2005) Tumor-specific targeting of an anticancer drug delivery system by LHRH peptide. *Proc Natl Acad Sci U S A* **102:** 12962-12967

Dhiman HK, Ray AR, Panda AK (2005) Three-dimensional chitosan scaffold-based MCF-7 cell culture for the determination of the cytotoxicity of tamoxifen. *Biomaterials* **26:** 979-986

Doillon CJ, Gagnon E, Paradis R, Koutsilieris M (2004) Three-dimensional culture system as a model for studying cancer cell invasion capacity and anticancer drug sensitivity. *Anticancer Res* **24:** 2169-2177

Dolznig H, Rupp C, Puri C, Haslinger C, Schweifer N, Wieser E, Kerjaschki D, Garin-Chesa P (2011) Modeling colon adenocarcinomas in vitro a 3D co-culture system induces cancer-relevant pathways upon tumor cell and stromal fibroblast interaction. *The American journal of pathology* **179:** 487-501

Donehower LA, Harvey M, Slagle BL, McArthur MJ, Montgomery CA, Jr., Butel JS, Bradley A (1992) Mice deficient for p53 are developmentally normal but susceptible to spontaneous tumours. *Nature* **356:** 215-221

Dowsett M, Jones A, Johnston SR, Jacobs S, Trunet P, Smith IE (1995) In vivo measurement of aromatase inhibition by letrozole (CGS 20267) in postmenopausal patients with breast cancer.

Clinical cancer research : an official journal of the American Association for Cancer Research **1:** 1511-1515

Dufau ML (1998) THE LUTEINIZING HORMONE RECEPTOR1. *Annual Review of Physiology* **60:** 461-496

Durand RE, Olive PL (2001) Resistance of tumor cells to chemo- and radiotherapy modulated by the three-dimensional architecture of solid tumors and spheroids. *Methods in cell biology* **64:** 211-233

Early Breast Cancer Trialists' Collaborative G, Davies C, Godwin J, Gray R, Clarke M, Cutter D, Darby S, McGale P, Pan HC, Taylor C, Wang YC, Dowsett M, Ingle J, Peto R (2011) Relevance of breast cancer hormone receptors and other factors to the efficacy of adjuvant tamoxifen: patient-level meta-analysis of randomised trials. *Lancet* **378:** 771-784

Easton DF (1999) How many more breast cancer predisposition genes are there? *Breast cancer research : BCR* **1:** 14-17

Edge SB, Compton CC (2010) The American Joint Committee on Cancer: the 7th edition of the AJCC cancer staging manual and the future of TNM. *Annals of surgical oncology* **17:** 1471-1474

Ehrenstein G, Lecar H (1977) Electrically gated ionic channels in lipid bilayers. *Q Rev Biophys* **10:** 1-34

Elston CW, Ellis IO (2002) Pathological prognostic factors in breast cancer. I. The value of histological grade in breast cancer: experience from a large study with long-term follow-up. *Histopathology* **41:** 154-161

Emanuele MA, Wezeman F, Emanuele NV (2002) Alcohol's effects on female reproductive function. *Alcohol Res Health* **26:** 274-281

Emons G, Kaufmann M, Gorchev G, Tsekova V, Gründker C, Günthert AR, Hanker LC, Velikova M, Sindermann H, Engel J, Schally AV (2010) Dose escalation and pharmacokinetic study of AEZS-108 (AN-152), an LHRH agonist linked to doxorubicin, in women with LHRH receptor-positive tumors. *Gynecologic Oncology* **119:** 457-461

Emons G, Ortmann O, Becker M, Irmer G, Springer B, Laun R, Holzel F, Schulz KD, Schally AV (1993) High affinity binding and direct antiproliferative effects of LHRH analogues in human ovarian cancer cell lines. *Cancer Res* **53:** 5439-5446

Engel J, Emons G, Pinski J, Schally AV (2012a) AEZS-108 : a targeted cytotoxic analog of LHRH for the treatment of cancers positive for LHRH receptors. *Expert opinion on investigational drugs* **21:** 891-899

Engel JB, Schally AV, Buchholz S, Seitz S, Emons G, Ortmann O (2012b) Targeted chemotherapy of endometrial, ovarian and breast cancers with cytotoxic analogs of luteinizing hormone-releasing hormone (LHRH). *Arch Gynecol Obstet* **286:** 437-442

Etzioni R, Urban N, Ramsey S, McIntosh M, Schwartz S, Reid B, Radich J, Anderson G, Hartwell L (2003) The case for early detection. *Nature reviews Cancer* **3:** 243-252

Excellence NIfHaCr. (2013) NICE and cancer drugs - the facts December 242013 http://www.nice.org.uk/newsroom/nicestatistics/niceandcancerdrugsthefacts.jsp

Fackenthal JD, Olopade OI (2007) Breast cancer risk associated with BRCA1 and BRCA2 in diverse populations. *Nature reviews Cancer* **7:** 937-948

Fadnes B, Uhlin-Hansen L, Lindin I, Rekdal O (2011) Small lytic peptides escape the inhibitory effect of heparan sulfate on the surface of cancer cells. *BMC Cancer* **11:** 116

Ferguson SS (2001) Evolving concepts in G protein-coupled receptor endocytosis: the role in receptor desensitization and signaling. *Pharmacol Rev* **53:** 1-24

Fichtner-Feigl S, Strober W, Kawakami K, Puri RK, Kitani A (2006) IL-13 signaling through the IL-13alpha2 receptor is involved in induction of TGF-beta1 production and fibrosis. *Nature medicine* **12:** 99-106

Finn RS, Crown JP, Lang I, Boer K, Bondarenko IM, Kulyk SO, Ettl J, Patel R, Pinter T, Schmidt M, Shparyk Y, Thummala AR, Voytko NL, Fowst C, Huang X, Kim ST, Randolph S, Slamon DJ (2015) The cyclin-dependent kinase 4/6 inhibitor palbociclib in combination with letrozole versus letrozole alone as first-line treatment of oestrogen receptor-positive, HER2-negative, advanced breast cancer (PALOMA-1/TRIO-18): a randomised phase 2 study. *Lancet Oncol* **16:** 25-35

Fischbach C, Chen R, Matsumoto T, Schmelzle T, Brugge JS, Polverini PJ, Mooney DJ (2007) Engineering tumors with 3D scaffolds. *Nature methods* **4:** 855-860

Fisher B, Bryant J, Wolmark N, Mamounas E, Brown A, Fisher ER, Wickerham DL, Begovic M, DeCillis A, Robidoux A, Margolese RG, Cruz AB, Jr., Hoehn JL, Lees AW, Dimitrov NV, Bear HD (1998) Effect of preoperative chemotherapy on the outcome of women with operable breast cancer. *Journal of clinical oncology : official journal of the American Society of Clinical Oncology* **16:** 2672-2685

Flanagan JM, Cocciardi S, Waddell N, Johnstone CN, Marsh A, Henderson S, Simpson P, da Silva L, kConFab I, Khanna K, Lakhani S, Boshoff C, Chenevix-Trench G (2010) DNA methylome of familial breast cancer identifies distinct profiles defined by mutation status. *American journal of human genetics* **86:** 420-433

Fletcher J, Clark MD, Sutton FA, Wellings R, Garas K (1999) The cost of MRI: changes in costs 1989-1996. *The British journal of radiology* **72:** 432-437

Frankel AE (2004) Reducing the Immune Response to Immunotoxin: Commentary re R. Hassan et al., Pretreatment with Rituximab Does Not Inhibit the Human Immune Response against the Immunogenic Protein LMB-1. Clin. Cancer Res., 10: 16–18, 2004. *Clinical Cancer Research* **10:** 13-15

Friedlander ML, Stockler MR, Butow P, King MT, McAlpine J, Tinker A, Ledermann JA (2013) Clinical trials of palliative chemotherapy in platinum-resistant or -refractory ovarian cancer: time to think differently? *Journal of clinical oncology : official journal of the American Society of Clinical Oncology* **31:** 2362

Friedrich J, Ebner R, Kunz-Schughart LA (2007) Experimental anti-tumor therapy in 3-D: Spheroids – old hat or new challenge? *International Journal of Radiation Biology* **83:** 849-871

Friedrich J, Seidel C, Ebner R, Kunz-Schughart LA (2009) Spheroid-based drug screen: considerations and practical approach. *Nature protocols* **4:** 309-324

Friess H, Büchler M, Kiesel L, Krüger M, Beger H (1991) LH-RH receptors in the human pancreas. *Int J Pancreatol* **10:** 151-159

Froehner M, Wirth MP (2014) Enzalutamide in Metastatic Prostate Cancer before Chemotherapy. *New Engl J Med* **371:** 1755-1755

Fujisawa T, Joshi B, Nakajima A, Puri RK (2009) A novel role of interleukin-13 receptor alpha2 in pancreatic cancer invasion and metastasis. *Cancer Res* **69:** 8678-8685

Fujisawa T, Joshi BH, Puri RK (2011) Histone modification enhances the effectiveness of IL-13 receptor targeted immunotoxin in murine models of human pancreatic cancer. *J Transl Med* **9:** 37

Gabbert H, Wagner R, Höhn P (1983) The relation between tumor cell proliferation and vascularization in differentiated and undifferentiated colon carcinomas in the rat. *Virchows Archiv B Cell Pathol* **42:** 119-131

Gaspar D, Veiga AS, Castanho MA (2013) From antimicrobial to anticancer peptides. A review. *Frontiers in microbiology* **4:** 294

Gebauer G, Fehm T, Beck EP, Berkholz A, Licht P, Jäger W (2003) Cytotoxic effect of conjugates of doxorubicin and human chorionic gonadotropin (hCG) in breast cancer cells. *Breast Cancer Research and Treatment* **77:** 125-131

Gebauer G, Mueller N, Fehm T, Berkholz A, Beck EP, Jaeger W, Licht P (2004a) Expression and regulation of luteinizing hormone/human chorionic gonadotropin receptors in ovarian cancer and its correlation to human chorionic gonadotropin-doxorubicin sensitivity. *Am J Obstet Gynecol* **190:** 1621-1628; discussion 1628

Gebauer G, Mueller N, Fehm T, Berkholz A, Beck EP, Jaeger W, Licht P (2004b) Expression and regulation of luteinizing hormone/human chorionic gonadotropin receptors in ovarian cancer and its correlation to human chorionic gonadotropin–doxorubicin sensitivity. *American Journal of Obstetrics and Gynecology* **190:** 1621-1628

Geyer CE, Forster J, Lindquist D, Chan S, Romieu CG, Pienkowski T, Jagiello-Gruszfeld A, Crown J, Chan A, Kaufman B, Skarlos D, Campone M, Davidson N, Berger M, Oliva C, Rubin SD, Stein S, Cameron D (2006) Lapatinib plus capecitabine for HER2-positive advanced breast cancer. *N Engl J Med* **355:** 2733-2743

Gilbert SF (2010) Developmental biology, ninth edition. *Sinauer Assiciates*

Gillet JP, Calcagno AM, Varma S, Marino M, Green LJ, Vora MI, Patel C, Orina JN, Eliseeva TA, Singal V, Padmanabhan R, Davidson B, Ganapathi R, Sood AK, Rueda BR, Ambudkar SV, Gottesman MM (2011) Redefining the relevance of established cancer cell lines to the study of mechanisms of clinical anti-cancer drug resistance. *Proc Natl Acad Sci U S A* **108:** 18708-18713

Gillet JP, Gottesman MM (2010) Mechanisms of multidrug resistance in cancer. *Methods in molecular biology* **596:** 47-76

Gimbrone MA, Leapman SB, Cotran RS, Folkman J (1972) TUMOR DORMANCY IN VIVO BY PREVENTION OF NEOVASCULARIZATION. *The Journal of Experimental Medicine* **136:** 261-276

Gnanapragasam VJ, Darby S, Khan MM, Lock WG, Robson CN, Leung HY (2005) Evidence that prostate gonadotropin-releasing hormone receptors mediate an anti-tumourigenic response to analogue therapy in hormone refractory prostate cancer. *The Journal of Pathology* **206:** 205-213

Goldhirsch A, Winer EP, Coates AS, Gelber RD, Piccart-Gebhart M, Thurlimann B, Senn HJ, Panel m (2013) Personalizing the treatment of women with early breast cancer: highlights of the St Gallen International Expert Consensus on the Primary Therapy of Early Breast Cancer 2013. *Annals of oncology : official journal of the European Society for Medical Oncology / ESMO* **24:** 2206-2223

Goldsmith PC, McGregor WG, Raymoure WJ, Kuhn RW, Jaffe RB (1983) Cellular localization of chorionic gonadotropin in human fetal kidney and liver. *J Clin Endocrinol Metab* **57:** 654-661

Gonzalez-Moreno O, Calvo A, Joshi BH, Abasolo I, Leland P, Wang Z, Montuenga L, Puri RK, Green JE (2005) Gene expression profiling identifies IL-13 receptor alpha 2 chain as a therapeutic target in prostate tumor cells overexpressing adrenomedullin. *International journal of cancer Journal international du cancer* **114:** 870-878

Graff CP, Wittrup KD (2003) Theoretical analysis of antibody targeting of tumor spheroids: importance of dosage for penetration, and affinity for retention. *Cancer Res* **63:** 1288-1296

Griffith LG, Swartz MA (2006) Capturing complex 3D tissue physiology in vitro. *Nat Rev Mol Cell Biol* **7:** 211-224

Grundker C, Emons G (2003) Role of gonadotropin-releasing hormone (GnRH) in ovarian cancer. *Reprod Biol Endocrinol* **1:** 65

Grundker C, Schlotawa L, Viereck V, Eicke N, Horst A, Kairies B, Emons G (2004) Antiproliferative effects of the GnRH antagonist cetrorelix and of GnRH-II on human endometrial and ovarian cancer cells are not mediated through the GnRH type I receptor. *European journal of endocrinology / European Federation of Endocrine Societies* **151:** 141-149

Grundker C, Volker P, Schulz KD, Emons G (2000) Luteinizing hormone-releasing hormone agonist triptorelin and antagonist cetrorelix inhibit EGF-induced c-fos expression in human gynecological cancers. *Gynecol Oncol* **78:** 194-202

Hagspiel KD, Neidl KFW, Eichenberger AC, Weder W, Marincek B (1995) Detection of Liver Metastases - Comparison of Superparamagnetic Iron Oxide-Enhanced and Unenhanced Mr-Imaging Art 1.5 T with Dynamic Ct, Intraoperative Us, and Percutaneous Us. *Radiology* **196:** 471-478

Hallett MA, Venmar KT, Fingleton B (2012) Cytokine stimulation of epithelial cancer cells: the similar and divergent functions of IL-4 and IL-13. *Cancer Res* **72:** 6338-6343

Halmos G, Arencibia JM, Schally AV, Davis R, Bostwick DG (2000) High incidence of receptors for luteinizing hormone-releasing hormone (LHRH) and LHRH receptor gene expression in human prostate cancers. *The Journal of urology* **163:** 623-629

Hamilton G (1998) Multicellular spheroids as an in vitro tumor model. *Cancer Letters* **131:** 29-34

Hammond ME, Hayes DF, Dowsett M, Allred DC, Hagerty KL, Badve S, Fitzgibbons PL, Francis G, Goldstein NS, Hayes M, Hicks DG, Lester S, Love R, Mangu PB, McShane L, Miller K, Osborne CK, Paik S, Perlmutter J, Rhodes A, Sasano H, Schwartz JN, Sweep FC, Taube S, Torlakovic EE, Valenstein P, Viale G, Visscher D, Wheeler T, Williams RB, Wittliff JL, Wolff AC (2010) American Society of Clinical Oncology/College of American Pathologists guideline recommendations for immunohistochemical testing of estrogen and progesterone receptors in breast cancer. *Archives of pathology & laboratory medicine* **134:** 907-922

Hanahan D, Weinberg RA (2000) The hallmarks of cancer. *Cell* **100:** 57-70

Hanahan D, Weinberg RA (2011) Hallmarks of cancer: the next generation. *Cell* **144:** 646-674

Hancock RE, Diamond G (2000) The role of cationic antimicrobial peptides in innate host defences. *Trends Microbiol* **8:** 402-410

Hansel W (2005) Targeting breast, prostate, ovarian, and testicular cancers through their hormone receptors. *Biology of reproduction* **73:** 850-850

Hansel W, Enright F, Leuschner C (2007a) Destruction of breast cancers and their metastases by lytic peptide conjugates in vitro and in vivo. *Molecular and cellular endocrinology* **260–262:** 183-189

Hansel W, Leuschner C, Enright F (2007b) Conjugates of lytic peptides and LHRH or PCG target and cause necrosis of prostate cancers and metastases. *Molecular and cellular endocrinology* **269:** 26-33

Hapgood JP, Sadie H, van Biljon W, Ronacher K (2005) Regulation of expression of mammalian gonadotrophin-releasing hormone receptor genes. *Journal of neuroendocrinology* **17:** 619-638

Harisinghani MG, Barentsz J, Hahn PF, Deserno WM, Tabatabaei S, van de Kaa CH, de la Rosette J, Weissleder R (2003) Noninvasive detection of clinically occult lymph-node metastases in prostate cancer. *N Engl J Med* **348:** 2491-2499

Harris AL, Hochhauser D (1992) Mechanisms of multidrug resistance in cancer treatment. *Acta oncologica* **31:** 205-213

Hayashi Y, Emoto T, Futaki S, Sekiguchi K (2004) Establishment and characterization of a parietal endoderm-like cell line derived from Engelbreth-Holm-Swarm tumor (EHSPEL), a possible resource for an engineered basement membrane matrix. *Matrix biology : journal of the International Society for Matrix Biology* **23:** 47-62

He H, Xu J, Nelson PS, Marshall FF, Chung LWK, Zhau HE, He D, Wang R (2010) Differential expression of the α2 chain of the interleukin-13 receptor in metastatic human prostate cancer ARCaPM cells. *The Prostate* **70:** 993-1001

Hebbes TR, Thorne AW, Crane-Robinson C (1988) A direct link between core histone acetylation and transcriptionally active chromatin. *EMBO J* **7:** 1395-1402

Hegedus R, Manea M, Orban E, Szabo I, Kiss E, Sipos E, Halmos G, Mezo G (2012) Enhanced cellular uptake and in vitro antitumor activity of short-chain fatty acid acylated daunorubicin-GnRH-III bioconjugates. *European journal of medicinal chemistry* **56:** 155-165

Heidenreich A, Aus G, Bolla M, Joniau S, Matveev VB, Schmid HP, Zattoni F, European Association of U (2008) EAU guidelines on prostate cancer. *European urology* **53:** 68-80

Heil J, Gondos A, Rauch G, Marme F, Rom J, Golatta M, Junkermann H, Sinn P, Aulmann S, Debus J, Hof H, Schutz F, Brenner H, Sohn C, Schneeweiss A (2012) Outcome analysis of patients with primary breast cancer initially treated at a certified academic breast unit. *Breast* **21:** 303-308

Hershey GKK (2003) IL-13 receptors and signaling pathways: An evolving web. *Journal of Allergy and Clinical Immunology* **111:** 677-690

Hilchie A, Doucette C, Pinto D, Patrzykat A, Douglas S, Hoskin D (2011) Pleurocidin-family cationic antimicrobial peptides are cytolytic for breast carcinoma cells and prevent growth of tumor xenografts. *Breast Cancer Research* **13:** R102

Hirschhaeuser F, Menne H, Dittfeld C, West J, Mueller-Klieser W, Kunz-Schughart LA (2010) Multicellular tumor spheroids: an underestimated tool is catching up again. *Journal of biotechnology* **148:** 3-15

Honrado E, Osorio A, Palacios J, Benitez J (2006) Pathology and gene expression of hereditary breast tumors associated with BRCA1, BRCA2 and CHEK2 gene mutations. *Oncogene* **25:** 5837-5845

Huang YB, Wang XF, Wang HY, Liu Y, Chen Y (2011) Studies on mechanism of action of anticancer peptides by modulation of hydrophobicity within a defined structural framework. *Molecular cancer therapeutics* **10:** 416-426

Hubalek M, Brantner C, Marth C (2010) Adjuvant endocrine therapy of premenopausal women with early breast cancer: an overview. *Wiener medizinische Wochenschrift* **160:** 167-173

Hudson PJ, Souriau C (2003) Engineered antibodies. *Nature medicine* **9:** 129-134

Hundt W, Petsch R, Helmberger T, Reiser M (2000) Signal changes in liver and spleen after Endorem administration in patients with and without liver cirrhosis. *Eur Radiol* **10:** 409-416

Iles RK, Delves PJ, Butler SA (2010) Does hCG or hCG beta play a role in cancer cell biology? *Molecular and cellular endocrinology* **329:** 62-70

Institute TNCRr. (2013) NCRI Cancer Research Database December 242013 http://www.ncri.org.uk/what-we-do/research-database

Isbarn H, Boccon-Gibod L, Carroll PR, Montorsi F, Schulman C, Smith MR, Sternberg CN, Studer UE (2009) Androgen deprivation therapy for the treatment of prostate cancer: consider both benefits and risks. *European urology* **55:** 62-75

Ivascu A, Kubbies M (2006) Rapid generation of single-tumor spheroids for high-throughput cell function and toxicity analysis. *J Biomol Screen* **11:** 922-932

Iwasaki T, Ishibashi J, Tanaka H, Sato M, Asaoka A, Taylor D, Yamakawa M (2009) Selective cancer cell cytotoxicity of enantiomeric 9-mer peptides derived from beetle defensins depends on negatively charged phosphatidylserine on the cell surface. *Peptides* **30:** 660-668

Jang SH, Wientjes MG, Lu D, Au JL (2003) Drug delivery and transport to solid tumors. *Pharm Res* **20:** 1337-1350

Jankowitz RC, McGuire KP, Davidson NE (2013) Optimal systemic therapy for premenopausal women with hormone receptor-positive breast cancer. *Breast* **22 Suppl 2:** S165-170

Jarboe JS, Johnson KR, Choi Y, Lonser RR, Park JK (2007) Expression of Interleukin-13 Receptor α2 in Glioblastoma Multiforme: Implications for Targeted Therapies. *Cancer Res* **67:** 7983-7986

Jemal A, Bray F, Center MM, Ferlay J, Ward E, Forman D (2011) Global Cancer Statistics. *Ca-Cancer J Clin* **61:** 69-90

Ji Q, Chen P, Aoyoma C, Liu P (2002) Increased expression of human luteinizing hormone/human chorionic gonadotropin receptor mRNA in human endometrial cancer. *Mol Cell Probes* **16:** 269-275

Jia L, Noker PE, Piazza GA, Leuschner C, Hansel W, Gorman GS, Coward LU, Tomaszewski J (2008) Pharmacokinetics and pharmacodynamics of Phor21-βCG(ala), a lytic peptide conjugate. *J Pharm Pharmacol* **60:** 1441-1448

Joensuu H, Gligorov J (2012) Adjuvant treatments for triple-negative breast cancers. *Annals of oncology : official journal of the European Society for Medical Oncology / ESMO* **23 Suppl 6:** vi40-45

Johnson JI, Decker S, Zaharevitz D, Rubinstein LV, Venditti JM, Schepartz S, Kalyandrug S, Christian M, Arbuck S, Hollingshead M, Sausville EA (2001) Relationships between drug activity in NCI preclinical in vitro and in vivo models and early clinical trials. *British journal of cancer* **84:** 1424-1431

Johnstone RW, Ruefli AA, Lowe SW (2002) Apoptosis: A Link between Cancer Genetics and Chemotherapy. *Cell* **108:** 153-164

Johnstone SA, Gelmon K, Mayer LD, Hancock RE, Bally MB (2000) In vitro characterization of the anticancer activity of membrane-active cationic peptides. I. Peptide-mediated cytotoxicity and peptide-enhanced cytotoxic activity of doxorubicin against wild-type and p-glycoprotein over-expressing tumor cell lines. *Anticancer Drug Des* **15:** 151-160

Jones PA, Laird PW (1999) Cancer epigenetics comes of age. *Nature genetics* **21:** 163-167

Joshi BH, Kawakami K, Leland P, Puri RK (2002) Heterogeneity in interleukin-13 receptor expression and subunit structure in squamous cell carcinoma of head and neck: Differential sensitivity to chimeric fusion proteins comprised of interleukin-13 and a mutated form of Pseudomonas exotoxin. *Clinical Cancer Research* **8:** 1948-1956

Joshi BH, Puri RA, Leland P, Varricchio F, Gupta G, Kocak M, Gilbertson RJ, Puri RK, Consortium USPBT (2008) Identification of interleukin-13 receptor alpha2 chain overexpression in situ in high-grade diffusely infiltrative pediatric brainstem glioma. *Neuro Oncol* **10:** 265-274

Kakutani H, Kondoh M, Saeki R, Fujii M, Watanabe Y, Mizuguchi H, Yagi K (2010) Claudin-4-targeting of diphtheria toxin fragment A using a C-terminal fragment of Clostridium perfringens enterotoxin. *European Journal of Pharmaceutics and Biopharmaceutics* **75:** 213-217

Kamb A, Wee S, Lengauer C (2007) Why is cancer drug discovery so difficult? *Nature reviews Drug discovery* **6:** 115-120

Kanamarlapudi V, Owens SE, Lartey J, Lopez Bernal A (2012a) ADP-ribosylation factor 6 expression and activation are reduced in myometrium in complicated pregnancies. *PLoS One* **7:** e37954

Kanamarlapudi V, Thompson A, Kelly E, Bernal AL (2012b) ARF6 Activated by the LHCG Receptor through the Cytohesin Family of Guanine Nucleotide Exchange Factors Mediates the Receptor Internalization and Signaling. *Journal of Biological Chemistry* **287:** 20443-20455

Kang SK, Cheng KW, Ngan ES, Chow BK, Choi KC, Leung PC (2000) Differential expression of human gonadotropin-releasing hormone receptor gene in pituitary and ovarian cells. *Molecular and cellular endocrinology* **162:** 157-166

Kaufman B, Mackey JR, Clemens MR, Bapsy PP, Vaid A, Wardley A, Tjulandin S, Jahn M, Lehle M, Feyereislova A, Revil C, Jones A (2009) Trastuzumab plus anastrozole versus anastrozole alone for the treatment of postmenopausal women with human epidermal growth factor receptor 2-positive, hormone receptor-positive metastatic breast cancer: results from the randomized phase III TAnDEM study. *Journal of clinical oncology : official journal of the American Society of Clinical Oncology* **27:** 5529-5537

Kaufmann M, Hortobagyi GN, Goldhirsch A, Scholl S, Makris A, Valagussa P, Blohmer J-U, Eiermann W, Jackesz R, Jonat W, Lebeau A, Loibl S, Miller W, Seeber S, Semiglazov V, Smith R, Souchon R, Stearns V, Untch M, von Minckwitz G (2006) Recommendations From an International Expert Panel on the Use of Neoadjuvant (Primary) Systemic Treatment of Operable Breast Cancer: An Update. *Journal of Clinical Oncology* **24:** 1940-1949

Kawakami K, Kawakami M, Puri RK (2004) Specifically targeted killing of interleukin-13 (IL-13) receptor-expressing breast cancer by IL-13 fusion cytotoxin in animal model of human disease. *Molecular cancer therapeutics* **3:** 137-147

Kawakami K, Takeshita F, Puri RK (2001) Identification of Distinct Roles for a Dileucine and a Tyrosine Internalization Motif in the Interleukin (IL)-13 Binding Component IL-13 Receptor α2 Chain. *Journal of Biological Chemistry* **276:** 25114-25120

Kawakami M, Kawakami K, Kasperbauer JL, Hinkley LL, Tsukuda M, Strome SE, Puri RK (2003) Interleukin-13 Receptor α2 Chain in Human Head and Neck Cancer Serves as a Unique Diagnostic Marker. *Clinical Cancer Research* **9:** 6381-6388

Kawamoto M, Horibe T, Kohno M, Kawakami K (2011) A novel transferrin receptor-targeted hybrid peptide disintegrates cancer cell membrane to induce rapid killing of cancer cells. *BMC Cancer* **11:** 359

Keller G, Schally AV, Nagy A, Baker B, Halmos G, Engel JB (2006) Effective therapy of experimental human malignant melanomas with a targeted cytotoxic somatostatin analogue without induction of multi-drug resistance proteins. *International journal of oncology* **28:** 1507-1513

Keller G, Schally AV, Nagy A, Halmos G, Baker B, Engel JB (2005) Targeted chemotherapy with cytotoxic bombesin analogue AN-215 can overcome chemoresistance in experimental renal cell carcinomas. *Cancer* **104:** 2266-2274

Kero J, Poutanen M, Zhang FP, Rahman N, McNicol AM, Nilson JH, Keri RA, Huhtaniemi IT (2000) Elevated luteinizing hormone induces expression of its receptor and promotes steroidogenesis in the adrenal cortex. *J Clin Invest* **105:** 633-641

Khaitan D, Dwarakanath BS (2006) Multicellular spheroids as an in vitro model in experimental oncology: applications in translational medicine. *Expert Opinion on Drug Discovery* **1:** 663-675

Kim S, Kim S, Bang Y, Kim S, Lee B (2003) In vitro activities of native and designed peptide antibiotics against drug sensitive and resistant tumor cell lines. *Peptides* **24:** 945 - 953

Kioi M, Kawakami K, Puri RK (2004) Analysis of antitumor activity of an interleukin-13 (IL-13) receptor-targeted cytotoxin composed of IL-13 antagonist and Pseudomonas exotoxin. *Clinical Cancer Research* **10:** 6231-6238

Kioi M, Kawakami M, Shimamura T, Husain SR, Puri RK (2006a) Interleukin-13 receptor alpha2 chain: a potential biomarker and molecular target for ovarian cancer therapy. *Cancer* **107:** 1407-1418

Kioi M, Kawakami M, Shimamura T, Husain SR, Puri RK (2006b) Interleukin-13 receptor α2 chain. *Cancer* **107:** 1407-1418

Kirkpatrick J (1998) Biochemical outcome after radical prostatectomy, external beam radiation therapy, or interstitial radiation therapy for clinically localized prostate cancer. *Journal of insurance medicine* **30:** 204-205

Klapper LN, Waterman H, Sela M, Yarden Y (2000) Tumor-inhibitory antibodies to HER-2/ErbB-2 may act by recruiting c-Cbl and enhancing ubiquitination of HER-2. *Cancer Res* **60:** 3384-3388

Kobayashi H, Brechbiel MW (2003) Dendrimer-based macromolecular MRI contrast agents: characteristics and application. *Mol Imaging* **2:** 1-10

Kobayashi H, Man S, Graham CH, Kapitain SJ, Teicher BA, Kerbel RS (1993) Acquired multicellular-mediated resistance to alkylating agents in cancer. *Proc Natl Acad Sci U S A* **90:** 3294-3298

Koenig JA, Edwardson JM (1997) Endocytosis and recycling of G protein-coupled receptors. *Trends Pharmacol Sci* **18:** 276-287

Kola I, Landis J (2004) Can the pharmaceutical industry reduce attrition rates? *Nature Reviews Drug Discovery* **3:** 711-715

Kondo S, Shinomura Y, Miyazaki Y, Kiyohara T, Tsutsui S, Kitamura S, Nagasawa Y, Nakahara M, Kanayama S, Matsuzawa Y (2000) Mutations of the bak gene in human gastric and colorectal cancers. *Cancer Res* **60:** 4328-4330

Kraus S, Naor Z, Seger R (2001) Intracellular signaling pathways mediated by the gonadotropin-releasing hormone (GnRH) receptor. *Arch Med Res* **32:** 499-509

Krebs LJ, Wang XP, Nagy A, Schally AV, Prasad PN, Liebow C (2002) A conjugate of doxorubicin and an analog of Luteinizing Hormone-Releasing Hormone shows increased efficacy against oral and laryngeal cancers. *Oral Oncol* **38:** 657-663

Kroeze WK, Sheffler DJ, Roth BL (2003) G-protein-coupled receptors at a glance. *J Cell Sci* **116:** 4867-4869

Kunwar S, Prados MD, Chang SM, Berger MS, Lang FF, Piepmeier JM, Sampson JH, Ram Z, Gutin PH, Gibbons RD, Aldape KD, Croteau DJ, Sherman JW, Puri RK (2007) Direct Intracerebral Delivery of Cintredekin Besudotox (IL13-PE38QQR) in Recurrent Malignant Glioma: A Report by the Cintredekin Besudotox Intraparenchymal Study Group. *Journal of Clinical Oncology* **25:** 837-844

Kunz-Schughart LA, Freyer JP, Hofstaedter F, Ebner R (2004) The use of 3-D cultures for high-throughput screening: the multicellular spheroid model. *J Biomol Screen* **9:** 273-285

Kunz-Schughart LA, Heyder P, Schroeder J, Knuechel R (2001) A heterologous 3-D coculture model of breast tumor cells and fibroblasts to study tumor-associated fibroblast differentiation. *Experimental cell research* **266:** 74-86

Kurebayashi J, Otsuki T, Moriya T, Sonoo H (2001) Hypoxia reduces hormone responsiveness of human breast cancer cells. *Jpn J Cancer Res* **92:** 1093-1101

Kuroda H, Mandai M, Konishi I, Yura Y, Tsuruta Y, Hamid AA, Nanbu K, Matsushita K, Mori T (1998) Human chorionic gonadotropin (hCG) inhibits cisplatin-induced apoptosis in ovarian cancer cells: possible role of up-regulation of insulin-like growth factor-1 by hCG. *Int J Cancer* **76:** 571-578

Kuszyk BS, Corl FM, Franano FN, Bluemke DA, Hofmann LV, Fortman BJ, Fishman EK (2001) Tumor Transport Physiology: Implications for Imaging and Imaging-Guided Therapy. *American Journal of Roentgenology* **177:** 747-753

Labialle S, Dayan G, Michaud M, Barakat S, Rigal D, Baggetto LG (2005) Gene therapy of the typical multidrug resistance phenotype of cancers: a new hope? *Semin Oncol* **32:** 583-590

Landry J, Freyer JP, Sutherland RM (1981) Shedding of mitotic cells from the surface of multicell spheroids during growth. *Journal of cellular physiology* **106:** 23-32

le Roux L, Volgin A, Maxwell D, Ishihara K, Gelovani J, Schellingerhout D (2008) Optimizing Imaging of Three-Dimensional Multicellular Tumor Spheroids with Fluorescent Reporter Proteins Using Confocal Microscopy. *Molecular Imaging* **7:** 214-221

Lee E, Rosca EV, Pandey NB, Popel AS (2011) Small peptides derived from somatotropin domain-containing proteins inhibit blood and lymphatic endothelial cell proliferation, migration, adhesion and tube formation. *The international journal of biochemistry & cell biology* **43:** 1812-1821

Lee SM, Lee EJ, Hong HY, Kwon MK, Kwon TH, Choi JY, Park RW, Kwon TG, Yoo ES, Yoon GS, Kim IS, Ruoslahti E, Lee BH (2007) Targeting bladder tumor cells in vivo and in the urine with a peptide identified by phage display. *Molecular cancer research : MCR* **5:** 11-19

Lenhard M, Lennerova T, Ditsch N, Kahlert S, Friese K, Mayr D, Jeschke U (2011) Opposed roles of follicle-stimulating hormone and luteinizing hormone receptors in ovarian cancer survival. *Histopathology* **58:** 990-994

Lenhard M, Tereza L, Heublein S, Ditsch N, Himsl I, Mayr D, Friese K, Jeschke U (2012a) Steroid hormone receptor expression in ovarian cancer: progesterone receptor B as prognostic marker for patient survival. *Bmc Cancer* **12**

Lenhard M, Tsvilina A, Schumacher L, Kupka M, Ditsch N, Mayr D, Friese K, Jeschke U (2012b) Human chorionic gonadotropin and its relation to grade, stage and patient survival in ovarian cancer. *BMC cancer* **12:** 2-2

Leung PC, Choi JH (2007) Endocrine signaling in ovarian surface epithelium and cancer. *Human reproduction update* **13:** 143-162

Leurs U, Lajko E, Mezo G, Orban E, Ohlschlager P, Marquardt A, Kohidai L, Manea M (2012) GnRH-III based multifunctional drug delivery systems containing daunorubicin and methotrexate. *European journal of medicinal chemistry* **52:** 173-183

Leuschner C, Enright FM, Gawronska-Kozak B, Hansel W (2003a) Human prostate cancer cells and xenografts are targeted and destroyed through luteinizing hormone releasing hormone receptors. *Prostate* **56:** 239-249

Leuschner C, Enright FM, Gawronska B, Hansel W (2003b) Membrane disrupting lytic peptide conjugates destroy hormone dependent and independent breast cancer cells in vitro and in vivo. *Breast Cancer Res Treat* **78:** 17-27

Leuschner C, Enright FM, Melrose PA, Hansel W (2001) Targeted destruction of androgen-sensitive and -insensitive prostate cancer cells and xenografts through luteinizing hormone receptors. *Prostate* **46:** 116-125

Leuschner C, Hansel W (2005) Targeting breast and prostate cancers through their hormone receptors. *Biol Reprod* **73:** 860-865

Leuschner C, Kumar CSSR, Hansel W, Hormes J (2005) Targeting Breast Cancer Cells and Their Metastases Through Luteinizing Hormone Releasing Hormone (LHRH) Receptors Using Magnetic Nanoparticles. *J Biomed Nanotechnol* **1:** 229-233

Li C, Hall WA, Jin N, Todhunter DA, Panoskaltsis-Mortari A, Vallera DA (2002) Targeting glioblastoma multiforme with an IL-13/diphtheria toxin fusion protein in vitro and in vivo in nude mice. *Protein engineering* **15:** 419-427

Li MQ, Tang ZH, Zhang Y, Lv SX, Yu HY, Zhang DW, Hong H, Chen XS (2014) LHRH-peptide conjugated dextran nanoparticles for targeted delivery of cisplatin to breast cancer. *J Mater Chem B* **2:** 3490-3499

Li Q, Chen C, Kapadia A, Zhou Q, Harper MK, Schaack J, LaBarbera DV (2011) 3D models of epithelial-mesenchymal transition in breast cancer metastasis: high-throughput screening assay development, validation, and pilot screen. *J Biomol Screen* **16:** 141-154

Limanond P, Raman SS, Sayre J, Lu DSK (2004) Comparison of dynamic ferumoxides-enhanced gadolinium-enhanced and MRI of the liver on highand low-field scanners. *J Magn Reson Imaging* **20:** 640-647

Limonta P, Montagnani Marelli M, Mai S, Motta M, Martini L, Moretti RM (2012) GnRH receptors in cancer: from cell biology to novel targeted therapeutic strategies. *Endocr Rev* **33:** 784-811

Limonta P, Moretti RM, Marelli MM, Motta M (2003) The biology of gonadotropin hormone-releasing hormone: role in the control of tumor growth and progression in humans. *Front Neuroendocrin* **24:** 279-295

Lin RZ, Chang HY (2008) Recent advances in three-dimensional multicellular spheroid culture for biomedical research. *Biotechnology journal* **3:** 1172-1184

Ling J, Liao H, Clark R, Wong MS, Lo DD (2008) Structural constraints for the binding of short peptides to claudin-4 revealed by surface plasmon resonance. *The Journal of biological chemistry* **283:** 30585-30595

Liotta LA, Kohn EC (2001) The microenvironment of the tumour-host interface. *Nature* **411:** 375-379

Liu S, Yang H, Wan L, Cheng JQ, Lu XF (2013) Penetratin-Mediated Delivery Enhances the Antitumor Activity of the Cationic Antimicrobial Peptide Magainin II. *Cancer Biother Radio* **28:** 289-297

Liu TF, Cai JZ, Gibo DM, Debinski W (2009) Reoxygenation of Hypoxic Glioblastoma Multiforme Cells Potentiates the Killing Effect of an Interleukin-13-Based Cytotoxin. *Clinical Cancer Research* **15:** 160-168

Lojun S, Bao S, Lei ZM, Rao CV (1997) Presence of functional luteinizing hormone/chorionic gonadotropin (hCG) receptors in human breast cell lines: implications supporting the premise that hCG protects women against breast cancer. *Biology of reproduction* **57:** 1202-1210

Ma HL, Jiang Q, Han S, Wu Y, Cui Tomshine J, Wang D, Gan Y, Zou G, Liang XJ (2012) Multicellular tumor spheroids as an in vivo-like tumor model for three-dimensional imaging of chemotherapeutic and nano material cellular penetration. *Mol Imaging* **11:** 487-498

MacDonald HR, Sordat B (1980) The multicellular tumor spheroid: a quantitative model for studies of in situ immunity. *Contemporary topics in immunobiology* **10:** 317-342

Mackiewicz-Wysocka M, Pankowska M, Wysocki PJ (2012) Progress in the treatment of bone metastases in cancer patients. *Expert opinion on investigational drugs* **21:** 785-795

Madhankumar AB, Mintz A, Debinski W (2004) Interleukin 13 mutants of enhanced avidity toward the glioma-associated receptor, IL13Ralpha2. *Neoplasia (New York, NY)* **6:** 15-22

Maeda H, Wu J, Sawa T, Matsumura Y, Hori K (2000) Tumor vascular permeability and the EPR effect in macromolecular therapeutics: a review. *J Control Release* **65:** 271-284

Mai JC, Mi Z, Kim SH, Ng B, Robbins PD (2001) A proapoptotic peptide for the treatment of solid tumors. *Cancer Res* **61:** 7709-7712

Mann BS, Johnson JR, Cohen MH, Justice R, Pazdur R (2007) FDA approval summary: vorinostat for treatment of advanced primary cutaneous T-cell lymphoma. *The oncologist* **12:** 1247-1252

Mauri D, Pavlidis N, Ioannidis JP (2005) Neoadjuvant versus adjuvant systemic treatment in breast cancer: a meta-analysis. *Journal of the National Cancer Institute* **97:** 188-194

McGregor DP (2008) Discovering and improving novel peptide therapeutics. *Current Opinion in Pharmacology* **8:** 616-619

Medical Nr. (2012) Aeterna Zentaris reaches SPA agreement with FDA for AEZS-108 Phase 3 trial in endometrial cancer 05/012013 http://www.news-medical.net/news/20121229/Aeterna-Zentaris-reaches-SPA-agreement-with-FDA-for-AEZS-108-Phase-3-trial-in-endometrial-cancer.aspx

Meduri G, Charnaux N, Loosfelt H, Jolivet A, Spyratos F, Brailly S, Milgrom E (1997) Luteinizing hormone/human chorionic gonadotropin receptors in breast cancer. *Cancer Res* **57:** 857-864

Meduri G, Charnaux N, Spyratos F, Hacene K, Loosfelt H, Milgrom E (2003) Luteinizing hormone receptor status and clinical, pathologic, and prognostic features in patients with breast carcinomas. *Cancer* **97:** 1810-1816

Meijers-Heijboer H, van Geel B, van Putten WL, Henzen-Logmans SC, Seynaeve C, Menke-Pluymers MB, Bartels CC, Verhoog LC, van den Ouweland AM, Niermeijer MF, Brekelmans CT, Klijn JG (2001) Breast cancer after prophylactic bilateral mastectomy in women with a BRCA1 or BRCA2 mutation. *N Engl J Med* **345:** 159-164

Melo MN, Ferre R, Castanho MARB (2009) Antimicrobial peptides: linking partition, activity and high membrane-bound concentrations. *Nat Rev Micro* **7:** 245-250

Mendelsohn J, Baselga J (2003) Status of epidermal growth factor receptor antagonists in the biology and treatment of cancer. *Journal of clinical oncology : official journal of the American Society of Clinical Oncology* **21:** 2787-2799

Mertens-Walker I, Baxter RC, Marsh DJ (2012) Gonadotropin signalling in epithelial ovarian cancer. *Cancer Letters* **324:** 152-159

Metzger-Filho O, Tutt A, de Azambuja E, Saini KS, Viale G, Loi S, Bradbury I, Bliss JM, Azim HA, Jr., Ellis P, Di Leo A, Baselga J, Sotiriou C, Piccart-Gebhart M (2012) Dissecting the heterogeneity of triple-negative breast cancer. *Journal of clinical oncology : official journal of the American Society of Clinical Oncology* **30:** 1879-1887

Mikhail AS, Eetezadi S, Allen C (2013) Multicellular tumor spheroids for evaluation of cytotoxicity and tumor growth inhibitory effects of nanomedicines in vitro: a comparison of docetaxel-loaded block copolymer micelles and Taxotere(R). *PLoS One* **8:** e62630

Millar R, Lowe S, Conklin D, Pawson A, Maudsley S, Troskie B, Ott T, Millar M, Lincoln G, Sellar R, Faurholm B, Scobie G, Kuestner R, Terasawa E, Katz A (2001) A novel mammalian receptor for the evolutionarily conserved type II GnRH. *Proc Natl Acad Sci U S A* **98:** 9636-9641

Millar RP, Lu ZL, Pawson AJ, Flanagan CA, Morgan K, Maudsley SR (2004) Gonadotropin-releasing hormone receptors. *Endocr Rev* **25:** 235-275

Miller BE, Miller FR, Heppner GH (1985) Factors affecting growth and drug sensitivity of mouse mammary tumor lines in collagen gel cultures. *Cancer Res* **45:** 4200-4205

Miller Lr. (2007) Quantifying western blots without expensive commercial quantification software. 11 March2015 http://www.lukemiller.org/journal/2007/08/quantifying-western-blots-without.html

Minchinton AI, Tannock IF (2006) Drug penetration in solid tumours. *Nature reviews Cancer* **6:** 583-592

Minko T, Dharap SS, Pakunlu RI, Wang Y (2004) Molecular targeting of drug delivery systems to cancer. *Curr Drug Targets* **5:** 389-406

Minn AJ, Gupta GP, Siegel PM, Bos PD, Shu W, Giri DD, Viale A, Olshen AB, Gerald WL, Massague J (2005) Genes that mediate breast cancer metastasis to lung. *Nature* **436:** 518-524

Minty A, Chalon P, Derocq JM, Dumont X, Guillemot JC, Kaghad M, Labit C, Leplatois P, Liauzun P, Miloux B (1993) Interleukin-13 is a new human lymphokine regulating inflammatory and immune responses. *Nature* **362:** 248-250

Moghimi SM, Hunter AC, Murray JC (2001) Long-circulating and target-specific nanoparticles: theory to practice. *Pharmacol Rev* **53:** 283-318

Momparler RL, Bovenzi V (2000) DNA methylation and cancer. *Journal of cellular physiology* **183:** 145-154

Monneret C (2007) Histone deacetylase inhibitors for epigenetic therapy of cancer. *Anti-cancer drugs* **18:** 363-370

Morbeck DE, Roche PC, Keutmann HT, McCormick DJ (1993) A receptor binding site identified in the region 81-95 of the beta-subunit of human luteinizing hormone (LH) and chorionic gonadotropin (hCG). *Molecular and cellular endocrinology* **97:** 173-181

Moretti RM, Montagnani Marelli M, Van Groeninghen JC, Limonta P (2002) Locally expressed LHRH receptors mediate the oncostatic and antimetastatic activity of LHRH agonists on melanoma cells. *J Clin Endocrinol Metab* **87:** 3791-3797

Morgan FJ, Birken S, Canfield RE (1975) The amino acid sequence of human chorionic gonadotropin. The alpha subunit and beta subunit. *Journal of Biological Chemistry* **250:** 5247-5258

Morikawa K, Walker SM, Nakajima M, Pathak S, Jessup JM, Fidler IJ (1988) Influence of Organ Environment on the Growth, Selection, and Metastasis of Human-Colon Carcinoma-Cells in Nude-Mice. *Cancer Res* **48:** 6863-6871

Mueller-Klieser W (2000) Tumor biology and experimental therapeutics. *Critical reviews in oncology/hematology* **36:** 123-139

Muller T, Gromoll J, Simoni M (2003) Absence of exon 10 of the human luteinizing hormone (LH) receptor impairs LH, but not human chorionic gonadotropin action. *J Clin Endocrinol Metab* **88:** 2242-2249

Nagy A, Schally AV (2005) Targeting of cytotoxic luteinizing hormone-releasing hormone analogs to breast, ovarian, endometrial, and prostate cancers. *Biology of reproduction* **73:** 851-859

Nagy A, Schally AV, Armatis P, Szepeshazi K, Halmos G, Kovacs M, Zarandi M, Groot K, Miyazaki M, Jungwirth A, Horvath J (1996) Cytotoxic analogs of luteinizing hormone-releasing hormone containing doxorubicin or 2-pyrrolinodoxorubicin, a derivative 500-1000 times more potent. *Proc Natl Acad Sci U S A* **93:** 7269-7273

Nakashima H, Fujisawa T, Husain SR, Puri RK (2010) Interleukin-13 receptor alpha 2 DNA prime boost vaccine induces tumor immunity in murine tumor models. *J Transl Med* **8**

Nestor CE, Ottaviano R, Reinhardt D, Cruickshanks HA, Mjoseng HK, McPherson RC, Lentini A, Thomson JP, Dunican DS, Pennings S, Anderton SM, Benson M, Meehan RR (2015) Rapid reprogramming of epigenetic and transcriptional profiles in mammalian culture systems. *Genome biology* **16:** 11

Noci I, Pillozzi S, Lastraioli E, Dabizzi S, Giachi M, Borrani E, Wimalasena J, Taddei GL, Scarselli G, Arcangeli A (2008) hLH/hCG-receptor expression correlates with in vitro invasiveness in human primary endometrial cancer. *Gynecologic Oncology* **111:** 496-501

O'Regan RM, Jordan VC (2001) Tamoxifen to raloxifene and beyond. *Semin Oncol* **28:** 260-273

Obort AS, Ajadi MB, Akinloye O (2013) Prostate-Specific Antigen: Any Successor in Sight? *Reviews in Urology* **15:** 97-107

Olesen SP (1986) Rapid increase in blood-brain barrier permeability during severe hypoxia and metabolic inhibition. *Brain research* **368:** 24-29

Olive PL, Banath JP, Evans HH (1993) Cell killing and DNA damage by etoposide in Chinese hamster V79 monolayers and spheroids: influence of growth kinetics, growth environment and DNA packaging. *British journal of cancer* **67:** 522-530

Oren Z, Shai Y (1998) Mode of action of linear amphipathic alpha-helical antimicrobial peptides. *Biopolymers* **47:** 451-463

Organization TWHr. (2015) Cancer 3 Feb2015 http://www.who.int/cancer/detection/breastcancer/en/

Overgaard M, Jensen MB, Overgaard J, Hansen PS, Rose C, Andersson M, Kamby C, Kjaer M, Gadeberg CC, Rasmussen BB, Blichert-Toft M, Mouridsen HT (1999) Postoperative radiotherapy in high-risk postmenopausal breast-cancer patients given adjuvant tamoxifen: Danish Breast Cancer Cooperative Group DBCG 82c randomised trial. *Lancet* **353:** 1641-1648

Ozben T (2006) Mechanisms and strategies to overcome multiple drug resistance in cancer. *FEBS letters* **580:** 2903-2909

Padera TP, Stoll BR, Tooredman JB, Capen D, di Tomaso E, Jain RK (2004) Pathology: cancer cells compress intratumour vessels. *Nature* **427:** 695

Pakarainen T, Ahtiainen P, Zhang FP, Rulli S, Poutanen M, Huhtaniemi I (2007) Extragonadal LH/hCG action--not yet time to rewrite textbooks. *Molecular and cellular endocrinology* **269:** 9-16

Pakarinen P, Vihko KK, Voutilainen R, Huhtaniemi I (1990) Differential response of luteinizing hormone receptor and steroidogenic enzyme gene expression to human chorionic gonadotropin stimulation in the neonatal and adult rat testis. *Endocrinology* **127:** 2469-2474

Pandya H, Gibo DM, Garg S, Kridel S, Debinski W (2012) An interleukin 13 receptor α 2–specific peptide homes to human Glioblastoma multiforme xenografts. *Neuro-Oncology* **14:** 6-18

Pantel K, Muller V, Auer M, Nusser N, Harbeck N, Braun S (2003) Detection and clinical implications of early systemic tumor cell dissemination in breast cancer. *Clinical cancer research : an official journal of the American Association for Cancer Research* **9:** 6326-6334

Pantel K, Otte M (2001) Occult micrometastasis: enrichment, identification and characterization of single disseminated tumour cells. *Semin Cancer Biol* **11:** 327-337

Papo N, Seger D, Makovitzki A, Kalchenko V, Eshhar Z, Degani H, Shai Y (2006) Inhibition of tumor growth and elimination of multiple metastases in human prostate and breast xenografts by systemic inoculation of a host defense-like lytic peptide. *Cancer Res* **66:** 5371-5378

Papo N, Shahar M, Eisenbach L, Shai Y (2003) A novel lytic peptide composed of DL-amino acids selectively kills cancer cells in culture and in mice. *The Journal of biological chemistry* **278:** 21018-21023

Parhi P, Mohanty C, Sahoo SK (2012) Nanotechnology-based combinational drug delivery: an emerging approach for cancer therapy. *Drug Discovery Today*

Pati D, Habibi HR (1995) Inhibition of Human Hepatocarcinoma Cell-Proliferation by Mammalian and Fish Gonadotropin-Releasing Hormones. *Endocrinology* **136:** 75-84

Pharmaceuticals Er. (2009) Clinical Trial EP-100 06/012013 http://www.esperancepharma.com/content/clinical-trials

Pharmaceuticals Er. (2012) Esperance Pharmaceuticals Presents Results From Phase 1 Study of EP-100 in Advanced, Refractory LHRH-Receptor Expressing Solid Tumors at ASCO 06/012013 http://www.esperancepharma.com/content/news-and-information#news01

Pilepich MV, Winter K, Lawton CA, Krisch RE, Wolkov HB, Movsas B, Hug EB, Asbell SO, Grignon D (2005) Androgen suppression adjuvant to definitive radiotherapy in prostate carcinoma--long-term results of phase III RTOG 85-31. *International journal of radiation oncology, biology, physics* **61:** 1285-1290

Piltonen T, Koivunen R, Morin-Papunen L, Ruokonen A, Huhtaniemi IT, Tapanainen JS (2002) Ovarian and adrenal steroid production: regulatory role of LH/HCG. *Human Reproduction* **17:** 620-624

Pouny Y, Rapaport D, Mor A, Nicolas P, Shai Y (1992) Interaction of Antimicrobial Dermaseptin and Its Fluorescently Labeled Analogs with Phospholipid-Membranes. *Biochemistry* **31:** 12416-12423

Press MF, Bernstein L, Thomas PA, Meisner LF, Zhou JY, Ma YL, Hung G, Robinson RA, Harris C, ElNaggar A, Slamon DJ, Phillips RN, Ross JS, Wolman SR, Flom KJ (1997) HER-2/neu gene amplification characterized by fluorescence in situ hybridization: Poor prognosis in node-negative breast carcinomas. *Journal of Clinical Oncology* **15:** 2894-2904

Price JC, Bromfield JJ, Sheldon IM (2013) Pathogen-associated molecular patterns initiate inflammation and perturb the endocrine function of bovine granulosa cells from ovarian dominant follicles via TLR2 and TLR4 pathways. *Endocrinology* **154:** 3377-3386

Puri R, Leland P, Obiri N, Husain S, Kreitman R, Haas G, Pastan I, Debinski W (1996) Targeting of interleukin-13 receptor on human renal cell carcinoma cells by a recombinant chimeric protein composed of interleukin-13 and a truncated form of Pseudomonas exotoxin A (PE38QQR). *Blood* **87:** 4333-4339

Qvarnstrom OF, Simonsson M, Eriksson V, Turesson I, Carlsson J (2009) gammaH2AX and cleaved PARP-1 as apoptotic markers in irradiated breast cancer BT474 cellular spheroids. *International journal of oncology* **35:** 41-47

Rahaman SO, Sharma P, Harbor PC, Aman MJ, Vogelbaum MA, Haque SJ (2002) IL-13Rα2, a Decoy Receptor for IL-13 Acts As an Inhibitor of IL-4-dependent Signal Transduction in Glioblastoma Cells. *Cancer Res* **62:** 1103-1109

Rahman NA, Rao CV (2009) Recent progress in luteinizing hormone/human chorionic gonadotrophin hormone research. *Molecular Human Reproduction* **15:** 703-711

Raja J, Ramachandran N, Munneke G, Patel U (2006) Current status of transrectal ultrasound-guided prostate biopsy in the diagnosis of prostate cancer. *Clinical radiology* **61:** 142-153

Rakha EA, Ellis IO (2009) Triple-negative/basal-like breast cancer: review. *Pathology* **41:** 40-47

Rampino N, Yamamoto H, Ionov Y, Li Y, Sawai H, Reed JC, Perucho M (1997) Somatic frameshift mutations in the BAX gene in colon cancers of the microsatellite mutator phenotype. *Science* **275:** 967-969

Rangarajan A, Hong SJ, Gifford A, Weinberg RA (2004) Species- and cell type-specific requirements for cellular transformation. *Cancer cell* **6:** 171-183

Rejniak KA, Estrella V, Chen T, Cohen AS, Lloyd MC, Morse DL (2013) The role of tumor tissue architecture in treatment penetration and efficacy: an integrative study. *Frontiers in oncology* **3:** 111

Rivero-Muller A, Vuorenoja S, Tuominen M, Waclawik A, Brokken LJS, Ziecik AJ, Huhtaniemi I, Rahman NA (2007) Use of hecate-chorionic gonadotropin beta conjugate in therapy of lutenizing hormone receptor expressing gonadal somatic cell tumors. *Molecular and cellular endocrinology* **269:** 17-25

Roberts DL, Williams KJ, Cowen RL, Barathova M, Eustace AJ, Brittain-Dissont S, Tilby MJ, Pearson DG, Ottley CJ, Stratford IJ, Dive C (2009) Contribution of HIF-1 and drug penetrance to oxaliplatin resistance in hypoxic colorectal cancer cells. *British journal of cancer* **101:** 1290-1297

Robinson PJ (2000) Imaging liver metastases: current limitations and future prospects. *The British journal of radiology* **73:** 234-241

Robson ME, Offit K (2004) Breast MRI for women with hereditary cancer risk. *Jama-J Am Med Assoc* **292:** 1368-1370

Rodday B, Hirschhaeuser F, Walenta S, Mueller-Klieser W (2011) Semiautomatic growth analysis of multicellular tumor spheroids. *J Biomol Screen* **16:** 1119-1124

Rodrigues EG, Dobroff ASS, Cavarsan CF, Paschoalin T, Nimrichter L, Mortara RA, Santos EL, Fazio MA, Miranda A, Daffre S, Travassos LR (2008) Effective topical treatment of subcutaneous murine B16F10-Nex2 melanoma by the antimicrobial peptide gomesin. *Neoplasia* **10:** 61-68

Rofstad EK, Eide K, Skoyum R, Hystad ME, Lyng H (1996) Apoptosis, energy metabolism, and fraction of radiobiologically hypoxic cells: A study of human melanoma multicellular spheroids. *International Journal of Radiation Biology* **70:** 241-249

Roodman GD (2004) Mechanisms of bone metastasis. *N Engl J Med* **350:** 1655-1664

Rosca EV, Koskimaki JE, Rivera CG, Pandey NB, Tamiz AP, Popel AS (2011) Anti-Angiogenic Peptides for Cancer Therapeutics. *Curr Pharm Biotechno* **12:** 1101-1116

Ruggiero C, Pastorino L, Herrera OL (2010) Nanotechnology based targeted drug delivery. *Conf Proc IEEE Eng Med Biol Soc* **2010:** 3731-3732

Russnes HG, Vollan HK, Lingjaerde OC, Krasnitz A, Lundin P, Naume B, Sorlie T, Borgen E, Rye IH, Langerod A, Chin SF, Teschendorff AE, Stephens PJ, Maner S, Schlichting E, Baumbusch LO, Karesen R, Stratton MP, Wigler M, Caldas C, Zetterberg A, Hicks J, Borresen-Dale AL (2010) Genomic architecture characterizes tumor progression paths and fate in breast cancer patients. *Science translational medicine* **2:** 38ra47

Saad F (2013) Evidence for the efficacy of enzalutamide in postchemotherapy metastatic castrate-resistant prostate cancer. *Therapeutic advances in urology* **5:** 201-210

Sahl REWHH-G (2006) Antimicrobial and host-defense peptides as new anti-infective therapeutic strategies. *Nature Biotechnology* **24:** 6

Sansom MS (1993) Alamethicin and related peptaibols--model ion channels. *Eur Biophys J* **22:** 105-124

Santini MT, Rainaldi G (1999) Three-dimensional spheroid model in tumor biology. *Pathobiology : journal of immunopathology, molecular and cellular biology* **67:** 148-157

Savranoglu P, Obuz F, Karasu S, Coker A, Secil M, Sagol O, Igci E, Dicle O, Astarcioglu I (2006) The role of SPIO-enhanced MRI in the detection of malignant liver lesions. *Clin Imag* **30:** 377-381

Schally A, Nagy A (1999) Cancer chemotherapy based on targeting of cytotoxic peptide conjugates to their receptors on tumors. *European Journal of Endocrinology* **141:** 1-14

Schally AV, Comaru-Schally AM, Nagy A, Kovacs M, Szepeshazi K, Plonowski A, Varga JL, Halmos G (2001) Hypothalamic hormones and cancer. *Front Neuroendocrinol* **22:** 248-291

Schang AL, Querat B, Simon V, Garrel G, Bleux C, Counis R, Cohen-Tannoudji J, Laverriere JN (2012) Mechanisms underlying the tissue-specific and regulated activity of the Gnrhr promoter in mammals. *Frontiers in endocrinology* **3:** 162

Schwartz G (2002) Hypothesis: Does ochratoxin A cause testicular cancer? *Cancer Causes Control* **13:** 91-100

Seok J, Warren HS, Cuenca AG, Mindrinos MN, Baker HV, Xu W, Richards DR, McDonald-Smith GP, Gao H, Hennessy L, Finnerty CC, López CM, Honari S, Moore EE, Minei JP, Cuschieri J, Bankey PE, Johnson JL, Sperry J, Nathens AB, Billiar TR, West MA, Jeschke MG, Klein MB, Gamelli RL, Gibran NS, Brownstein BH, Miller-Graziano C, Calvano SE, Mason PH, Cobb JP, Rahme LG, Lowry SF, Maier RV, Moldawer LL, Herndon DN, Davis RW, Xiao W, Tompkins RG, Inflammation t, Host Response to Injury LSCRP (2013) Genomic responses in mouse models poorly mimic human inflammatory diseases. *Proceedings of the National Academy of Sciences*

Sethi A, Delatte J, Foil L, Husseneder C (2014) Protozoacidal Trojan-Horse: Use of a Ligand-Lytic Peptide for Selective Destruction of Symbiotic Protozoa within Termite Guts. *PLoS ONE* **9:** e106199

Shai Y (1999) Mechanism of the binding, insertion and destabilization of phospholipid bilayer membranes by alpha-helical antimicrobial and cell non-selective membrane-lytic peptides. *Biochim Biophys Acta* **1462:** 55-70

Shai Y (2002) Mode of action of membrane active antimicrobial peptides. *Biopolymers* **66:** 236-248

Shai Y, Oren Z (2001) From "carpet" mechanism to de-novo designed diastereomeric cell-selective antimicrobial peptides. *Peptides* **22:** 1629-1641

Shang B, Cao Z, Zhou Q (2012) Progress in tumor vascular normalization for anticancer therapy: challenges and perspectives. *Frontiers of medicine* **6:** 67-78

Shanks N, Greek R, Greek J (2009) Are animal models predictive for humans? *Philosophy, ethics, and humanities in medicine : PEHM* **4:** 2

Shaw KR, Wrobel CN, Brugge JS (2004) Use of three-dimensional basement membrane cultures to model oncogene-induced changes in mammary epithelial morphogenesis. *Journal of mammary gland biology and neoplasia* **9:** 297-310

Shenker A (2002) Activating mutations of the lutropin choriogonadotropin receptor in precocious puberty. *Receptors Channels* **8:** 3-18

Shenoy VS, Vijay IK, Murthy RSR (2005) Tumour targeting: biological factors and formulation advances in injectable lipid nanoparticles. *J Pharm Pharmacol* **57:** 411-421

Shimamura T, Fujisawa T, Husain SR, Joshi B, Puri RK (2010) Interleukin 13 Mediates Signal Transduction through Interleukin 13 Receptor α2 in Pancreatic Ductal Adenocarcinoma: Role of IL-13 Pseudomonas Exotoxin in Pancreatic Cancer Therapy. *Clinical Cancer Research* **16:** 577-586

Shoemaker RH (2006) The NCI60 human tumour cell line anticancer drug screen. *Nature reviews Cancer* **6:** 813-823

Simoni M, Gromoll J, Nieschlag E (1997) The follicle-stimulating hormone receptor: Biochemistry, molecular biology, physiology, and pathophysiology. *Endocrine Reviews* **18:** 739-773

Singh M, Zuo J, Li X, Ambrus G, Lei ZM, Yussman MA, Sanfilippo JS, Rao CV (1995) Decreased expression of functional human chorionic gonadotropin/luteinizing hormone receptor gene in human uterine leiomyomas. *Biology of reproduction* **53:** 591-597

Sionvardi N, Kaneti J, Segalabramson T, Giat J, Levy J, Sharoni Y (1992) Gonadotropin-Releasing-Hormone Specific Binding-Sites in Normal and Malignant Renal Tissue. *J Urology* **148:** 1568-1570

Slamon DJ, Leyland-Jones B, Shak S, Fuchs H, Paton V, Bajamonde A, Fleming T, Eiermann W, Wolter J, Pegram M, Baselga J, Norton L (2001) Use of chemotherapy plus a monoclonal antibody against HER2 for metastatic breast cancer that overexpresses HER2. *New Engl J Med* **344:** 783-792

Sotiriou C, Pusztai L (2009) Gene-expression signatures in breast cancer. *N Engl J Med* **360:** 790-800

Sower SA, Chiang YC, Lovas S, Conlon JM (1993) Primary structure and biological activity of a third gonadotropin-releasing hormone from lamprey brain. *Endocrinology* **132:** 1125-1131

Steinmeyer C, Berkholz A, Gebauer G, Jager W (2003) The expression of hCG receptor mRNA in four human ovarian cancer cell lines varies considerably under different experimental conditions. *Tumour biology : the journal of the International Society for Oncodevelopmental Biology and Medicine* **24:** 13-22

Stephen ZR, Kievit FM, Zhang MQ (2011) Magnetite nanoparticles for medical MR imaging. *Mater Today* **14:** 330-338

Straub B, Muller M, Krause H, Schrader M, Miller K (2003) Real-time quantitative reverse transcriptase-polymerase chain reaction for luteinizing hormone-releasing hormone receptor gene mRNA expression in human prostate cancer. *Urology* **62:** 172-176

Sun J, Zhou SB, Hou P, Yang Y, Weng J, Li XH, Li MY (2007) Synthesis and characterization of biocompatible Fe3O4 nanoparticles. *J Biomed Mater Res A* **80A:** 333-341

Sutherland RM, McCredie JA, Inch WR (1971) Growth of Multicell Spheroids in Tissue Culture as a Model of Nodular Carcinomas. *Journal of the National Cancer Institute* **46:** 113-120

Sutton MA, Gibbons RP, Correa RJ (1991) Is deleting the digital rectal examination a good idea? *Western Journal of Medicine* **155:** 43-46

Szende B, Srkalovic G, Timar J, Mulchahey JJ, Neill JD, Lapis K, Csikos A, Szepeshazi K, Schally AV (1991) Localization of receptors for luteinizing hormone-releasing hormone in pancreatic and mammary cancer cells. *Proc Natl Acad Sci U S A* **88:** 4153-4156

Takenouchi M, Hirai S, Sakuragi N, Yagita H, Hamada H, Kato K (2011) Epigenetic modulation enhances the therapeutic effect of anti-IL-13R(alpha)2 antibody in human mesothelioma xenografts. *Clinical cancer research : an official journal of the American Association for Cancer Research* **17:** 2819-2829

Tammela T (2004) Endocrine treatment of prostate cancer. *J Steroid Biochem* **92:** 287-295

Tan N, Margolis DJ, McClure TD, Thomas A, Finley DS, Reiter RE, Huang J, Raman SS (2011) Radical prostatectomy: value of prostate MRI in surgical planning. *Abdom Imaging*

Tao YX, Bao S, Ackermann DM, Lei ZM, Rao CV (1997a) Expression of luteinizing hormone human chorionic gonadotropin receptor gene in benign prostatic hyperplasia and in prostate carcinoma in humans. *Biology of reproduction* **56:** 67-72

Tao YX, Bao S, Ackermann DM, Lei ZM, Rao CV (1997b) Expression of luteinizing hormone/human chorionic gonadotropin receptor gene in benign prostatic hyperplasia and in prostate carcinoma in humans. *Biology of reproduction* **56:** 67-72

Teicher BA (2006) Tumor models for efficacy determination. *Molecular cancer therapeutics* **5:** 2435-2443

Teicher BA (2009) Acute and chronic in vivo therapeutic resistance. *Biochemical Pharmacology* **77:** 1665-1673

Temkin SM, Fleming G (2009) Current treatment of metastatic endometrial cancer. *Cancer Control* **16:** 38-45

Thompson A, Kanamarlapudi V (2014) The regions within the N-terminus critical for human glucagon like peptide-1 receptor (hGLP-1R) cell Surface expression. *Sci Rep-Uk* **4**

Thurber GM, Wittrup KD (2008) Quantitative spatiotemporal analysis of antibody fragment diffusion and endocytic consumption in tumor spheroids. *Cancer Res* **68:** 3334-3341

Tieva A, Stattin P, Wikstrom P, Bergh A, Damber JE (2001) Gonadotropin-releasing hormone receptor expression in the human prostate. *Prostate* **47:** 276-284

Todorovska A, Roovers RC, Dolezal O, Kortt AA, Hoogenboom HR, Hudson PJ (2001) Design and application of diabodies, triabodies and tetrabodies for cancer targeting. *Journal of immunological methods* **248:** 47-66

Torisawa YS, Shiku H, Yasukawa T, Nishizawa M, Matsue T (2005) Multi-channel 3-D cell culture device integrated on a silicon chip for anticancer drug sensitivity test. *Biomaterials* **26:** 2165-2172

Trinchard-Lugan I, Khan A, Porchet HC, Munafo A (2002) Pharmacokinetics and pharmacodynamics of recombinant human chorionic gonadotrophin in healthy male and female volunteers. *Reproductive biomedicine online* **4:** 106-115

Tschentscher P, Wagener C, Neumaier M (1997) Sensitive and specific cytokeratin 18 reverse transcription polymerase chain reaction that excludes amplification of processed pseudogenes from contaminating genomic DNA. *Clin Chem* **43:** 2244-2250

Twentyman PR (1980) Response to chemotherapy of EMT6 spheroids as measured by growth delay and cell survival. *British journal of cancer* **42:** 297-304

Uehiro N, Horii R, Iwase T, Tanabe M, Sakai T, Morizono H, Kimura K, Iijima K, Miyagi Y, Nishimura S, Makita M, Ito Y, Akiyama F (2014) Validation study of the UICC TNM classification of malignant tumors, seventh edition, in breast cancer. *Breast cancer* **21:** 748-753

Ujihara M, Yamamoto K, Nomura K, Toyoshima S, Demura H, Nakamura Y, Ohmura K, Osawa T (1992) Subunit-specific sulphation of oligosaccharides relating to chargeheterogeneity in porcine lutrophin isoforms. *Glycobiology* **2:** 225-231

UK CRr. (2009) Cancer Research UK Statistics December 20132013 http://www.cancerresearchuk.org/cancer-info/cancerstats/world/

UK CRr. (2012) Worldwide cancer statistics December 242013 http://www.cancerresearchuk.org/cancer-info/cancerstats/world/

Utsugi T, Schroit AJ, Connor J, Bucana CD, Fidler IJ (1991) Elevated expression of phosphatidylserine in the outer membrane leaflet of human tumor cells and recognition by activated human blood monocytes. *Cancer Res* **51:** 3062-3066

Vajpeyi R (2005) WHO Classification of Tumours: Pathology and Genetics of Tumours of the Breast and Female Genital Organs. *Journal of Clinical Pathology* **58:** 671-672

van der Hage JA, van de Velde CJ, Julien JP, Tubiana-Hulin M, Vandervelden C, Duchateau L (2001) Preoperative chemotherapy in primary operable breast cancer: results from the European Organization for Research and Treatment of Cancer trial 10902. *Journal of clinical oncology : official journal of the American Society of Clinical Oncology* **19:** 4224-4237

Van Dyke T, Jacks T (2002) Cancer modeling in the modern era: progress and challenges. *Cell* **108:** 135-144

van Groeninghen JC, Kiesel L, Winkler D, Zwirner M (1998) Effects of luteinising-hormone-releasing hormone on nervous-system tumours. *Lancet* **352:** 372-373

van Zoggel H, Carpentier G, Dos Santos C, Hamma-Kourbali Y, Courty J, Amiche M, Delbe J (2012) Antitumor and Angiostatic Activities of the Antimicrobial Peptide Dermaseptin B2. *Plos One* **7**

Voskoglou-Nomikos T, Pater JL, Seymour L (2003) Clinical Predictive Value of the in Vitro Cell Line, Human Xenograft, and Mouse Allograft Preclinical Cancer Models. *Clinical Cancer Research* **9:** 4227-4239

Vousden KH, Lane DP (2007) p53 in health and disease. *Nat Rev Mol Cell Biol* **8:** 275-283

Vu T, Claret FX (2012) Trastuzumab: updated mechanisms of action and resistance in breast cancer. *Frontiers in oncology* **2:** 62

Wachter S, Gerstner N, Dorner D, Goldner G, Colotto A, Wambersie A, Potter R (2002) The influence of a rectal balloon tube as internal immobilization device on variations of volumes and dose-volume histograms during treatment course of conformal radiotherapy for prostate cancer. *International journal of radiation oncology, biology, physics* **52:** 91-100

Wang C, Li HB, Li S, Tian LL, Shang DJ (2012) Antitumor effects and cell selectivity of temporin-1CEa, an antimicrobial peptide from the skin secretions of the Chinese brown frog (Rana chensinensis). *Biochimie* **94:** 434-441

Wang L, Menon KM (2005) Regulation of luteinizing hormone/chorionic gonadotropin receptor messenger ribonucleic acid expression in the rat ovary: relationship to cholesterol metabolism. *Endocrinology* **146:** 423-431

Wang YS, Li D, Shi HS, Wen YJ, Yang L, Xu N, Chen XC, Chen X, Chen P, Li J, Deng HX, Wang CT, Xie G, Huang S, Mao YQ, Chen LJ, Zhao X, Wei YQ (2009) Intratumoral Expression of Mature Human Neutrophil Peptide-1 Mediates Antitumor Immunity in Mice. *Clinical Cancer Research* **15:** 6901-6911

Wang YX, Hussain SM, Krestin GP (2001) Superparamagnetic iron oxide contrast agents: physicochemical characteristics and applications in MR imaging. *European Radiology* **11:** 2319-2331

Warner E, Plewes DB, Hill KA, Causer PA, Zubovits JT, Jong RA, Cutrara MR, DeBoer G, Yaffe MJ, Messner SJ, Meschino WS, Piron CA, Narod SA (2004) Surveillance of BRCA1 and BRCA2 mutation carriers with magnetic resonance imaging, ultrasound, mammography, and clinical breast examination. *Jama-J Am Med Assoc* **292:** 1317-1325

Webber MM, Bello D, Kleinman HK, Hoffman MP (1997) Acinar differentiation by non-malignant immortalized human prostatic epithelial cells and its loss by malignant cells. *Carcinogenesis* **18:** 1225-1231

Weichert JP, Clark PA, Kandela IK, Vaccaro AM, Clarke W, Longino MA, Pinchuk AN, Farhoud M, Swanson KI, Floberg JM, Grudzinski J, Titz B, Traynor AM, Chen HE, Hall LT, Pazoles CJ, Pickhardt PJ, Kuo JS (2014) Alkylphosphocholine analogs for broad-spectrum cancer imaging and therapy. *Science translational medicine* **6:** 240ra275

Weidle UH, Maisel D, Klostermann S, Schiller C, Weiss EH (2011) Intracellular Proteins Displayed on the Surface of Tumor Cells as Targets for Therapeutic Intervention with Antibody-related Agents. *Cancer Genom Proteom* **8:** 49-63

Weigelt B, Peterse JL, van 't Veer LJ (2005) Breast cancer metastasis: markers and models. *Nature reviews Cancer* **5:** 591-602

Weigelt B, Reis-Filho JS (2009) Histological and molecular types of breast cancer: is there a unifying taxonomy? *Nat Rev Clin Oncol* **6:** 718-730

Weinberg RA (1983) Oncogenes and the molecular biology of cancer. *The Journal of cell biology* **97:** 1661-1662

Weinberg RA (2002) Cancer Biology and Therapy: the road ahead. *Cancer biology & therapy* **1:** 3

Weindel K, Moringlane JR, Marme D, Weich HA (1994) Detection and quantification of vascular endothelial growth factor/vascular permeability factor in brain tumor tissue and cyst fluid: the key to angiogenesis? *Neurosurgery* **35:** 439-448; discussion 448-439

Westberry JM, Prewitt AK, Wilson ME (2008) Epigenetic regulation of the estrogen receptor alpha promoter in the cerebral cortex following ischemia in male and female rats. *Neuroscience* **152:** 982-989

Whiteside GT, Adedoyin A, Leventhal L (2008) Predictive validity of animal pain models? A comparison of the pharmacokinetic-pharmacodynamic relationship for pain drugs in rats and humans. *Neuropharmacology* **54:** 767-775

Wolff AC, Hammond ME, Hicks DG, Dowsett M, McShane LM, Allison KH, Allred DC, Bartlett JM, Bilous M, Fitzgibbons P, Hanna W, Jenkins RB, Mangu PB, Paik S, Perez EA, Press MF, Spears PA, Vance GH, Viale G, Hayes DF, American Society of Clinical O, College of American P (2014)

Recommendations for human epidermal growth factor receptor 2 testing in breast cancer: American Society of Clinical Oncology/College of American Pathologists clinical practice guideline update. *Archives of pathology & laboratory medicine* **138:** 241-256

Wong M, Pavlakis N (2011) Optimal management of bone metastases in breast cancer patients. *Breast cancer* **3:** 35-60

Wu AH, Low WC (2002) Molecular cloning of the rat IL-13 alpha 2 receptor cDNA and its expression in rat tissues. *J Neurooncol* **59:** 99-105

Wu HM, Wang HS, Huang HY, Lai CH, Lee CL, Soong YK, Leung PC (2013) Gonadotropin-releasing hormone type II (GnRH-II) agonist regulates the invasiveness of endometrial cancer cells through the GnRH-I receptor and mitogen-activated protein kinase (MAPK)-dependent activation of matrix metalloproteinase (MMP)-2. *BMC Cancer* **13:** 300

Wu W, He QG, Jiang CZ (2008) Magnetic Iron Oxide Nanoparticles: Synthesis and Surface Functionalization Strategies. *Nanoscale Res Lett* **3:** 397-415

Wykosky J, Gibo DM, Stanton C, Debinski W (2008) Interleukin-13 Receptor α2, EphA2, and Fos-Related Antigen 1 as Molecular Denominators of High-Grade Astrocytomas and Specific Targets for Combinatorial Therapy. *Clinical Cancer Research* **14:** 199-208

Xia W, Mullin RJ, Keith BR, Liu LH, Ma H, Rusnak DW, Owens G, Alligood KJ, Spector NL (2002) Anti-tumor activity of GW572016: a dual tyrosine kinase inhibitor blocks EGF activation of EGFR/erbB2 and downstream Erk1/2 and AKT pathways. *Oncogene* **21:** 6255-6263

Xu H, Chen CX, Hu J, Zhou P, Zeng P, Cao CH, Lu JR (2013) Dual modes of antitumor action of an amphiphilic peptide A(9)K. *Biomaterials* **34:** 2731-2737

Xu X, Farach-Carson MC, Jia X (2014) Three-dimensional in vitro tumor models for cancer research and drug evaluation. *Biotechnology Advances* **32:** 1256-1268

Yamauchi J, Itoh H, Shinoura H, Miyamoto Y, Hirasawa A, Kaziro Y, Tsujimoto G (2001) Involvement of c-Jun N-Terminal Kinase and p38 Mitogen-Activated Protein Kinase in α1B-Adrenergic Receptor/Gαq-Induced Inhibition of Cell Proliferation. *Biochemical and Biophysical Research Communications* **281:** 1019-1023

Yang L, Horibe T, Kohno M, Haramoto M, Ohara K, Puri RK, Kawakami K (2012) Targeting interleukin-4 receptor alpha with hybrid peptide for effective cancer therapy. *Molecular cancer therapeutics* **11:** 235-243

Yoon DJ, Liu CT, Quinlan DS, Nafisi PM, Kamei DT (2011) Intracellular Trafficking Considerations in the Development of Natural Ligand-Drug Molecular Conjugates for Cancer. *Ann Biomed Eng* **39:** 1235-1251

Zelezetsky I, Pacor S, Pag U, Papo N, Shai Y, Sahl HG, Tossi A (2005) Controlled alteration of the shape and conformational stability of alpha-helical cell-lytic peptides: effect on mode of action and cell specificity. *The Biochemical journal* **390:** 177-188

Zhang M, Shi H, Segaloff DL, Van Voorhis BJ (2001) Expression and localization of luteinizing hormone receptor in the female mouse reproductive tract. *Biology of reproduction* **64:** 179-187

Zhang Y, Fatima N, Dufau ML (2005) Coordinated changes in DNA methylation and histone modifications regulate silencing/derepression of luteinizing hormone receptor gene transcription. *Mol Cell Biol* **25:** 7929-7939

Zhao Z, Wang L, Xu W (2014) IL-13Ralpha2 mediates PNR-induced migration and metastasis in ERalpha-negative breast cancer. *Oncogene*

Zhong J, Chau Y (2008) Antitumor activity of a membrane lytic peptide cyclized with a linker sensitive to membrane type 1-matrix metalloproteinase. *Molecular cancer therapeutics* **7:** 2933-2940

Zhou R, Qian S, Gu X, Chen Z, Xiang J (2013) Interleukin-13 and its receptors in colorectal cancer (Review). *Biomedical reports* **1:** 687-690

Ziecik AJ, Kaczmarek MM, Blitek A, Kowalczyk AE, Li X, Rahman NA (2007) Novel biological and possible applicable roles of LH/hCG receptor. *Molecular and cellular endocrinology* **269:** 51-60

Zietman AL, Chung CS, Coen JJ, Shipley WU (2004) 10-year outcome for men with localized prostate cancer treated with external radiation therapy: results of a cohort study. *The Journal of urology* **171:** 210-214

Zong WX, Ditsworth D, Bauer DE, Wang ZQ, Thompson CB (2004) Alkylating DNA damage stimulates a regulated form of necrotic cell death. *Genes Dev* **18:** 1272-1282

Zurawski SM, Vega F, Huyghe B, Zurawski G (1993) Receptors for interleukin-13 and interleukin-4 are complex and share a novel component that functions in signal transduction. *The EMBO journal* **12:** 2663-2670